THE UNIVERSITY *of* EDINBURGH

The Role of Tyrosine Phosphorylation of Synaptophysin in the Synaptic Vesicle Lifecycle

THE UNIVERSITY *of* EDINBURGH

Alexander James Johnson

Thesis Presented for the Degree of Doctor of Philosophy

May 2012

Contents

List of Figures

List of Tables

Declaration

I, Alexander James Johnson, have composed this thesis myself. The work and the results reported herein are my own except where indicated, and have not been submitted for any other degree or professional qualification.

Acknowledgements

Giselle and Penny, you are always the inspiration, motivation and most enjoyable distractions. This thesis exists because of you.

Thanks to my parents, without their support of all my choices, I would have never made it this far.

A big thank you to Mike for supporting, teaching and advising me throughout the project. But mostly for accepting me as a student in the first place! I have been helped out throughout the project greatly by advice from Dr. Gareth Evans. And I am very grateful for input, and collaboration efforts, from Dr. Peter Haines and Prof. Phil Robinson. Thanks to all the members of the CIP that have helped me, whether by letting me steal some enzymes or teaching me some techniques.

Finally I would like to thank anyone who has helped me keep the Scottish Breweries and distilleries in business over the last few years; it has been great having a range of friends to forget/talk about work with.

"La hauteur de l'habileté est d'être capable de le cacher"

- Francois De La Rochefoucauld, c.1650

Abstract

Synaptophysin (Syp) is a major integral synaptic vesicle (SV) protein; there are 31 copies of Syp per vesicle, which totals up to 10% of the total SV protein content. Despite being the major SV protein, little is known about the interaction partners of Syp and as a result there has been no clear role attributed to it. One key feature of Syp is that its cytoplasmic C-terminus contains 10 pentapeptide repeats, nine of which are initiated by a tyrosine residue. Syp is the major tyrosine phospho-protein on SVs. The kinase thought to phosphorylate Syp *in vivo* is the ubiquitously expressed non-receptor kinase C-Src. There are two splice variants of C-Src, N1- and N2-Src, which are only expressed in neuronal tissues. Although the 3 Srcs are structurally similar, they differ by a small insert of amino acids into their SH3 domains (the N-Src loop).

Examination of the amino acid sequence of the cytosolic C-terminus of Syp revealed a putative type one SH3 domain interaction motif. A screen using SH3 domains of synaptic proteins as bait in GST-pull downs from nerve terminal lysate allowed an inventory of potential interaction partners of Syp to be created. Reciprocal experiments using the C-terminal of Syp as bait confirmed many of these interactions. Single point mutations of the SH3 interaction motif on Syp highlighted that syndapin and C-Src bound to Syp via this motif. These binding mutants were inserted in Syp superecliptic synaptophluorin (SypHy) to determine the functional consequences of these interactions. These mutants did not affect the trafficking of Syp when expressed in cortical neurons derived from Syp knockout mice. However,

the SH3 interaction motif was fundamental for the retrieval of VAMP (vesicle associated membrane protein) when expressed in Syp knockout cultures. Importantly, this role is not mediated through a direct interaction with VAMP with the SH3 interaction motif implicating either syndapin, C-Src or both in Syp-dependent VAMP retrieval.

The 3 different Srcs had different methods of interaction with Syp, and *in vitro* protein kinase assays the ability of the three Src splice variants to phosphorylate Syp was assessed. Key differences in both speed and efficiency of Syp phosphorylation was observed for the different Src splice variants. Mutagenesis of either all 9 tyrosine residues, only previously identified sites resulted in changes in Syp interactions in GST-pull down assays from nerve terminal lysates. To investigate the role of Syp phosphorylation in the SV lifecycle, the tyrosine pentapeptide repeats were truncated from the C-terminal of Syp in both a mCerulean tagged Syp and SypHy. The experiments showed that these potential tyrosine phosphorylation sites were not involved in the trafficking of Syp but key in the retrieval of VAMP from the plasma membrane during the SV lifecycle.

I have indentified an SH3 interaction motif on the C-terminal of Syp that is critical in forming a complex of proteins that are responsible for the retrieval of VAMP during the SV lifecycle. Further experiments have shown that this key interaction is potentially phosphorylation dependent. My preliminary mass spectrometry analysis has provided a catalogue of proteins that can potentially interact with Syp, identifying proteins that may bind to either the Syp C-terminus SH3 interaction

motif or to other regions in a phosphorylation dependent manner. This has provided a list of potential candidate proteins for the VAMP retrieval complex.

Abbreviations

4AP	4-aminopyridine
AP1	Adaptor protein 1
AP180	Adaptor protein 180
AP2	Adaptor protein 2
ATP	Adenosine-5'-triphosphate
Bar domain	Bin–Amphiphysin–Rvs domain
BSA	Bovine serum albumin
C2	Protein kinase C homologous
CaMK 2	Calcium/calmodulin-dependent protein kinase 2
Cer	mCerulean
CLAP domain	Clathrin/AP-2-binding domain
COV	Coefficient of variance
CSPα	Cysteine string protein alpha
DNA	Deoxyribonucleic acid
DIV	Days *in vitro*
ECL	Electrochemiluminescence

FBS	Fetal bovine serum
FL	Full length
FRET	Förster resonance energy transfer
GFP	Green fluorescent protein
GSH	Glutathione
GST	Glutathione S-transferase
GTP	Guanosine 5'-triphosphate
His	Histidine
Hsc 70	Heat shock protein 70
IPTG	Isopropyl β-D-1-thiogalactopyranoside
LTP	Long term potentiation
MARVEL	MAL and related proteins for vesicle trafficking and membrane link
mRNA	Messenger Ribonucleic acid
Munc 18	Mammalian homologue of uncoordinated
N1-Src	Neuronal splice variant of Src 1
N2-Src	Neuronal splice variant of Src 2

MEM	Minimum essential media
NMDA	N-Methyl-D-aspartic acid
NSF	N-ethylmaleimide sensitive factor
NT	Neurotransmitter
PC12	Pheochromocytoma derived cell line
PCR	Polymerase chain reaction
PDL	Poly-d-lysine
Phospho	Phosphorylation
PI(4,5)P2	PtdIns 4,5-bisphosphate
PMSF	Phenylmethanesulfonylfluoride
RNAi	Ribonucleic acid interference
PP2	Src kinase inhibitor
ROI	Region of interest
SCAMPs	Secretory membrane proteins
SDS-PAGE	Sodium dodecyl sulfate polyacrylamide gel electrophoresis
SH1	Src homology domain 1
SH2	Src homology domain 2

SH3	Src homology 3 domain
SH-PTP1	Tyrosine phosphatase
Siah	Seven in absentia homologue
SNAP25	Synaptosomal-associated protein 25
SNARE	Soluble N-ethylmaleimide sensitive factor attachment protein receptor
Src	Non-receptor tyrosine kinase
SV	Synaptic vesicle
Syp	Synaptophysin
SypHy	Superecliptic synaptophysin phluorin
t-SNARE	Target SNARE
VAMP	Vesicle associated membrane protein
v-SNARE	Vesicle SNARE
WT	Wild type

Chapter 1 Introduction

Neurotransmission, the process of releasing neurotransmitter (NT) in a directional manner between different neurons to allow propagation of an action potential, is fundamental to life. Without it, neurons would be unable to develop networks and therefore regulate countless processes that occur throughout the body; ranging from simply staring out the window to the complex regulation of idea formation and writing a thesis. The specialised domain of the neuron which allows regulation of this process is the synapse, where the NT is released from the pre-synaptic side to another neuron on the post-synaptic side. There are two key properties that characterise neurons; they are long and they are able to conduct neuronal transmission at very high speed. The packets of NT are called synaptic vesicles (SVs), and their membranes are full of proteins which regulate trafficking, NT release and SV formation.

The two defining characteristics could present a potential problem to neurons. As they are long in cellular terms, the synapse is located a long way from the site of SV synthesis in the cell. If SVs were supplied by the cell body, then the neuron would be able to propagate a single action potential but then fail to propagate further action potentials that are in rapid succession. This is because the nerve terminal would eventually run out of NT, as the SVs would be used up faster than the time it would take to syntheses new SVs *de novo* and traffic to the synapse. To overcome this, neurons have evolved a method of recycling the protein machinery that is involved in neuronal transmission at the synapse, and this is called the SV lifecycle.

1.1 - The Synaptic Vesicle Lifecycle

As NTs are compounds that can elicit responses from neurons, it is important that they are contained and only released when needed. As a result, they are packaged in SVs which undergo a cycle of release and retrieval following the appropriate signal from an action potential (figure 1.1). The SVs are located near the pre-synaptic membrane and following an influx of Ca^{2+} into neurons, caused by the arrival of an action potential, the SVs fuse with the membrane in a process called exocytosis. This causes the NT cargo to be released into the synaptic cleft, which then diffuses across to the post-synaptic membrane to facilitate the propagation of an action potential. The SV membrane and the proteins are then retrieved from the membrane to maintain the surface area of the cell during endocytosis, and to allow the SVs to be re-constituted and re-filled in order to participate in further propagations of action potentials.

1.2 - Molecular Components of Exocytosis

The SNARE (soluble N-ethylmaleimide sensitive factor attachment protein receptor) complex is essential in mediating SV exocytosis. It comprises of three proteins; synaptobrevin, also known as VAMP (vesicle associated membrane protein), which is attached to the vesicle (v-SNARE), and the target-SNAREs syntaxin1 and SNAP-25 (synaptosomal-associated protein 25) which are located on the plasma membrane (Burgoyne and Morgan, 2003). It has been demonstrated that these SNARE

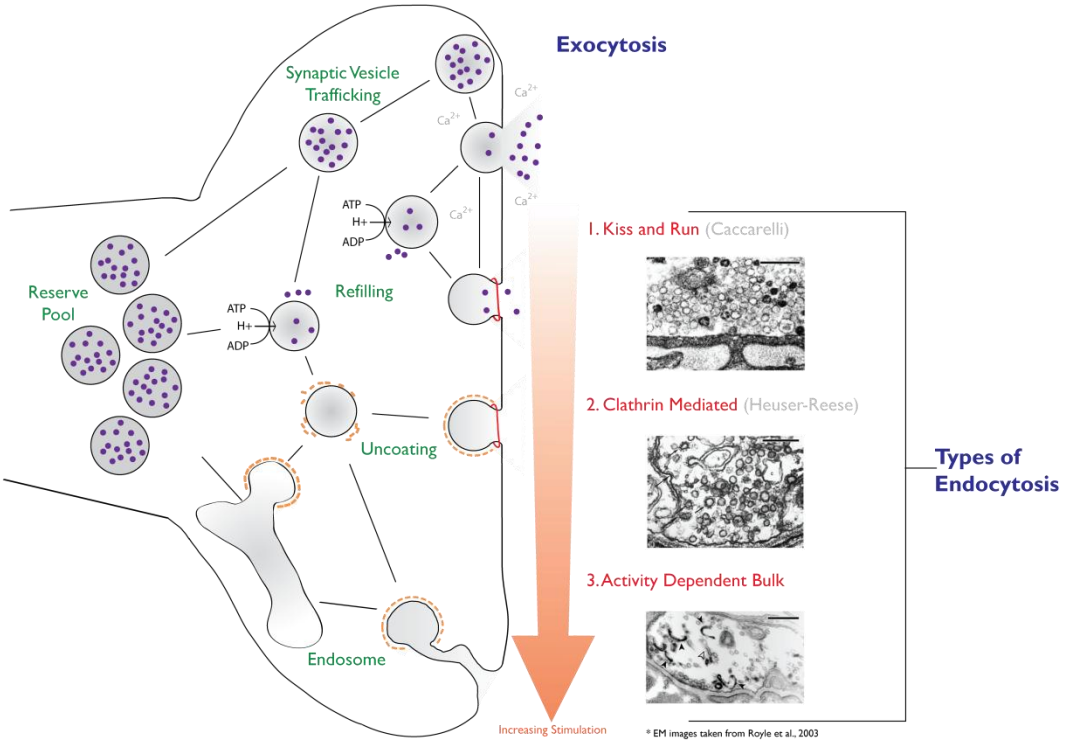

Figure 1-1 Schematic of the Synaptic Vesicle Lifecycle

Neurotransmitter is packaged inside vesicles of membrane called synaptic vesicles. They are stored in the nerve terminal in pools or clusters of vesicles and are trafficked to the plasma membrane, where they are docked. Following Ca^{2+} influx, the vesicle fuses into the plasma membrane, a process that is mediated by a complex of proteins called the SNARE complex, and this causes the release of the neurotransmitter. This fusion event is termed exocytosis. Following exocytosis the synaptic vesicle membrane and proteins are then retrieved from the plasma membrane, this is called endocytosis. At present there are 3 main types defined; Kiss and Run, Clathrin mediated and activity dependent bulk endocytosis. **1)** Kiss and run is a rapid form of endocytosis, the vesicle creates a transient fusion pore instead of fully fusing with the plasma membrane, and as a result is thought to be very rapid. **2)** Clathrin mediated endocytosis requires that a clathrin coat is surrounds the invaginating vesicle membrane. As there are many proteins involved in the coating and uncoating process, it is a slower form of endocytosis. **3)** Activity dependent bulk endocytosis is only thought to occur under periods of high stimulation. A large section of the membrane is invaginated and from this vesicles can form, potentially via a clathrin mediated budding process. Once the vesicles are formed from the plasma membrane, they are refilled with neurotransmitter, and therefore are able to be released in following rounds of exocytosis.

proteins are the substrates for the neurotoxins botulinum and tetanus toxins, and application of these toxins prevents NT release from the pre-synaptic nerve terminals (Blasi et al., 1993a, Blasi et al., 1993b, Schiavo et al., 1992). Further proof that the SNARE proteins are fundamental to SV exocytosis was provided by SNARE gene knockout studies in *Caenorhabditis elegans, Saccharomyces cerevisiae, Drosophila melanogaster* and mice, where stimulated content release was abolished (Nonet et al., 1998, Schoch et al., 2001, Schulze et al., 1995, Washbourne et al., 2002).

The complex has been described as a molecular zipper (Rizo and Sudhof, 2002), as it was proposed to function by each of the SNARE proteins contributing an α-helix, except SNAP-25 which contributes 2 (Sutton et al., 1998), which then coil together and force the SV and plasma membrane together resulting in fusion and NT release (Hanson et al., 1997, Rizo and Sudhof, 2002) (figure 1.1). This complex is very stable and requires energy provided by the ATPase NSF, to dissociate the complex, which requires the adaptor protein α-SNAP (soluble NSF attachment protein) (Mayer et al., 1996, Sollner et al., 1993).

The formation of the SNARE complex relies on chaperone proteins. For example, munc-18 (a mammalian homologue of the *Drosophila melanogaster* protein uncoordinated 18) interacts with syntaxin and regulates its trafficking to the plasma membrane (Medine et al., 2007), and how syntaxin enters the SNARE complex. There are three different reported modes of interactions between munc-18 and syntaxin which are spatially distinct. Munc-18 can interact with; a closed form of

syntaxin, which occurs primarily on intracellular membranes, the N-terminal of syntaxin is called mode 2 and mode 3 based on the idea that syntaxin is alone or in the SNARE complex (Dulubova et al., 1999, Rickman et al., 2007). It has been shown biochemically that SNAP25 is chaperoned by cysteine-string protein-α (CSPα) (Sharma et al., 2011). The physiological effects of this interaction are highlighted by CSPα knockout studies in *Drosophila melanogaster* and mice, as they display pre-synaptic dysfunction (Fernandez-Chacon et al., 2004, Umbach et al., 1994). It has been suggested that synaptophysin (Syp) (a integral SV membrane protein) might be the chaperone for VAMP and may even regulate its entry into the SNARE complex (Becher et al., 1999, Bonanomi et al., 2007, Calakos and Scheller, 1994, Edelmann et al., 1995, Pennuto et al., 2003).

Synaptotagmin is a transmembrane protein that contains multiple domains, most notably it has a cytoplasmic region which contains two C2 domains (C2A and C2B) (Perin et al., 1991, Rizo and Rosenmund, 2008, Sudhof, 2002). There are 17 isoforms where synaptotagmin 1 or 2 are expressed in most neurons along with synaptotagmin 3 (Ullrich et al., 1994, Dean et al., 2012). Synaptotagmin has been reported to be a fundamental protein in exocytosis, as it is proposed to be the Ca^{2+} sensor that couples Ca^{2+} influx caused by the action potential propagation to SV fusion (Martens et al., 2007). This hypothesis is based on the fact that synaptotagmin shares a direct interaction with syntaxin and phopholipids (Bennett et al., 1992, Martens et al., 2007) which is mediated by the C2 domain of synaptotagmin. The interaction between synaptotagmin and phospholipds is mediated by basic residues in the C2A and C2B domains and it is thought to be the

key interaction in coupling Ca^{2+} influx with SV fusion (Martens et al., 2007). The interaction of synaptotagmin and syntaxin is dependent on the C2A domain binding three Ca^{2+} ions (Ubach et al., 1998). The C2B domain has been shown to be important for, and sufficient for spontaneous, binding of synaptotagmin to membranes, which brings them in close proximity of each other in a Ca^{2+} dependent manner (Arac et al., 2006). It has also been shown, in PC12 cells, that the Ca^{2+} dependent manner in which synaptotagmin binds to the syntaxin in the SNARE complex and inserts itself in to the membrane is important in the expansion of the fusion pore (Lynch et al., 2008). Further evidence of the importance of synaptotagmin in exocytosis is provided by synaptotagmin knockout mice which displayed defects in Ca^{2+} induced neurotransmission, which suggests a defect in a stage of exocytosis (Geppert et al., 1994).

1.3 - Endocytosis

At the pre-synaptic nerve terminals, there is a limited supply of SVs, as few as two hundred or less (Dittman and Ryan, 2009). Therefore, following exocytosis, in order to maintain a supply of SVs for subsequent rounds of exocytosis during a prolonged stimulation, it is important that the SVs are continuously recycled and re-filled (Figure 1.1). This process of recycling is endocytosis, and SV endocytosis was first observed in the frog neuromuscular junction by the use of electron microscopy and horse-radish peroxidase in 1973 (Heuser and Reese, 1973). The type of endocytosis that was detected by Heuser and Reese was clathrin-mediated and a kinetic examination revealed that this process was slow; first characterised as 1 minute for total completion of endocytosis (Miller and Heuser, 1984) and more recently, due

to advancements in imaging techniques, it has been defined as a τ value of 13 seconds for a single SV (Balaji and Ryan, 2007). As this time scale does not seem to fit with the idea of rapid neuronal communication, it was hypothesised that a faster form of endocytosis must also exist. In 1973, Ceccarelli *et al.* proposed a rapid form of endocytosis, where vesicles only partially fuse with the plasma membrane and can rapidly be fissioned away (Ceccarelli et al., 1973). This was later dubbed 'kiss-and-run' (Fesce et al., 1994). More recently, a third type of endocytosis has been proposed, entitled 'activity dependent bulk endocytosis' (Clayton et al., 2008, Royle and Lagnado, 2003), which refined early observations of large invaginations in the frog neuromuscular junction (Miller and Heuser, 1984). During periods of high stimulation, there is a high volume of exocytosis, which greatly increases the surface of the cell membrane. As a result, large invaginations of the plasma membrane are retrieved and SVs can subsequently bud from this (figure 1.1).

1.3.1 - Rapid Endocytosis (Kiss-and-Run)

There is still a lot of active debate as to whether the rapid form of endocytosis, 'kiss-and-run', is real and functions physiologically in an active neuron. The biggest reason for this is in the very nature of the process, it is too rapid to allow characterisation of the potential mechanism; with some reporting that it occurs in less than 1 second (Beutner et al., 2001, Neves et al., 2001). Further to this, many of the studies attempting to characterise this rapid endocytosis have been conducted in neuroendocrine cells using techniques that are unsuitable for most forms of neuronal analysis (for example, capacitance recordings and amperometry).

Therefore, neuronal studies have had to rely on indirect fluorescent imaging methods which are often subjective.

Capacitance and amperometry recordings of chromaffin cells, and the Calyx of Held, provide the strongest direct evidence of a transient fusion pore that would represent kiss-and-run. In such studies, it was reported that between 10-17% of single vesicle fusion events were transient in their nature (Albillos et al., 1997, He et al., 2006). However, technical difficulties make interpretation of these results somewhat difficult; for example, SV turnover had to be elicited by non-physiological stimuli, and also the recording electrode might not be located at sites of SV recycling.

Imaging of neurons in conjunction with labelling with lipophilic FM dyes has also failed to provide a definitive answer to the kiss-and-run debate, providing evidence for (Aravanis et al., 2003, Harata et al., 2006, Klingauf et al., 1998, Pyle et al., 2000, Richards et al., 2005) and against (Fernández-Alfonso et al., 2006, Ryan et al., 1996, Zenisek et al., 2002). These studies exploit the fact that FM dyes only fluoresce when inserted into membrane and the idea that they might be able to differentially label full fusion vesicle and kiss-and-run vesicle membrane. This differential labelling was achieved by using three different FM dyes, which differ in their length of the nonpolar hydrocarbon chain (which is the domain of the compound that inserts into the membrane), FM1-43, FM1-84 and FM2-10. The different side chains affect how 'sticky' the dyes are; FM2-10 has the shortest side chain so would dissociate from the membrane faster than FM1-43 and FM1-84, FM1-84 has a

longer side chain so dissociates slower then FM2-10 and FM1-43. Therefore FM1-84 might be able to 'escape' being released in a full fusion event (Ryan et al., 1996). However, after advancement of the technique, manly by removing high levels of background staining by the FM dyes, it was shown in 2008 that following action potential stimulation of neurons there was complete destain of the neuron (Chen et al., 2008). This suggests that either kiss-and-run did not occur, or that FM dyes are not able to detect these transient fusion events.

The advent of quantum dots, which are a very photo-stable nano-particles, with a diameter of 15 nm (Larson et al., 2003)) allowed researchers to examine the ratio of full fusion events with transient fusion events, since the large size of the quantum dot excludes it from entering a transient fusion pore, and thus being released only when a SV completes full fusion. Combined with FM dye labelling, it was found that the quantum dot unloading was slower than FM dyes, thereby highlighting that there are two pathways (Zhang et al., 2007). Further work took advantage of the fact the quantum dots' fluorescence was pH-sensitive, where it was shown with bafilomycin A1 that the quantum dots were able to label two different endocytosis pathways (Zhang et al., 2009). However, skeptics say that this slower unloading of the quantum dots was due to its large size relative to the SV; potentially stabilising the vesicle during fusion (Dittman and Ryan, 2009).

It is clear that, even though there is debate in the SV field about its role in neuronal SV recycling, that there must be a more rapid form of endocytosis that is clathrin

independent to balance endocytosis with the rapid rate of exocytosis, or neurons would fail to continue to communicate during periods of high stimulation.

Identification of the major proteins involved in this rapid form of endocytosis would help greatly in providing a definitive answer to the 'kiss-and-run' debate. It is worth highlighting that VAMP has been reported to be essential for a fast form of synaptic vesicle endocytosis (Deak et al., 2004). This combined with its role in exocytosis, allows the hypothesis that VAMP could be a key protein in kiss-and-run; potentially providing a starting block for unraveling the molecular machinery that is involved in rapid 'kiss-and-run' endocytosis.

1.3.2 - Clathrin Mediated Endocytosis

Clathrin mediated endocytosis is the most characterised type of endocytosis and the main reason for this is that it is slower than kiss and run. This has allowed many of the molecular components to be identified and their roles characterised. The molecular players have been examined since discovery of clathrin mediated endocytosis in 1973 (Heuser and Reese, 1973). It has been reported to be the dominant form of endocytosis in the neuron at mild stimulations; where endocytosis was monitored using the genetic reporter superecliptic synaptophysin phluorin (SypHy) in hippocampal neurons subjected to stimulation of 20 Hz for 2 seconds with either clathrin knocked down using RNAi or overexpression of AP180 (Granseth et al., 2006).

Superecliptic synaptophysin phluorins are pH-sensitive fluorescent genetic reporter of local pH environments which allow direct monitoring of pre-synaptic activity

(Sankaranarayanan et al., 2000). The pH-sensitive fluorophore is expressed inside the SV lumen, where the pH is ~5.5; at this acidic pH the fluorophore is quenched. When the SV undergoes exocytosis the pH that the fluorophore is exposed to is ~7.4, and at this pH the fluorophore is able to fluoresce, thereby creating an increase in fluorescent signal. As endocytosis occurs, the fluorophore is removed from the cell surface resulting in a decay of the fluorescence signal. However, it is worth noting that this decay is also produced by SV re-acidification (for further details refer to section 2.5.2 and figure 2.3).

It has been demonstrated that this type of endocytosis occurs on the periphery of the active zones (Gad et al., 2000, Roos and Kelly, 1999). Clathrin Mediated Endocytosis can be broken down into sequential stages of, activation, nucleation, invagination, fission and uncoating (figure 1.2).

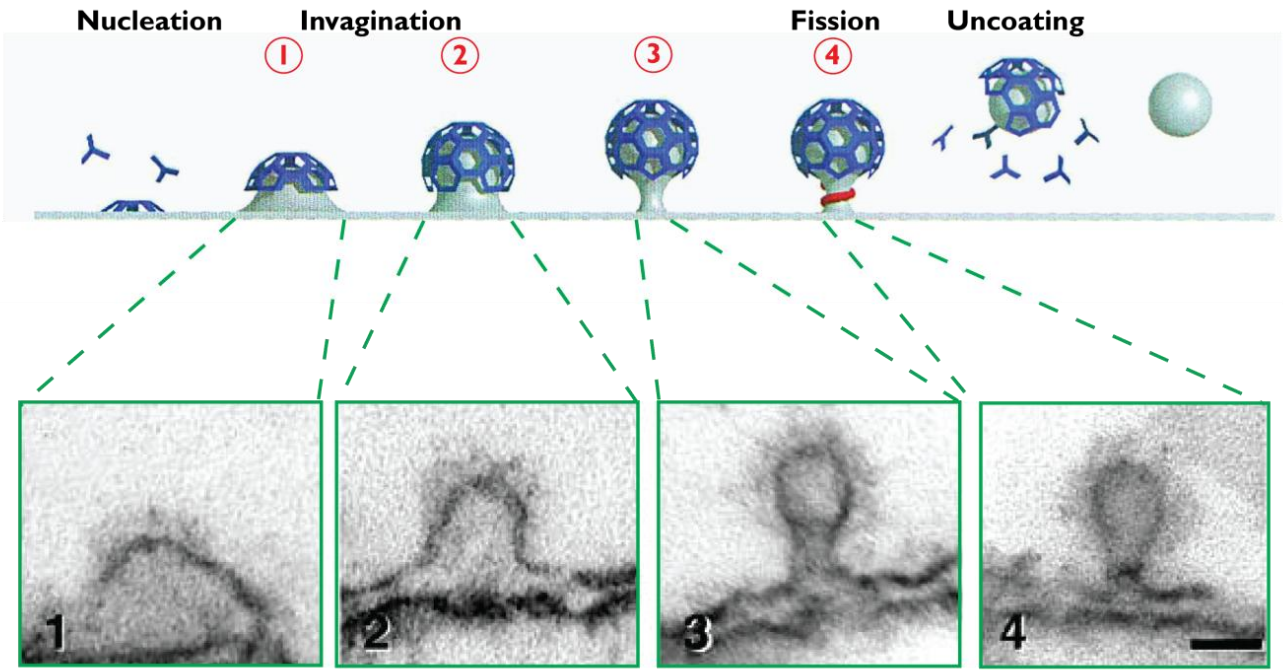

Figure 1-2 Schematic of Clathrin Mediated Endocytosis

The process of clathrin mediated endocytosis can be broken down into different steps, which are all regulated by a different set of proteins. Once the process is activated the invagination begins. (1) Nucleation is the starting point of the formation of the clathrin coat (blue). 2-3) The vesicle then begins to start to further invaginate, a process driven by proteins which help induce curvature of the membrane. 4) Once the vesicle is ready to be fissioned away from the plasma membrane, amphiphysin recruits the GTPase dynamin (red ring) to the neck of the budding vesicle where its activity fissions the vesicle from the plasma membrane. Once the vesicle is freed from the plasma membrane, the clathrin coat is removed, and the vesicle is then re-filled and able to re-enter in to the SV lifecycle. (Adapted from Gad *et al*., 2000).

1.3.2.1 - Nucleation of Clathrin Mediated Endocytosis

A key protein complex in the nucleation stage of clathrin mediated endocytosis is adaptor protein 2 (AP2). It binds to the vesicle proteins which are in the plasma membrane, and this interaction is thought to be mediated by the C2B domain of synaptotagmin (Jorgensen et al., 1995). Once AP2 is bound to synaptotagmin, it is able to bind to other endocytoic proteins that contain specific tyrosine motifs (Yxxϕ, where ϕ is a large hydrophobic residue) (Haucke and De Camilli, 1999). Such proteins include Syp, SCAMPs and SV2a (Haucke and De Camilli, 1999). It has been shown that the disruption of the interaction between AP2 and synaptotagmin results in blockage of receptor mediated endocytosis (Haucke et al., 2000), which uses the same molecular pathway as clathrin mediated endocytosis.

The AP2 protein is a tetramer made up of 4 different subunits, α, β2, μ2 and σ2 (Schroder and Ungewickell, 1991, Robinson, 1997). The α and μ subunits are responsible for anchoring AP2s with the plasma membrane by directly binding with the membrane lipid PI(4,5)P2 (Gaidarov and Keen, 1999). Once anchored to the membrane the hinge domain of the β2 subunit can then recruit clathrin and AP180 (Hao et al., 1999, Shih et al., 1995), which begins the process of nucleation.

Besides its role in the assembly of the clathrin coat structure, AP2 is also important in the selection of cargo proteins into the coated pits. There are several typical sequences which are AP2 cargo recognition motifs; tyrosine based, di-leucine, acidic clusters, dilysine, ubiquitin addition and a reported synaptic vesicle targeting sequence ((Collins et al., 2002, Kelly et al., 2008) and reviewed in (Kirchhausen et

al., 1997)). However, further reports are casting doubt as to whether many of these motifs are physiological and function in an *in vivo* situation. For example, the dilysine motif has been reported to bind directly to the heavy chain of clathrin and not to AP2 (Kibbey et al., 1998). The di-leucine motif was reported, by *in vitro* biochemical assays, to interact directly with the μ subunit of AP2 (Bremnes et al., 1998), but there are contradictory reports that suggest that this motif binds indirectly to AP2 via other proteins, such as β-actin and Nef (Hua and Cullen, 1997, Piguet et al., 1998, Rapoport et al., 1998). The Yxxσ motif interaction with the μ2 subunit of AP2 has been shown to be important in the nucleation of clathrin coated pits (Haucke and De Camilli, 1999, Haucke et al., 2000), but how this interaction mediates that effect is unclear as different reports detail differences in the cargo that binds. Mutations were made in the Yxxσ motif, that bound the epidermal growth factor (EGF) receptor to AP2 and no significant effects were seen of the internalisation of the receptor (Nesterov et al., 1995, Sorkin et al., 1996). Recent work has shown the importance of AP2 in endocytosis, a knockdown of AP2 significantly slowed endocytosis (Kim and Ryan, 2009). However, in this report it was found the knockdown did not prevent the retrieval of vGlut, Syp, synaptotagmin and VAMP. Therefore, despite a well range of characterised cargo motifs for the μ subunit of AP2, further work is required to determine if they are functionally significant *in vivo*.

Clathrin is a triskelion, containing three heavy and three light chains, that is capable of forming a spherical basket structure without the requirement of any other proteins (Heuser, 1980, Kirchhausen and Harrison, 1981). Further to this, it has

been demonstrated that only the heavy chain is required for the coat formation, as removal of the light chain failed to abolish formation of normal clathrin coats (Schmid et al., 1982). Truncations of the C-terminal of the heavy chain revealed that it is important in forming normal and functional clathrin coated vesicles (Lemmon et al., 1991). As clathrin forms a defined stereotypical polyhedral cage, solved to 21 angstroms, where each triskelion of clathrin contributes two edges to the coat structure (Smith et al., 1998), clathrin is important in forming typical SVs of a similar size (Cheng et al., 2007). It has been shown that the adaptor proteins AP2 and AP180 interact directly with clathrin and promote the formation of vesicle coat (Hao et al., 1999).

1.3.2.2 - Invagination

Invagination relies on a set of proteins that help induce membrane curvature, as this is the step that sees the most dramatic change in shape (flat membrane to the round vesicle).

Epsin has been suggested to be a key protein in this process. Based on data showing that it was able to induce lipid tubulation (Ford et al., 2002). Further to this, it was shown that the N-terminus of epsin binds to $PI(4,5)P_2$ and this interaction results in a change of the shape of epsin (formation of the helix 0, which inserts into the membrane), suggesting that epsin penetrates to the membrane lipid and then induces curvature of the vesicle membrane (Ford et al., 2002).

Endophilin has also been shown to induce lipid tubulation, and this process was regulated by its N-terminal of BAR domain (Farsad et al., 2001). It is suggested that

a pair of helices, located on the BAR domain, insert into the plasma membrane to help promote membrane curvature (Masuda et al., 2006). *In vivo* interference studies, micro injections of antibodies in the lamprey, showed that without endophilin function, endocytosis appeared to be arrested at the invagination stage, as there was a large number of clathrin coated pits (Ringstad et al., 1999). Further evidence of a role for endophilin in invagination is provided by a study which disrupted the SH3 mediated interaction of endophilin; the SH3 domain of endophilin is known to interact with dynamin and synaptojanin. It was found that there was an increase of clathrin coated pits (Gad et al., 2000), suggesting that endocytosis is arrested at the invagination and uncoating stages.

1.3.2.3 - Fission of Clathrin Coated vesicles

The fission of vesicles away from the plasma membrane during clathrin mediated endocytosis is mainly conducted by the GTPase Dynamin 1, and it is recruited to the budding vesicle neck by amphiphysin.

1.3.2.3.1 - Dynamin 1

The role of dynamin 1 in endocytosis was first highlighted in a temperature sensitive *Drosophila melanogaster* mutant, *shibire* (Koenig and Ikeda, 1989). This mutant fly has a mutation in the GTPase domain of dynamin 1 which was temperature sensitive. At the restrictive temperature of 29°C the GTPase domain of dynamin 1 could not function. After 8 minutes exposure to 29°C during stimulation, it was found that there was a complete depletion of SVs in the nerve terminals, with many dynamin rings found around invaginations of SVs. To really show that the activity of

dynamin 1 is important in endocytosis, flies exposed to restrictive temperature were 'rescued' by a 2 minute exposure to the permissive temperature at 19°C (van der Bliek and Meyerowitz, 1991) which showed that dynamin 1 was essential for SV endocytosis and suggested that it was the GTPase activity that regulated the fission events.

In 1998, it was shown that it was indeed the GTPase activity which was ultimately responsible for fissioning the vesicles away from membrane (Sweitzer and Hinshaw, 1998). However, the exact mechanism of this process is still subject to debate. Three main ideas have arisen. First, it has been hypothesised that dynamin 1 acts as a 'pinchase', based on the evidence that GTP application to dynamin and microtubules resulted in a decrease in tube diameter and production of SVs (Sweitzer and Hinshaw, 1998). Secondly, dynamin 1 may be a 'poppase' based on the fact that GTP application resulted in dynamin 1 rings around nanotubules to increase their pitch (e.g. stretching the tube to breaking point) (Stowell et al., 1999). Thirdly, imaging of GTP application to dynamin 1 and lipid tubules tagged with mirco-beads revealed that dynamin 1 actually twists the lipid tubes, increasing the tension until the tube breaks off (Roux et al., 2006), therefore acting as a 'twistase'.

Knockout studies of mice where the dynamin 1 gene was ablated showed that the mice are able to form functional synapses, however they were not viable postnatally (Ferguson et al., 2007). One of the reasons that the knockout failed to show a total failure of synapses is that dynamin has 3 isoforms, encoded by different genes and various splice variants. Dynamin 1 and 3 are expressed

neuronally, whereas dynamin 2 is ubiquitously expressed (Cao et al., 1998, Ferguson et al., 2007, Gray et al., 2003). Dynamin 2 is reported to be important in fission events in micropinocyosis (Cao et al., 2007), so it is easy to imagine that there is compensation for the loss of dynamin 1 by dynamin 2, and potentially dynamin 3; however little is known about the function of dynamin 3. This idea of compensation is supported by a recent paper using a double knockout of dynamin 1 and dynamin 3, where they were found to have overlapping roles (Raimondi et al., 2011).

1.3.2.3.2 Amphiphysin

The role of amphiphysin is to recruit dynamin to the neck of the budding vesicle, and it is proposed to do this using specific protein domains present in both the amphiphysin isoforms (amphiphysin 1 and 2). It has a BAR (bin/amphiphysin/Rvs) domain on its N-terminus, which has been shown to bind to curved membranes like that of an invaginated vesicle (Peter et al., 2004). The CLAP domain is known to bind to clathrin and AP2 (David et al., 1996, Evergren et al., 2004), and the C-terminal Src homology (SH3) domain is thought to bind to the proline rich domain of dynamin (David et al., 1996). This then suggests that amphiphysin recruits dynamin by interacting with it via its SH3 domain, and this complex is then recruited to the invagination site via an interaction mediated by the CLAP domain. Finally, the amphiphysin may locate dynamin to the neck of the invagination based on the membrane curvature sensing ability of the BAR domain.

Amphiphysin 1 knockout mice have cemented this critical role of amphiphysin in SV recycling. The knockout mice showed major learning defects, and a high frequency

of irreversible tonic seizures resulting in death of the subject (Di Paolo et al., 2002). This was shown to be caused by a block of endocytosis, determined by use of electron microscopy with horseradish peroxidase to label newly formed SVs. During high stimulation (like seizures) with rapid exocytosis, if there is defective endocytosis, the SVs would not be recycled, therefore leaving the nerve terminal unable to function during neuronal transmission. Further evidence is provided by studies in the large lamprey reticulospinal synapse, it was subjected to microinjection of the SH3 domain of amphiphysin 1 to disrupt the amphiphysin and dynamin interaction, it was found that SV recycling was arrested at the invagination stage (Shupliakov et al., 1997). This suggests that no SVs were able to fission from the plasma membrane because there was no dynamin acting on their budding necks.

1.3.2.3 - Uncoating and Re-filling of Synaptic vesicles

Once the vesicle is fissioned away from the plasma membrane, the clathrin coat needs to be removed so the SV can be re-filled with NT. There are at least three proteins charged with this role; synaptojanin, auxilin and a heat shock protein of 70 kDa (Hsc70). Synaptojanin has been shown to be essential in this process in both cultured cortical neurons and the large lamprey reticulospinal synapse by means of electrophysiological recordings of brain slices and ultra-structural analysis (Cremona et al., 1999, Gad et al., 2000). It is thought that it is recruited to the vesicle via its proline rich domain interacting with the SH3 domain of endophilin (Milosevic et al., 2011). Work in the giant squid axon, where competitive binding peptides were injected in to the axon, demonstrated that both auxlin and Hsc70

were also both essential for removing the clathrin coat once the vesicle is internalised (Morgan et al., 2001).

Once the vesicle is uncoated, it is refilled with NT. This process is conducted by NT transport proteins which make use of a proton-motive force, generated by V-type ATPases present on the SV (Naito and Ueda, 1985).

1.3.3 - Activity Dependent Bulk Endocytosis

Bulk endocytosis is termed bulk as it invaginates more membrane that is required for a single vesicle, creating bulk endosomes and from this, vesicles can form inside the nerve terminal. Physiologically, it does not make much sense to greatly reduce the surface area of the nerve terminal in response to anything less than high stimulation (where there would be little fusion of vesicles to the membrane), so the bulk invaginations only occur in response to high levels of stimulation which results in a large increase of the nerve terminal surface area. There has been some debate as to whether the elevated stimulation required to elicit such a response is within the physiological threshold.

The first reports of bulk endocytosis were from studies of the frog neuromuscular junction (Miller and Heuser, 1984), however the simulation used to induce endocytosis was not physiological. Further work in this system showed that bulk invaginations could occur in response to tetanic action potential stimulations (Richards et al., 2005, Richards et al., 2003). However, evidence that bulk invaginations occur within the physiological scale was provided by work in the snake motor boutons, where a bulk response was observed in response to a relatively

mild stimulation (5 Hz for 30 seconds) (Teng and Wilkinson, 2000). It has also been shown that bulk endocytosis can occur in central nerve terminals in response to physiological stimulation; using retinal bipolar neurons stimulated by Ca^{2+} (Paillart et al., 2003), Calyx of Held stimulated by 1 second of 10 Hz of stimulation (Wu and Wu, 2007) and in cultured cerebellar granule neurons trains of action potential (40 Hz for 10 seconds) induced bulk invaginations (Clayton et al., 2008). Therefore, the stimulation required to initiate bulk endocytosis is within the physiological threshold, albeit at the higher end of the scale. The implication of this is that bulk endocytosis could be a potential target for seizures in condition where there is up regulation of inappropriate neuronal activity, such as epilepsy.

The mechanism relies on dynamin acting to fission the bulk invagination away from the plasma membrane. It is recruited to the neck of the invagination by a stimulation and phosphorylation dependent interaction with syndapin (Anggono et al., 2006, Clayton et al., 2009).

1.3.3.1 - Syndapin

Syndapin has an SH3 domain, which means it is capable of interacting with many proteins that contain a proline rich domain. One of these SH3 mediated interactions is one that it shares with dynamin (Anggono et al., 2006). However, for this interaction to occur, dynamin must be dephosphorylated by calcineurin (Clayton et al., 2009). This dephosphorylation is also stimulation dependent as dynamin is only dephosphorylated during high stimulation (Clayton et al., 2009).

Another key domain of syndapin is its F-BAR domain, and this differs in the sensitivity of the curvature of membranes that it can detect in relation to the N-BAR domain of amphiphysin (Henne et al., 2007). This suggests that syndapin and amphiphysin could be targeting different types of invaginations due to their differences in sensitivity to membrane curvatures; N-BAR domains sense sharp convex curvatures of about 30° and F-BAR domains prefer angles of about 10° (as reviewed in (Qualmann et al., 2011)).

This allows the hypothesis that under periods of high activity, dynamin is dephosphorylated, and this selectivity mediates the interactions with syndapin and not amphyphysin (Anggono et al., 2006). And it is this interaction with syndapin that then recruits dynamin to the neck of the bulk invagination, due to the sensitivity of the F-BAR domain of syndapin.

Evidence to support this is provided by the syndapin knockout mouse, where the knockout mice suffer a high frequency of seizures and there is a high level of accumulations of endocytic intermediates (Koch et al., 2011). This suggests that syndapin is an important protein in maintaining the SV recycling pathway under high stimulation. This supports the idea that syndapin is involved in activity dependent bulk endocytosis as at high stimulation, like seizures, there will be high levels of exocytosis and clathrin mediated endocytosis would not be efficient enough to meet the demands of SV recycling, therefore bulk invaginations occur. Under high stimulation dynamin is dephosphorylated and can therefore bind to syndapin, and recruit it to bulk invaginations, based on the sensitivity of the F-BAR

domain of syndapin. So if syndapin is absent, then dynamin would not be recruited to the invaginations and therefore arrest bulk endocytosis creating endocytosis intermediates.

1.4 - Synaptophysin

Syp is the most expressed protein found on the SV, making up 10.2% of the overall protein content of a typical SV, which amounts to 31.5 copies per SV (Takamori et al., 2006). As Syp is such an abundant protein, it was no surprise that it was the first integral SV membrane protein to be isolated (Jahn et al., 1985, Wiedenmann and Franke, 1985) and subsequently cloned (Buckley et al., 1987, Leube et al., 1987, Sudhof et al., 1987). However, since its discovery in 1985, very little progress has been made into defining a clear physiological role for Syp. To highlight this fact, its main function in the current literature is as a synaptic marker, where it has been used as a synaptic marker in nearly 3000 published studies (Valtorta et al., 2004), which greatly outnumbers the papers published to address the functional significance of Syp. The main reason why there has been no clear physiological role characterised and defined for Syp is that Syp knock out studies have failed to produce an obvious phenotype.

The first papers to try and address the function of Syp were conducted before genetic knockout mice were readily available, therefore they had to use other systems to try and determine the physiological role of Syp. Micro-injection of Syp antibodies into early blastomeres of *Xenopus* embryos followed by electrophysiological whole cell recordings showed that there was a reduction in

both the spontaneous and evoked neurotransmission events (Alder et al., 1992) suggesting that Syp is involved in a stage of exocytosis. Further to this, it was shown that injection of Syp mRNA into the *Xenopus* embryo, causing an overexpression of Syp, resulted in an increase in NT release frequency (Alder et al., 1995), further suggesting a role for Syp in facilitating exocytosis.

1.4.1 - Synaptophysin Knockout Studies

The first examinations of Syp knockout mice failed to offer a great insight to any potential function of Syp, and failed to reproduce the exocytosis effects seen in the *Xenopus* system used by Alder *et al,* (Alder et al., 1995, Alder et al., 1992). It was reported that the Syp knockout mice were viable, fertile and even formed typical SVs (Eshkind and Leube, 1995).

1.4.3.1.1 - Evidence for a Role of Synaptophysin in Exocytosis Provided by Synaptophysin Knockout Mice

Further work showed that the Syp deficient mice displayed no major morphological changes in their brain structure, and electrophysiological methods showed that there was no difference in evoked and spontaneous release of NT (McMahon et al., 1996). One of the reasons that the Syp knockout mice failed to produce an obvious phenotype might be due to compensation provided by isoforms of Syp. It was found that it has two neuronal homologues in the form of Syp II (synaptoporin) (Knaus et al., 1990) and synaptogyrin (Stenius et al., 1995). Further to this, non-neuronal homologues were identified as pantophysin (Haass et al., 1996), mitsugumin29 (Takeshima et al., 1998) and SCAMPs (secretory membrane proteins)

(Singleton et al., 1997). However, examination of the mRNA levels of Syp II and pantophysin showed that there was no 'drastic' up regulation of isoforms of Syp in the Syp knockout mouse (Eshkind and Leube, 1995). This suggests that there may not be much compensation afforded to the Syp knockout mouse from the isoforms of Syp. To rule out the potential compensation of the Syp homologues and thus determine a physiological role for Syp, a double knock out mouse was made. Both the genes that encoded Syp and synaptogyrin was ablated and the resulting mouse was subjected to electrophysiological examination of the hippocampal CA1 region (Janz et al., 1999). One of the outcomes of this paper was that it confirmed that finding by McMahon (McMahon et al., 1996); that Syp did not appear to be essential for NT release. These two results suggest that the role of Syp was unlikely to be in exocytosis.

1.4.1.2 - Evidence for a Role of Synaptophysin in Long-Term Potentiation Provided by Synaptophysin Knockout Mice

Long term potentiation (LTP) is where a tetanic stimulation can alter the properties of a synapse to make it more efficient (Bliss and Lomo, 1970), and is thought to be the molecular mechanism that underpins learning and memory (Morris et al., 1986). As LTP relies on a tetanic stimulation, it therefore also relies on lots of NT being released in response to high stimulation. As NT is released from SVs, it therefore also relies on efficient SV recycling. Therefore, if defective LTP is observed in Syp knockout mice then it might be indicative that Syp indeed has a role in regulating recycling of SVs.

Use of the Syp and synaptogyrin double knockout mouse found that both short- and long-term potentiation were 'severely reduced' in the double knockout mice when compared to wild type (WT) mice (Janz et al., 1999). However, this severe reduction failed to present itself on a morphological level as hippocampal regions were reported to be normal. It was only with the advancement of experimental approaches that the subtle changes in the learning and memory of Syp deficient mice were proven. The behavioural differences found in Syp knockout mouse were highlighted by a decrease in novel object recognition and an increased in learning time in spatial memory tasks (Schmitt et al., 2009).

Therefore, Syp has been shown to be important in regulation of learning and memory (Schmitt et al., 2009), and this is determined by LTP. As it has been shown that Syp does not alter the release of NT (Janz et al., 1999, McMahon et al., 1996), it is possible that Syp is regulating synaptic strength during LTP inducing stimulations. A possible mechanism for how Syp achieves this could be by limiting the availability of SVs, and a potential site of action for Syp to be able to regulate this could be endocytosis; where a slower endocytosis would result in fewer SVs available for release in subsequent rounds of exocytosis.

1.4.1.3 - Evidence for a role of Synaptophysin in Endocytosis Provided by Synaptophysin Knockout Mice

It is important to consider that at the time of publication of many of the Syp knockout studies, there were very few techniques available to directly investigate endocytosis in neurons. However, there is plenty of evidence that endocytosis is

indeed affected in the Syp knockout mice. For example, when rod photoreceptor cells from Syp knockout mice were subjected to high levels of activity, they were found, from ultra-structural analysis, to have a decreased number of SVs and significant plasma membrane deformations (Spiwoks-Becker et al., 2001). The reason rod photorececptor cells were used was because in WTs they express high levels of Syp, but do not express Syp II in the WT or knockout situation. These observations in the rod photorececptor cells are indicative of defects in endocytosis. A further observation in this paper states that in WT cells, there was an activity-dependent decrease in the SV diameter, and this was not found in the knockouts (Spiwoks-Becker et al., 2001). This observation suggests that there are two different types of endocytosis occurring, Syp-dependent and -independent types. Due to the overall decrease in the SV number found in the Syp knockout cells, it is likely that the Syp-independent pathway of endocytosis is less efficient. Or it works perfectly well but cannot compensate for the Syp-dependent mode of endocytosis.

Further evidence that Syp is important in regulating a rapid form of endocytosis is provided, although not in Syp knockout, by a study where the C-terminal of Syp, which was tagged with a glutathione S-transferase (GST) tag, was injected into the squid giant synapse (Daly et al., 2000). The injection resulted in a decrease of SV availability and an increase of clathrin coated SVs inside the cell, interpretation of these results by the authors suggest that Syp regulates a clathrin independent form of endocytosis and does not affect clathrin mediated endocytosis (Daly et al., 2000).

A recent paper, which was published in the last year, applied modern imaging techniques to Syp knockout neurons, which are able to directly examine endocytosis, have complemented the hypothesis in earlier Syp knockout papers that Syp appears to be regulating a rapid form of endocytosis during high stimulation. Using superecliptic synaptophluorins of synaptotagmin and SV2A, combined with electrophysiology, it was shown that Syp was required for kinetically efficient SV retrieval during sustained stimulation (Kwon and Chapman, 2011). Further to this, truncations of Syp protein used to rescue the knockout revealed that it was this section of the C-terminus of Syp that appeared to be regulating endocytosis during, but not after, sustained synaptic transmission (Kwon and Chapman, 2011).

1.4.2 - Synaptophysin Structure

In 1987 hydrophobicity plots of the amino acid sequence of rat Syp revealed that Syp contained 4 transmembrane domains (Sudhof et al., 1987), where the NH_2 and COOH termini were located on the cytosolic side of the SV (figure 1.3). The structure predicted by these hydrophobicity plots was confirmed by use of several antibodies targeted to different predicted regions of Syp (Johnston et al., 1989). This means that there are two inter-luminal domains, and present on these domains are two cysteines, with the potential to form disulphide bridges (Johnston and Sudhof, 1990), and an N-linked glycosylation site (Rehm et al., 1986). It is predicted that the disulphide bridges form within each of the domain, rather than with the different intra-luminal domains (Johnston and Sudhof, 1990). The functional

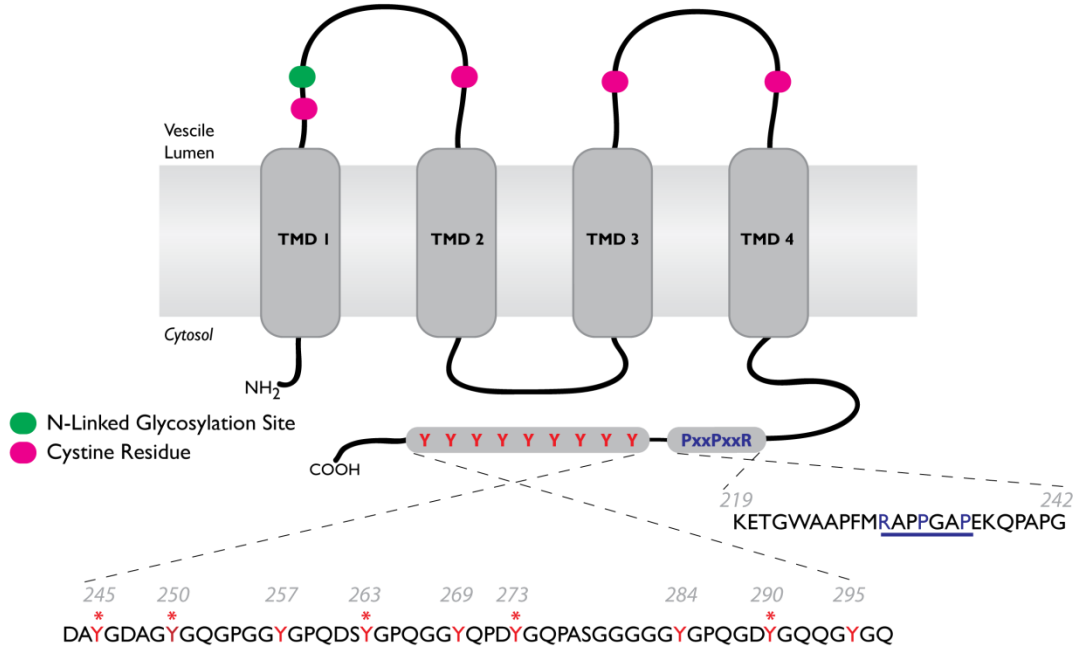

Figure 1-3 Schematic of Synaptophysin

Synaptophysin has four transmembrane domains (TMD), with cytosolic N- and C-termini. On its two intra-vesicular domains there are 4 cysteines, which can form di-sulphide bonds with one another, and an N-linked glycosylation site. On its C-terminal there are two interesting peptide motifs, one is a putative type one SH3 interaction motif and the other is a pentapeptide repeat. This pentapeptide repeat is a potential tyrosine phosphorylation motif and is repeated nine times. Although it is known that Syp is subjected to tyrosine phosphorylation, it is not known which of the tyrosine residues are phosphorylated. NetPhos (an online phosphorylation prediction database) has predicted that 5 of these sites are phosphorylated physiologically, and they are highlighted by an asterisk.

significance of both these disulphide bridges and the N-linked glycosylation is unknown.

1.4.2.1 - The Synaptophysin C-Terminal

The cytosolic C-terminal of Syp represents the potentially most interesting domain of Syp. The reason for this is that in 1990, Linstedt *el al* showed that the C-terminal of Syp was fundamental to the retrieval of Syp during endocytosis (Linstedt and Kelly, 1991). Therefore, this suggests that the C-terminal of Syp contained a motif that is critical to the trafficking of Syp during endocytosis. On the short 90 amino acid C-terminal, there are two different motifs which could potentially act as a regulator of its endocytosis and thus endocytosis of other synaptic proteins; we have identified a putative type one SH3 interaction motif (RxxPxxR) and there are ten pentapeptide repeats (YG(P/Q)QG) (Sudhof et al., 1987) (figure 1.3 and 1.4).

The SH3 interaction motif conforms perfectly with the putative type one SH3 interaction motif defined as two prolines are found in a sequence (which form two hydrophobic interactions with residues in the SH3 domain), separated by two amino acids, and an arginine (which forms a salt bridge with a key residues in the SH3 domain) is two amino acids upstream of the first proline (RxxPxxP) (Mayer and Eck, 1995, Weng et al., 1995, Cesareni et al., 2002). Specificity of SH3 domains to such SH3 interaction motifs are regulated by the flanking sequences of the SH3 ligand, as different flanking regions alter the access to the motif, therefore regulate specificity of the motif (Cesareni et al., 2002, Mayer and Eck, 1995, Weng et al., 1995).

Of the ten pentapeptide repeats, nine are initiated by a tyrosine residue and this makes Syp a target for tyrosine kinases. In agreement, biochemical kinase assays combined with immunoprecipitations showed it to be the major tyrosine-phosphorylation protein on the SV (Pang et al., 1988). These potential tyrosine sites are particularly interesting, as they have been recently proposed to be important in regulating the kinetics of endocytosis during sustained stimulation (Kwon and Chapman, 2011). Therefore, in order to start to understand the function of Syp during the SV lifecycle, one must understand how Syp can interact with SH3 domains and how tyrosine might affect these interactions.

1.4.3 - Interactions of Synaptophysin

One of the major reasons that there has been little advancement in defining a physiological role for the most expressed synaptic vesicle protein Syp, is that there has yet to be a definitive study to catalogue the interaction partners of Syp. Often, there are conflicting papers which debate the conditions of how the interaction is achieved. One of the key problems in determining interaction partners of Syp is that it is not expressed in its natural transmembrane state, as it is a 4 transmembrane containing protein. This makes it difficult to determine which interactions detected are real as full length Syp will not express in many bacterial cell lines.

Using a rational approach, if one was to identify which proteins Syp interacts with, then one might gain clues as to which stage of the SV lifecycle Syp acts upon, and

thus elucidate the physiological role of Syp. Examples of this are detailed in the following sections.

1.3.3.1 - Interaction of Synaptophysin with VAMP

The best characterised interaction of Syp is one with the v-SNARE VAMP (Calakos and Scheller, 1994, Edelmann et al., 1995), which is a key protein in SV fusion during exocytosis (Schiavo et al., 1992). One of the reasons that this interaction is potentially very exciting is that VAMP has been shown to be important in the rapid retrieval of SVs to maintain the readily releasable pool (Deak et al., 2004), and in the Syp knockout studies it was found that Syp is important in regulating a clathrin-independent rapid form of endocytosis (Daly et al., 2000, Spiwoks-Becker et al., 2001). Therefore, it has been hypothesised that the interaction between Syp and VAMP could be a controlling interaction for this rapid endocytosis (Edelmann et al., 1995, Kwon and Chapman, 2011).

Evidence to support this hypothesis, and the importance of the Syp-VAMP association, was provided by the use of superecliptic phluorins in Syp knockout cortical neurons, where it was demonstrated that Syp was fundamental to the retrieval of VAMP following exocytosis (Gordon et al., 2011). Further to this, the retrieval of other key SV endocytosis proteins was slowed which is in agreement with other reports (Kwon and Chapman, 2011).

It could be hypothesised that the interplay of Syp and VAMP could regulate a rapid type of endocytosis, which is the same type of endocytosis found defective in Syp knockout neurons, the actual interaction between the two proteins is not clearly

defined. Although there is indirect FRET imaging evidence that Syp and VAMP do interact in cultured rat hippocampal neurons (Pennuto et al., 2002), there is some debate as to under which conditions this interaction may occurs. This is mostly focused on whether stimulation promotes or disrupts the heterodimer complex formation of Syp and VAMP (Khvotchev and Sudhof, 2004, Pennuto et al., 2002, Prekeris and Terrian, 1997, Reisinger et al., 2004). It was first suggested that if stimulation disrupts the heterodimer complex of Syp and VAMP, then this could act as a mechanism to regulate the entry of VAMP into the SNARE complex, and thus modulate fusion events (Calakos and Scheller, 1994). This idea gained further strength when it was shown that syntaxin (a t-SNARE protein) was excluded from the SNARE VAMP/SYP complex, and conversely, when syntaxin and VAMP formed a complex, Syp was excluded (Edelmann et al., 1995). This suggested that Syp acted as a chaperone for VAMP (Bonanomi et al., 2007, Pennuto et al., 2003), and following stimulation from Ca^{2+} influx, VAMP was released and was able to enter the SNARE complex and result in SV fusion with the plasma membrane.

However, *in vivo* cross linking studies showed that the Syp/VAMP heterodimer complex actually increased 6 fold following stimulation induced by KCl, α-latrotoxin, or ionomycin (Khvotchev and Sudhof, 2004). Thus, due to differences in *in vitro* and synaptosome preparations, the mechanism, and therefore the functional significance, of the interaction between Syp and VAMP is still unclear.

A potential reason as to why it had been difficult to evaluate the functional significance of this interaction is that the interaction is only found in mature

neurons, and the Syp-VAMP heterodimer is not found in embryonic rat brain and developing neurons before synaptogenesis (Becher et al., 1999). It has been suggested that the developmental promotion of this interaction is dependent on post-translational modifications, such as phosphorylation (Evans and Cousin, 2005), disulphide bonds (Becher et al., 1999, Edelmann et al., 1995), or cholesterol content in the SV membrane (Mitter et al., 2003). Despite the complications in the formation of the Syp-VAMP complex, the site of interaction on VAMP has been suggested to be on the C-terminal domain (Yelamanchili et al., 2005), which consists mostly of a transmembrane domain. But there has been no reports detailing the site of interaction on Syp. It is unlikely to be on the C-terminus of Syp as deletion of the 73 amino acids of the C-terminus of Syp has no effect on the VAMP interaction (Bonanomi et al., 2007, Felkl and Leube, 2008).

1.4.3.2 - Interaction of Synaptophysin with Dynamin 1

Coimmunoprecipitation from rat brain extracts show that Syp can form interaction complexes with dynamin (Daly et al., 2000). As dynamin is essential for most forms of endocytosis (Marks et al., 2001), the Daly paper went on to hypotheses that the Syp-dynamin interaction is a regulatory step in endocytosis, but in a clathrin independent manner. The interaction of Syp and dynamin is thought to be mediated by the C-terminal of Syp (Daly and Ziff, 2002, Gonzalez-Jamett et al., 2010), and in experiments similar to Alder *et al* and Daly *et al*, it was shown using micro injection of the C-terminal of Syp that the quantal size of NT release was altered in chromaffin cells (Gonzalez-Jamett et al., 2010)

Further work showed that the Syp-dynamin interaction was Ca^{2+} dependent (Daly and Ziff, 2002), and this added strength to the argument that this interaction was important in regulating endocytosis as Ca^{2+} is essential for SV endocytosis to occur (Cousin, 2000). Daly and Ziff refined their original hypothesis by showing that the Syp-dynamin interaction is promoted once the Syp has left its interaction with VAMP, suggesting that the purpose of Syp was to recruit dynamin to the vesicle membrane. However, the Ca^{2+} concentrations used in the Daly and Ziff paper to stimulate the formation of the Syp-Dyn interaction were very high. 150 µM was reported to induce half of the maximal binding (Daly and Ziff, 2002). This concentration is closely matched to that of active zones (the sites of exocytosis) (Llinas et al., 1992), and it is thought that endocytosis does not occur in the high Ca^{2+} concentrations of the active zones, but on the periphery of the active zones where the Ca^{2+} concentration is much lower. This suggests that if the interaction of Syp and dynamin is physiological then it is acting within the active zone which might be the site of a rapid form of endocytosis.

1.4.3.3 - Interaction of Synaptophysin with Cholesterol

The cholesterol content of SVs membrane is highly enriched when compared to other neuronal membrane types (Westhead, 1987), with reports of this figure being up to 40% (Takamori et al., 2006). This is important as it has been implicated in facilitating the interaction of Syp and VAMP (Felkl and Leube, 2008, Mitter et al., 2003). One of the reasons cholesterol is able to promote interactions of Syp, is that it is suggested, by use of photo-activatable lipids, that Syp is a major cholesterol binding protein (Thiele et al., 2000).

Cholesterol has been reported to be important in endocytosis. Depletion of cholesterol with methyl-beta-cyclodextrin blocked clathrin mediated endocytosis of transferrin and EGF (Rodal et al., 1999). Ultra-structural analysis further revealed that an acute application of methyl-cyclodextrin arrested clathrin mediated endocytosis at the invagination, as many clathrin coated pits were still observed (Subtil et al., 1999).

Thiele *et al* suggested that an interaction between Syp and cholesterol was important in the biogenesis of 'synaptic-like mircovesicles'. By pharmacologically depleting cholesterol, there was no defect in overall endocytotic activity, but an abolishment of biogenesis of 'synaptic-like mircovesicles' (Thiele et al., 2000). This allowed the hypothesis that the interaction between Syp and cholesterol is important in the biogenesis of vesicles by Syp somehow aiding the membrane to induce the curvature required to form vesicles.

It has also been suggested that Syp might be responsible for the recruitment of cholesterol to the SV membranes (as reviewed in (Hannah et al., 1999, Valtorta et al., 2004)). It has also been reported that the function of this interaction might not be specific to just nerve terminals, but also at the trans-Golgi network where vesicles are initially created (Regnier-Vigouroux et al., 1991).

However, it is important to note that a lot of the studies that report the interaction between Syp and cholesterol have not been conducted in neurons, so comparing the data of the biogenesis and transportation of 'synaptic-like mircovesicles' to SVs requires some caution.

Despite all these studies, the functional consequence of the Syp and cholesterol interaction remains unknown and even how they might interact is uncharacterised.

1.4.3.4 - Interaction of Synaptophysin with Other Synaptic Proteins

A potential role for Syp in the SV lifecycle is further highlighted by its interactions with other proteins that are involved in the same process. It has been reported, based on evidence provided by immunoprecipitations and immunohistochemical analysis, that Syp can interact with the vesicular proton pump v-ATPase which is an important protein in providing the proton motive force required for NT transporter proteins in re-filling the vesicles with NT once they have been subjected to endocytosis (Carrion-Vazquez et al., 1998, Galli et al., 1996, Thomas and Betz, 1990). An interaction with myosin V has also been reported. Myosin V is located on the SV and thought to be important in the trafficking of SVs (Prekeris and Terrian, 1997). Further work using glutaraldehyde-fixed synatposomes suggested that this interaction might be involved in docking of SVs, or even fusion events on the pre-synaptic membrane (Thomas and Betz, 1990).

An interaction, apparently mediated by the C-terminus of Syp, with AP1 was also observed in studies that have used yeast-two hybrid systems to identify potential Syp interaction partners (Horikawa et al., 2002).

In the most recent attempt to define the interactions, use of yeast two hybrid screens in combination with the split-ubiquitin YTH system identified some novel interaction partners of Syp; VAMP 2, secretory carrier-associated membrane protein 1, synaptogyrin 3, synaptotagmin 3, stathmin-3, Rho-related GTP-binding

protein RhoN and Arfaptin2 (Felkl and Leube, 2008). However, although all these interactions were confirmed in yeast and FRET experiments, when immunoprecipitations experiments were conducted only the interactions of Syp with VAMP and synaptogyrin 3 were found. In a further FRET experiment in the same paper, it was shown that SH2 domain of Src was able to interact with Syp.

The closest any study has come to molecularly mapping an interaction of Syp with any other protein is provided by a study investigating an interaction of Syp with Seven in Absentia homologue (Siah 1a). GST-pull downs were conducted using truncations of the C-terminal of Syp, and it was found that the end of the C-terminal (residues 276-309) contained the binding site for this interaction (Wheeler et al., 2002). The significance of this interaction is that Siah 1a can facilitate the ubiquitination of Syp, by interactions of Siah 1a with the brain-enriched E2 ubiquitin-conjugating enzyme UbcH8, as over expression of Siah 1a promotes the ubiquitination and degradation of Syp (Wheeler et al., 2002).

Therefore, the interaction partners of Syp are still poorly defined and appear to be relatively small in number.

1.4.4 - Tyrosine Phosphorylation of Synaptophysin

The C-terminal of Syp contains ten pentapeptide repeats, nine of which are initiated by a tyrosine residue (Sudhof et al., 1987) (figure 1.4). This large number of potential tyrosine phosphorylation sites makes Syp the major tyrosine phosphorylation protein in the nerve terminal (Pang et al., 1988). In order to understand what effect this post-translational modification has on the physiological

role of Syp during the SV, one must characterise the relationship Syp has with its tyrosine kinase and which of the pentapeptide repeats are phosphorylated.

It was shown *in vitro* that Syp is phosphorylated by the non-receptor tyrosine kinase Src (Barnekow et al., 1990). Surprisingly, even though Syp was discovered in 1985, none of the physiological tyrosine phosphorylation sites have yet been identified. A major reason for this could be due to a lack of any trypsin cleavage sites on the C-terminus of Syp, so any fragments digested with the aim of identifying the phosphorylation sites with mass spectrometry would fail to produce specific phospho-fragments. When the C-terminus of Syp is passed through a phosphorylation prediction database program (NetPhos), five of the tyrosine repeats are predicated to be phosphorylated (Evans and Cousin, 2005); these are Y245, Y250, Y263, Y273 and Y290 (figure 1.4). The closest any published study has come to identifying which of the nine potential sites are phosphorylated was in 2009, where the C-terminal of Syp was subjected to tyrosine phosphorylation following oxidative stress indicated by the application of Peroxynitrite and Fyn (a Src family kinase member) phosphorylation *in vitro* by means of TKB1 Escherichia coli cells (Mallozzi et al., 2009). Here, they reported that Y263 and Y273 were phosphorylated, however, this is unlikely to represent a normal method of tyrosine phosphorylation during the SV lifecycle as neurons are not always in a state of oxidative stress.

1.4.4.1 - Dephosphorylation of Synaptophysin

As phosphorylation is a reversible reaction, it is also important to identify what the tyrosine phosphatase might be. At present, no potential candidate has been identified in the literature. However, it has been proposed that SH-PTP1 might be the responsible phosphatase (Evans and Cousin, 2005). This is based on the fact that it is found in a complex with Syp and Src (Jena et al., 1997), and has a direct interaction with Src (Falet et al., 1996). However, it has never been reported to share a direct interaction with Syp.

1.4.4.2 - In vivo Tyrosine Phosphorylation of Synaptophysin

It is known that Syp is phosphorylated under basal conditions in neurons (Jena et al., 1997, Mullany and Lynch, 1998). It was purified from rat brain lysates using

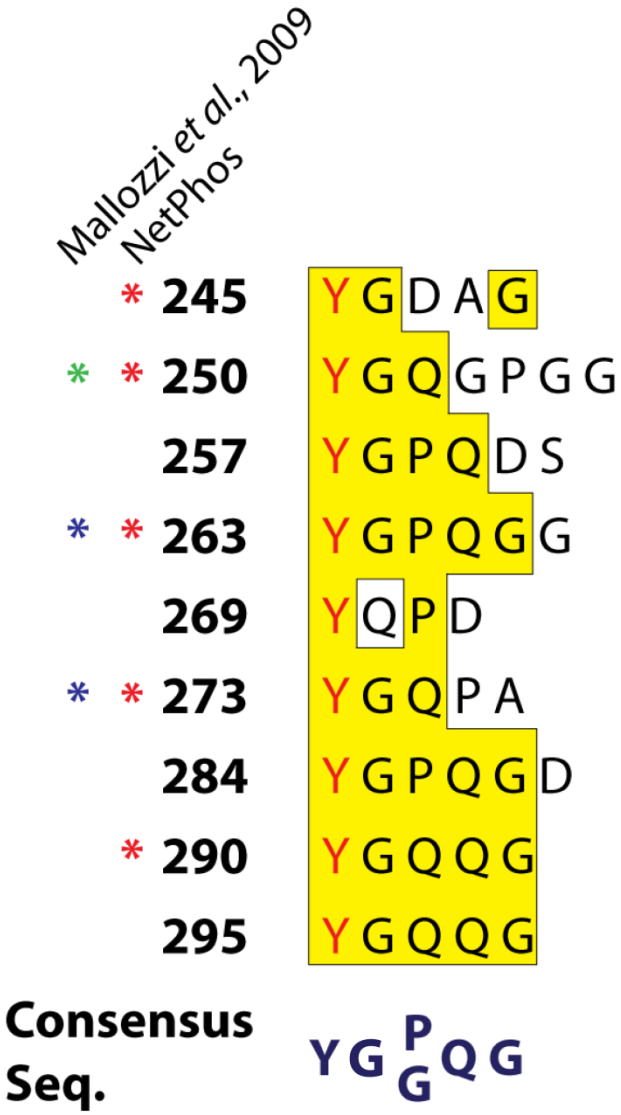

Figure 1-4 The Nine Pentapeptide Tyrosine Repeats of the C-terminus of Synaptophysin

The nine pentapeptide repeats share a high degree of sequence homology, and can produce a consensus sequence of YG(P/G)QG. Five of the tyrosine residues have been predicted to be phosphorylated by the online phosphorylation prediction database NetPhos, and they are highlighted by the red asterisks. A group (Mallozzi *et al*., 2009) investigated which of the tyrosine residues were phosphorylated following peroxide nitrate treatment, the blue asterisks note the residues which displayed tyrosine phosphorylation and the green asterisk notes the site of nitration.

immunoprecitiations and the use of tyrosine phosphate antibodies have shown that it is phosphorylated. Further evidence of this was provided by metabolic labelling experiments in synaptosomes (Pang et al., 1988). In an attempt to determine the effects of stimulation on the tyrosine phosphorylation state of Syp *in vivo*, metabolic radiolabelling experiments were conducted on brain slices in conjunction with application of KCl (Rubenstein et al., 1993). It was found that there was no incorporation of the γ-^{32}P phosphates upon the depolarising KCl stimulation, suggesting that the tyrosine phosphorylation of Syp is not regulated by stimulation of SV recycling.

This lack of stimulation dependency of tyrosine phosphorylation suggests that the phosphorylation of Syp might not be involved in the SV lifecycle. In fact, tyrosine phosphorylation has been reviewed to not have a direct influence upon the SV lifecycle (Gurd, 1997). A more popular view of how tyrosine phosphorylation can regulate the SV lifecycle is by modifying channels and receptors (Evans and Cousin, 2005, Evans and Pocock, 1999, Jovanovic et al., 2000), thus not excluding the possibility that the tyrosine phosphorylation is fundamental to the role of Syp in the SV lifecycle. This is highlighted by reports that show tyrosine phosphorylation is an important post translational modification during LTP (Kalia et al., 2004, Purcell and Carew, 2003). Usually, LTP relies on post synaptic modification, and this depends on a tetanic stimulation, which is released from the pre-synaptic side and where the SV lifecycle occurs. It is thus conceivable that when SV recycling becomes defective, the LTP stimulation would be reduced, altering the LTP effects on the post-synaptic side.

As tyrosine phosphorylation is a critical process in LTP, and the Syp knockout studies show that Syp is critical in regulation of LTP, it is tempting to hypothesise that it is tyrosine phosphorylation of Syp that regulates the apparent role of Syp modulating synaptic strength and SV availability. This idea is complemented by studies which showed that tyrosine phosphorylation of Syp increased with glutamate release from synaptosomal preparations from hippocampal slices subjected to a LTP stimulus (Mullany and Lynch, 1998). It has also been suggested that the tyrosine phosphorylation of Syp may display a stimulation dependency, but only for an LTP inducing stimulation (Evans and Cousin, 2005). This idea was based on the fact that the Syp-Src interaction was found to be upregulated in hippocampal brain slices of trained rat subjects in spatial memory learning tasks (Zhao et al., 2000), suggesting that Syp would be more phosphorylated due to an increased association with Src. This is further complemented by a suggestion that the pentapeptide repeats are important in regulating endocytosis during periods of sustained stimulation (Kwon and Chapman, 2011).

1.4.4.3 - Other types of Phosphorylation of Synaptophysin

The C-terminal of Syp has also been demonstrated to be a substrate for the serine phospho kinase calcium/calmodulin-dependent protein kinase 2 (CaMKII) (Rubenstein et al., 1993). Unlike tyrosine, these serine phospho sites are phosphorylated in a stimulation dependent manner *in vivo*. However, again due to a lack of trypsin cleavage sites on the C-terminus of Syp, the identity of the specific serine phosphorylation sites remain elusive. Mass spectrometry analysis has revealed that 3 of the 4 potential sites are serine phosphorylated in an *in vitro*

situation (Rubenstein et al., 1993). It is worthy of note, that none of the 4 potential serine phosphorylation sites are representative of the typical CaMKII consensus sequence of RxxS (Evans and Cousin, 2005).

1.4.5 - Other Proposed Functions of Synaptophysin

Syp is known to form homo-multimeric complexes *in vitro*, ranging from dimers to hexamers (Jahn et al., 1985, Johnston and Sudhof, 1990, Thomas et al., 1988), and it has been reported that the hexamer complex of Syp is able to form channels when reconstituted into planer lipid bilayers (Thomas et al., 1988). The channel activity of Syp was characterised and shown to display specific activity for K+ ions (Gincel and Shoshan-Barmatz, 2002). Syp was later identified as a member of the MARVEL (MAL and related proteins for vesicle trafficking and membrane link) family of integral membrane proteins associated with membrane juxtapositions (Sanchez-Pulido et al., 2002), and its structure has been solved using 3D single particle electron microscopy reconstruction (Arthur and Stowell, 2007). *In vivo* evidence confirmed that Syp is able to form oligomers on the surface of the SVs membrane by FRET imaging experiments (Pennuto et al., 2002). This led to the hypothesis that Syp might be able to form a proteinaceous fusion pore that regulates fusion events during exocytosis (Arthur and Stowell, 2007, Gincel and Shoshan-Barmatz, 2002, Thomas et al., 1988, Valtorta et al., 2004). Evidence for this is provided by the fact that studies have been able to record a K^+ current from a channel formed by reconstituting Syp into planer lipid bilayers (Thomas et al., 1988). Interestingly, the C-terminal of Syp is not required in order for Syp to be able to form oligomers *in vivo* (Pennuto et al., 2002).

1.5 - Non-Receptor Tyrosine Kinase Src

It was demonstrated that Syp is a substrate for the non-receptor tyrosine kinase Src (Barnekow et al., 1990). Cellular Src (C-Src) was first discovered in 1977 (Varmus et al., 1977), and since then it has been discovered that there are two neuronal splice variants of the ubiquitously expressed C-Src; N1- and N2-Src (Chan and Black, 1995, Levy et al., 1987, Matsunaga et al., 1993, Pyper and Bolen, 1989). Structurally, the three different Srcs are almost identical with the exception of a short string of additional amino acids in the SH3 domains which is generated by alternative splicing of the C-Src gene (Chan and Black, 1995); N1-Src contains 6 extra amino acids whereas, N2-Src contains 17 extra amino acids (figure 1.5).

1.5.1 - Src Domains

The 'unique' domain of Src is able to be myristoylated, and this is thought to be mediate the attachment of Src to membranes which might be important in the function of Src within the cell (Roskoski, 2004, Song et al., 1997). The SH1 domain of the kinase is the site of ATP binding (Tatosyan and Mizenina, 2000).

1.5.1.1 - The SH3 domain

The SH3 domain has been suggested to be important in the regulation of the kinase activity of Src. Src is hypothesised to exist in two confirmations, open and clamped (Yeatman, 2004), which represent an active and inactive form of the kinase, respectively. The SH3 domain is thought to be one of the molecular switches that changes the confirmation of the kinase as it is able to interact with a small linker

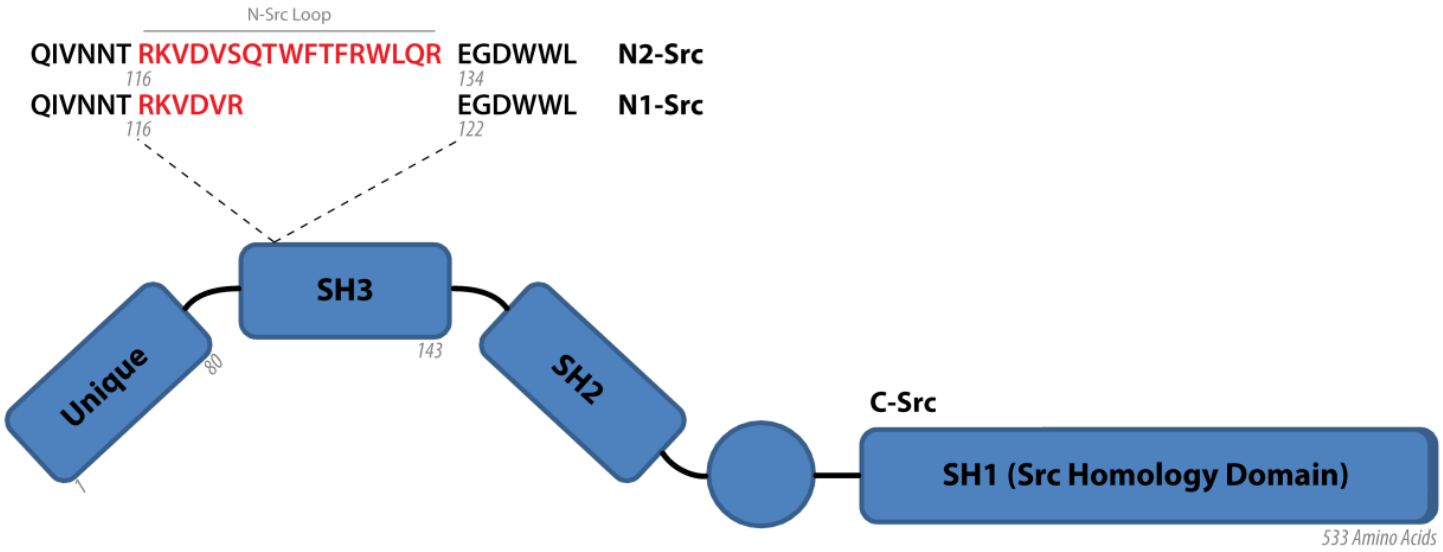

Figure 1-5 A schematic of the non-receptor C-Src and its splice variants

C-Src contains 4 domains; unique, SH1, SH2 and an SH3 domain. C-Src is ubiquitously expressed and has two splice variants which are specific to neuronal tissue. These are termed neuronal N1- and N2-Src. They are almost identical to C-Src with the exception of an addition of a short N-Src loop to their SH3 domains. N1-Src has 6 and N2-Src has 17 extra amino acids in their SH3 domains.

region between the SH1 and SH2 domains (Boggon and Eck, 2004, Brabek et al., 2002, Xu et al., 1997) (figure 1.5). Therefore, any proteins binding to the SH3 domain can displace the linker binding and thus promote changes to the open conformation.

Another possible role in regulating the Src kinase activity of the SH3 domain is that it might be involved defining the substrates of the kinase. SH3 domains are known to interact with proline rich domains of other proteins which contain SH3 interaction motifs (Feng et al., 1994, Tatosyan and Mizenina, 2000). Therefore, the interactions of the SH3 domain are critical in regulating the activity and help define the selectivity of the kinase, and it is postulated that as the neuronal splice variants of Src differ in their respective SH3 Domains, then this would vary the substrate specificity of the differing Srcs (Feng et al., 1995, Miller, 2003).

1.5.1.2 - The SH2 Domain

The SH2 domain of Src has been reported to bind to short sequences of proteins that contain tyrosine that have been phosphorylated (Bradshaw et al., 1999, Bradshaw and Waksman, 2002). Theses phospho-tyrosine short sequences are thought to be 3-6 residues in length with a loose consensuses sequence of pYEEI (pY = a phosphorylated tyrosine) (Songyang et al., 1993). This therefore suggests that the SH2 domain of Src participates in regulating protein interactions of the kinase.

It has been suggested that both SH3 and SH2 domains are fundamental to substrate phosphorylation by Src. The SH3 domain may first bind the kinase to an SH3 interaction motif, and after the kinase has phosphorylated a tyrosine residue, this

will create further binding motifs for the SH2 domain, thus increasing the ability of the kinase to phosphorylate a substrate (Evans and Cousin, 2005). Evidence to support this idea is provided by an interaction study; yeast-two hybrid system screens and GST pull downs have shown that the SH2 domain of Src is capable of interacting with Syp (Felkl and Leube, 2008, Mallozzi et al., 2009).

1.5.2 - Localisation Differences of the Three Srcs

Firstly, it should be noted that there is very little data provided by the literature about N2-Src, so at present it is only possible to review the differences between C-Src and the neuronal splice variant N1-Src. C- and N1-Src were found to have different levels of expression in different brain areas; the majority of N1-Src mRNA was found in the mesencephalon, cerebellum, pons, medulla and telecephalon while C-Srcs mRNA was at its highest in the hippocampus, thalamus and cerebellum (Sugrue et al., 1990, Yagi, 1994). These differences are further highlighted by differences in their expression in neurons. Immunohistochemical analysis highlighted that N1-Src was localised to cell soma and dendritic processes, and very little N1-Src was found in axons and nerve terminals (Sugrue et al., 1990). This is different to C-Src, which is readily found in nerve terminals (Walaas et al., 1988). When comparisons are made of the amount of C-Src purified from brain lysates to purified SV lysates, a 4-5 fold higher concentration in the SV lysates was found (Greengard et al., 1993). N1-Src was found to be enriched in synaptic membranes preparations when compared to SV preparations (Onofri et al., 2007), suggesting that the functions of the different splice variants of Src might be different.

1.5.3 - The Role of Src in Synaptic Vesicle Recycling

As the different Srcs were found to be localised to the SVs and sites of exocytosis and endocytosis, these splice variants may play different roles in the SV lifecycle. At present, however, the role for Src modulating exocytosis is still unclear.

1.5.3.1 - Src in Exocytosis

There have been reports showing that in the presence of a Src inhibitors (PP2) NT release from PC12 cells is increased (Ohnishi et al., 2001). In this study they showed that the release of dopamine was only increased during Ca^{2+} stimulation, which was induced by ionomycin application. This result was complemented by the fact that over expression of a constitutive version of Src also increased the amount of NT release.

However, there are contradictory reports from synaptosome preparations, where the effect reported of PP2 on glutamate release either enhanced of decreased glutamate release. When cerebrocortical synaptosomes were incubated with PP2 and stimulated using a high concentration of 4-aminopyridine (4AP) (3 mM), it was found that there was a decrease of glutamate release (Wang, 2003). However, it is important to consider how the stimulation was induced. The concentration of the 4AP used is unlikely to represent a physiological level of Ca^{2+} influx. In support of this idea, studies which used a lower concentration, representing a more physiological level of Ca^{2+}, showed that inhibition of Src increased NT release. Rat synaptosomes were incubated with PP2, and using assays to determine the amount of glutamate release and FM dye unloading, it was shown that inhibition of kinase

active of Src increased exocytosis following stimulation induced by KCl, or 4AP (0.3 mM), application (Baldwin et al., 2006).

1.5.3.2 - Src in Endocytosis

Src has been shown to play an important role in the receptor internalisation of the angiotensin II complex (Fessart et al., 2005). Here, the interaction of Src with the angiotensin II receptor is thought to initiate the binding of AP2 to the receptor, which is critical in the recruitment of clathrin. This mechanism of Src mediated phosphorylation interaction with AP2 is thought to be a common mechanism for the internalisation of many other types of receptors (Zimmerman et al., 2009).

Further evidence that Src is important in regulating endocytosis is provided by a report that caveolae endocytosis of plasma macromolecules, which is dependent on the fission action of dynamin 2, is dependent on Src activation (Sverdlov et al., 2007). This was shown as overexpression of dominant negative versions of Src and use of the kinase inhibitor PP2 blocked caveolae endocytosis. In support of the idea that Src mediates caveolae endocytosis by phosphorylation of dynamin 2, it has been shown that phosphorylation of dynamin 2 by Src increased dynamin GTPase activity (Ahn et al., 2002)

1.5.3.3 - Src in Learning and Memory

As Src has been implicated in both exocytosis and endocytosis, it is possible that it may regulate LTP events during learning and memory. After spatial maze learning tests, mice were found to have elevated levels of C-Src mRNA in the CA3 region of the hippocampus, and this increased mirrored an increase of Src activity in

hippocampal synaptosome preparations from these subjects (Zhao et al., 2000). Src has been well reported to have a role in enhancing the function of the post synaptic N-methyl-D-aspartate (NMDA) receptor (Kalia et al., 2004, Lu et al., 1998, Salter and Kalia, 2004, Yu et al., 1997, Yu and Salter, 1999). But interestingly, Zhao et al. showed that there was an increase in the association of Src with the pre-synaptic proteins synapsin and Syp in mice subjected to learning and memory tasks (Zhao et al., 2000). This implies that the role of Src in LTP may be both pre- and post-synaptic.

1.6 - Project Aims

The physiological role of Syp has yet to be defined, the major reason for this is that the knockout mouse displays a subtle phenotype that has yet to be convincingly characterised. Further to this, as the interactions of Syp are poorly defined it has been hard to narrow down the specific steps of the SV cycle that Syp might be involved in, potentially hiding its role further.

Despite the lack of overt phenotype in the Syp knockout mouse, one must entertain the idea that Syp is an important protein to the SV lifecycle, most simply because it is expressed at such high levels on the SV. Mother Nature, or evolution, would not waste so much energy in expressing a redundant protein to what amounts to 10.6% of the SV protein content (Takamori et al., 2006). Another feature of Syp that suggests that it has an important role is the fact that it is the pre-dominant tyrosine phospho protein on the vesicle (Pang et al., 1988), which is facilitated by nine tyrosine peptide repeats on its C-terminus, suggesting that regulation of Syp may be

important to the SV lifecycle. The role that phosphorylation of Syp plays has also yet be defined; investigations have been hampered by a lack of protease cleavage sites on the C-terminal of Syp to identify which of the nine potential tyrosine phosphorylation sites are physiologically relevant, and the lack of a definition of a Syp function has not helped.

Based on the limited understanding of the interactions of Syp and the Syp knockout mice showing apparent plasma membrane defects, it is likely that Syp has a role in endocytosis.

In this thesis, I set out to test the hypothesis that tyrosine phosphorylation of Syp controls its physiological role in the SV lifecycle.

To test this hypothesis, I hope to define the role of Syp, and this will be broken into two main research arms;

1 - To define the interactions of the C-terminus of Syp; once the interactions and binding sites are determined, one can postulate as to the step of endocytosis that Syp functions in. Mapping the binding sites will allow binding mutants to be created to determine the functional consequences of the interactions mapped.

2 - To characterise the phosphorylation of Syp; characterisation of the phosphorylation reaction, and identification of the physiological tyrosine phosphorylation sites, combined with functional imaging assays will help define a role of tyrosine phosphorylation of Syp. If a role of phosphorylation is defined, then it would provide clues to the overall function of Syp in the SV lifecycle.

These aims will be achieved using a combination of biochemistry assays combined with functional imaging assays of neurons with a Syp knockout background.

Chapter 2 Materials and Methods

2.1 - Materials

2.1.1 - Key Molecular Biology Materials

pGEX Vectors, ON# 27-4580-01 GElifesciences, Buckinghamshire, United Kingdom, for sequence see appendix figure 1

Pfu DNA Polymerase, ON# M774, LigaFast™ Rapid DNA Ligation System, ON# M8221 (http://www.promega.com), Promega, Southampton, United Kingdom

Expand High Fidelity PCR System, Roche, ON# 11732641001, (http://www.roche.co.uk), Roche Products Limited (Pharmaceuticals), Welwyn Garden City, United Kingdom

Primers, designed by self, made by Eurogentec Ltd., (http://www.eurogentec.com/eu-home.html), Southampton, United Kingdom

Fast Digest enzymes, Age1, Bham1, Bsp14071, EcoR1, Hind III, Not1, SalI, Xba1, Xho1, Fermentas, (http://www.fermentas.com/en/home), York, United Kingdom

TOP10 Cells, gift from Dr. Luke Chamberlain, University of Strathclyde,

BL21 cells, Invitrogen, ON# C6070-03, (http://www.invitrogen.com/site/us/en/home.html), Paisley, UK

2.1.2 - Key Biochemistry Materials

Glutathione Resin, GeneScript, ON# L00206, (http://www.genscript.com), GenScript USA Inc., Piscataway, USA

MicroSpin G-50 columns, GE lifescience, ON#27-5330-02, http://www.gelifesciences.com/webapp/wcs/stores/servlet/Home/en/GELifeSciences), Buckinghamshire, United Kingdom

SDS-PAGE Protein 3 mini gel kit, Large gel protein gel system mark 2 system, Large gel gradient former - model 385, Protein transfer tank - Trans blot cell (www.bio-rad.com), Bio-Rad Laboratories Ltd., Hemel Hempstead, United Kingdom

Ponceau Stain, Sigma, ON# P7170, (http://www.sigmaaldrich.com/united-kingdom.html), Sigma-Aldrich Company Ltd., Gillingham, United Kingdom

Coomassie brilliant blue, Merck, ON# K36988153708, (http://www.merck.com/index.html), Merck Sharp & Dohme Limited, Hoddesdon, Hertfordshire, United Kingdom

ATP, [γ-32P] 10Ci/mmol, Perkin-Elmer, ON# BLU002250UC, (http://www.perkinelmer.com), Cambridge, United Kingdom

2.1.3 - Key Cell Preparation Materials

Neurobasal media, Invitrogen, ON# 12348-017

Papain, Sigma, ON# P3375

Cytosine β-D-arabinofuranoside (Ara-C), Sigma, ON# C1768

2.1.4 - Key Imagine Analysis Tools

ImageJ 1.44p, NIH, http://imagej.nih.gov/ij/

ImageJ plugins downloads; for colocalisation analysis - WCIF ImageJ bundle (http://www.uhnresearch.ca/facilities/wcif/imagej/installing_imagej.htm), for time series analysis (http://rsbweb.nih.gov/ij/plugins/time-series.html)

2.1.5 - Constructs Made and Used

See Table One.

2.1.6 - Solutions

Basic NaCl Buffer; 136 mM NaCl, 2.5 mM KCl, 2 mM $CaCl_2$, 1.3 mM $MgCl_2$, 10 mM glucose, 10 mM HEPES, pH 7.4

Coomassie stain; 0.15% (w/v) Coomassie Blue G-250, 20% (v/v) methanol, and 10% (v/v) acetic acid

DMEM; supplemented with 1 % v/v of penicillin/streptomycin solution

ECL solution 1; 100 mM Tris, 2.5 mM of luminol (made up in DMSO), 9 mM of p-Coumaric acid (made up in 2.5 ml DMSO)

ECL solution 2; 100 mM Tris, 3% H_2O_2

Elution Buffer; 100 mM Tris (pH to 8), 20 mM glutathione, 100 mM NaCl, Protease inhibitor cocktail

Full neurobasal medium; supplemented with 1 % v/v of penicillin/streptomycin solution, 10% foetal bovine serum

Table 1 DNA Constructs Made and Used

General Biochemistry Constructs

	Tag	Domain	Vector	Residues	Species	Source
Amphiphysin 1	GST	SH3	pGEX 4T-1	596-683	Rat	HM
Amphiphysin 2	GST	SH3	pGEX 4T-1	494-588	Rat	HM
C-Src	GST	SH3	pGEX 4T-1	81-142	Rat	MAC Lab
Endophillin	GST	SH3	pGEX 4T-1	290-352	Rat	MP
Gst	GST	Tagged Vector	pGEX 4T-1	258-930		Amersham
GST KG	GST	Tagged Vector	pGEX KG	258-1014		CR
N1-Src	GST	SH3	pGEX 4T-1	81-148	Rat	MAC Lab
N2-Src	GST	SH3	pGEX 4T-1	81-159	Rat	MAC Lab
P85	GST	SH3	pGEX 4T-1	2-83	Cow	TP
Syndapin 1	GST	SH3	pGEX 4T-1	386-441	Mouse	MP
C-Src	Active Kinase	Full Length	pGEX-4T-1-PTP1B-3C-His-d80	1-533	Rat	GE
N1-Src	Active Kinase	Full Length	pGEX-4T-1-PTP1B-3C-His-d80	1-539	Rat	GE
N2-Src	Active Kinase	Full Length	pGEX-4T-1-PTP1B-3C-His-d80	1-550	Rat	GE

Synaptophysin Constructs

	Tag	Domain	Vector	Residues	Species	Source
C-Syp	GST	C-Terminal	pGEX 4T-1	219-308	Mouse	MAC Lab
C-Syp	GST	C-Terminal	pGEX KG	219-308	Mouse	AJ
C-Syp	HIS	C-Terminal	pET28a	224-308	Mouse	MAC Lab
C-Syp 2E (Y263,273E)	GST	C-Terminal	pGEX KG	219-308	Mouse	AJ and MAC
C-Syp 2F (Y263,273F)	GST	C-Terminal	pGEX KG	219-308	Mouse	AJ and MAC
C-Syp 6F (Y245,250,257,263,273,290F)	GST	C-Terminal	pGEX 4T-1	219-308	Mouse	AJ
C-Syp 9E	GST	C-Terminal	pGEX KG	219-308	Mouse	AJ and MAC
C-Syp 9F	GST	C-Terminal	pGEX KG	219-308	Mouse	AJ and MAC
C-Syp AA (PP232,235AA)	GST	C-Terminal	pGEX 4T-1	219-308	Mouse	MAC Lab
C-Syp AA (PP232,235AA)	GST	C-Terminal	pGEX KG	219-308	Mouse	AJ
C-Syp AA (PP232,235AA)	HIS	C-Terminal	pET28a	224-308	Mouse	MAC Lab
C-Syp End	GST	C-Terminal	pGEX KG	277-308	Mouse	AJ
C-Syp R	GST	C-Terminal	pGEX KG	219-308	Mouse	AJ
C-Syp RA	GST	C-Terminal	pGEX KG	219-308	Mouse	AJ
C-Syp T1	GST	C-Terminal	pGEX 4T-1	219-238	Mouse	AJ
C-Syp T1	GST	C-Terminal	pGEX KG	219-238	Mouse	AJ
C-Syp T1	GST	C-Terminal	pGEX KG	219-238	Mouse	AJ
C-Syp T1 R	GST	C-Terminal	pGEX KG	219-238	Mouse	AJ
C-Syp T1 RA	GST	C-Terminal	pGEX KG	219-238	Mouse	AJ
C-Syp T2	GST	C-Terminal	pGEX 4T-1	219-257	Mouse	AJ
C-Syp T2	GST	C-Terminal	pGEX KG	219-257	Mouse	AJ
C-Syp T3	GST	C-Terminal	pGEX 4T-1	219-270	Mouse	AJ
C-Syp T3	GST	C-Terminal	pGEX KG	219-270	Mouse	AJ

C-Syp T4	GST	C-Terminal	pGEX 4T-1	219-290	Mouse	AJ
C-Syp T4	GST	C-Terminal	pGEX KG	219-290	Mouse	AJ
C-Syp Y245F	GST	C-Terminal	pGEX 4T-1	219-308	Mouse	AJ
C-Syp Y273F	GST	C-Terminal	pGEX 4T-1	219-308	Mouse	AJ
C-Syp Y290F	GST	C-Terminal	pGEX 4T-1	219-308	Mouse	AJ
FL-C-Src	HIS	Full Length	pQE30	1-533	Rat	MAC Lab
FL-N1-Src	HIS	Full Length	pQE30	1-539	Rat	MAC Lab
FL-N2-Src	HIS	Full Length	pQE30	1-550	Rat	MAC Lab

Imaging Constructs

	Tag	**Domain**	**Vector**	**Residues**	**Species**	**Source**
Cer	Cer	Tagged Vector	N1-Cer	1-238		MAC Lab
WT Syp	Cer	Full Length	N1-Cer	1-308	Mouse	AJ
RA Syp	Cer	Full Length	N1-Cer	1-308	Mouse	AJ
SypHy	EGFP	Full Length	pCI-neo	1-308	Rat	LL
SypHy R	EGFP	Full Length	pCI-neo	1-308	Rat	AJ
VAMP pH	EGFP	Full Length	pCI-neo	1-116	Rat	GM

AJ	Alex Johnson
CR	C. Rickman, Herriot-Watt, Edinburgh, UK
GE	G. Evans, University of York, York, UK
GM	G. Miesenböck, Oxford, UK
HM	H. McMahon, MRC-LMB, Cambridge, UK
MAC Lab	From the lab of M. Cousin
MP	M. Plomann, University of Cologne,
TP	T. Pawson, Samuel Lunenfeld Research Institute, Toronto, Canada

Krebs Buffer (-Ca^{2+}); NaCl 188.5 mM, KCl 4.7 mM, $MgSO_4$ 1.18 mM, Glucose 1 mM, $Na_2P_4.H_2O$ 1 mM, HEPES 20 mM, pH 7.4 with a saturated Tris base

Krebs (Ca^{2+}) Buffer; Krebs buffer + 500 µM $CaCl_2$

Kinase Reaction Buffer; 100 mM Tris (pH 7.2 with HCl), 25 mM MgCl2, 2 mM EGTA, 2 mM DTT, 250 µM $NaVO_4^{3-}$, 5 mM $MnCl_2$

LB media; 10 g/l tryptone, 5 g/l yeast extract, 170 mM NaCl pH to 7.4 with NaOH

Laemmli buffer (1x); 63 mM Tris pH 6.8, 10 % Glycerol, 0.1% EGTA, 2 % SDS, 0.0025% bromophenol blue, 8% β-Mercaptoethanol

Lysis Buffer; 1% Triton X-100, 25 mM Tris-HCl, pH 7.4 ,150 mM NaCl, 1 mM EGTA, 1 mM EDTA , 20 µg/ml leupeptin, 1 mM PMSF, Complete protease inhibitor tablet (Roche)

MeOH/acetic acid SDS PAGE destain; 40% Methanol, 10% Acetic Acid Glacial, 50% dH_2O

Modified Lysis Buffer; 150 mM NaCl, 20 mM Tris, 1 mM EDTA, 2% Triton X-100

NH_4Cl Buffer; 86 mM NaCl, 2.5 mM KCl, 2 mM CaCl2, 1.3 mM $MgCl_2$, 10 mM glucose, 10 mM HEPES, 50mM NH_4Cl, pH 7.4

PBS; 0.37 M NaCl, 4 mM KCl, 20 mM Na_2HPO_4, adjust pH using $NaH_2PO_4.H_2O$

Papain; diluted to 10 units per ml

Ponceau stain; 0.5 % ponceau S stain in 1 % acetic acid

Sucrose/ EDTA; 0.32 M sucrose, 1 mM EDTA, 5 mM Tris, pH 7.4 with 0.1 M HCL

Super Media; 85 mM NaCl, 15 g/l tryptone, 25 g/l Yeast extract

STE; 10 mM Tris, 150mM NaCl, 1mM EDTA pH 8

TBE buffer; 89 mM Tris, 89 mM Boric Acid, 2 mM EDTA.

TFB1; 30 mM Potassium acetate, 10 mM $CaCl_2$, 50 mM $MnCl_2$, 100 mM $RbCl_2$, 15% glycerol - pH to 5.8 with 1 M acetic acid

TFB2; 10 mM MOPs, 75 mM $CaCl_2$, 10 mM $RbCl_2$, 15% glycerol - pH to 6.5 with 1 M KOH

Transfer Buffer; 25 mM Tris, 192 mM Glycine, 20 % methanol

Upper electrode buffer; 250 mM Tris, 200 mM Glycine, 1 % SDS, pH to 8.3

2.1.7 - Antibodies Used

The primary antibodies and the concentrations used are listed in table 2.

2.2 - Molecular Methods

2.2.1 - Polymerase Chain Reaction

For this project, several different types of polymerases were used;

- Pfu DNA polymerase (Promega) - for site directed mutagenesis
- Expand DNA polymerase (Roche) - Taq based enzyme for Polymerase Chain Reaction (PCR) cloning
- Go-Taq DNA polymerase (Promega) - for colony screening

Table 2 - List of Antibodies Used

Primary Antibodies

Antibody	Species	Use	Dilution (1 in X)	Manufacturer
Amphiphysin	Mouse	WB	2000	AbCam
Dynamin	Goat	WB	1000	Santa Cruz Biotechnology Inc
His	Mouse	WB	3000	Sigma
PY20	Mouse	WB	500	BD Biosciences
Synapsin	Mouse	ICC	100	Synaptic Systems
Synapsin	Mouse	WB	1000	Synaptic Systems
Synaptophysin	Rabbit	WB	1000	Synaptic Systems
Synaptophysin	Mouse	IP	500	AbCam
Syndapin	Mouse	WB	2000	BD Biosciences
Syndapin	Mouse	WB	1000	AbCam
VAMP	Mouse	ICC	250	AbCam
VAMP	Mouse	WB	1000	AbCam

Secondary antibodies

Antibody	Species	Use	Dilution (1 in X)	Manufacturer
Alexa 468	Mouse	ICC	1000	BD Bioscience
Anti Goat	Mouse	WB	10000	Sigma
Anti Mouse	Goat	WB	10000	Sigma
Anti Rabbit	Goat	WB	10000	Sigma

A standard reaction is listed below;

Solution	Volume used
10X Supplied Buffer	5 µl
dNTPs (100 ng/µl)	1 µl
Sense Primer (100 µM)	0.5 µl
Anti-Sense Primer (100 µM)	0.5 µl
DNA	<0.5 µg
Polymerase	1.25 u/50 µl

Samples were then placed in a GeneAmp PCR system 9700 PCR machine (Applied Biosystems California) and subjected to the following programs.

For site directed mutagenesis and colony screening;

1. Initial Denaturation - 95°C for 30 seconds
2. 18 Cycles of;
    a. Denaturation - 95°C for 30 seconds
    b. Annealing - 55°C for 1 minute
    c. Extension - 68°C for a time calculated as 2 minutes for every 1kb to be amplified
3. Finish and hold at 4°C

For PCR cloning with Expand DNA Polymerase;

1. Initial Denaturation - 95°C for 5 minutes
2. 18 Cycles of;
    a. Denaturation - 95°C for 30 seconds
    b. Annealing - 55°C for 45 seconds

c. Extension - 72°C for a time calculated as 2 minutes for every 1kb to be amplified

3. Final Extension - 72°C for 10 minutes
4. Finish and hold at 4°C

Site directed mutagenesis PCR products were then digested with the restriction enzyme DpN1 (see method; Restriction Digestions) before being transformed into competent bacteria (see method; Transformation of Competent Cells). DNA was extracted from the bacteria using a mini-prep (see method; Mini Prep of DNA) and sequenced (Source BioScience). Expand PCR products were ligated into a TA based vector (pGEM), using a T4 ligase (Promega). To determine the result of a colony screen, a 5 µl sample of the finished PCR reaction was run on an agarose gel.

2.2.2 - Restriction Digestions

Typical restriction digest reactions used Fermatas' fast digest enzymes, where the solutions were prepared at room temperature. The typical reaction mixture was, 14 µl of distilled H_2O, 2 µl of fast digest green buffer, 1 µg of DNA and then 1 µl of each of the desired enzymes. The solution was then gently mixed and then incubated at 37°C for 5 minutes. The whole reaction was run on an agarose gel to determine if the digestion was successful or to allow purification of a DNA fragment by gel extraction.

2.2.3 - Agarose Gels and Gel Extraction

Typically, 0.7% agarose gels were used to separate DNA. 0.7% (w/v) of agarose was added to TBE buffer (section 2.1.5), where the solution was heated in a microwave

and gently mixed to ensure that the agarose had fully dissolved. SYBR safe (Invitrogen) was added at a dilution of 1:10000, and the solution was poured into a casting mould. Samples were run at an electrical current of 140 volts for 45 minutes. To visualise DNA separation, the gel was imaged under a ultra-violet light source.

If required, digested DNA was purified using a gel extraction kit following the manufactures' instructions (QIAgen).

2.2.4 - DNA Ligations

Once two digested products with complementary sticky ends had been purified, T4 ligafast from Promega was used to ligate the products together (figure 2.1[1]). The basic reaction consisted of; the DNA insert, the digested DNA vector, 2X rapid ligase buffer and T4 DNA ligase. The amounts of DNA used were calculated using this formula;

$$\frac{ng\ of\ vector\ \times\ kb\ size\ of\ insert}{kb\ size\ of\ vector} \times molar\ ratio\ of\ \frac{Insert}{Vector} = ng\ of\ insert$$

Normally, a final reaction volume of 20 µl was used.

After a gentle mix, the reaction was incubated at room temperature for 10 minutes. The product of the ligation reaction was then used to transform bacteria, which allowed amplification of the new DNA.

2.2.5 - Preparation of Competent Cells

Two types of competent cell stocks were made; TOP10 cells (which were used to harvest recombinant DNA), or BL21 cells (which were used to express large amounts of recombinant protein).

To prepare competent cells, a 5 ml solution of LB media was inoculated with a scraping from a frozen stock of the competent cells, and this was incubated overnight (16 hours) at 37°C with shaking at 200 rpm. The culture was then transferred to a 1 l flask which contained 250 ml of LB media supplemented with 20mM $MgSO_4$. A 1-l flask was used to allow sufficient aeration to help the growth of the bacteria. This was then incubated at 37°C, 200 rpm until the solution reached the bacteria's exponential growth phase (indicated by an optical density of 0.4-0.8).

The culture was then subjected to centrifugation for 5 minutes at 4500 g and 4°C. The supernatant was discarded while the pellet was gently re-suspended in 100 ml of ice cold TFB1 solution. The cells were then pelleted again by centrifugation (at 4500 g, 4°C for 5 minutes) and re-suspended very gently using 1/25th volume (10ml) of ice cold TFB2. The cell/TFB2 solution was then incubated on ice for 30 minutes. After this incubation, the solution was aliquoted at 200 µl per tube into pre-chilled eppendorf tubes. These tubes were then rapidly frozen using a dry ice and isopropanol bath, and subsequently stored at -70°C until needed.

2.2.6 - Transformation of Competent Cells

Tubes of competent cells were removed from a -70°C freezer and defrosted slowly on ice. When they were completely defrosted, the DNA of interest was then added

to the cell solution (normally 1 µg/µl of DNA was used). After gentle mixing, the solution was incubated on ice for 30 minutes to allow the DNA to stick to the outside of the cells. After the incubation the solutions were then subjected to a heat shock at 42°C for 50 seconds to stimulate the cells to take up the DNA. An incubation on ice was then preformed for 2 minutes to allow recovery. LB media (250 µl) was added to each tube and the solutions were incubated at 37°C while shaking at 200 rpm for 45 minutes. This was then plated at an appropriate volume (typically 30-100 µl) onto agar plates containing appropriate antibiotics and incubated overnight at 37°C to allow colony development.

2.2.7 - Mini-Prep of DNA

To harvest plasmid DNA from bacteria mini-prep kits from QIAgen were used. An overnight culture was created by inoculating 5 ml of LB media and the appropriate antibiotic with a single colony from an agar plate of transformed bacteria or a scraping from a frozen stock of bacteria. After incubation at 37°C and shaking at 200 rpm for 16 hours, the culture was centrifuged at 4500 g and 4°C for 10 minutes. The supernatant was discarded while the DNA was extracted using a mini-prep kit in accordance to the manufactures' instructions. However the final step differed from the manual as 30 µl of distilled H_2O was used to elute the DNA from the mini prep column. The concentration of the DNA was then measured using optical density at wavelength of 260 nm.

2.3 - Biochemical Methods

2.3.1 - Expression of Recombinant Proteins

To start expressing a recombinant protein for biochemistry (figure 2.1[2]) a 'seeder' culture was established. This was a 5 ml solution of LB media containing the appropriate antibiotic (100 mg/l for ampicillin or and 30 mg/l for kanamycin) to which a scrape of a frozen stock, or a colony from an agar plate, of the bacteria that had to be grown was added. The 'seeder' culture was then incubated overnight at 37°C while shaking at 200 rpm.

After this incubation the 'seeder' culture was decanted into a bigger volume of growth media with the appropriate antibiotic, this growth media was either LB media or 'super' media. The choice of which media and which volume used depended on which recombinant protein is being grown. For example, the pGEX 4T-1 N2-Src SH3 construct was grown in a 1 l culture of 'super' media since it did not express well. In contrast, pGEX 4T-1 GST expresses very well in bacteria so a volume of 250 ml of LB media was sufficient. The flask was then shaken at 37°C and 200 rpm until the bacteria reached its exponential growth phase, which was detected by measuring the optical density of the growth solution (optical density reading of 0.6-0.8). At this stage the culture was then induced with 1 mM IPTG (Calbiochem) to start expression of the recombinant protein. After the addition of IPTG the culture was shaken at 200 rpm for either 4 hours at 37°C or 16 hours at 19°C dependent on the protein expressed.

After this, the culture was centrifuged at 4500 g at 4°C for 10 minutes. The supernatant was removed and the bacterial pellet was re-suspended in 30 ml of buffer, either 'pull down buffer for bugs' or STE buffer. The suspension was centrifuged at 4500 g at 4°C for 10 minutes, the supernatant was removed and the dry pellet stored at -80° until required.

2.3.2 - Preparation of GST Fusion Proteins

A frozen bacterial pellet of the protein of interest was re-suspended in 30 ml of STE buffer, 1 mM PMSF (Sigma), 30 µl of protease inhibitor cocktail solution (Sigma) and 5 µM of the reducing agent DTT (Sigma). After re-suspension Lysozyme was added (at a final concentration of 5.7 µM) to break down the bacterial cell wall. The bacteria and Lysozyme solution was then incubated on ice for 30 minutes.

After this incubation the detergent Triton X-100 was added (final concentration of 1%) to the solution. The solution was then subjected to sonication which consisted of 6 cycles of 30 seconds at 10 microns followed by 30 seconds of mixing, where all steps were conducted on ice. To clarify the lysate, the solution was centrifuged at 17000 g 4°C for 30 minutes.

GSH beads (GeneScript) were aliquoted into a 50 ml flacon tube (1.33 ml per 1 l of bacteria culture, which is determined by the binding capacity of the GSH beads; >20 mg of GST). 10 ml of PBS was added to the beads followed by vortexing. The bead solution was centrifuged for 5 minutes at 500 g and 4°C. The supernatant was aspirated and the wash step was repeated a further 4 times. Afterwards the beads were re-suspended with sufficient PBS to ensure that they were in a 50% slurry.

The supernatant of the bacterial lysate containing the recombinant protein was then added to the prepared GSH bead 50% mixture and incubated at 4°C with agitation for 1 hour.

The beads bound to the recombinant protein of interest were pelleted by centrifugation at 500 g and 4°C for 5 minutes. They were transferred to a 15 ml falcon tube and re-suspended with 10 ml PBS. The beads underwent this 'wash and centrifuge cycle' a further 2 times. This is followed by an additional wash using PBS supplemented with 1.2 M NaCl. This was to remove any proteins that are not strongly bound to the GSH beads. After this, the beads underwent another 2 further washes with PBS. After the final centrifugation, the beads were re-suspended with PBS to ensure that they were in a 50% slurry (figure 1[3]).

A sample of the GST-fused protein slurry was run on an SDS-PAGE gel against known concentrations of BSA standards to quantify how much protein is on the beads.

2.3.3 - GST-Pull down Assay from Synaptosomal Lysate

GST-Pull Downs were performed in the following manner. The spin columns (GE Lifesciences) were pre washed using lysis buffer and plugged. Normally 50 µg of GST-tagged protein was used and then 200 µl of synatposomal lysate (5 mg/ml) was added. The beads were then incubated with the protein lysate 4°C with agitation for one hour (figure 2.1[3]).

After this incubation the columns were unplugged and placed in a collection eppendorf tube where they were centrifuged for 10 seconds at 2000 g and 4°C. This first through was kept and used as a control. The beads were then re-

suspended in 450 µl of ice cold lysis buffer and centrifuged again at 2000 g, 4°C for 10 seconds (figure 2.1[4]). The through was discarded, and the wash was repeated with lysis buffer. A further wash was conducted using 450 µl of lysis buffer supplemented with 500 mM NaCl. Beads were then subjected to one more wash with lysis buffer and a further two washes with 20 mM Tris. The columns were then plugged and 50 µl of SDS laemmli solution was added to separate bound protein from the bait (figure 2.1[5]). After a 1 minute incubation, the columns were unplugged and transferred to collection eppendorf tubes where they were centrifuged for 10 seconds at 2000 g and 4°C to elute protein previously bound to complex (figure 2.1[6]). The through was boiled for 5 minutes and kept at -20°C until they were separated on an SDS-PAGE gel.

2.3.4 - GST-Pull Down Assay Using Bacterial Lysate

Bacterial lysates were produced using the same method as "Preparing the GST Fusion Proteins", but the STE buffer was replaced with modified lysis buffer.

The protocol was essentially the same as the GST-Pull Down from synaptosomal lysate, with the following exceptions; the GST fusion protein was incubated with the protein lysate for 2 hours at 4°C with agitation, and instead of lysis buffer, modified lysis buffer was used for the washing steps.

2.3.5 - SDS Polyacrylamide Gel Electrophoresis (SDS-PAGE)

To prepare a mini SDS-PAGE gel, a 'mini-protein mark 3 kit' (bio-rad) was used. The concentration of the gel was determined by the molecular weight of the protein of interest. For example, a protein of 30 kDa would best been seen on a 10% gel as it

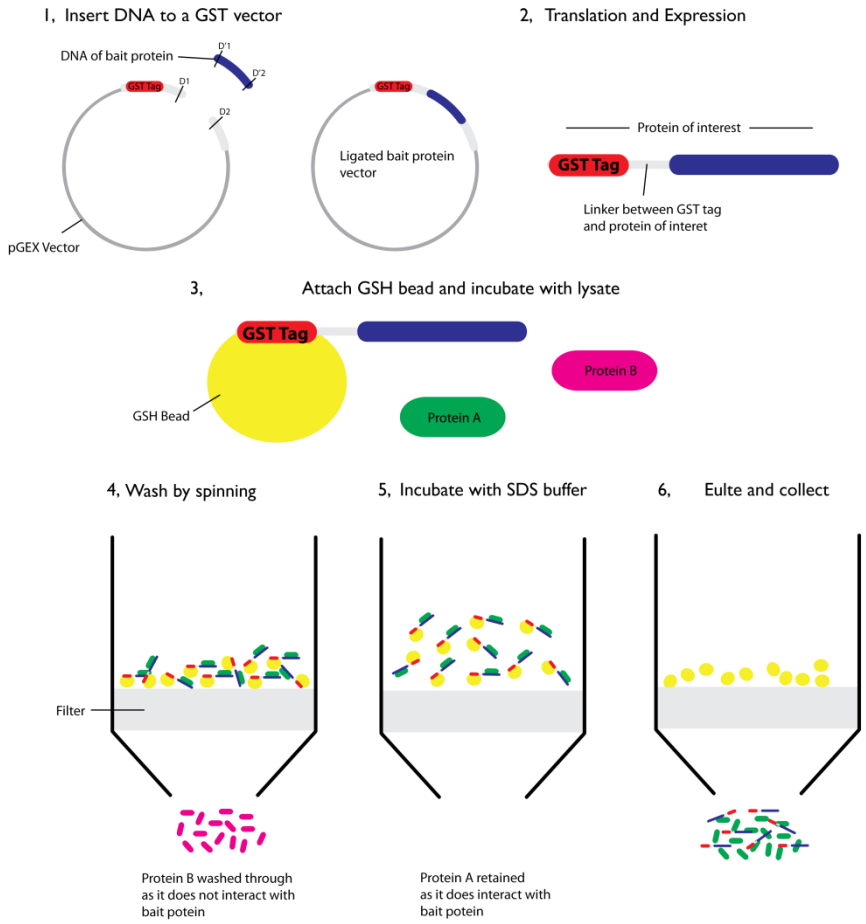

Figure 2-1 A Schematic of a GST Pull Down experiment

(1) A DNA sequence of interest (blue) is first subjected to a restriction digest, using either endogenous or artificially added restriction sites (D'1 and D'2), to produce sticky overhanging ends. It is then inserted into a GST tagged vector (such as the pGEX family) cut using the same restriction sites (D1 and D2). T4 ligase was used to ligate the insert into the vector. (2) The plasmid is then used to transform competent cells of bacteria. (3) The bacteria were then lysed and the protein lysate was collected and incubated with GSH beads (yellow). GSH beads bind to GST tags with a high affinity. Therefore, the beads are able to bind to the protein of interest in the lysate and form a large complex. This complex of beads and fused protein is then incubated with another protein lysate. This was either synaptosomal lysate or a recombinant overexpressed protein. If any interactions occur from this lysate, then that interaction partner will join the large complex attached to the beads. The beads were then transferred to a spin column (4), which has a filter which is too small for the beads to pass through. Therefore, anything that was not attached to the beads or the interaction complex will pass through (pink). After removing any proteins that are not bound to the bait protein by multiple washes, SDS buffer is used to elute any proteins that have remained bound (5; green). The through is then collected (6) and separated by use of SDS-PAGE. Any protein found here is indicative of an interaction with the GST-Fused bait protein.

displays the most separation at the range of 25-75 kDa. The compositions of the gels were;

	7.5%	10%	12.5%	15%	Stack
30% bis-Acrylamide	25%	33.4%	41.6%	50%	15%
dH2O	50%	40.2%	31.8%	10%	60%
0.5M Tris pH 6.8		-	-	-	25%
1.5M Tris pH 8	25%	25%	25%	-	-
2.5M Tris pH 8		-	-	40%	-
Glycerol		-	-	15%	-
10% SDS	0.1%	0.1%	0.1%	0.1%	0.1%
APS	0.04%	0.04%	0.04%	0.04%	0.04%
TEMED	0.08%	0.08%	0.08%	0.08%	0.08%

Larger gels were made using a BIO-RAD protein gel system mark 2. They were designed to contain a gradient of concentration ranging from 7.5-15% which was generated using a gradient former from BIO-RAD (model 385).

Once the gels were loaded with samples they were placed into a tank containing upper electrode buffer. The mini gels were run at 100 volts to pass the samples through the stack phase of the gel, and after which point the voltage was turned up to 160 v. The current was stopped when the dye front of the samples reached the bottom of the gel. Large gels were run at 100 volts to pass through the stack phase, after which point, the voltage was turned up to 180 and was left to run overnight (16-18 hours) with cooling.

After running, the gels were either subjected to a Coomassie blue stain (for at least 30 minutes), where one could see all the protein on the gel by destaining the coomassie using a MeOH/acetic acid de-staining solution overnight with shaking. Alternatively, the gels were used in western blots to detect a single protein.

2.3.6 - Western Blotting

The transfers were conducted in a BIO-RAD mini trans blot cell. The gel was removed from the SDS-PAGE tank and placed in transfer buffer to equilibrate. During this time a membrane was prepared. For most blots, a nitrocellulose membrane was used except for the phosphorylation blots where a PVDF membrane was used. Nitrocellulose membranes were washed in transfer buffer before use while the PVDF membrane needed to be activated before use. This consisted of a 10 second wash in methanol before a wash in transfer buffer. When the membranes were prepared, the gels were then sandwiched next to the membrane in the transfer cassettes, where pressure was applied by the addition of filter paper and sponge pads. The cassette was then placed in the transfer tank, which was filled with transfer buffer and an ice pack was added to the tank to prevent overheating. The transfer took place at 90 volts for 90 minutes, or 30 volts overnight. After transfer, the membranes were subjected to a ponceau stain, which was later removed using distilled water, to confirm whether the successful transfer. The membrane was then blocked for one hour at 4°C using either a 5% milk powder PBS-0.5% PVP-40 solution, or, for phosphorylation blots, a 3% BSA TBS-0.1% tween-20 solution. After blocking, the membranes were washed with 5% milk powder PBS-0.5% PVP-40 solution, or a 3% BSA TBS-0.1% tween-20 solution for

phosphorylation blots. The primary antibody (at an appropriate dilution) was added, and incubated for 2 hours with rotation at 4°C. The membranes were then subjected to 3 washes, each lasting 5 minutes each, in the buffer used to make the primary antibody solution. The secondary antibody was then added to the membrane, at an appropriate dilution. After a 1 hour incubation at 4°C with rotation, the membranes were washed with rotation 4 times, for 5 minutes each, in the buffer which was used to make up the antibody. This is followed by a 1-2 minute incubation of the membrane in an ECL solution. The excess was removed by pressing the membrane with filter paper. A cling-film protective wrap was then created to encase the membrane, and this was transferred to an X-ray cassette. The membrane was then exposed to X-ray films over appropriate exposure time. The film was then placed in developer solution until the protein bands could be seen on the film. This was then washed with water and placed in fix solution and washed again with water and placed in the film dryer.

2.3.7 - Analysis of SDS Page Gels and Western Blots

To analyse the results of many of the biochemical experiments, ImageJ (NIH) was used. The general principle was to normalise the amount of protein detected (by western blotting) to the amount of loaded protein in the same experiment. To determine this, optical density of the western blot and coomassie gel was calculated using ImageJ (plot lane function in the gel analyse section). After this, a ratio was obtained by dividing the western blot values with the coomassie values. These ratios were normalised to the maximum value for each gel to allow comparison across different experiments. For example, after a GST-Pull down, western blotting

was used to determine if certain proteins interacted. To assess the amount of protein loaded, either the membrane was subjected to ponceau staining, or another gel was run with same amounts of protein and then subjected to a coomassie stain (figure 2.2).

Digital copies of gels stained with coomassie, ponceau stained membranes or western blot films were scanned, using a CannonScan IDL 60. Adobe Photoshop CS3 was used to align the images and prepare them for analysis; ensuring that the bands were horizontal. The files were opened in ImageJ and a box was drawn on the image, enclosing the protein bands of interest, and the box is converted into a 'gel lane' of interest. The program then determined the relative densitometry of the bands within the region of interest, and produced a graph showing the peaks of intensities. Afterwards, lines were drawn to separate the different sample lanes, the area under the graph of each peak is calculated using an automated function of ImageJ (using the 'wand trace function'). As a result, a ratio of the normalised amounts of protein detected by western blotting over the amounts of protein loaded was produced. Statistical analysis was conducted using GraphPad Prism. Typically a One Way ANOVA was used with a Dunnett post test conducted to compare all lanes against one control lane.

2.3.8 - Glutathione Elution of GST-Fusion Protein from GSH Beads

A saturating excess solution of glutathione can 'out-compete' a GST-tagged protein binding to the GSH beads, which allows for elution of the GST-fused protein.

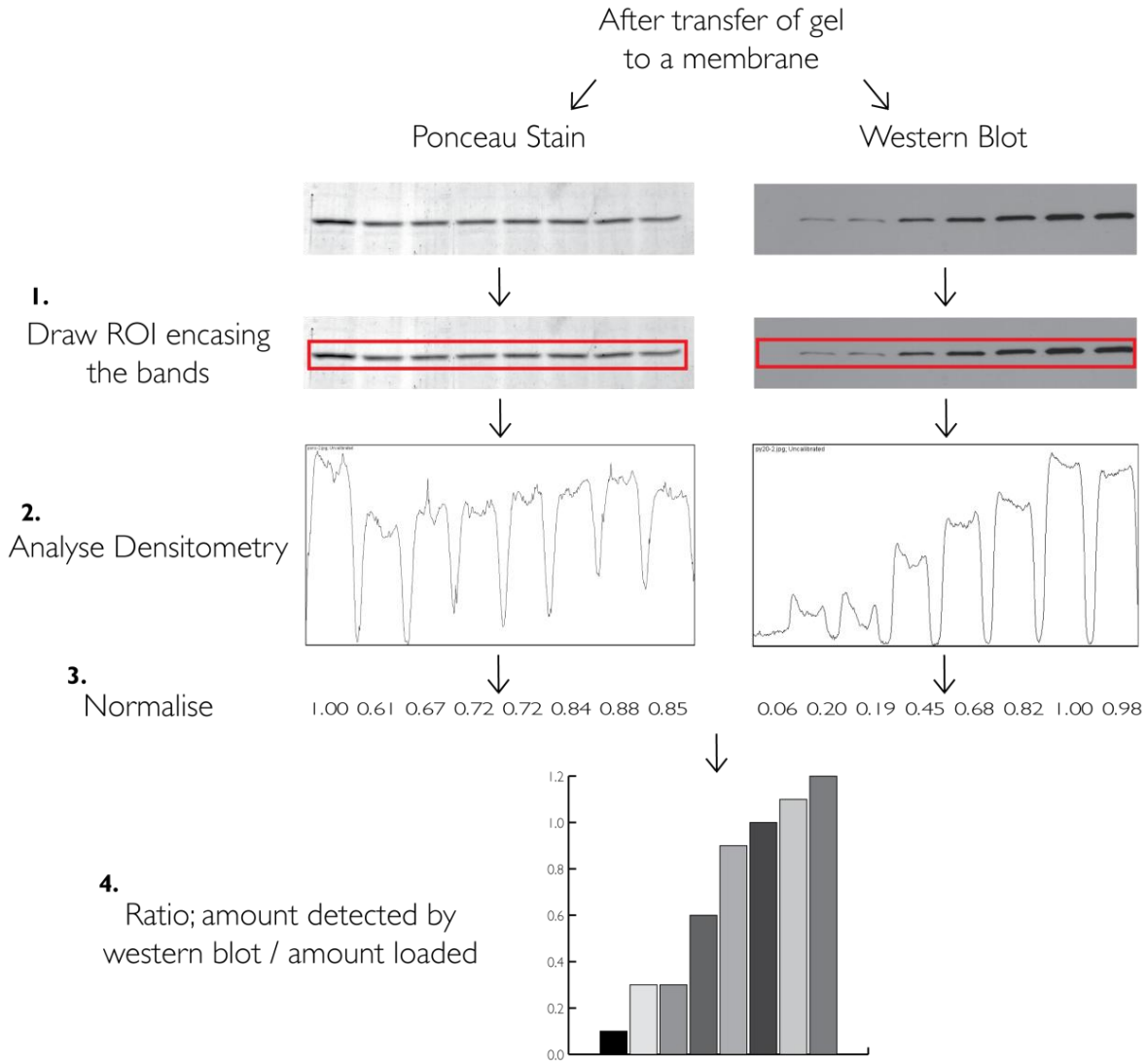

Figure 2-2 Analysis of Western Blots

After the transfer of proteins from an SDS-PAGE gel to a membrane, it was stained with ponceau and scanned to obtain a digital copy, which shows the amount of protein that was loaded onto the membrane (1 – left). The ponceau stain was then removed by washing with distilled H_2O and the membrane was subjected to western blotting. The resulting X-ray film was also scanned to provide the amount of the protein of interest detected (1-right). (2) The scanned images were then analysed using ImageJ software. If required, they were first converted to greyscale and aligned to ensure that the bands were horizontal. A region of interest (red box) was drawn around all bands that were analysed. (3) The densitometry of each band was then extracted using a graph function the area under the curve. (4) These raw values were then normalised to the maximum value of each membrane. (5) A ratio of the amount of protein detected divided by the amount of protein loaded for each experiment was then calculated.

To perform this, 400 µl of the GST-fused protein 50% slurry was taken and transferred into a pre-chilled 1.5 ml eppendorf. The beads were then pelleted using a 10 second pulse at 4000 g using a bench top centrifuge. The supernatant was removed and replaced by the addition of 100 µl of ice cold elution buffer. The tubes were then incubated at 4°C with agitation for 20 minutes. The beads were then pelleted using a 10 second pulse at 4000 g and at 4°C. The supernatant was collected and then replaced with another 100 µl of ice cold elution buffer. The beads were incubated for a further 20 minutes. This cycle of pelleting and collection of the supernatant was repeated until there were at least 4 elutions.

A 5 µl sample of the elutions was run on an SDS-PAGE gel, and the elutions were pooled if no significant degradation had occurred. A 5 µl sample of the combined elution was run against BSA standards on an SDS-PAGE gel to establish a final concentration. The eluted protein was then diluted to the desired final concentration, using an appropriate buffer, and stored in aliquots at -70°C until required for use.

2.3.9 - Tyrosine Kinase Phosphorylation Assay

After prior optimization of the conditions, the kinase assays were conducted using a kinase (Src) concentration of 2.5 µM and a saturating ATP concentration of 250 µM. The substrate concentration varied depending on whether it was a time-course assay, where 500 mM was used, or an endpoint assay, where a range of concentrations were used. To generate the different concentrations of the proteins

and compounds used, kinase reaction buffer (KRB) buffer was used to dilute the stock solutions.

The reaction tubes, and solutions, were pre-heated to 30°C. Then the substrate and kinase were added and mixed in the reaction tube. To initiate the reaction ATP was added and thoroughly mixed. The reaction was incubated for the desired time; then a sample of the reaction was added to ice cold Laemmli solution to stop the reaction. The samples were then subjected to SDS-PAGE where the resulting phosphorylation was detected using a phospho-tyrosine antibody and western blotting.

For a time course assay, samples were taken at 0, 0.5, 1, 2, 5, 10, 30 and 60 minutes. This allowed analysis to determine differences between different kinases and provided a suitable time point to conduct an endpoint assay. An endpoint assay was used to calculate a Km value for a kinase; here varying concentrations of the substrate were used. A sample was taken during the rapid phase of the time-course, and using standard Michaelis Menten kinetics, a Hanes–Woolf plot was produced to give the Km values for each kinase tested.

To further characterise the phosphorylation of synaptophysin, ATP-γ-^{32}P was also used. A concentration of 4 mCi was used. To measure the amount of γ-^{32}P incorporation, samples were run on an SDS-PAGE gel, coomassie stained and dried on a gel drier. It was then placed in a film cassette and exposed to X-Ray film, where exposure ranged from one to two weeks. Once the autoradiography film was developed, the dried gel was scanned onto a computer and used as a loading

control for the autoradiography blots during analysis. The assays were conducted using the same protocol as the non-heat assays

2.3.10 - Immunoprecipitation of Synaptosome Proteins

Protein G beads were prepared by placing 200 µl of a 25% slurry into a pre-washed spin column; the column was then centrifuged at 2000 g, 4°C for 10 seconds. After discarding the through, 400 µl of ice cold lysis buffer was added to the beads and the column was centrifuged again at 2000 g, 4°C for 10 seconds. After a further 2 washes with lysis buffer, the columns were plugged and 50 µl of lysis buffer plus protease inhibitors was added. The antibody was then added to the beads and the column was then incubated for one hour at 4°C with agitation. After the incubation the columns were then centrifuged at 2000 g, 4°C for 10 seconds, and the through was discarded and the synaptosome lysate (200 µl of a 5 mg/ml solution) was added to the beads. The columns were then incubated for one hour at 4°C with agitation. The columns were then centrifuged at 2000 g, 4°C for 10 seconds to remove to the lysate, and the pelleted beads where then washed by re-suspension with 400 µl of ice cold lysis buffer and centrifugation at 2000 g, 4°C for 10 seconds. This wash was repeated once more with lysis buffer, then with 400 µl of lysis buffer supplemented with 500 mM NaCl, once more with lysis buffer and then a further two washes with 20 mM Tris. The beads were then incubated with 50 µl of SDS laemmli buffer and the columns were then transferred into eppendorf collection tubes, where a final centrifugation of 2000 g, 4°C for 10 seconds eluted the sample from the beads. This sample was then stored at -20°C until analysis by SDS-PAGE and western blotting.

2.4 - Cell Preparations

2.4.1 - Production of Crude P2 Synaptosomes

An adult rat (>2 months) was stunned, subjected to a cervical dislocation then decapitated. The forebrain was removed, but the cerebellum and visible white matter were discarded, and washed in 40 ml sucrose solution. The solution was then homogenised, by use of a homogeniser drill, and then centrifuged at 1075 g, 4°C for 10 minutes. The supernatant from this spin (S1 fraction) was kept on ice while the pellet was re-suspended in sucrose/EDTA solution and centrifuged at 1075 g, 4°C for 10 minutes. This supernatant was combined with the other S1 fraction and centrifuged at 20200 g, 4°C for 30 minutes. The P2 pellet was then gently re-suspended with ice cold Krebs buffer and subjected to further centrifugation at 20200 g, 4°C for 30 minutes. This pellet was re-suspended using a Ca/Krebs solution and aliquoted into eppendorf tubes and incubated in a 37°C water bath for 5 minutes. Samples were then centrifuged at 20200 g for 2 minutes, and after aspirating away the supernatant the pellets were re-suspended with 400 µl lysis buffer and incubated on ice for 15 minutes with vortexing every 5 minutes. After the incubation the tubes were centrifuged at 31000 g, 4°C for 5 minutes and the supernatants were pooled. This solution was then aliquoted into eppendorfs and stored at -80°C until required.

2.4.2 - Primary Culture of Embryonic Cortical Neurons

Coverslips were rinsed in ethanol, and then water, before being autoclaved. Once sterilised, they were placed in a 50 ml falcon tube of poly-D-lysine (PDL) and

incubated overnight at 4°C. The coverslips were then dried and placed in multi-well plates and supplemented with a 50 µl drop of Laminin (1 mg/ml) and full Neurobasal media. The plates were then stored in the incubator (37°C, 5% CO_2) for at least two hours.

A pregnant mouse with an E18.5 litter was subjected to cervical dislocation and then collected from the animal house. The embryos were removed and placed in a petri dish containing PBS with 1% penicillin/streptomycin (Pen/Strep). They were then decapitated and the heads were subjected to dissection to remove the brain, and then further dissection removed the cortices. The cortices were then incubated in Papain (10 units/ml) for 20 minutes at 37°C. Afterwards, the excess Papain was removed (by pipetting) and the tissue was disaggregated using DMEM/FBS/pen-strep media. This cell suspension was then centrifuged for 3.5 minutes at 1500 g and at room temperature, where the supernatant was discarded. The pellet was re-suspended in sufficient full Neurobasal media to ensure that the cells were at a density of 10^7cells/ml. The cell suspension was added to the 50 µl Laminin drop on each of the cover slips; the amount varied depending on the desired use of the plate. For example, for live imaging assays, the cells were plated at 10^5 cells/ml. The plates were then returned to the incubator (37°C, 5% CO2). After 72 hours, a partial media change was conducted where the newly added media contained Ara-C (Sigma) to produce a final concentration of 1 µM. The Ara-C inhibits DNA replication (Politis et al., 1985) and is used in this case to kill glial cells to prevent overgrowth of neurons.

2.4.3 - Transfection of Cortical Neurons

After 7 days *in vitro* (DIV), the cells were subjected to transfection. MEM media was equilibrated in the incubator (37°C, 5% CO_2) for 45 minutes and then used to replace the conditioned media. The conditioned media was collected and stored in the incubator. The cells were incubated with the MEM media in the incubator (37°C, 5% CO_2) for 30 minutes.

DNA and Lipofectamine 2000 solution was prepared in this manner; the volumes of the solutions in this paragraph are all on a 'per well' bases. 1 µl of lipofectamine was added to 250 µl of MEM, and 1 µg of DNA was also added to 250 µl of MEM. After a 5 minute incubation, these two solutions were mixed and incubated at room temperature for 30 minutes. 500 µl of the DNA/Lipofectamine solution was added dropwise to the centre of the well. The plates were then incubated (37°C, 5% CO_2) for 2 hours. After this incubation, the well was washed with 1.5 ml MEM and the conditioned media was returned to the well. The plates were then returned to the incubator (37°C, 5% CO_2).

2.5 - Cellular Imaging Techniques

2.5.1 - Immunocytochemistry of Cultured Neurons

The cells were removed from the incubator and incubated in Na Basic solution for 10 minutes. After this incubation the cells were washed 3 times by the addition and aspiration of PBS. A 20 minute incubation with 4% paraformaldehyde (in dH_2O) was then used to fix the cells, and then a further 3 washes with PBS were conducted. The cells were then incubated for 10 minutes with PBS supplemented with 50 mM

NH_4Cl, and then subjected to another 3 PBS washes. A 30 minute incubation of the cells then followed, using a solution of 0.1% Triton X-100 and 1% BSA in PBS. The appropriate primary antibody was diluted with PBS and 1% BSA, and a drop was placed onto a parafilm layer in a humidified chamber. The coverslip was placed on top of the droplet and underwent a two hour incubation. 3 PBS washes were used to remove any residual primary antibody. The secondary antibody was diluted with PBS and 1% BSA and 50 µl droplets were placed on clean parafilm in a humidified chamber, then the coverslips were placed onto the drops and incubated for 1 hour. The coverslips were then washed 3 times in PBS, and a final wash with distilled H_2O. Any excess liquid was removed by touching the side of the coverslip onto a tissue, and the coverslips were mounted onto slides; where they were placed on to a 15 µl drop of Mowiol. The slides were then left to dry overnight, ensuring that they were covered from any light.

When the slides were ready for use, the images of the cells were acquired by using epifluorescence microscopy. A Carl Zeiss Axio Observer.A1 Microscope was used and images were captured with a AxioCam MRm Rev. 3 Digital Camera. Analysis of the images was conducted using ImageJ. To examine the distribution pattern across the length of a neuron, to determine if the proteins are expressed in a puncate pattern, a coefficient of variation was calculated. This value is the standard deviation divided of the fluorescent signal by mean fluorescent intensity of pixels in a length of axon (Lyles et al., 2006). Therefore, ROIs were drawn along lengths of the neuron and the fluorescence intensity of the pixels was measured. If the

coefficient of variation is low, this is indicative that the staining is diffuse, whereas a high coefficient of variation indicates that the staining is more puncatate.

To examine the co-localisation of proteins, a Pearson's value use calculated using a plugin in ImageJ. A Pearson's value measures the overlap of fluorescent signal of two channels for a pixel, therefore if two fluorescently labelled proteins are present in the same pixel then a high Pearson's value would be recorded, which is indicative that the two proteins are in the same area that the pixel of the captured image. A low Pearson's value would indicate that there is no fluorescent signal overlap, which indicates that the two fluorescent labelled proteins do no occupy the same pixels of the image. Lengths of neurons were defined as ROIs, by hand tracing the path of the neuron, and the ImageJ plugin analysed the mean Pearson's value for the length of neuron traced.

2.5.2 - Imaging Cultured Neurons with Superecliptic Synaptophluorins

Superecliptic Synaptophluorins make use of a pH-sensitive fluorophore (enhanced superecliptic GFP) to provide information about the environment of synaptic vesicle cargo (figure 2.3).

Transfected cells were incubated (37°C, 5% CO_2) for 5-7 days. After this they were transferred to a Warner imaging chamber, with embedded parallel platinum wires (RC-21BRFS), and mounted on to a Carl Zeiss Axio Observer A1 Microscope. The chamber was subjected to constant perfusion (5 ml/min) of Basic NaCl buffer. A wavelength of 500 nm was used to detect any synaptophluorin transfected cells

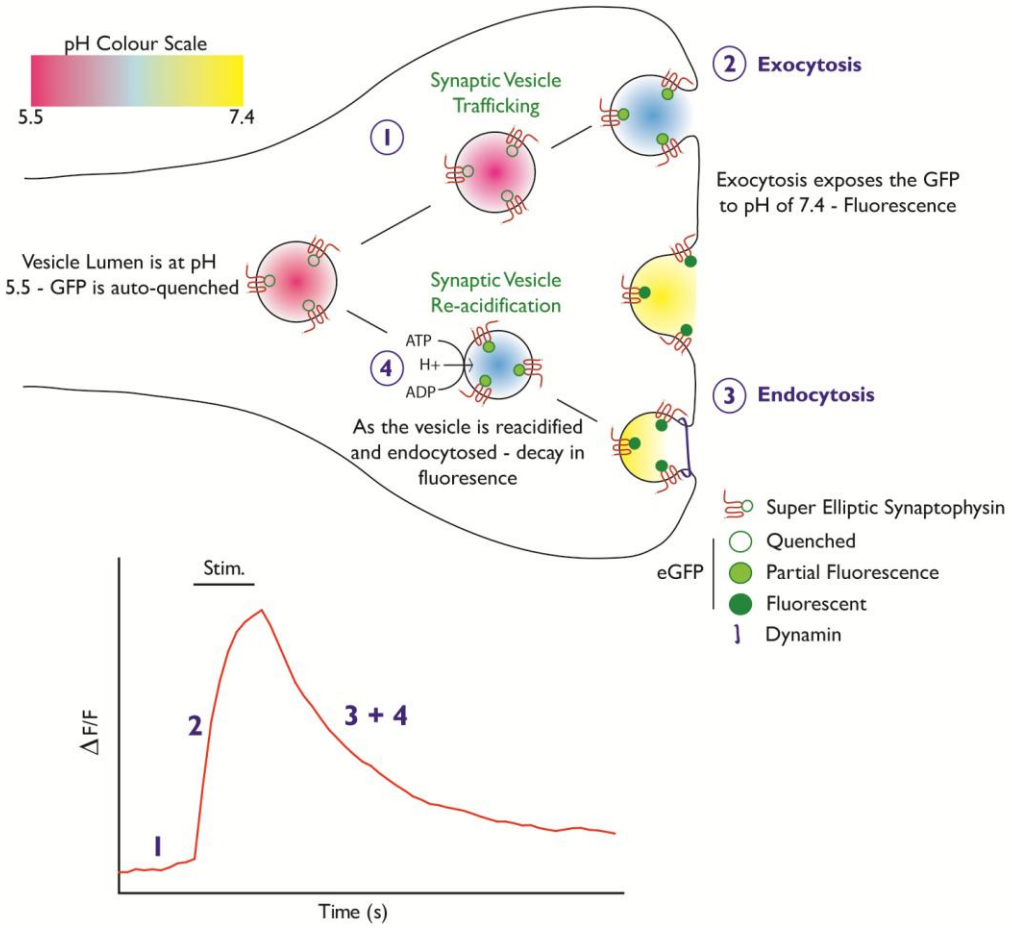

Figure 2-3 Supereclipticic Synaptophluorins

A diagram explaining the use of supereclipticic synaptophlurins in synaptic vesicle recycling is shown. Supereclipticic synaptophluorins are expressed on the surface of synaptic vesicles, and contain a pH-sensitive fluorophore on the luminal side where (1) an acidic pH of 5.5 inside the vesicles quenches the fluorophore. When the vesicle undergoes exocytosis (2), the fusion pore allows the fluorophore to be exposed to the outside of the cell, which has a pH of 7.4. And at this pH the fluorescence of the fluorophore is enhanced. (3) After exocytosis, endocytosis occurs. This moves the fluorophore away from the surface, and results in a decrease in detectable fluorescence. (4) Shortly after the vesicle has undergone endocytosis, it is refilled with neurotransmitter driven by a protomotive force. As a result, the vesicle becomes re-acidified to a pH of 5.5. This causes the fluorophore to become quenched once again. The graph on the bottom left shows changes in fluorescence level (normalised to baseline; ΔF/F) over time during an event described in the schematic diagram with corresponding numbers. Black bar (Stim.) denotes a stimulus applied to trigger vesicle recycling. An upstroke of the trace represents increase in fluorescence upon exocytosis.

using a ×40 oil-immersion objective. Transfected cells were imaged using a AxioCam MRm Rev. 3 Digital Camera, where images were captured every 4 seconds with an exposure time of 400 ms. After acquiring 10 frames to establish a baseline of background fluorescence, the cells were electrically stimulated at 10 Hz for 30 seconds. A 30 second perfusion of NH_4Cl buffer was introduced after the 60^{th} frame to reveal the total pool of fluorescently labelled vesicles, the NH_4Cl reveals the whole pool as it is able to diffuse arose membranes and removes the acidic pH gradient in the SVs, therefore causing all the fluorophores to fluoresce.

2.5.3 - Analysis of Synaptophluorin Assay

Results obtained from the synaptophluorin assay were analysed using ImageJ, Microsoft Excel and Graphpad Prism. The acquired image stack was opened in ImageJ and aligned using a StackReg plugin if required; this corrected for any horizontal drift during image acquisition. If there was any significant vertical drift the experiment was discarded.

To select regions of interest (ROIs) a macro was created which highlighted spots that responded to both electrical stimulation and the NH_4Cl pulse. This meant that only areas which displayed synaptic events were used in the analysis. The macro worked by doing two image subtractions (figure 2.4);

1. To highlight the electrical stimulation response - the image at the end of the stimulation minus the frame previous to the stimulation.
2. To highlight the NH_4Cl response - the image at the height of the NH_4Cl pulse had the image previous to the NH_4Cl pulse subtracted from it.

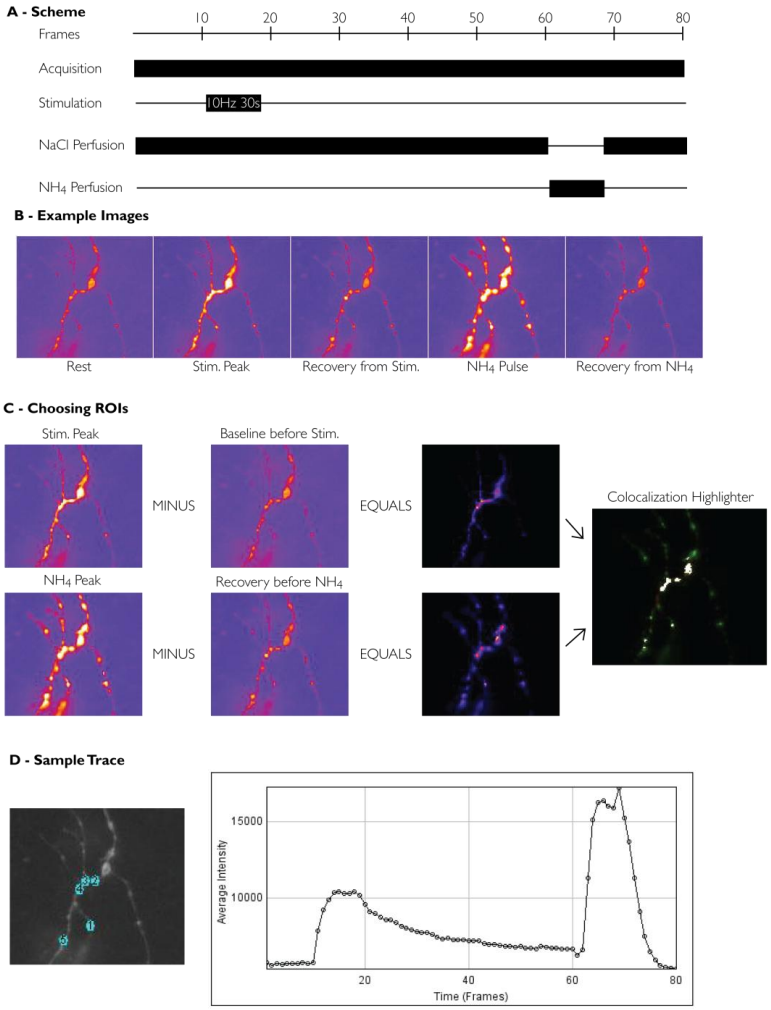

Figure 2-4 Analysis of Synaptophluorin Assay

(A) A scheme of a synaptophluorin assay experiment is shown. It typically consisted of 80 acquisition frames (1 frame every 4 seconds) captured during constant perfusion of buffers. The first 10 frames were used to establish a baseline fluorescence. After this, electrical stimulation was applied at 10 Hz for 30 seconds. At frame 60, NH_4Cl was applied to the cell for 30 seconds. (B) Sample images of the same neuron at different time points indicated are shown. False colour was applied to better reveal fluorescence changes. (C) The same frames were used to select regions of interests (ROIs) for analysis. With the use of a macro, images of the peak intensity during electrical stimulation and the NH_4Cl pulse were subtracted by their corresponding baseline images. The resulting images were co-localised to highlight areas which had responded to both the electrical stimulation and the NH_4Cl pulse. (D) An image showing 5 selected ROIs is shown on the left. A trace plotted on the right displays average integrated intensities of the ROIs over time generated using a time series plugin.

The two resulting images were then subjected to a co-localisation plugin, which highlighted any areas which showed more than a signal of 5% in increase of fluorescence from baseline and co-localised at a ratio of more than 10%. Identical circular ROIs of 5 pixels (0.85 μm, giving a ROI of 0.55 μm^2) in diameters were drawn around any highlighted points. ROIs were not drawn around spots that were significantly larger (experience from the MAC lab has shown that the typical synapse is smaller than this size); also they were never drawn on overlapping highlighted points. The ROIs are slightly larger than the typical synapse, as this allows for minor drift in the experimental setup. Once the ROIs are drawn around the highlighted synapses that have responded to both the electrical stimulation and the NH_4Cl pulse, the ROIs are re-centred using a function of the time series analyser (which determines the mean centre of the synapse throughout the captured image). The average integrated intensities of the signal within each ROI was analysed by use of a Time Series Analysis plugin. These raw values were normalised in Excel to their starting value by dividing by baseline fluorescence, and a trace of each ROI was produced to confirm that the macro had correctly selected it. The values were then either normalised to the peak of the NH_4Cl pulse (the proportion of recycling vesicles to the total pool) or to the peak of the stimulation response (to determine kinetic information) and plotted in Prism as a function of $\Delta F/F$. Statistical analysis comparing different constructs with the same synaptophluorin reporter was conducted using two way ANOVA.

2.5.4 - mCerulean Synaptophysin Trafficking Assay

mCerulean tagged proteins of interest, after being transfected into a neuron, allowed monitoring of how that protein is trafficked in rounds of the SV lifecycle as described by (Li and Murthy, 2001) (figure 2.5).

Transfected cells were mounted on the microscope as described in the previous section. Once mounted on to the microscope, the cells were subjected to constant perfusion (5 ml/min) of Basic NaCl buffer. A ×40 oil-immersion objective, and a wavelength of 430 nm, was used to image a mCerulean transfected cell. An AxioCam MRm Rev. 3 Digital Camera captured images every 4 seconds for 10 frames, in order to establish a baseline reading. And then stimulation (10 Hz for 20 seconds) was applied to the chamber, and a further 50 frames were captured. The image was then analysed in ImageJ, Microsoft Excel and Graphpad Prism.

After using a StackReg plugin (to correct the image for any horizontal drift), identical oval ROIs (5 pixel diameter) were placed in the centre of every synapse (figure 6B). A Time Series Analysis plugin detailed the integrative intensity of each of the ROIs, and the raw values were transferred into Excel; where the data was normalised to the starting value of the experiment. The first 10 points were used to create a line of fluoresce decay (which results from exposure to the laser light), and this was used to correct the whole data set. These values were then plotted in Prism as a function of $\Delta F/F_0$.

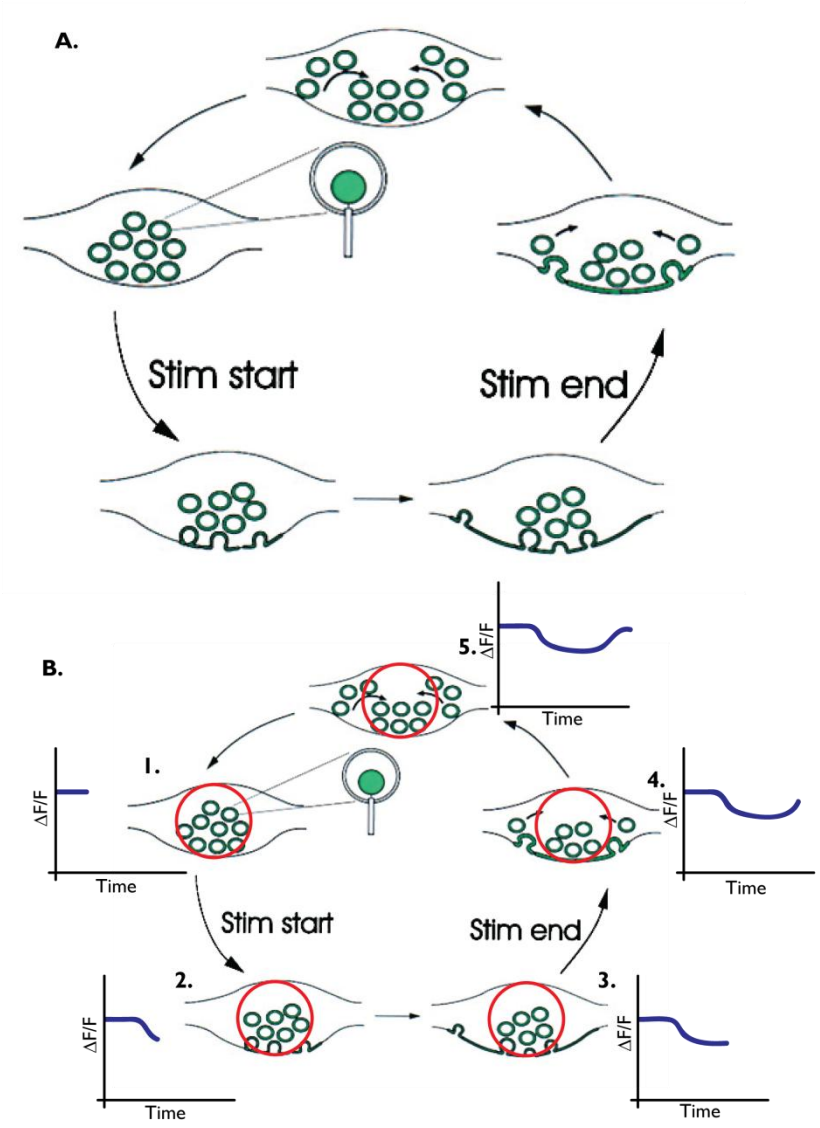

Figure 2-5 mCerulean trafficking assay

A) A schematic to show a model of how synaptic proteins are trafficked during SV recycling. B) At rest the labelled protein will be located in the centre of the nerve terminal as the SVs are in clusters. Following stimulation the SVs fuse with the plasma membrane and the fluorescence signal will diffuse out to the periphery of the nerve terminal. As endocytosis occurs, the SV proteins will be retrieved and as the SVs form clusters, the fluorescent signal will increase back to baseline levels. A ROI is drawn around the nerve terminal to measure the change in fluorescence during the SV recycling lifecycle. Adapted from (Li and Murthy, 2001).

Chapter 3 Defining the SH3 Domain Interactions of Synaptophysin

3.1 - Introduction

Syp, until recently, had no known role in SV recycling. This changed with recent work which shows the Syp is required for VAMP retrieval (Gordon et al., 2011), while its absence slows SV endocytosis in general (Gordon et al., 2011, Kwon and Chapman, 2011), but what is still unknown is the molecular mechanism underpinning how Syp retrieves VAMP from the plasma membrane.

To develop an understanding of the molecular action of Syp in VAMP retrieval, clues can be gained by characterising which proteins it interacts with. With a catalogue of interaction partners of Syp, one could begin to further elucidate at which stage of the SV lifecycle Syp is involved. Many of the studies investigating the interactions of Syp have failed to produce detailed characterisations of its interactions. For example, there is still debate as to whether Syp actually has a physiological interaction with VAMP; some papers suggest there is a direct interaction based on immunoprecipitations and cross-linking (Calakos and Scheller, 1994, Edelmann et al., 1995, Washbourne et al., 1995), however this interaction is only thought to occur in mature systems (Becher et al., 1999), which makes interpretation of the significance of this interaction difficult. As such, there are many hypotheses that the function of this interaction could range from regulating targeting of VAMP to the SVs (Pennuto et al., 2003) to actually regulating fusion events (Edelmann et al.,

1995). Despite the broad speculation of the function of this interaction, only the Syp binding site on VAMP is known, and even this is not mapped to specific residues, it is suggested that it is the N-terminal part of VAMP that is imporant in this interaction (Yelamanchili et al., 2005, Washbourne et al., 1995).

Syp is also reported to have an interaction with dynamin (Daly and Ziff, 2002, Gonzalez-Jamett et al., 2010). This interaction is Ca^{2+} dependent, however as the concentrations required are akin to the active zone (Daly and Ziff, 2002). Amperometric recordings of chromaffin cells, which had been subjected to micro injection of antibodies for either Syp or dynamin, suggest that the interaction might regulate quantal size (Gonzalez-Jamett et al., 2010). It has been reported that the site of interaction for dynamin is the C-terminus of Syp, where increasing lengths of the C-terminal increased the interaction, suggesting that dynamin binds to the pentapeptide repeats (Daly and Ziff, 2002).

At present, the most complete attempt to create a catalogue of interaction partners of Syp relied heavily on a yeast-two hybrid screen (Felkl and Leube, 2008). This could produce false positives in the form of interactions that occur outside the physiological setting on an intact nerve terminal. For example, 6 potential interaction partners of Syp were found using this system, which were reported to be confirmed by FRET. However, only two of these interactions were confirmed by immunoprecipitation; these were interactions with VAMP and synaptogyrin 3. Further work showed that the SH2 domain of Src interacts with Syp, however, no interaction site was defined.

Another yeast two-hybrid screen identified an interaction of Syp with AP1γ, and further characterisation by immunoprecipitation and immunocytochemistry revealed that this interaction was mediated by the C-terminal of Syp (Horikawa et al., 2002). Again, no specific residues were mapped for this interaction.

An interaction with Siah-1a, a ubiquitin-protein ligase, has been demonstrated (Wheeler et al., 2002). Biochemical interaction assays using truncations of the C-terminus of Syp showed that the site of interaction was on the extreme end of the C-terminal of Syp.

With this in mind, there is a real need to catalogue the interaction partners of Syp (to gain an insight as to at which stage of the SV lifecycle Syp might be acting) and to molecularly map these interactions (to allow binding mutants to be tested in physiological assays).

Work conducted in 1991 highlighted the importance of the C-terminal of Syp in endocytosis, where a truncation of the whole C-terminus arrested endocytosis (Linstedt and Kelly, 1991). This suggests that there is potentially an interaction motif on the C-terminal of Syp that is critical to its own endocytosis, therefore we examined the primany structure of the C-terminus and found a potential type one SH3 interaction motif (Feng et al., 1995). The importance of this interaction site was highlighted by further sequence analysis where it was found to be conserved across a wide range of mammalian species (figure 3.1). It is potentially exciting as many synaptic proteins contain SH3 domains. It provides a potential interaction platform for Syp regulation.

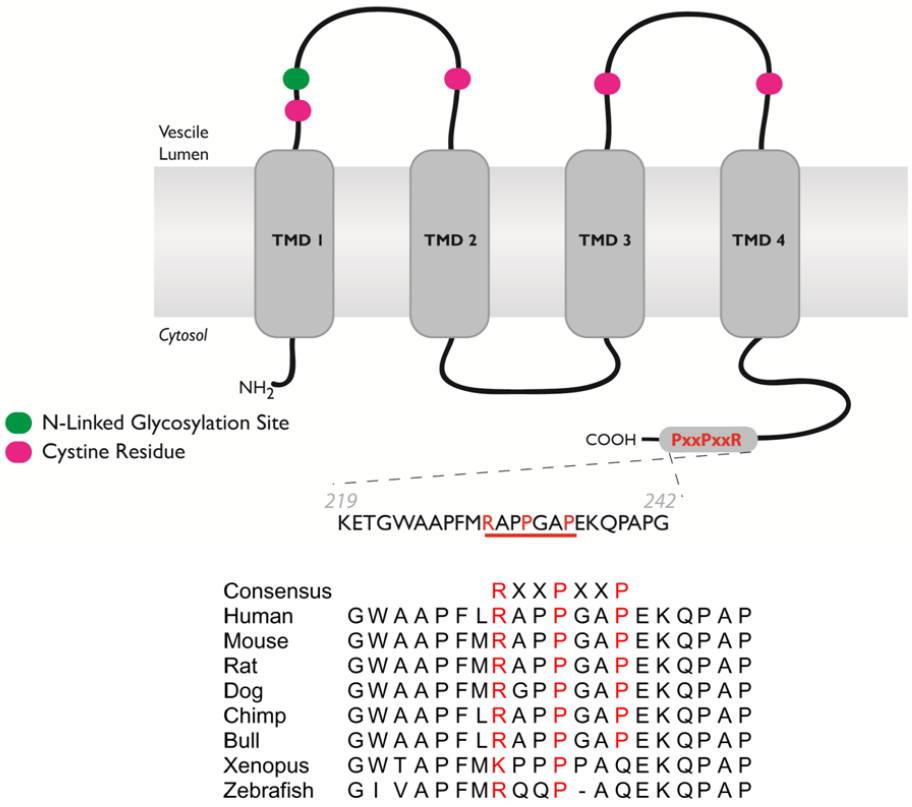

Figure 3-1 The SH3 Interaction Motif of Synaptophysin is Conserved across Species

The putative type one SH3 interaction motif (RxxPxxP) on the C-terminus of Syp is conserved in mammals. The only disruption of the SH3 interaction motif is found in non-mammalian vertebrates' such as the *Xenopus* and Zebrafish.

Taken together, we were presented with a novel starting point to begin to define some SH3 domain-mediated interactions of Syp.

3.2 - Results

3.2.1 - Synaptophysin has Specific Interactions with SH3 Domains of Synaptic Proteins

Syp has a putative type one SH3 domain interaction motif where the motif is RxxPxxP and the Syp sequence is RAPPGAP, which is on its C-terminus. Therefore it could potentially interact with proteins that contain an SH3 domain (figure 3.1). As many synaptic proteins contain SH3 domains, and the synapse is the localisation of Syp, it is hypothesised that this SH3 interaction motif could be key in the function of Syp by regulating its interactions with other synaptic proteins. At present, the wealth of papers published about Syp have failed to characterise in molecular terms which proteins Syp interacts with. Therefore, as a starting point in this project, a screen of potential SH3 domain interaction partners of Syp was conducted. SH3 domains of synaptic proteins (amphiphysin 1 and 2, endophilin 1, P85, C-Src, N1-Src and N2-Src) were used as bait in GST-pull down experiments using synaptosomal lysates.

First, to validate this approach and methodology, western blotting of the GST-pull down samples with antibodies of known interaction partner proteins that contained a SH3 interaction motif were conducted (figure 3.2 A-D, E). For example, since dynamin 1 was known to bind to all of the bait SH3 domains with the exception of N1- and N2-Src (Anggono et al., 2006, Graham et al., 2007, Hill et al., 2001,

Qualmann et al., 1999, Simpson et al., 1999, Solomaha et al., 2005, Takei et al., 1999), the samples collected from the GST-pull down were subjected to western blotting with a dynamin 1 antibody. As predicted, the SH3 domains of N1- and N2-Src significantly interacted less with dynamin 1 than all the other bait SH3 domains, with the exception of endophilin 1 (figure 3.2C, E). Further blotting for amphiphysin 1 and 2 (figure 3.2A, B, E) showed that there were high levels of interaction with endophilin, and this interaction has been previously characterised (Micheva et al., 1997). It has been reported that synapsin is able to interact with the SH3 domains of endophilin, C-Src and P85 (Cousin et al., 2003, Onofri et al., 2000, Onofri et al., 1997). When samples from the SH3 GST-pull down screens were subjected to western blotting with a synapsin antibody, these were the interactions that were found (figure 3.2D E). Therefore, these results show that the experimental approach is valid.

To define interactions of Syp with synaptic SH3 domain containing proteins, western blotting the GST-pull down samples with a Syp antibody (figure 3.3A, B) was performed to determine which of the domains interacted with Syp. Two SH3 domains which extracted the most Syp were C-Src and N2-Src. The amphiphysins and P85 SH3 domains showed some affinity for Syp, where endophilin and N1-Src showed no affinity for Syp.

These results indicate that Syp can interact with SH3 domains and is selective in its interactions (C- and N2-Src being the most effective). This specificity could be generated by the type one SH3 interaction motif found on the C-terminal of Syp.

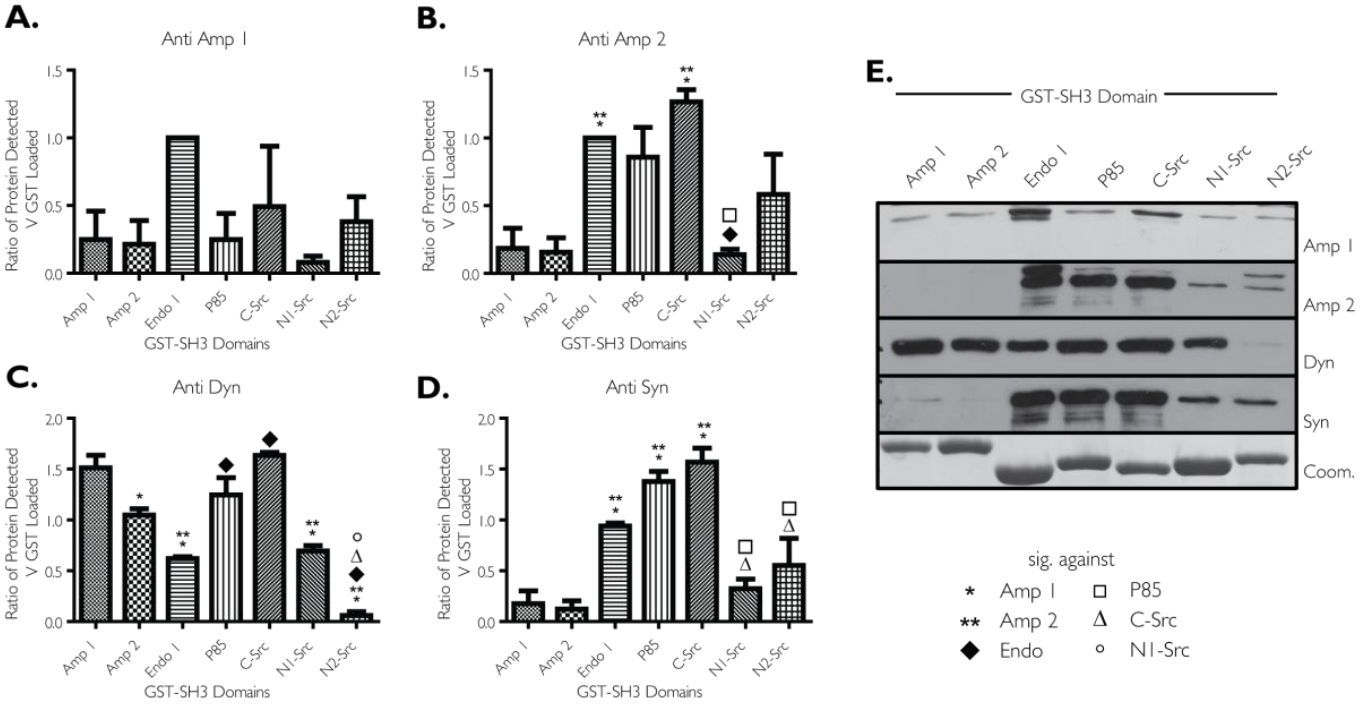

Figure 3-2 GST-Pull Down Experiments using Synaptosome Lysates Revealed Interactions between Synaptic Proteins

GST baits were generated from SH3 domains of amphiphysin 1 and 2 (Amp 1, Amp 2), endophilin 1 (Endo 1), P85, C-, N1- and N2-Src. Pull-down experiments were performed using synaptosome lysates and quantified using western blotting. Coomassie staining was used as an internal control for the amount of GST loaded in each lane. Densitometry analysis of the relative amounts of protein detected normalised to GST loaded and plotted for antibodies against A) Amp 1, B) Amp 2, C) Dynamin (Dyn), and D) Synapsin (Syn). Graph bars are means ± SEM. Statistical significance against the various conditions are indicated by symbols explained as shown. One-way ANOVA, n=3 independent experiments for all of the conditions, $p<0.05$. E) Representative western blots for each set of data are shown.

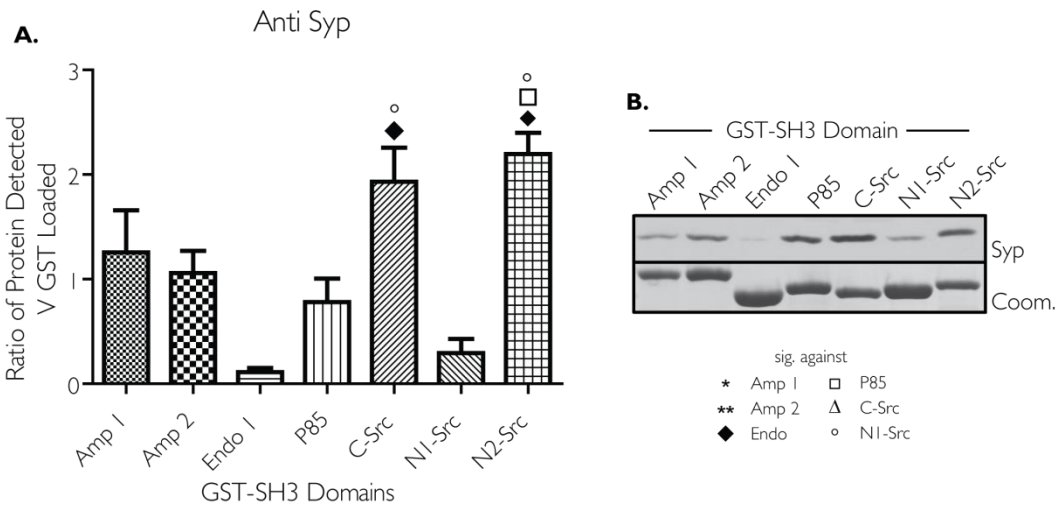

Figure 3-3 Synaptophysin has Specific Interactions with Synaptic Proteins

GST baits of the SH3 domains of amphiphysin 1 and 2 (Amp 1, Amp 2), endophilin 1 (Endo 1), P85, C-, N1- and N2-Src. Pull-down experiments were performed using synaptosome lysates and quantified using western blotting. Coomassie staining was used as an internal control for the amount of GST loaded in each lane. Densitometry analysis of the relative amounts of protein detected normalised to GST loaded and plotted for antibodies against A) synaptophysin (Syp). Graph bars are means ± SEM. Statistical significance against the various conditions are indicated by symbols explained as shown. One-way ANOVA, n=3 independent experiments for all of the conditions, $p<0.05$. B) Representative western blots of the GST-pull downs.

3.2.2 - The SH3 Domain of N2-Src Interacts Directly with the C-Terminus of Synaptophysin

GST-Pull Downs using SH3 domains of synaptic proteins as bait demonstrated that Syp can be specifically extracted from synaptosomal lysate by C-, N2-Src, and to a lesser extent the amphiphysin SH3 domains (figure 3.3A, B). However, as these results were from synaptosomal lysates, it is possible that they might be false positives. Such results can occur because all the proteins in a nerve terminal are present in the lysate and many of these proteins exist in complexes. Therefore the protein of interest might be detected via western blotting as a result of an indirect interaction. For example, the bait protein might be interacting with a protein in such a complex rather than directly with the protein detected by western blotting.

To overcome this, GST-pull downs were conducted from bacterial lysates expressing a synaptic protein of interest. In this scenario, is it less likely that any protein complexes will be formed because the overexpressed proteins natural interaction partners in a nerve terminal are not present in the lysate. Therefore, any Syp-dependent interactions detected are much more likely to be a result of a direct interaction.

GST-Pull Down experiments were therefore conducted using a bacterial lysate of the C-terminal of Syp tagged with His as a recognition epitope. These experiments should also provide evidence as to whether the SH3 domains interact with Syp via its C-terminus which contains the SH3 interaction motif (figure 3.4).

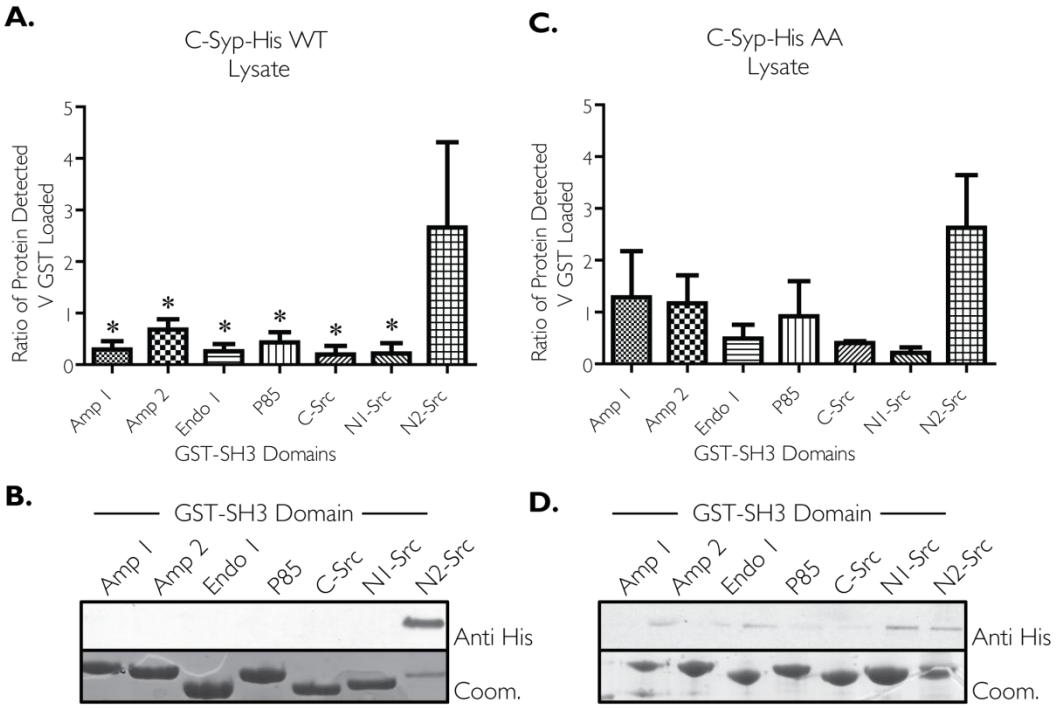

Figure 3-4 Synaptophysin Interacts Specifically with N2-Src when Pulling Down from Bacterial Lysate Expressing the C-Terminus of Synaptophysin

The SH3 domains of amphiphysin 1 and 2 (Amp 1, Amp 2), endophilin 1 (Endo 1), P85, C-, N1- and N2-Src were used as bait in pull down experiments that used bacterial lysate expressing the C-terminal of Syp. The lysate expressed either the WT C-terminal of Syp (C-Syp-His WT), or one that carried two mutations of the SH3 interaction motif (C-Syp-His AA, P232, 235A). Coomassie staining was used as an internal control for the amount of GST loaded in each lane. Densitometry analysis of the relative amounts of protein detected normalised to GST loaded and plotted for antibodies against His for experiments using the A) WT C-terminus or the C) SH3 interaction mutant C-terminal. One-way ANOVA, n=3 independent experiments for all of the conditions, a * denotes significance for when $p<0.05$ when compared to N2-Src. Graph bars are means ± SEM. B) and D) are representative western blots of the GST-pull downs.

Only the SH3 domain of N2-Src pulled down the C-terminal of Syp from bacterial lysate (figure 3.4A, B). This interaction was significant when compared to the other bait SH3 domains ($p < 0.05$). This implies that the interaction between Syp and the SH3 domain of N2-Src is direct and via the C-terminus of Syp. The other interactions (amphiphysin 1, 2 and C-Src) seen when using synaptosomal lysate (figure 3.3A, B) were not found using the C-Syp lysate.

To more directly test if the SH3 domains were binding to Syp via the SH3 interaction motif, single point mutations of two key residues of the motif (P232,235A) were made and this was used as a protein lysate for the bait SH3 domains. GST-pull down experiments using the mutated C-Syp AA (figure 3.4C, D) did not disrupt the SH3 domain interaction with N2-Src. This suggests that the SH3 interaction motif is unlikely to be the site of interaction for the SH3 domain of N2-Src.

These data have confirmed an interaction with the SH3 domain of N2-Src to the C-terminal of Syp. Interestingly, this interaction is not by the putative SH3 interaction motif. The data also highlights the need to investigate further the interactions with the other SH3 bait domains; especially C-Src.

3.2.3 - Mutations in the SH3 Domain Binding Motif disrupt the Direct Interaction of the C-Terminus of Synaptophysin with Full Length C-Src

While GST SH3 domains of C- and N2-Src were found to significantly interact with Syp when pulling down from synaptosomal lysate, and the N2-Src SH3 domain interacts with a C-Syp when expressed in a bacterial lysate, it remains to be

confirmed whether the C-Src interaction is direct or mediated by a different domain of C-Src. Since GST pull downs from C-Syp lysate might give misleading results due to the tetramer formation, reciprocal experiments were conducted where GST C-Syp was used as bait to extract full length C- and N2-Src from bacterial lysate. Only C- and N2-Src were used as they showed the greatest levels of interaction in previous experiments. Similar to previous experiments the mutated SH3 interaction motif Syp (C-syp AA) was also used to investigate if the interaction between the Srcs and Syp is via the SH3 interaction motif on the Syp C-terminal.

The results from experiments using full length C-Src lysate and GST C-Syp suggested that there is a direct interaction between FL C-Src and the C-terminus of Syp (figure 3.5A, B). Another key finding was that C-Syp AA mutant showed a reduction in its ability to interact with C-Src compared to WT. This further suggested that the interaction between C-Src and Syp could be via the SH3 domain of C-Src and the SH3 interaction motif on the C-terminus of Syp, although this data set is only from 2 independent experiments. It also confirms that there is a direct interaction between the C-terminal of Syp and C-Src.

A significant interaction between C-Syp and full length N2-Src was also observed, confirming it as a binding partner of Syp (figure 3.5C, D). However, this interaction did not appear to be mediated via N2-Srcs SH3 domain as the C-Syp AA mutant SH3 interaction motif failed to disrupt the binding of N2-Src.

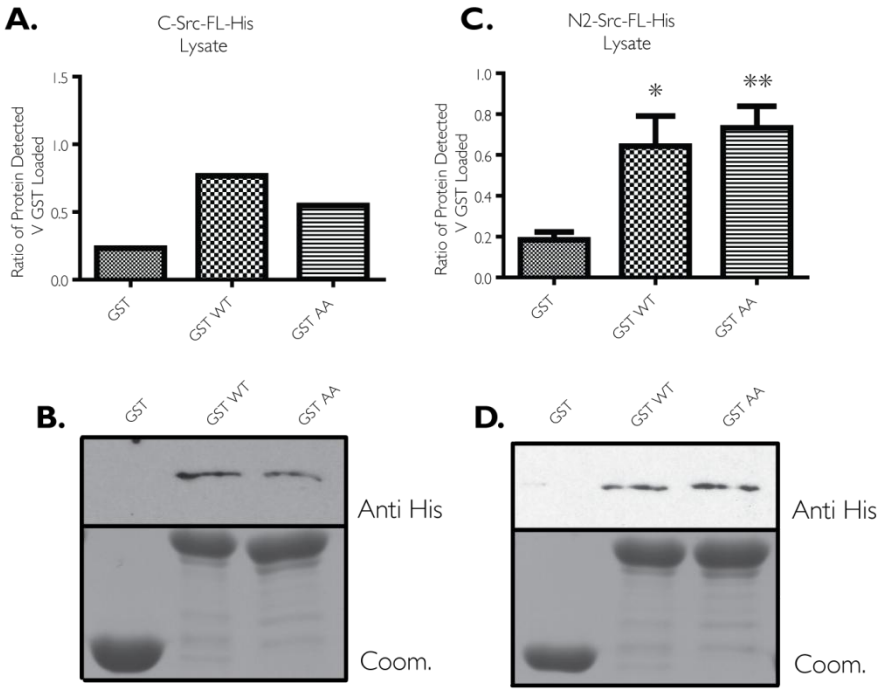

Figure 3-5 Mutations in the SH3 Domain Binding Motif disrupt the Direct Interaction of the C-terminus of Synaptophysin with Full Length C-Src

The WT and an SH3 interaction motif mutant (PP232,235AA) AA version of the C-terminal of Syp were used as bait in GST-pull downs from bacterial lysates. The bacterial lysates used were those expressing the full length C- and N2-Srcs and carried a His tag. Coomassie staining was used as an internal control for the amount of GST loaded in each lane. Densitometry analysis of the relative amounts of protein detected normalised to GST loaded and plotted for antibodies against the His tag of the overexpressed lysate protein for A)C-Src and C) N2-Src. Statistical significance is noted by the asterisks (* = $p<0.05$, ** = $p<0.01$) when compared to GST control. Graph bars are means ± SEM. A one-way ANOVA was conducted, where the C-Src data was from 2 independent experiments, while N2-Src data was from 5 independent experiments. Representative blots are shown for the B) C-Src and D) N2-Src pull downs.

3.2.4 - Truncations of the C-Terminus of Synaptophysin Suggest that the SH3 Interaction Motif is the Binding Site for C-Src

Pervious experiments suggested that C-Src might interact via its SH3 domain to the SH3 interaction motif on the C-terminus of Syp (section 3.2.3). To test if this was indeed the case the C-terminal of Syp was systematically truncated (figure 3.6). The shortest truncation was truncation 1 (T1) which was a short fragment (19 residues) of the C-terminus which contained the SH3 interaction motif. Therefore any proteins interacting with this fragment are highly likely to be interacting with the SH3 interaction motif. Further truncations T2, T3 and T4 containing the SH3 interaction motif and sequentially longer fragments of the Syp C-terminus were also made to study possible interactions that might use different motifs on the C-terminal of Syp.

The full length GST-WT C-Syp was compared to these truncations when used to pull down from C-Src bacterial lysate (figure 3.7A, D). The levels of interaction of T1 and the WT C-Syp with C-Src were almost identical. This shows that the SH3 interaction motif alone is sufficient to allow WT levels of interaction between C-Src and Syp, strongly suggesting that the SH3 motif is the site of this interaction. This result is strengthened by the fact that the longer truncations (T2-T4) showed similar levels as interaction to the WT. Thus additional regions of the C-terminal present in these truncations did not affect the levels of interaction detected.

The results differ when the C-Syp truncations were used to extract the N-Srcs from bacterial lysate. N1-Src displays much less binding to T1 when compared to WT C-

Figure 3-6 Schematic to Show the Truncations of the C-terminal of Synaptophysin

The C-terminus of Syp was truncated to produce different lengths of the C-terminal to begin to investigate potential interaction sites. Truncation 1 (T1) was designed to contain only the SH3 interaction motif, where the other truncations were subsequently longer versions of C-terminus that still contained the SH3 interaction motif (T2-T4).

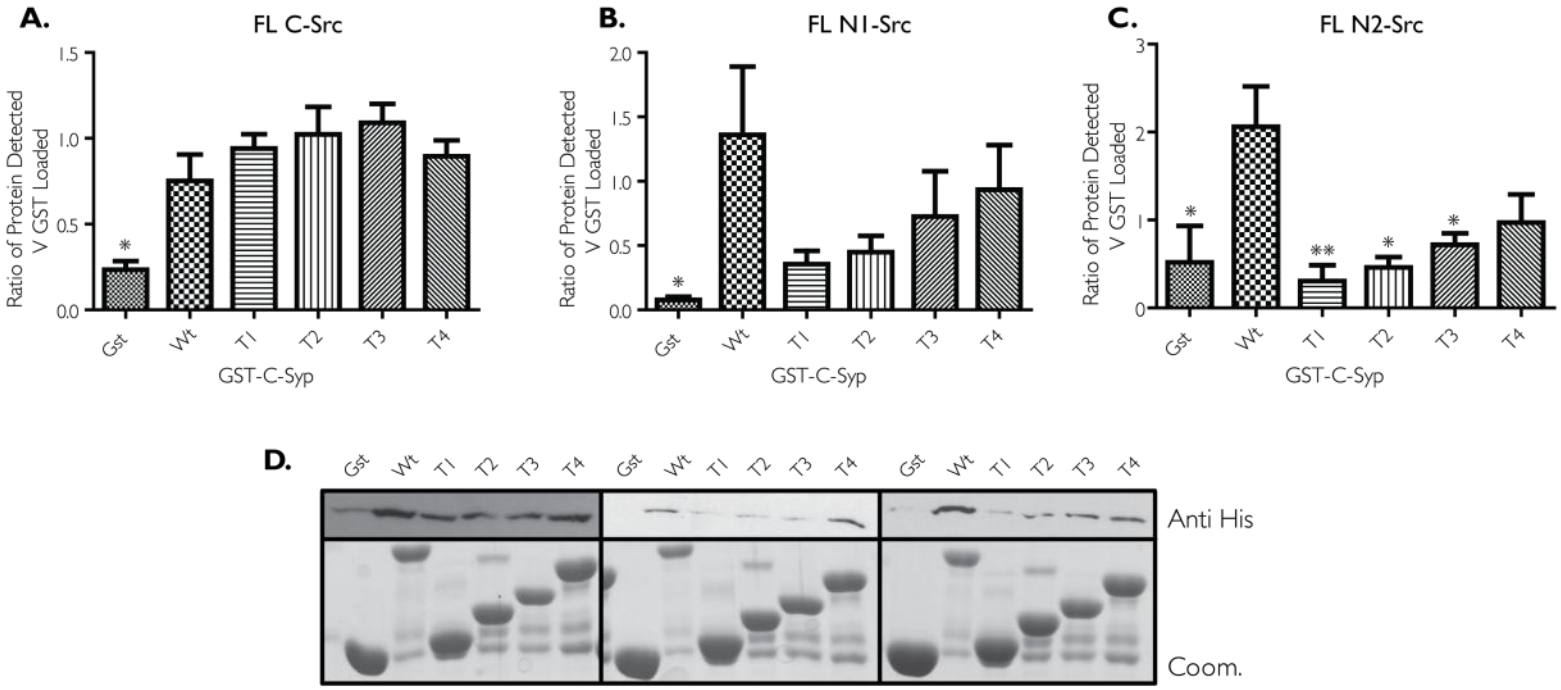

Figure 3-7 Src has Different modes of Binding to Synaptophysin for C, N1 and N2

GST bait proteins were made using WT and truncations of the C-terminal of Syp (figure 3.6); T1-T4. GST-pull down experiments were conducted using bacterial lysate that overexpressed His tagged full length A) C- B) N1- and C) N2-Src. The western blots were analysed by densitometry, and a ratio was produced by dividing this by the amount of protein loaded on a coomassie stained gel. Graph bars are means ± SEM. Statistical significance was conducted with an one-way ANOVA, where the data is n ≥ 3 independent experiments (* = $p<0.05$, ** = $p<0.01$ when compared to WT). D) Representative western blots for each set of data are shown.

Syp (figure 3.7B, D), although not quite statistically significant. Instead, there was a trend where the level of interaction increased with the length of the C-terminus, with the longest truncation (T4) almost restoring the interaction seen with the full length N1-Src with C-Syp. This suggests that N1-Src might bind to the pentapeptide repeats on the C-terminal (YD(P/G)QG). Together with the observation that the SH3 domain of N1-Src failed to pull down Syp from synaptosomal lysates (figure 3.3A, B), it is likely that another domain of N1-Src is responsible for the interaction detected with WT C-Syp, which uses a different mode of interaction compared to C-Src.

Pull down experiments from bacterial lysate expressing full length N2-Src showed a similar trend to N1-Src (figure 3.7C, D). There is little significant interaction with T1, and very little recovery of the interaction with the increase in length of the C-terminus. Even the longest truncation (T4) fails to recover to WT levels, suggesting that the interaction between N2-Src and Syp is not via the SH3 domain. The site of interaction could therefore be the end fragment (residues 289-308) of the syp C-terminal, as this is the only section missing in the final truncation.

Truncations of the C-terminus were made from WT C-syp in a pGEX-4T1 vector. This vector has no linker sequence designed between the GST tag and the start of the Syp sequence. This might prevent correct protein folding of the C-terminus, or more likely it might physically exclude access to the interaction motif (which is very close to the start of the C-terminus) for some SH3 interactions. To examine these possibilities, the C-terminus of Syp was cloned into at GST tagged vector (pGEX KG) which has an additional linker sequence of 22 residues before its

multiple cloning site, where the Syp C-terminal was inserted (figure 3.8). After the WT C-terminus was cloned into the pGEX KG vector, site directed mutagenesis was conducted to create the T1 truncation. GST-pull down experiments using the KG and pGEX 4T-1 Syps (WTs and T1s) as bait were conducted using the three different full length Src lysates. From the full length C-Src lysate, the pGEX 4T1 constructs showed a similar trend to the pervious experiment (figure 3.9A, D); where T1 is capable of interaction with C-Src. The KG constructs mirrored the result as seen previously with the pGEX 4T-1 Syps, where the WT C-terminus and the T1 truncation showed the same amount of interaction.

GST-pull downs from the N1-Src lysate (figure 3.9B, D) using the pGEX 4T-1 bait Syp proteins displayed the same results as seen previously where there was a greatly reduced interaction between N1-Src and the T1 truncation of Syp. When the KG bait Syps were used, there was more of an interaction found using the pGEX KG WT Syp when compared with the pGEX 4T-1 WT Syp. This suggests that the linker region between the GSH bead and the protein does improve the ability of the C-terminal of Syp to form an interaction with N1-Src.

Similarly, the results from GST-Pull Downs using the N2-Src lysate (figure 3.9C, D) showed that the KG WT C-terminal had a similar interaction to its pGEX 4T-1 counterpart. The key observation from this experiment is that the T1 truncation in the KG vector, still showed only little interaction as in the pGEX 4T-1 vector. This

Figure 3-8 Schematic to Show the Differences of Synaptophysin in a 4T-1 and KG-pGEX vectors

The C-terminal Syp 4T-1 construct does not contain a linker region between the start of the C-terminus and the GST tag. This might result in obstruction of the SH3 interaction motif, which is very close to the start of the C-terminal of Syp, when a GSH bead is bound to the construct. Therefore, the C-terminal of Syp was cloned into a KG-pGEX vector which has a linker region (grey) between the GST tag and the start of the C-terminal of Syp.

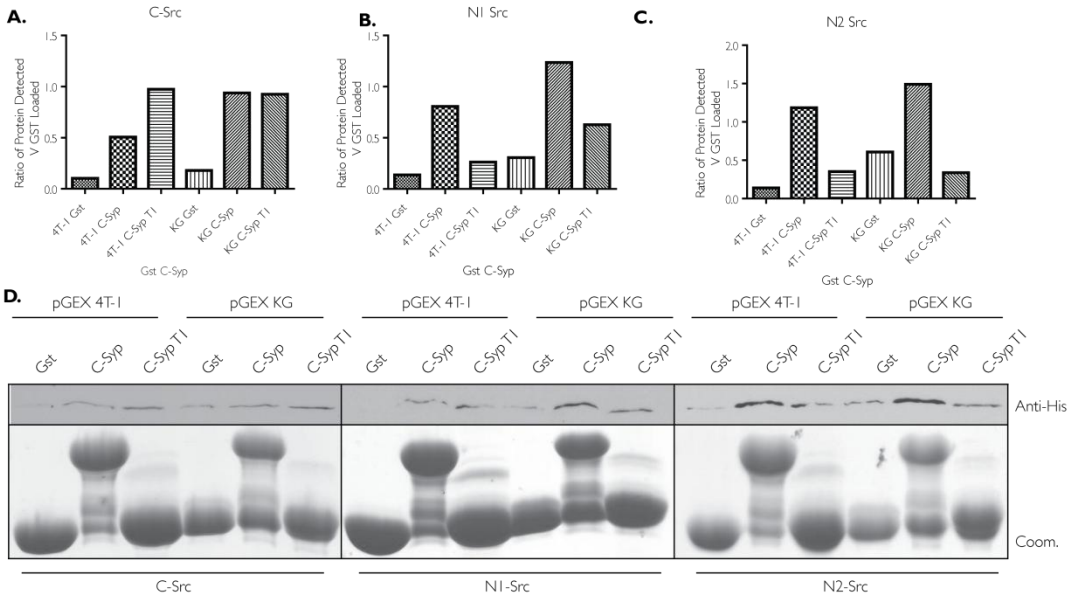

Figure 3-9 The KG vector does not Affect the Srcs interactions with Synaptophysin

GST bait proteins were made of the full length and the T1 truncation of the C-terminal of Syp, in both the 4T-1 (no linker region between the GST tag and the start of the C-terminal) and KG (25 amino acid linker region between the GST tag and the start of the Syp C-terminal) pGEX vectors. These were used as to extract overexpressed full length His tagged A) C-, B) N1- and C) N2-Src from bacterial lysate. The GST-pull downs samples were analysed by densitometry of a western blot conducted with an antibody raised against His. Coomassie stained gels were used as a loading control, and D) representative blots are shown. (The data for each condition is n = 2 independent experiments).

again provided evidence that N2-Src does not bind to the SH3 interaction motif on the C-terminal of Syp.

It can therefore be concluded that the 3 different Srcs all bind to the C-terminus of Syp but potentially have different modes of interaction; C-Src binds to a large truncation of Syp that contains the SH3 interaction motif and is mediated by its SH3 domain. N1-Src is capable of binding to the T1 truncation but it does not bind as well as WT levels of the interaction. N2-Src does not appear to bind via the SH3 interaction motif at all. Further to this, it can also be concluded that the KG Syp constructs allow greater accessibility to SH3 domains.

3.2.5 - The pGEX 4T-1 Synaptophysin Constructs Limit Access to the SH3 Interaction Motif

Previous experiments which investigated how the Srcs interacted with Syp showed that it was necessary to use a GST vector that had a linker region between the site of GSH bead binding and the start of the Syp C-terminal (section 3.2.4). These experiments showed that Syp is more available to interact with bacterial lysate proteins. It was therefore important to test if there were similar differences when pulling down from synaptosomal lysate.

Figure 3.10A shows the comparison between the pGEX 4T-1 vector, expressing WT C-syp or the T1 truncation of the C-terminal, and the pGEX KG vector from two independent GST-pull downs from synaptosomal lysate. The samples were run on a large gradient (7-15%) gel to allow maximal separation of the proteins, visualised using coomassie staining. Some differences in the extracted proteins were

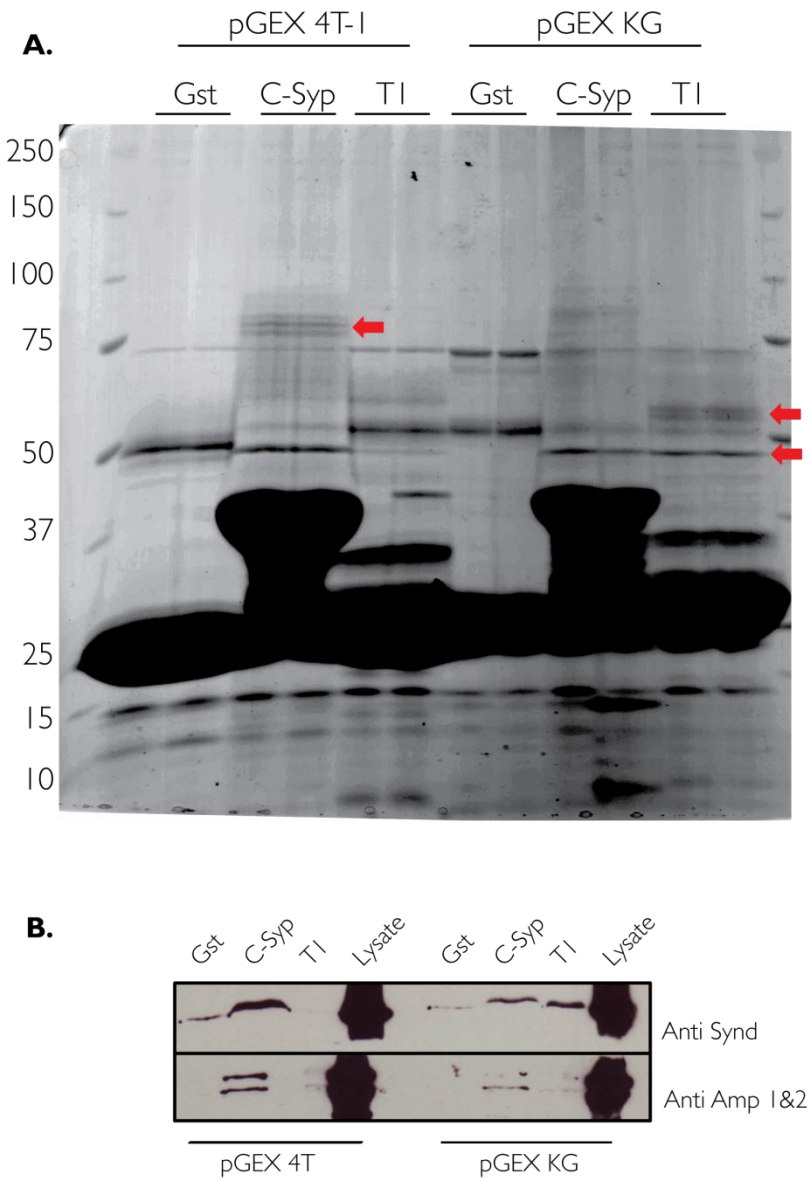

Figure 3-10 The pGEX 4T-1 Synaptophysin Constructs Limit Access to the SH3 Interaction Motif

GST bait proteins were created of the full length C-terminus of Syp and the truncation mutant T1, in both the 4T-1 and KG pGEX vectors (which either do not have or have a linker region between the GST tag and the start of the C-terminal of Syp). These bait proteins were used in a GST-pull down using synaptosomal lysate. A) The samples were separated on a large SDS-PAGE gradient gel (7-15%) and coomassie stained. Some of the differences in the proteins pulled down by the baits are highlighted by red arrows. B) Western blotting of the samples with syndapin (Synd), amphiphysin 1 (Amp1) and amphiphysin 2 (Amp2) antibodies were conducted and representative blots are shown.

observed when comparing the pGEX 4T-1 WT C-Syp vector with the KG vector; examples of these are highlighted in figure 3.10A. This again suggests that the close proximity of GSH beads might be interfering with the interaction sites on the pGEX 4T-1 C-syp. This result is highlighted further when comparing the T1 truncations in the different vectors. There are many additional bands of protein in the pGEX KG T1 lanes compared to the pGEX 4T-1 equivalents, for example a large band at about 50 kDa. This provided more evidence that the linker region in the pGEX KG vectors allows more access of SH3 domains to the SH3 interaction motif on the C-terminal of Syp.

To attempt to see if these additional protein bands were SH3 containing proteins, western blotting was conducted using antibodies for syndapin and amphiphysin (figure 3.10B). Western blots for syndapin clearly showed that syndapin does interact with WT C-Syp in the pGEX 4T-1 vector, but when it is truncated to make T1 the interaction is no longer detected (Figure 3.10B). In contrast, the T1 truncation with pGEX KG Syps was able to interact with syndapin at WT levels; suggesting that either the GSH beads block the interaction site on the T1 truncation or that, without a linker, the short fragment of the T1 was not in its natural conformation. These western blots also provide evidence that the syndapin interaction might also be mediated by the SH3 interaction motif on Syp in a similar manner to C-Src. A similar result is seen when the samples were subjected to western blotting for amphiphysin; the pGEX 4T-1 vector only allows interaction with the full length C-terminal, whereas the T1 truncation in the KG vector cannot bind amphiphysin 1 and 2.

Although the blots are from a single experiment, the result further supports the fact that the Syp C-terminal SH3 interaction motif is sufficient for some protein-protein interactions (Syndapin and C-Src) and the pGEX 4T-1 vector excludes some of these interactions by not having a linker region.

3.2.6 - The SH3 Domain of Syndapin Interacts with Synaptophysin

Data from GST-Pull Downs using the T1 truncation of Syp highlighted a possible interaction between syndapin and the C-terminal of Syp. It also suggested that the SH3 domain of syndapin may bind the SH3 interaction motif on Syp. To test this hypothesis further, a similar screen (to figure 3.2 and 3.3) of GST-SH3 domains were used as bait when pulling down from synaptosomal lysate (figure 3.11A). The results were similar to pervious experiments; where the SH3 domains of amphiphysin 1, amphiphysin 2, C-Src showed high levels of interaction with Syp while endophilin did not. Interestingly, a high level of interaction was also observed with the SH3 domain of syndapin (figure 3.11A). Next, 3 independent GST-Pull Downs were conducted using the SH3 domain of syndapin from synaptosomal lysates. A strong interaction between the SH3 domain of syndapin and Syp was confirmed (figure 3.11B). Thus, the SH3 domain of syndapin interacts with Syp, potentially via its C-terminal SH3 interaction motif.

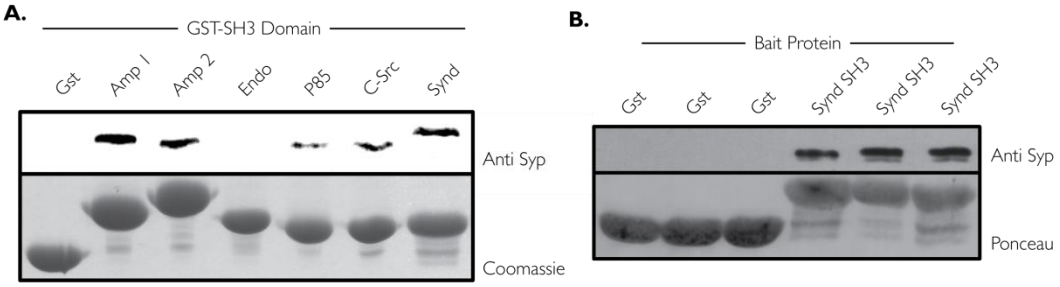

Figure 3-11 The SH3 domain of Syndapin Interacts with Syp

GST bait proteins of the SH3 domains of amphiphysin 1 and 2 (Amp 1 and 2), endophilin 1 (Endo), P85, C-Src and synadpin (Synd) were used in GST-pull downs using synaptosomal lysate. Western blotting with an antibody against Syp was used, to detect interactions of the SH3 domains with Syp. A) The results of the full range of SH3 domain bait proteins and a coomassie stained gel as a loading control from a single experiment. B) Further repeats of the experiment with the SH3 domain of syndapin with a ponceau stain of the nitrocellulose membrane as a loading control. This data is from 3 independent GST-pull downs.

3.2.7 - Single Point Mutation of the SH3 Domain Interaction Motif Showed that the Motif Is Essential for Interaction of Synaptophysin with C-Src and Syndapin

Studies so far have suggested that the SH3 interaction motif on the C-terminus of Syp could be the site of interaction for both C-Src and syndapin, and to a lesser extent amphiphysin 1 and 2. To directly test this, a single point mutant was made in the motif, where the initial residue of the motif (R) was mutated to reverse its charge (R/E). These mutants were made in both the full length C-terminus of Syp and the T1 truncation. The full length Syp C-terminus, full length C- Syp with a mutation of the SH3 interaction motif (C-Syp R), T1 truncation and T1 with the mutant interaction motif (T1 R) were used as bait in GST-Pull Down experiments using both synaptosomal and bacterial lysates (figure 3.12A).

When the pull down from synaptosomes was run on a coomassie stained large gradient gel, there are differences in proteins that interact with the different C-syp baits (figure 3.12B). The WT C-syp binds many bands that are also found in the T1 lane, suggesting the SH3 interaction motif alone is sufficient to mediate such interactions. There are also bands which are found in the full length C-syps (WT and the R point mutation) that are not present in the T1 (T1 and T1 R) lanes, reaffirming the conclusion that there might be other interaction motifs on the C-terminal or that some proteins are sensitive to the folding of the C-terminal.

To look at specific protein interactions, these GST-pull down samples were blotted for amphiphysin 1 and 2. This showed that the SH3 interaction motif is not the

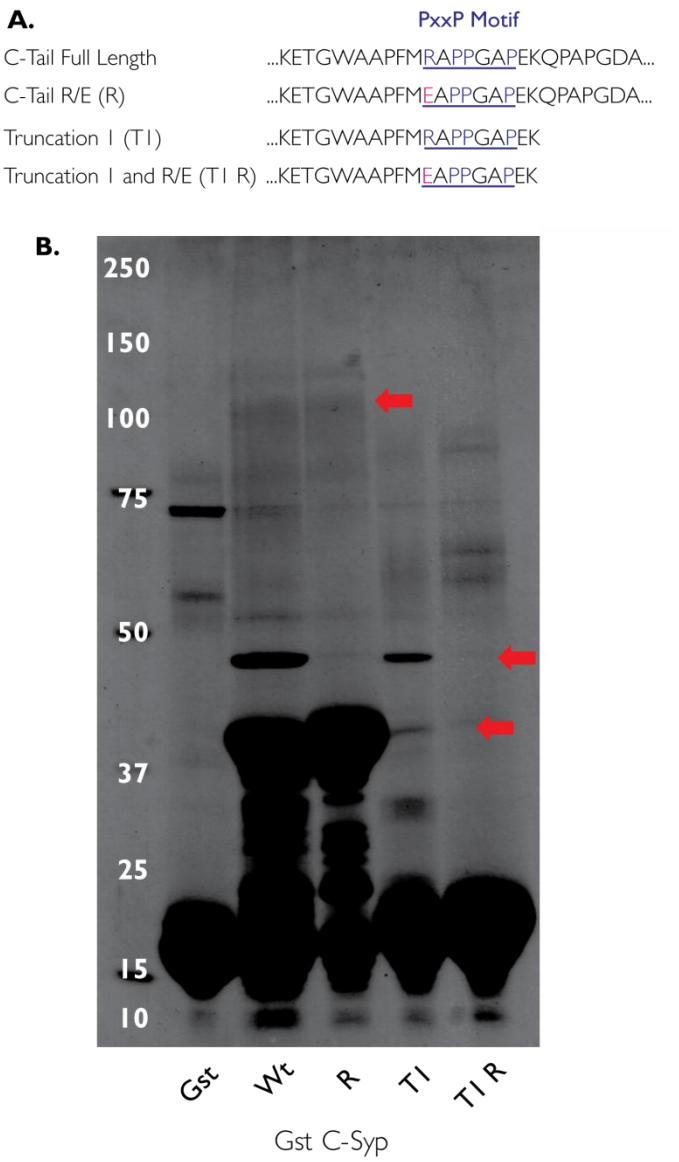

Figure 3-12 The SH3 Interaction Motif on the C-Terminal of Synaptophysin Regulates many Interactions

A) Single point mutations of the SH3 interaction motif were made, where the basic residue of the motif (RxxPxxP) was mutated (R to E). This mutation was made in both the full length and the T1 truncation of the C-terminus of Syp. B) GST bait proteins were generated of these SH3 interaction mutants of the C-terminal of Syp and were used in GST-pull down experiments with synaptosomal lysates. The samples were then separated by use of a large gradient SDS-PAGE gel, and subjected to coomassie staining. A few examples of differences in the protein that interact with the SH3 interaction motif are highlighted by red arrows.

primary site of interaction (figure 3.13A, B and D) since the single point mutation of the motif in the full length C-terminal failed to significantly reduce the interaction. The T1 truncation was significantly different when compared to the full length, in agreement that the SH3 motif is not the major interaction site for amphiphysin 1 and 2 (figure 3.10B). These data highlight that amphiphysin 1 and 2 do not use the SH3 interaction motif on Syp as their main site of interaction.

Previous pull downs using the pGEX 4T-1 Syp C-terminus suggested that syndapin could bind to the SH3 interaction motif (figure 3.10B). To test if the interaction between syndapin and Syp was mediated by the SH3 interaction motif western blotting was preformed for syndapin (figure 3.13C, D). The SH3 interaction motif mutant in the full length Syp C-terminal completely ablated the interaction. This strongly suggests that the SH3 interaction motif is the site of interaction for syndapin. Thus syndapin interacts with Syp via the SH3 interaction motif. This is corroborated by the fact that the single point mutation in T1 also ablates the interaction.

To test whether C-Src also interacted with the SH3 interaction motif on the C-terminal of Syp, GST-pull downs were performed from bacterially expressed full length C-Src, as there were no antibodies available which can differentiate between C-Src and the neuronal splice variants to allow use of synaptosomal lysate. A similar result to the syndapin was found; the single point mutation in both the full length C-terminal of syp and the T1 truncation significantly reduced the levels of interaction

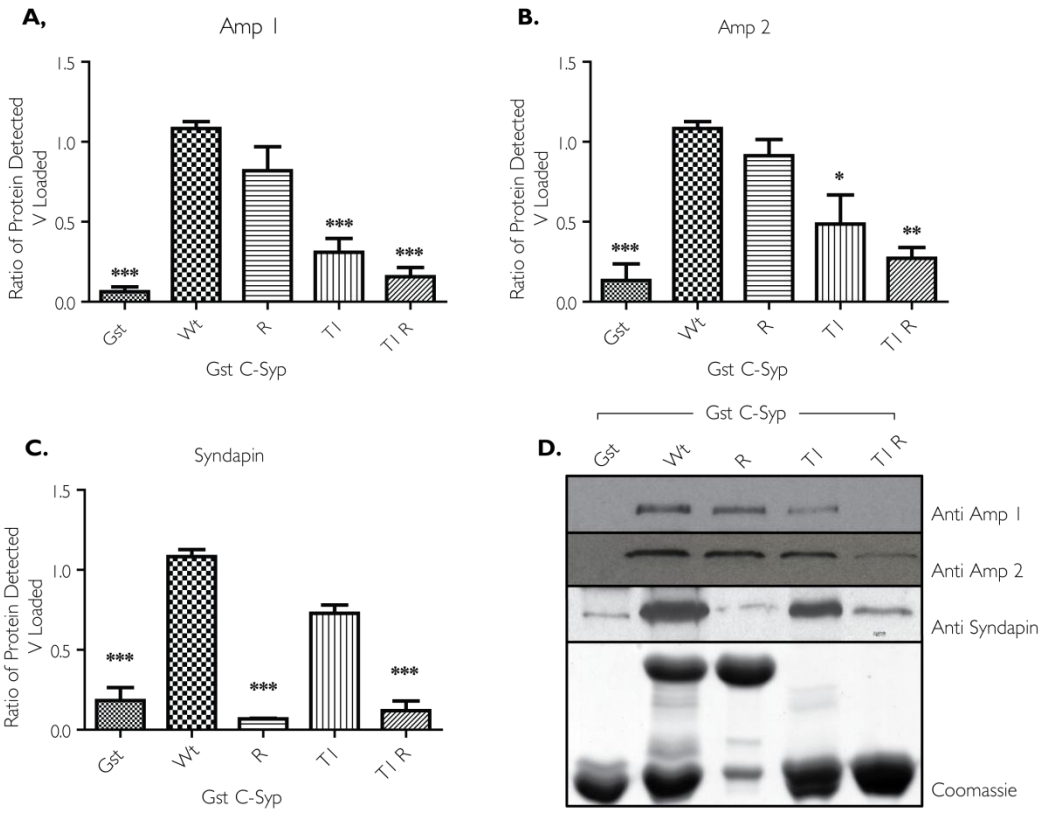

Figure 3-13 GST Syndapin Binds to the C-terminal of Synaptophsyin via the SH3 Interaction Motif

GST-pull down experiments were conducted using the SH3 interaction motif mutant versions of the C-terminal of Syp (as described in figure 3.12) as bait when pulling down from synaptosomal lysates. The amount of interaction of each of the conditions were analysed by densitometry of the western blots using antibodies for A) amphiphysin 1 (Amp 1) B) amphiphysin 2 (Amp 2) and C) syndapin. Coomassie staining was used as an internal control for the amount of GST loaded in each lane. One-way ANOVA, n= ≥3 independent experiments for all for the conditions, * = $p<0.05$, ** = $p<0.01$ and *** = $p<0.001$ when compared to WT. Graph bars are means ± SEM. D) Representative western blots for each set of data are shown.

when compared to the WT C-syp (figure 3.14A, B). Therefore, the SH3 domain of C-Src interacts with the SH3 interaction motif on the C-terminal of Syp.

The SH3 interaction motif is comprised of 3 key residues, a basic R and the 2 prolines. To conclude that the SH3 interaction motif binds to C-Src, there were further mutants were produced to test the involvement of all 3 residues for the interaction with C-Src. These were R229E (R), PP232 and 235AA (AA) and R229E combined with PP232, 235AA (RA). As before, these mutants were used as bait to extract full length C-Src from bacterial lysate. The results show that interaction between C-Src and the C-terminal of Syp is significantly disrupted by both the R and the AA Syps, and the RA Syp disrupted the interaction in an additive manner (figure 3.15A, B). This was complemented by results using the T1 truncation with the same key residues mutated; the single point mutation significantly reduces the levels of interaction and this reduction is increased when the triple mutant is used.

It can be there concluded that all three residues in the SH3 interaction motif are fundamental to the interactions of C-Src with Syp. This confirms that these interactions of Syp are via the SH3 domains of syndapin and C-Src and the SH3 interaction motif on the C-terminus of Syp.

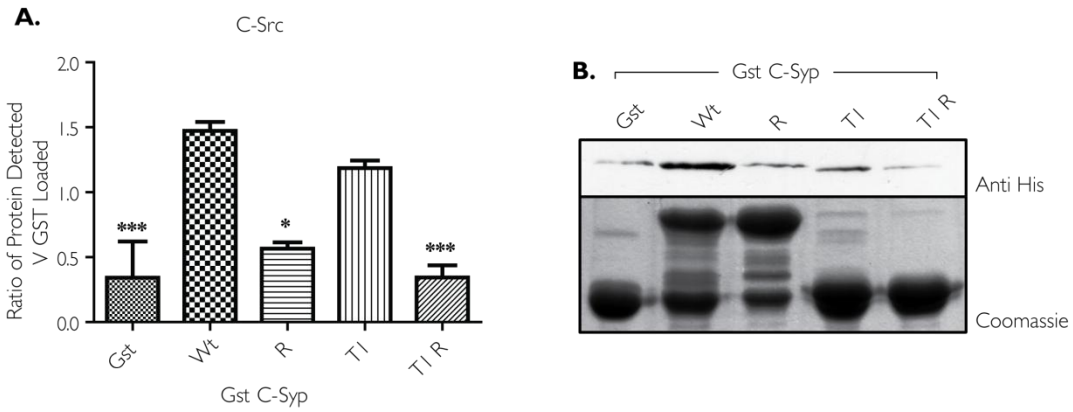

Figure 3-14 A Single Point Mutation in the SH3 Interaction Motif on the C-terminal of Synaptophysin Disrupts the Interaction with C-Src

GST bait proteins were made of the SH3 interaction mutants of the C-terminal of Syp (as described in figure 3.12) and used in GST-pull down experiments that used bacterial lysate overexpressing His tagged full length C-Src. The samples were quantified using western blotting using an antibody that detects His. Coomassie staining was used as an internal control for the amount of GST loaded in each lane. A) Densitometry analysis of the relative amounts of protein detected normalised to GST loaded and plotted for His. One-way ANOVA, n=5 independent experiments for all for the conditions, * = $p<0.05$ and *** $p=<0.001$ when compared to WT. Graph bars are means ± SEM. B) Representative western blots are shown.

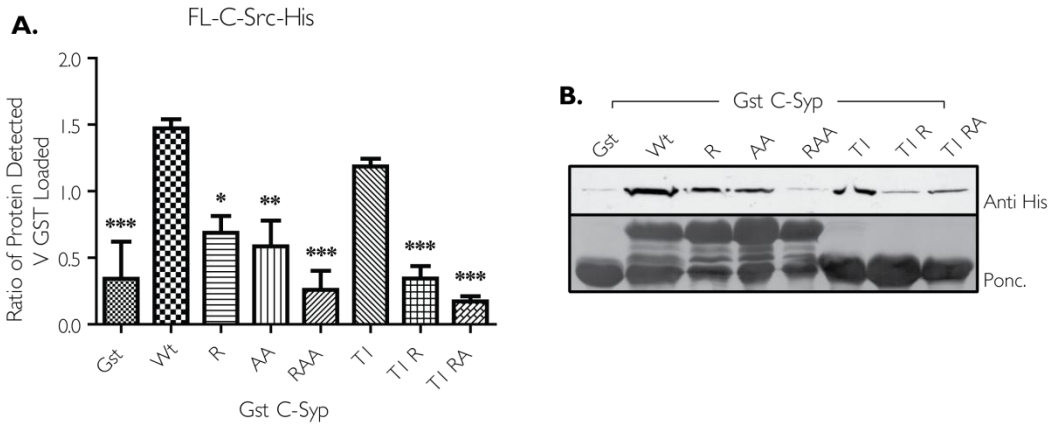

Figure 3-15 The Entire SH3 Interaction Motif on the C-terminal of Synaptophysin is Important for the Interaction with C-Src

GST-bait proteins of the C-terminal of Syp (R229E (R), PP232 and 235AA (AA) and R229E combined with PP232, 235AA (RA)) were made and used in GST-pull down experiments with bacteria lysate that overexpressed His tagged full length C-Src. Western blotting revealed the extent of interaction for each of these conditions. Coomassie staining was used as an control for the amount of GST loaded in each lane. A) Densitometry analysis of the relative amounts of protein detected normalised to GST loaded are plotted. One-way ANOVA, n=5 independent experiments for all for the conditions, * = $p<0.05$, ** =$p<0.01$ and *** $p=<0.001$ when compared with WT. Graph bars are means ± SEM. B) Representative western blots are shown.

3.2.8 Immunocytohistochemistry Staining Shows that Mutants of the SH3 Interaction Motif Result in Mis-Localisation of Syp and VAMP

The SH3 interaction motif on the C-terminal of Syp is a key interaction site for syndapin and C-Src binding. To test if these interactions had any obvious functional consequences, the binding mutants were created in mCerulean (Cer) tagged full length Syp (Cer-Syp) and transfected into Syp knockout cortical neurons (Eshkind and Leube, 1995). A screen was conducted using immunocytohistochemistry, where the synaptic proteins synapsin and VAMP were used as markers. Synapsin was used to determine whether the Cer-Syp constructs were localised to clusters of SVs, and VAMP was used as it would highlight any mis-localisation of VAMP from the nerve terminals. If the Cer-Syp RA (R229E combined with P232, 235A) did not localise with synapsin, it could be assumed that the SH3 motif, and the interactions it facilitates for Syp, might be responsible for Syp localisation to clusters of SVs.

To compare the co-localisation of endogenous synapsin and Syp (figure 3.16) a Pearson's coefficient was calculated. A value of 1 would indicate perfect co-localisation between the two proteins tested, where a value of 0 would prove that there is no co-localisation. The results revealed that both the Cer-Syp and the Cer-Syp RA mutant co-localised very well with synapsin; the Cer-Syp scored a Pearson's coefficient value of 0.56 ± 0.05 and Cer-Syp RA had a value of 0.66 ± 0.07.

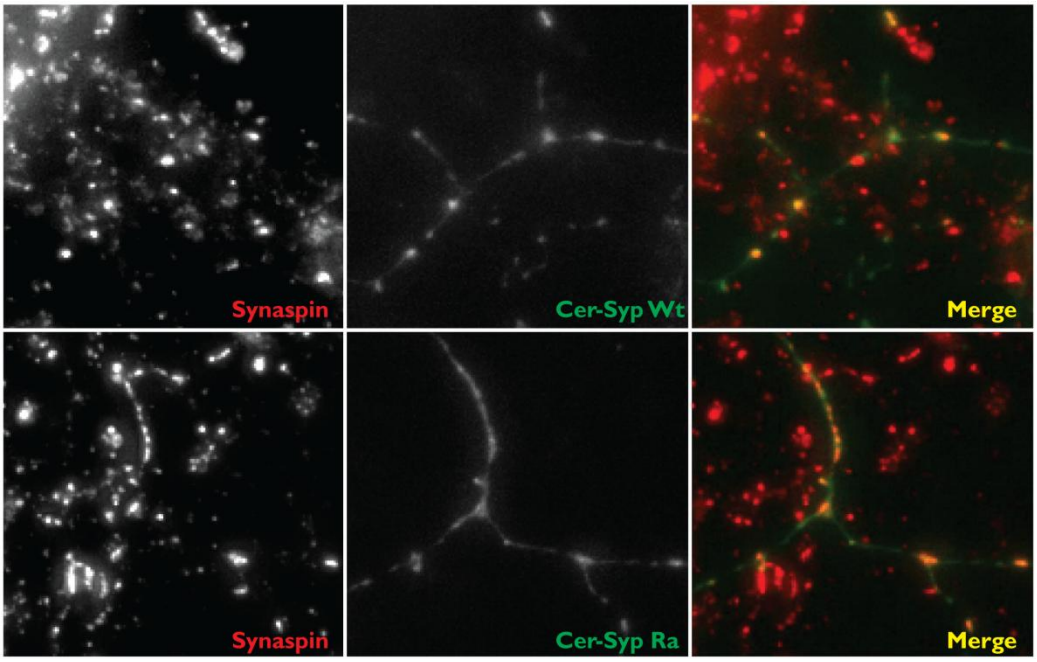

Figure 3-16 Expression Pattern of the SH3 Interaction Motif Mutant Synaptophysin with Synapsin

Representative images of cortical neurons derived from Syp knockout mice were transfected with mCerulean tagged Syp are shown. Cells were transfected with either the WT or a SH3 interaction mutant (R229E combined with PP232, 235AA (Ra) Green). The neurons were fixed and stained with a primary synapsin antibody (red). An Alexa 468 secondary antibody was then used to allow dual channel images to be captured to analyse the localisation of the Cer tagged Syps with synapsin. Overlay of the images are shown in the right panel.

Therefore, it was concluded that the SH3 interaction motif, and the interactions disrupted by the binding mutant (Cer-Syp RA), is not responsible for how Syp is localised to SVs clusters.

A coefficient of variance (COV) was also calculated from these images. This value provided information about the dispersion of fluorescence across the axon which can be interpreted as a measure of the punctuate nature of fluorescently labelled proteins, thus highlighting if the Wt and mutant Cer-Syps form the expected expression pattern of synaptic puncata. If a COV value is 1, then the expression of the fluorescence protein is very concentrated in one area along the length of neuron tested; which is suggestive of clustering in puncta. A value of 0 indicates that the protein is diffuse across the length of the neuron. Neurons that had been transfected with either Cer-Syp of Cer-Syp RA were compared using this measure, and no difference was detected (the COV for Cer-Syp was 0.64 ± 0.057 and 0.60 ± 0.053 for Cer-Syp RA). The same results was seen when comparing the synapsin staining in the Cer-Syp and Cer-Syp RA transfected cells, the COVs were not significantly different from each condition (Cer-Syp - 0.78 ± 0.09, and Cer-Syp RA - 0.56 ± 0.12). These data supports the notion that the SH3 interaction motif is not responsible for the localisation of Syp to clusters of SVs.

A VAMP antibody was also used on Syp knockout cortical neurons that had been transfected with the Cer tagged Syps. The localisation of VAMP should be very punctate as it is expressed on the SV, and as the SV is where Syp is classically thought to be localised, one would expect there to be high levels of co-localisation

with VAMP and Syp. This is what was found when neurons that had been transfected with the different Cer-Syp were fixed and stained for VAMP (figure 3.17). The WT Cer-Syp and VAMP had a Pearson's coefficient of 0.8, which indicates that the two proteins co-localise very well. The Cer-Syp transfected cells were also analysed to determine a COV value, and it was found that both VAMP and Cer-Syp form punctata; values of 1.0 and 0.9 respectively. This means that both VAMP and Cer-Syp have very high levels of co-localisation, and where they do co-localise they both form puncata; which could be on the SVs.

Cer-Syp RA was used to see if the SH3 interaction motif on the C-terminal of Syp is responsible for the co-localisation between Syp and VAMP and if the SH3 interaction motif causes the puncate expression pattern seen in the WT Cer-Syp transfected Syp knockout cortical neurons. Examination of neurons that had been transfected with Cer-Syp RA (figure 3.17) revealed that there were lower levels of co-localisation (a Pearson's coefficient of 0.58) with VAMP than the WT counterpart cells Pearson's value of 0.8). This suggests that the SH3 interaction motif might be the region of syp that localised Syp with VAMP and therefore the SVs, or it is located at the neuron cell surface.

When the COVs were compared between WT and RA transfected neurons, the puncate expression pattern of VAMP changed to a more diffuse expression throughout the whole neuron (in Cer-Syp transfected cells COV = 1, in Cer-Syp RA transfected cells = 0.53). A smaller difference was seen when comparing the COV of the transfected Cer Syp constructs; COV for WT Cer-Syp = 0.9, for Cer-Syp RA = 0.65.

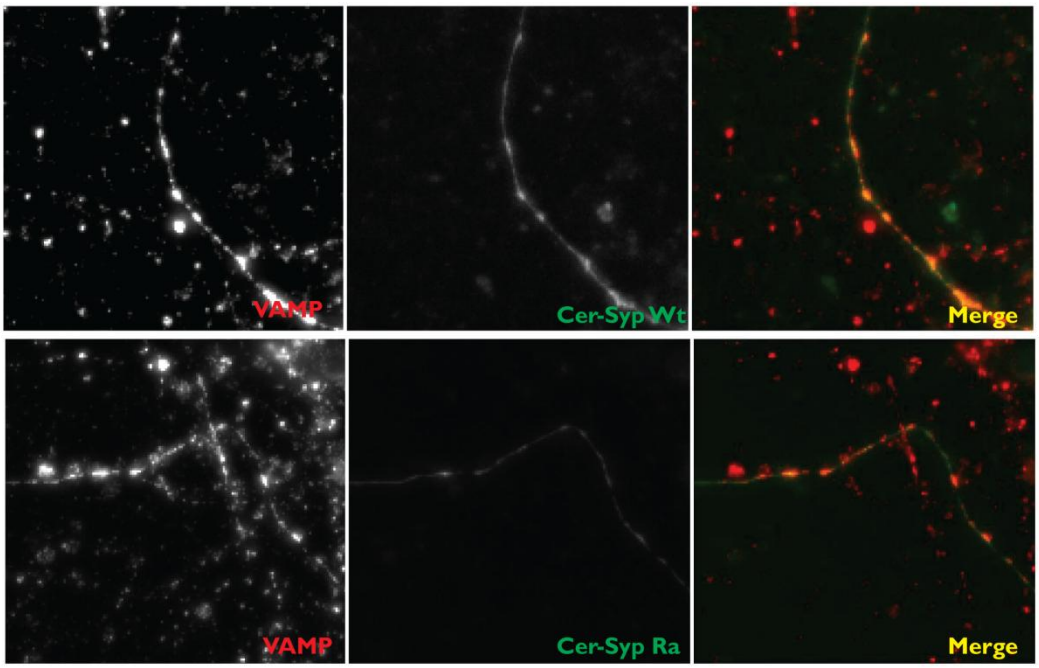

Figure 3-17 Expression Pattern of the SH3 Interaction Motif Mutant Synaptophysin with VAMP

Representative images of cortical neurons derived from Syp knockout mice were transfected with mCerulean tagged Syp are shown. Cells were transfected with either the WT or a SH3 interaction mutant (R229E combined with PP232, 235AA (Ra), green). The neurons were fixed and stained with a primary VAMP antibody (red). An Alexa 468 secondary antibody was then used to allow dual channel images to be captured to analyse the localisation of the Cer tagged Syps with VAMP. Overlay of the images are shown in the right panel.

Interestingly, some cells transfected with Cer-Syp RA mutants were observed to have 'blobs' of fluorescence at the end of processes. After re-examination of the RA (R229E combined with PP232, 235AA) mutant sequence it was found that the mutagenesis has resulted in the formation of a motif for ApaG domain (RAPPGAP to EAPAGAP) (Cicero et al., 2007). This was only found after extensive database searching, and could explain why the RA constructs produced a 'blobby' phenotype. These 'blobs' were only seen in the some of the cells, and cell in which they were present were discarded from analysis

Taken together, it can be concluded that the SH3 interaction motif of the C-terminal of Syp, although is not important for vesicle clustering, is key in the localisation of VAMP to nerve terminals.

3.2.9 - The SH3 Interaction Motif on the C-Terminal of Syp is not a Trafficking Motif

As it was found that mutations of the SH3 interaction motif of Syp displayed mis-localisation of VAMP (section 3.2.8) trafficking assays were conducted to see what effect the SH3 interaction motif has on Syp trafficking during the SV lifecycle. Syp knockout cortical neurons were transfected with the Cer tagged Syps and imaged during electrical stimulation. This was done by drawing ROIs around the synapses and monitoring how the tagged proteins are trafficked following electrical stimulation (10 Hz for 20 seconds). Previous work has shown that Syp leaves the nerve terminal upon the application of stimulation and then returns with a time constant of 115.4 ± 6.81 seconds (Li and Murthy, 2001). The movement out of the

synapse is indicative of SV exocytosis, and the recovery back in to the synapse highlights retrieval of SVs by endocytosis (figure 2.5). This is exactly what was seen in Syp knockout mice cortical preparations that had been transfected with WT Cer-Syp (figure 3.18A, B). A clear drop in fluorescence was measured upon stimulation which then slowly recovers to baseline levels.

Next the Cer-RA syp was tested to see if the SH3 interaction motif affects Syp trafficking during the SV lifecycle. The trafficking of Cer-Syp RA was similar to that of the WT Cer-Syp; showing movement away from the centre of the synapse followed by recovery (figure 3.18A). Sample images illustrate the diffusion and recovery of fluorescence (arrows, figure 3.18B).

It can be concluded that Cer-Syp RA is trafficked in a similar way as the WT, suggesting that the SH3 interaction motif of Syp is not involved in the trafficking of Syp.

3.2.10 - The SH3 Interaction Motif Does Not Control Synaptophysin Endocytosis

Superecliptic synaptophluorins are pH sensitive fluorescent proteins that are used as reporters of the SV lifecycle; their fluorescence is based on the pH they are exposed to and this allows one to monitor global effects of a specific protein on the SV lifecycle (figure 2.3). Different reporter proteins can provide information on how these proteins are recruited or retrieved during rounds of exocytosis and endocytosis.

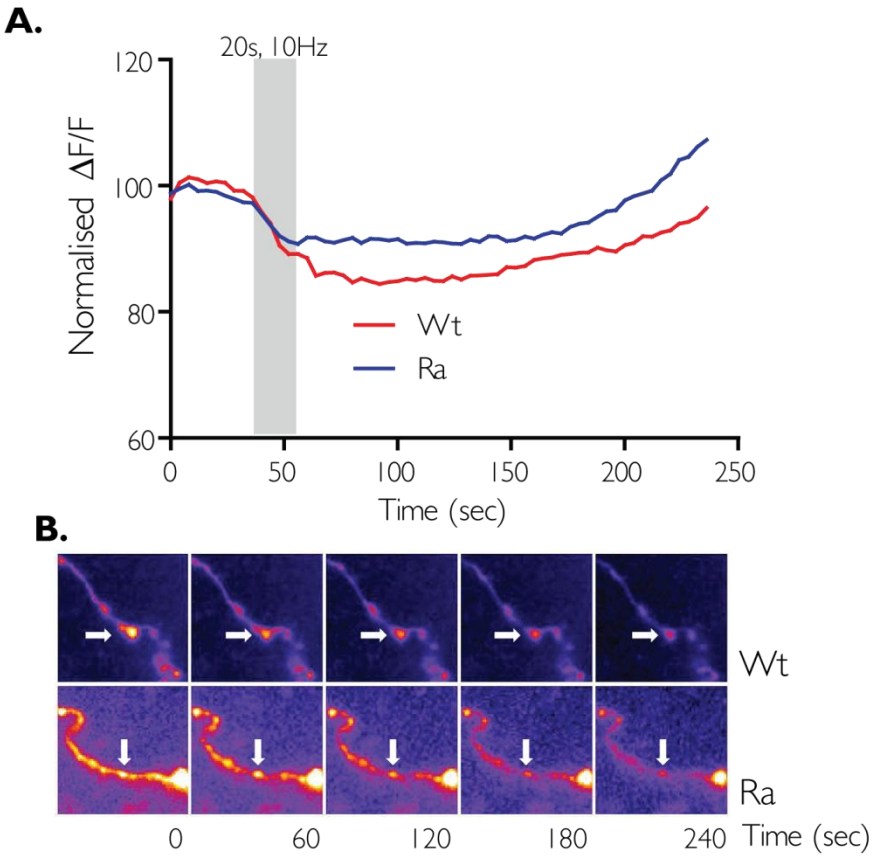

Figure 3-18 The SH3 Interaction Motif on the C-terminal of Synaptophysin is not a Trafficking Motif

Cortical neurons derived from Syp knockout mice were transfected with either WT or the SH3 mutant version (R229E combined with PP232, 235AA (Ra)) of Syp that are tagged with mCerulean. A) Cells were imaged for 10 frames (4 seconds apart) to establish a baseline level of fluorescence, and then electrical stimulation was applied (10 Hz for 20 seconds - highlighted by the grey shading). Images were captured for a further 50 frames (200 seconds). The change in fluorescence in defined ROIs was normalised to the baseline level and plotted against time. B) Representative images sampled at various time points during an experiment for each condition are shown in false colouring. (n=2 for both conditions). White arrows note an example ROI.

To further confirm that the SH3 interaction motif was not involved in the trafficking of Syp, and to see if the interactions that it regulates have an effect on the SV lifecycle, superecliptic synaptophluorins were used. Comparisons were made between a WT Syp phluorin (SypHy) and a single point mutant in the SH3 interaction motif Syp (R229E - SypHy R). Syp knockout cortical neurons were used and transfected with these constructs. The single point mutant of the SH3 interaction motif (R229E) was used in case the potential gain of function, caused by the triple mutation (R229E combined with PP232, 235AA) creating a potential ApaG interaction motif (APAG), affected the results.

Values of fluorescence intensities from the experiments using the WT SypHy and the SypHy R were normalised to the peak response during the NH_4Cl perfusion, which reports the size of the total pool of SVs (Kim and Ryan, 2009). This will provide details of the proportion of SVs that fused with the plasma membrane following a stimulation of 10 Hz for 30 seconds (figure 3.19A). Both the WT and the R Syp phluorin have a recycling pool of about 40% of the total pool of SVs labelled with the phluorin, and thus there is no clear difference between the traces of how these SVs undergo SV recycling, suggesting that there is no effect on SV exocytosis.

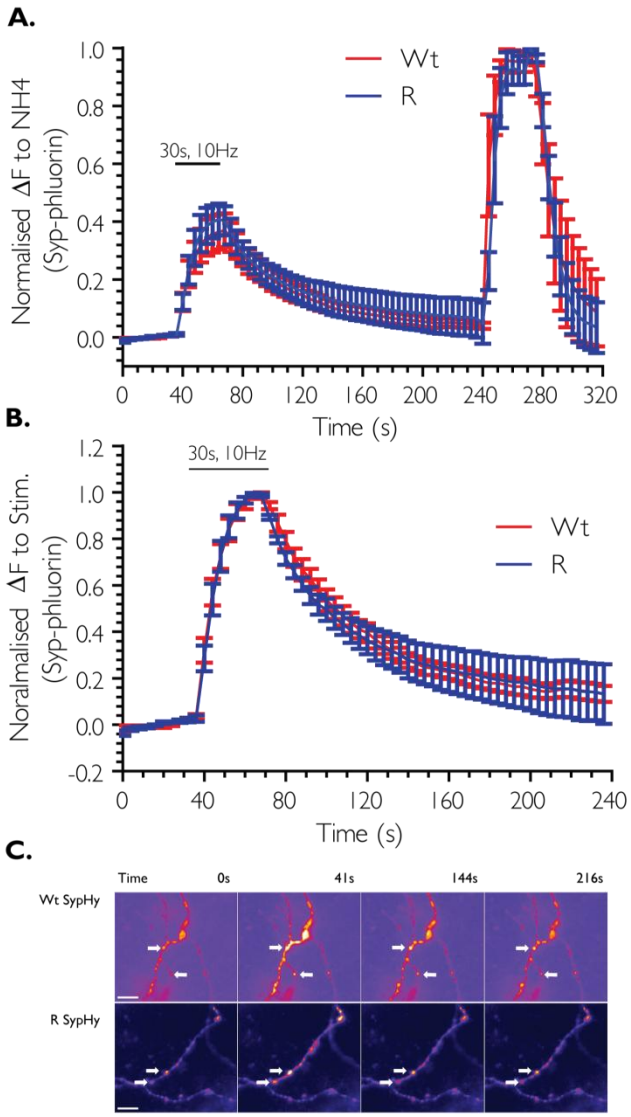

Figure 3-19 The SH3 Interaction Motif Mutant has no Role in the Recycling of Synaptophysin

Cortical neurons derived from Syp knockout mice were transfected with superecliptic Syp phluorin, either a WT or a single point SH3 interaction motif mutant (R229E (R)) version. The neurons were imaged for 40 seconds, to establish a baseline level of fluorescence, and then an electrical stimulation was applied to the neurons (10 Hz for 30 seconds). The cells were imaged for a further 200 seconds where a short perfusion of NH_4Cl was applied for 30 seconds. The changes in fluorescence over time were normalised to A) the peak during the NH4Cl perfusion or B) the peak of stimulation (where the NH4Cl induced change in fluorescence was removed for presentation purposes). Traces are mean ± SEM. C) Representative images are shown in false colouring at various time points. N=4 for both conditions. White arrows highlight example ROIs.

Although the recycling pool size is unchanged, the rate of retrieval might be affected by the mutant Syp. To determine the kinetics of SV retrieval, the fluorescent traces were normalised to their peak responses during stimulation (figure 3.19B, C). When comparing the WT and the R phluorins, there was no significant difference detected in the kinetics of fluorescent recovery to baseline levels (τ values of 42.5 ± 4.566 and 40.97 ±9.207 for the WT and the R phluorin respectively).

These data suggest that the SH3 interaction motif on the C-terminal of Syp is not responsible for the physiological trafficking of Syp in the recycling pool of SVs. Further to this, the interaction motif does not appear to mediate any interactions of Syp that disrupt the SV lifecycle following electrical stimulation.

3.2.11 - Synaptophysin is Fundamental in the Retrieval of VAMP from the Plasma Membrane and this is mediated via the SH3 Interaction Motif on Synaptophysin

Experiments detailed in section 3.2.10 showed that the SH3 interaction motif on the C-terminal of Syp is not important in the maintenance of SV recycling, or the trafficking of Syp. However, experiments in section 3.2.8 showed that there were defects in the localisation of VAMP in cells that had been transfected with the Cer-Syp RA construct. To see if this mis-localisation, which appeared to be mediated by the SH3 interaction motif, had a physiological affect on the trafficking of VAMP, a VAMP phluorin was used.

An empty Cer vector was transfected into Syp knockout cortical neurons as a control, and to provide data about how the knockout functions without Syp present. When the data of the Cer transfected cells were stimulated with 300 action potentials the fluorescent intensities were normalised to the peak intensity recorded during the NH_4Cl perfusion, the percentage of the vesicles that are available to undergo recycling in Syp knockout neurons is about 30% (figure 3.20A). There was also impartial recovery of fluorescence back to baseline compared to WT. This small impairment in recovery suggests that VAMP is not effectively retrieved from the plasma membrane following exocytosis (figure 3.21).

The results from neurons that had been transfected with Cer-Syp WT were somewhat different; the percentage of recycling vesicles is significantly different to neurons transfected with the Cer control (about 50% of the SVs are recycled, compared to 30% in the Cer transfected neurons) (figure 3.20A), and there is a decrease in fluorescence after stimulation, which suggests that Syp is responsible for retrieval of VAMP from the plasma membrane; this is in agreement with published reports (Gordon et al., 2011). It also shows that Syp is important in the regulation of the amount of VAMP phluorin labelled SVs that can recycle.

When the VAMP phluorin traces for the Cer and the Cer Syp were normalised to the peak of stimulation (figure 3.21A), the amount of fluorescence decrease seen in the WT cells is significantly different to those with the Cer vector. Further to this the

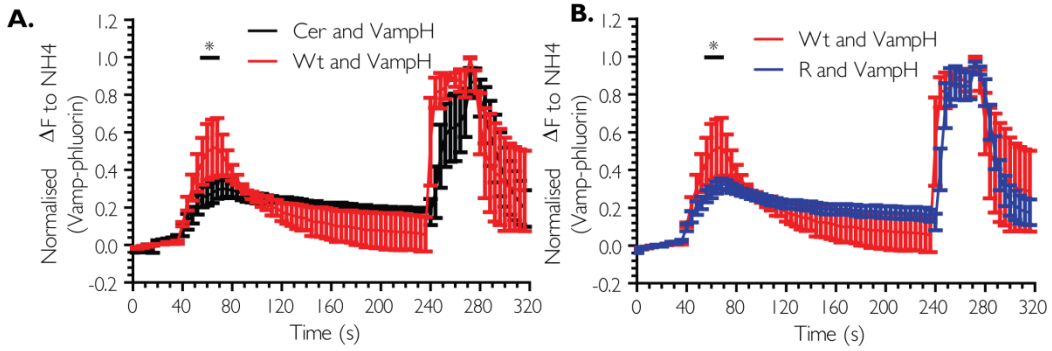

Figure 3-20 The Effect of the SH3 Interaction Motif Mutant on the Recycling Pool of VAMP

Cortical neurons derived from Syp knockout mice were transfected with superecliptic VAMP phluorin and a mCerulean construct of; the empty mCerulean vector (Cer), wild type Syp (WT) and a single point SH3 interaction motif mutant (R229E) version of Syp (R). The neurons were imaged for 40 seconds, to establish a baseline level of fluorescence, and then an electrical stimulation was applied to the neurons (10 Hz for 30 seconds). The cells were imaged for a further 200 seconds where a short perfusion of NH_4Cl was applied for 30 seconds. The changes in fluorescence over time were normalised to the peak during the NH4Cl perfusion to compare the effects of A) Cer with WT and B) Wt and R on VAMP recycling. Statistical testing was conducted by means of a two-way ANOVA, * indicates $p<0.05$. N = 4 for Cer, n = 3 for WT and n = 8 for R. Traces are the mean ± SEM.

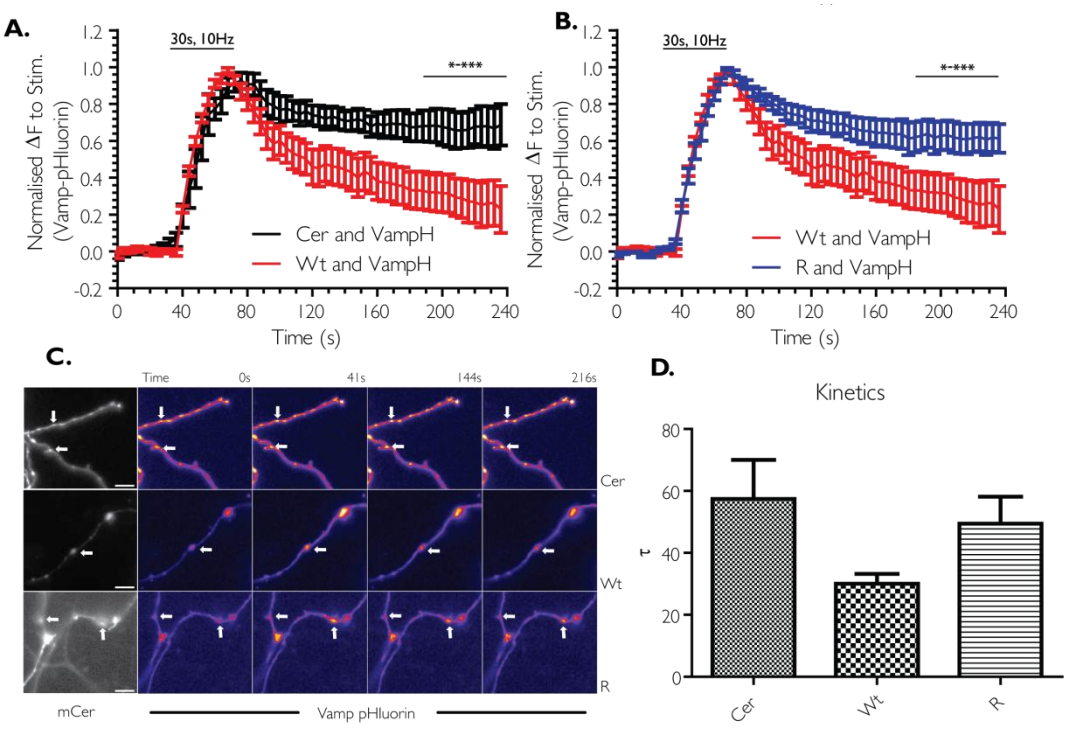

Figure 3-21 The SH3 Interaction Motif Mutant cannot Rescue VAMP Retrieval in Synaptophysin Knockout Mice

Cortical neurons derived from Syp knockout mice were transfected with superecliptic VAMP phluorin and a mCerulean construct of; the empty mCerulean vector (Cer), wild type Syp (WT) and a single point SH3 interaction motif mutant (R229E) version of Syp (R). The neurons were imaged for 40 seconds, to establish a baseline level of fluorescence, and then an electrical stimulation was applied to the neurons (10 Hz for 30 seconds). The cells were imaged for a further 200 seconds. The changes in fluorescence over time were normalised to the peak during stimulation to compare the effects of A) Cer with WT and B) Wt and R on VAMP retrieval. Plots are the mean ± SEM. Statistical testing was conducted by means of a two-way ANOVA, * indicates $p<0.05$, *** indicates $p<0.01$. C) Representative images are shown in false colouring at various time points. D) τ values for the VAMP retrieval are plotted as their means ± SEM. N = 4 for Cer, n = 3 for WT and n = 8 for R. White arrows highlight example ROIs.

rate of decrease is also faster; where the WT cells have a τ value of 30.06 ± 3.18 compared to the Cer τ value of 57.45 ± 12.06. Thus, Syp is responsible for the retrieval of VAMP from the plasma membrane following exocytosis, complementing published results (Gordon et al., 2011).

To determine if the SH3 interaction motif was responsible for these proposed roles of Syp, the Syp knockout cortical neurons were transfected with Cer-Syp R. The results mirrored those seen when comparing the Cer-Syp transfected neurons with the Cer controls transfected neurons. When the data was normalised to the peak of the NH_4Cl perfusion (figure 3.20B), the percent of the SVs in the recycling pools of the neurons transfected with Cer and the SH3 interaction mutant version of Syp were significantly different as shown by the difference in peak size. Also, in the Cer-Syp R traces, there was an impairment of florescent recovery following the applied stimulation, just as in the Cer cells This suggests that the single point mutation in Syps SH3 interaction motif renders the Syp protein unable to conduct its physiological role in the SV lifecycle.

Normalising the Cer-Syp R fluorescent traces to the peak of stimulation also showed the same result as the Cer control cells (figure 3.21B); the amount of fluorescence recovery following stimulation is significantly different when compared to the Cer-Syp transfected cells. The kinetics also reflects the data from the Cer control cells as the WT cells have a τ value of 30.06 ± 3.18 where the R transfected cells have 49.44 ± 8.7. Again, suggesting that the point mutation prevents Syp from completing its physiological role.

This data highlights that the SH3 interaction motif on the C-terminal of Syp is fundamental for the retrieval of VAMP from the plasma membrane during the SV lifecycle. Further to this, one can conclude that the SH3 interaction motif of Syp can regulate the percentage of VAMP phluorin labelled SVs that can enter the recycling pool.

It is possible that these results might be explained by the possibility that VAMP might interact with Syp via the SH3 interaction motif. Therefore, an important control for these VAMP phluorin experiments was conducted using a GST-pull down. The C-terminal of Syp was used as bait against synaptosomal lysate and western blotting for VAMP clearly showed that there was no interaction detected between C-Syp and VAMP (figure 3.22). Further to this, all the possible mutations of the SH3 interaction motif of C-Syp were also tested, and none showed any interaction with VAMP. Therefore VAMP is unable to interact with either WT or the mutated C-terminals of Syp. This means that the conclusion that Syp and its SH3 domain interaction motif is responsible for VAMP retrieval in the SV lifecycle still stands.

3.2.12 - A Mass Spectrometry Approach to Produce a Catalogue of Proteins that Interact with Synaptophysin

Section 3.2.11 showed that the retrieval of VAMP from the plasma membrane during the SV lifecycle is dependent on an interaction of Syp that depends on the SH3 interaction motif of Syp. Therefore it was important to identify every protein that interacts with Syp to see if there were any obvious candidate proteins that act

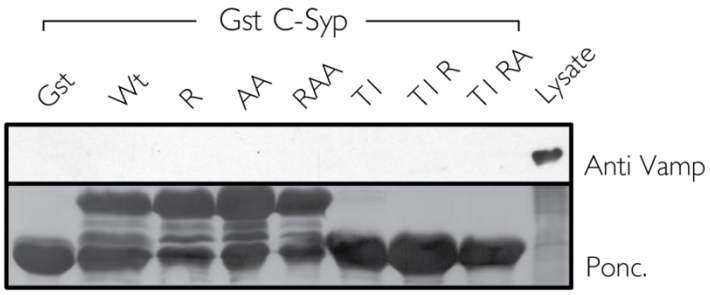

Figure 3-22 VAMP does not Interact with the C-terminal of Synaptophysin

GST-bait proteins of the C-terminal of Syp (R229E (R), PP232 and 235AA (AA) and R229E combined with PP232, 235AA (RA)) were made and used in GST-pull down experiments with synaptosomal lysate. Western blotting revealed the extent of interaction for each of these conditions by use of a VAMP antibody. Coomassie staining was used as a control for the amount of GST loaded in each lane. Lysate was added as a positive control. Representative western blots are shown from 3 independent experiments.

as the VAMP retrieval adaptor complex. And further to this it is important to determine which of these is mediated with the SH3 interaction motif on the C-terminal of Syp.

GST Pull downs were conducted from synaptosomal lysate using the WT C-terminal of Syp as bait. The sample was then run on a large SDS-PAGE gel, stained with colloidal coomassie and 1 centimetre slabs were cut from the WT C-Syp lane for identification of proteins by mass spectrometry (figure 3.23). A collaboration was founded with Prof. Phil Robinson and Dr. Peter Haines in the CMRI, University of Sydney, who conducted the mass spectrometry. They found 106 different proteins that were able to interact with the C-terminal of Syp (detailed in appendix table 1), of these protein 6 really stood out as interesting endocytosis proteins; amphiphysin 1 and 2, AP2, syndapin, synapsin and synaptotagmin.

To identify which of these might interact with the SH3 interaction motif, mutations and truncations of the C-terminal (figure 3.8) were used in the GST-pull downs, and 46 different proteins bands were cut from the large SDS-PAGE gel (figure 3.23). 10 of these bands were prioritised for analysis, and have provided some clues as to which of the 106 proteins are able to interact with Syp via the SH3 interaction motif. For example, band 27 (figure 3.23) was identified as synapsin, and this clearly shows differences in the amount that it can interact with the WT SH3 interaction motifs when compared to the mutant versions of Syp. For the full results see appendix table one.

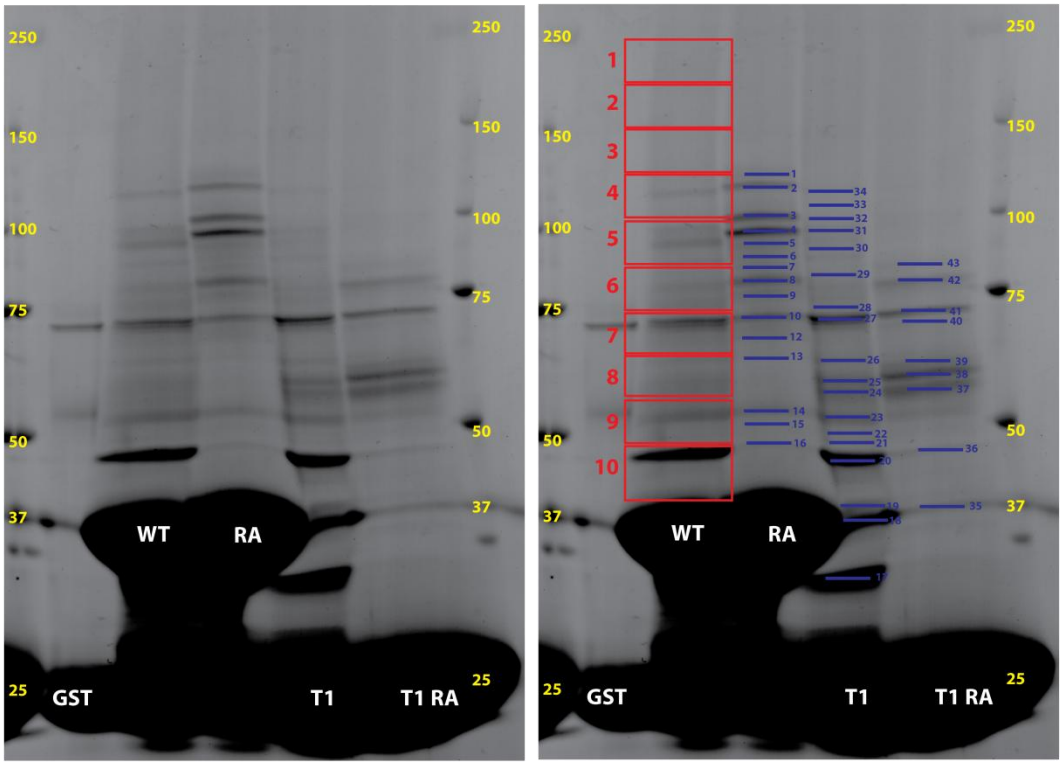

Figure 3-23 GST-Pull down from Synaptosomal Lysate using the SH3 Interaction Motif Mutants to Catalogue all SH3 mediated interactions of Synaptophysin

GST bait proteins were made of WT C-terminal, SH3 interaction motif mutant (R229E combined with PP232, 235AA (RA)), truncation containing just the SH3 interaction motif (T1) and the truncation containing the mutant SH3 interaction motif (T1 RA). These were used in GST-pull down experiments using synaptosomal lysates. The samples were run on a large gradient (7-15%) SDS-PAGE gel and subjected to coomassie staining (left). The gel was then cut (right) to produce about 1 cm 'slabs' of the WT lane, and single protein bands of the SH3 interaction mutant lanes.

The mass spectrometry has, in our knowledge, created the first catalogue of all the proteins that are able to interact with the C-terminal of Syp. It also confirmed that syndapin is an interaction partner of the C-terminal of Syp. The analysis of the cut bands to compare which proteins are mediated by the SH3 interaction motif on the C-terminal of Syp can act as an important step in identifying which proteins interact with Syp to allow the retrieval of VAMP from the plasma membrane during the SV lifecycle.

3.3 - Discussion

The experiments in this chapter have identified and elucidated a novel mechanism of how Syp conducts its physiological role during the SV lifecycle by retrieving VAMP from the plasma membrane. Analysis of the amino acid sequence of Syp revealed that there is a putative type one SH3 interaction motif on its C-terminus; which might be important for its function during the SV lifecycle. Using a rational biochemical approach to indentify interaction partners of Syp, it was found that the C-terminal of Syp has selective interactions with many SH3 containing synaptic proteins; amphiphysin 1 and 2, P85, syndapin, C- and N2-Src. Systematic mutations and truncations of the C-terminal of Syp confirmed that the SH3 interaction motif within it was indeed the site of interaction for C-Src and syndapin. Based on this, Syp binding mutants were then created to address the functional consequences of these interactions. Immunocytohistochemical experiments showed that the binding mutant disrupted the localisation of Syp with VAMP; but had no effect on the trafficking of Syp visualised using superecliptic Syp phluorin. When VAMP phluorin was used to monitor SV recycling in Syp knockout neurons transfected with

either WT Syp or the SH3 interaction mutant, it was observed that the interactions regulated by the SH3 interaction motif on the C-terminal of Syp are critical to the retrieval of VAMP from the plasma membrane. Furthermore, the retrieval of VAMP must be via a complex of proteins that interact with the SH3 interaction motif of Syp as no direct interaction between VAMP and the C-terminal of Syp was found. Preliminary mass spectrometry analysis has provided a catalogue of proteins that can potentially interact with the SH3 interaction motif on the C-terminal of Syp, thus providing a list of potential candidate proteins that form the VAMP retrieval complex and potentially even the VAMP adaptor protein.

3.3.1 - Appraisal of the Biochemical Experimental Approach

GST-pull downs are an *in vitro* method for detecting interactions, and this means that there are inherent advantages and disadvantages to using such a technique to investigate how proteins can interact outside their natural environment. The biggest caveat to consider is that protein lysate is not the natural environment for the proteins; they are no longer localised in their correct cellular compartment so will encounter a collection of proteins they would not normally be exposed to. This can lead to false positive identifications of physiological interaction partners. To minimise the risk of this occurring, the main screening lysate used was of synaptosomes, where only proteins in the nerve terminal would be present. Further to this, experiments in section 3.2.1 validated the methodological approach by examining a range of previously reported interactions and the results in figure 3.2 complemented the published data.

A more physiological method to test for interactions would be to perform immunoprecipitations from synaptosomal lysates. However, as binding mutants of Syp were being tested for their interactions, Syp knockout cells would need to be transfected with different mutant Syps. As transfection efficiency of the cortical neurons is low, HEK cells would have to be used. This presents a similar issue to GST-pull down experiments. HEK cells do not naturally express Syp, therefore Syp would not be in its natural environment and thus could interact differently with any proteins of interest.

In section 3.2.1, GST-SH3 domains were used as bait against synaptosomal lysates as a screen to test if Syp was indeed capable of interacting with SH3 domain containing proteins. In these screening experiments, a GST control was not used. The reason for this is that all the bait SH3 domains were in the same expression vector; therefore they all have the same GST tag. If the GST tag was responsible for the interactions detected, then this would appear as the background level of interaction in all of the samples. In addition, as some of the SH3 domains showed no interaction in the screens, it is unlikely that the GST tag was interacting with any of the proteins of interest.

Once it was found that Syp selectively interacted with certain SH3 domains (amphiphysin 1 and 2, P85, C- and N2-Src) from GST-pull downs from synaptosomal lysate (figure 3.3), it was important to test if these interactions were direct or indirect via a possible protein complex. To do this, a bacterial lysate expressing the C-terminal of Syp was used in similar GST-pull downs (section 3.2.2). Ideally, the

bacterial lysate should have expressed the full length Syp protein, but the full length Syp did not express at all in bacterial cell lines tried. The results from these GST-pull downs found that only N2-Src bound Syp, and amphiphysin 1 and 2, P85 and C-Src interactions were no longer detected (figure 3.4). Why these interactions were not detected could be explained in three ways. First, the interactions might be due to an indirect interaction via protein complexes. Another reason might be because these interactions are phosphorylation dependent. In the synaptosomal lysate there are many kinases present, and this means that many of the proteins (bait proteins and Syp) are phosphorylated. As these kinases are not present in the bacterial lysate, the proteins could be in a different phosphorylation state and therefore could unable their ability to interact with each other. Thirdly, it is also possible that the SH3 domains of C-Src, amphiphysin 1 and 2, do not bind to Syp via its C-terminus, since in the synaptosome GST-pull downs full length Syp was present rather than just the C-terminal.

To begin to investigate if the SH3 interactions detected when pulling down from synaptosomes were mediated by the SH3 interaction motif on the C-terminal of Syp, a mutant form of C-Syp (C-Syp AA) was used as a bacterially expressed lysate for the SH3 domains GST-pull downs (Figure 3.5). It was surprising to find that all the other SH3 domains appear to be able to interact better with the mutant C-Syp, when compared to experiments which used the WT C-Syp. So much so that the graph resembles the result of the pull down from synaptosomes, with the exception of the lack of C-Src SH3 interaction to the mutant C-Syp. Again, the lack of C-Src interaction could be explained by the interaction being phosphorylation dependent,

the interaction being indirect or the interaction site not being on the C-terminal of Syp. However, when reviewing the significance of the results from these experiments (section 3.2.2), it is important to note that western blotting with an anti-his antibody revealed that the C-Syp formed dimmers and tetramers. This could potentially exclude its ability to interact with the SH3 domains. This was detected more in the WT than the AA mutant C-Syp lysate, which may explain why there was a lot less interaction of the SH3 bait domains with the WT than the mutant lysates.

Experiments to further examine the interaction between C-, N2-Src and Syp were conducted using GST-C-Syp as bait from bacterial lysates expressing the full length Srcs. It was shown that the C-Src interaction was likely to be mediated by the SH3 interaction motif on the C-terminal of Syp (Section 3.2.3). A key experiment to confirm these results would have been to use the GST-C-Syp and the mutant Syp (GST-C-Syp AA) as bait against synaptosomal lysate; however at present there are no antibodies which can detect the different splice variants of the Srcs. We have twice attempted to generate N2-Src specific antibodies and even tested N1-Src antibodies with no success.

As the C-Syp AA still binds quite well to the C-terminal of Syp, it would have been interesting to perform similar GST-pull downs using the different domains of Src; such as the SH2 domain to see how much of a contribution to the interaction is afforded by the other Src domains.

To test if the SH3 interaction motif was sufficient for the interactions of C- and N2-Src with Syp, truncation mutations of the Syp C-terminus was made (figure 3.6). The truncations used were designed to test primarily the SH3 interaction motif, and as a result there is a possibility that the end fragment (residues 277-308) might be the site of interaction for the neuronal Srcs (N1- and N2-Src) as they failed to display a full recovery of the interaction when compared to WT C-Syp (figure 3.8). To test this, the end fragment of Syp was cloned into a pGEX vector and similar GST-pull downs were conducted (using full length N1- and N2-Src). Although the data generated was only from one experiment, there was no interaction between the end fragment of the C-terminus of Syp and the neuronal Srcs (data not shown). This suggests that the N2-Src only appears to be able to interact with the full length of the C-terminal, potentially suggesting that folding of the C-terminal maybe important for interactions of Syp, or that it binds to the pentapeptide repeats (YD(P/G)QG), in a similar manner to dynamin 1 (Daly and Ziff, 2002, Gonzalez-Jamett et al., 2010).

The strongest evidence that the SH3 interaction motif on the C-terminal of Syp is key in regulating the interactions between syndapin and C-Src is provided by section 3.2.7, where single point mutations of the motif significantly disrupted this interaction. This was demonstrated by the use of a single point mutation (R) of a triple residue motif (RxxPxxP), therefore only one of the key SH3 interaction motif residues was critical for this interaction with syndapin. However, to conclude that this interaction is mediated by the SH3 interaction motif on the C-terminal of Syp, a GST-pull down should have been conducted using the C-Syp mutants that carried all

the mutations of the SH3 interaction motif, as conducted with C-Src (figure 3.15). However, as shown previously the AA mutant formed an APAG motif, making interpretation of these results difficult. And ideally, this would have also been conducted using bacterial lysate that express the full length syndapin protein to show if the interaction was direct.

3.3.2 - Cellular Function Appraisal

In section 3.2.8, it was found that the SH3 interaction motif mutant of Cer-Syp (RA) showed less co-localisation with VAMP but not synapsin. This observation could be explained as follows; if both the Cer-Syp RA and VAMP are more diffuse in the neuron and not in puncta on the SV, then they are less likely to co-localise, as the area in which the protein is expressed is larger than a small synaptic puncta. The differences in the COV suggest that the SH3 interaction motif of Syp is important in the localisation of VAMP. The expression pattern of Syp into puncta does not appear to be mediated by the SH3 interaction motif; as synapsin staining showed no difference in the WT and RA transfected Syp knockout cells, and the VAMP staining only showed a small effect.

It is important to note that the imaging results for the VAMP staining are from cells from a single experiment, however the result that WT Syp is the protein that localise endogenous and exogenous VAMP to the vesicles was later confirmed by further work of a lab member (Gordon et al., 2011). In this study, WT cells with Syp knock out cells were compared and it was found in the knock out cells that VAMP

was more diffuse compared to WT cells. This serves as further proof that Syp co-localises with VAMP and this is mediated by the SH3 interaction motif of Syp.

Section 3.2.11 showed that there was no direct interaction between VAMP and the C-terminus of Syp, but that the SH3 interaction motif was important in the retrieval of VAMP during the SV recycling. As there is no direct interaction with the domain of Syp that was mutated, it is therefore possible that the retrieval of VAMP is a complex of proteins which have a key interaction with Syp via its SH3 interaction motif. If this is the case and the SH3 interaction motif on the C-terminal of Syp indeed interacts with a protein complex, one of the proteins in this complex may function as an adaptor protein for VAMP. When the interaction between Syp and the SH3 mediated complex is disrupted, the adaptor protein for VAMP is not effectively trafficked in the SV lifecycle, and as a result VAMP remains on the plasma membrane following fusion during exocytosis.

One of the major disadvantages with phluorin assays in this project is the decrease in fluorescence that is a balance of endocytosis and the re-acidification (figure 2.3). Therefore, an effect of VAMP phluorin reported endocytosis could be a result of defective vesicle re-acidification. It has been indeed reported that Syp can interact with the vesicular proton pump v-ATPase (Carrion-Vazquez et al., 1998, Galli et al., 1996, Thomas and Betz, 1990). In order to overcome this, one could conduct the phluorin based assays in the presence of bafilomycin. Bafilomycin inhibits this re-acidification process, which allows direct visualisation of the endocytosis trace during stimulation (Nicholson-Tomishima and Ryan, 2004).

However, it is unlikely that a defective vesicle re-acidification effect plays a role in our observations as the Syp phluorin traces with both the SH3 interaction motif and phosphorylation mutants show a normal trace of endocytosis and re-acidification. Further to this, other papers have used different phluorin tagged synaptic proteins, and bafilomycin, and reported no obvious differences in their endocytosis and re-acidification processes in Syp knockout neurons (Gordon et al., 2011, Kwon and Chapman, 2011).

In experiments where the Cer-tagged Syps were transfected in to a cell, the overall expression profile of WT Syp and single point mutant of the SH3 interaction motif (R) did not result in differences of expression throughout the whole of the neuron (observations of the MAC lab). The expression profile was very different to cells which had been transfect with just the Cer empty vector; therefore the single point mutation did not adversely affect the neurons handling of the mutant and tagged proteins.

3.3.3 - Further Discussion

VAMP phluorin imaging has revealed that the SH3 interaction motif is critical to the retrieval of VAMP from the plasma membrane in the SV lifecycle, and this retrieval was shown to be via an indirect interaction via a complex of proteins rather than a direct interaction between the two proteins. This result challenged previous reports in the field about the nature of the Syp and VAMP interaction. Previous reports have stated that Syp and VAMP interact directly to form a complex that can be purified by immunoprecipitation (Calakos and Scheller, 1994, Edelmann et al.,

1995). The techniques used may render their findings non-physiological, and could be a result of the fact that they purified the complex from synaptosomes rather than intact neurons, where the proteins would be expressed in their correct membrane structures. However, it was found by FRET imaging *in vivo* that it is likely that Syp and VAMP interact in a neuron (Pennuto et al., 2002). When further FRET experiments were conducted with a truncation of the C-terminal of Syp (which kept the SH3 interaction motif), it was found that there was no significant reduction in the interaction (Felkl and Leube, 2008, Pennuto et al., 2002), which suggests the SH3 interaction motif, or other domains of the protein, may be regulating the interaction of VAMP and Syp. However it is worth noting that FRET is not a reporter of interactions, but only an indicator that the proteins are within the distance that represents a molecular interaction. Therefore, it is possible to imagine that there would be high levels of FRET between the two most expressed SV proteins (VAMP has 70 copies and Syp 31 copies (Takamori et al., 2006)) on the small surface area of the SV. This limitation in the use of FRET implies that the experiments have not ruled out the possibility that the SH3 interaction motif on Syp may still interact with VAMP indirectly in the regulation of its retrieval.

One of the interactions that we successfully mapped to be mediated by the SH3 interaction motif that is fundamental to the retrieval of VAMP was an interaction with syndapin. This interaction had never been reported before. However, interpreting how syndapin might be involved in the retrieval of VAMP is difficult. Syndapin is known to interact with dynamin and recruit it to invaginating vesicles with a smaller membrane curvature than typical clathrin mediated endocytosis

vesicles (Clayton et al., 2009, Henne et al., 2007). Combined with the fact the VAMP has been implicated in a rapid form of endocytosis which is clathrin independent (Deak et al., 2004), it suggests that the nature of the endocytosis that retrieves VAMP differs from the classical clathrin mediated endocytosis. To further characterise the functional significance of the Syp and syndapin interaction, one could repeat the VAMP phluorin experiments in a system which has been subjected to shRNA knockdown of syndapin.

Another key interaction identified was with the non-receptor kinase C-Src. The significance of this interaction is highly suggestive that tyrosine phosphorylation of the C-terminal of Syp is indeed important for Syp in retrieving VAMP from the plasma membrane during the SV lifecycle. This interaction had previously been reported (Barnekow et al., 1990), but never mapped to a specific binding site. To further investigate if tyrosine phosphorylation afforded to Syp by a direct interaction could be responsible for the retrieval of VAMP, one could repeat the VAMP phluorin assay with the expression levels of C-Src knockdown with shRNAs. Further to this, a more direct way to test if tyrosine phosphorylation is important in the retrieval of VAMP would be to create a range of phospho-mutants of Syp and investigate their function in neurons.

In summary, a SH3 interaction motif has been identified on Syp that controls VAMP retrieval from the plasma membrane. Potential modulators of the retrieval are C-Src and syndapin.

Chapter 4 Tyrosine Phosphorylation of Synaptophysin

4.1 - Introduction

One of the interesting features of the C-terminal of Syp is that it contains ten pentapeptide repeats, nine of which are initiated by tyrosine residues (figure 1.3, 1.4), and as a result of all these potential tyrosine phosphorylation sites it is the major phospho-tyrosine SV associated protein (Pang et al., 1988). Characterisation of the phosphorylation reaction is lacking. It has been reported that Syp co-purifies in a complex, and can be a substrate for, the non-receptor tyrosine kinase C-Src (Barnekow et al., 1990). A phosphatase has yet to be identified, although it has been suggested to be SH-PTP1 (Evans and Cousin, 2005). Furthermore, identification of the physiological phosphorylation sites has been hampered by the lack of protease cleavage sites on the C-terminal. Online database analysis by NetPhos has predicted that five of the nine potential sites are likely to be phosphorylated *in vivo*. It is only recently that a study has devised a digestion protocol to produce sufficient peptides of the C-terminus to allow mass spectrometry analysis to identify Syp phosphorylation sites. However, this group was investigating tyrosine phosphorylation of Syp during oxidative stress conditions, rather than physiological stimulations (Mallozzi et al., 2009).

Phosphorylation of the C-terminal of Syp is an exciting prospect when imagining how the role of Syp in the SV lifecycle might be regulated. One reason for this is

that the C-terminal of Syp has been shown to be essential in its endocytosis (Linstedt and Kelly, 1991), and as the majority of the C-terminal is made up via these tyrosine repeats, it is tempting to hypothesis that phosphorylation is an important post translational modification that regulates the function of Syp. Another reason that phosphorylation is exciting is that dynamin 1, a fundamental protein in SV endocytosis, has been shown to interact with the tyrosine repeats on the C-terminal (Daly and Ziff, 2002), and phosphorylation is well known to regulate interactions. Indeed, in addition to dynamin, the previous chapter has shown that N1-, N2-Src, amphiphysin 1 and 2 may also bind to the pentapeptide repeats.

Therefore, to understand why the most tyrosine phosphorylated protein on the SV is phosphorylated, one must identify which of the nine potential sites are phosphorylated, and even how Syp is phosphorylated. Once this is achieved, it would offer an insight into what might be the physiological role of Syp in the SV lifecycle.

It has been reported that Syp is a substrate for Src, and the two proteins are found in a complex in intact neurons (Barnekow et al., 1990), suggesting that Src is the major physiological kinase that might phosphorylate Syp *in vivo*. Therefore, it was important to assess if their different modes of interaction with Syp (as described in chapter 3) resulted in a differing ability to phosphorylate it.

The three Srcs differ in their SH3 domains, where an additional short sequence of amino acids is present in the N-Srcs, creating the N-Src loop (N1-Src has 6 extra amino acids, and N2-Src has 17 extra amino acids in their SH3 domains (Chan and

Black, 1995, Matsunaga et al., 1993)) (figure 1.5). In the previous chapter, it was shown that the SH3 domains of C- and N2-Src were able to extract Syp from synaptosomal lysates to a significantly greater extent than N1-Src (figure 4.1A, B). The interaction between Syp and the C-Src SH3 domain was found to be mediated by the SH3 interaction motif on Syp (section 3.2.7). In contrast, while N2-Src is able to bind to Syp at similar levels as that of C-Src, the interaction site was not the SH3 interaction motif.

4.2 - Results

4.2.1 - Differential Phosphorylation of Synaptophysin by C-, N1- and N2-Src

As a starting point to characterising the phosphorylation reactions of the three different Srcs, *in vitro* time course assays were conducted to determine if there were any differences in the speed, and the amount, of phosphorylation of the Syp C-terminus by the Src kinases. Experiments were designed to monitor phosphorylation up to 2 hours while ensuring that the initial rate of reaction was captured with sufficient time resolution. A 2 hour endpoint was used to ensure that data was collected once the extent of phosphorylation had reached its plateau stage. The amount of phosphorylation was detected by western blotting with a PY20 antibody, which recognises any phosphorylated tyrosine residues (tested by the manufacture, BD Biosciences). After western blotting, the amount of phosphorylation detected by the PY20 antibody was normalised to the maximum value. Figure 4.2A shows there was no difference in the time course for the three

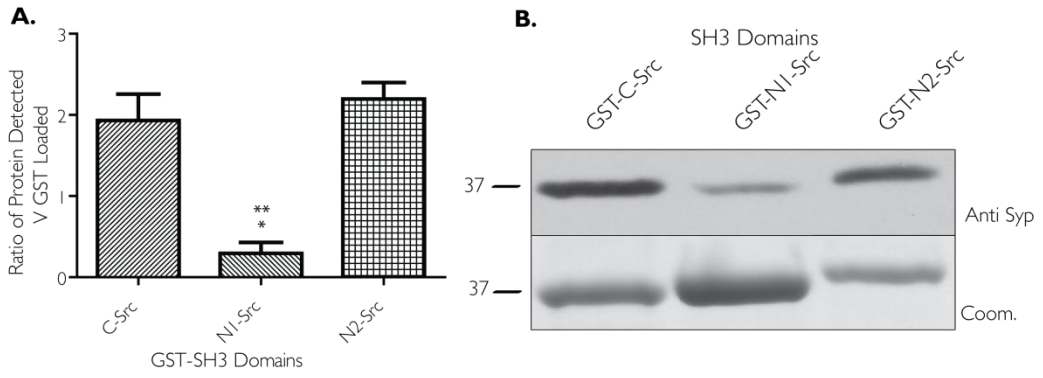

Figure 4-1 Synaptophysin Selectivity Binds to the SH3 Domains of C- and N2-Src

GST baits were generated from the SH3 domains of C-, N1- and N2-Src. Pull-down experiments were performed using synaptosome lysates and quantified using western blotting for Syp. Coomassie staining was used as a control for the amount of GST loaded in each lane. Densitometry analysis of the relative amounts of protein detected normalised to GST loaded and plotted for antibodies against synaptophysin (A). Graph bars are means ± SEM. * ($p<0.05$) and ** ($p<0.01$). One-way ANOVA, n=3 independent experiments for all for the conditions. B) Representative western blots for each set of data are shown.

different Srcs to maximally phosphorylate Syp. This suggests that the mechanism of phosphorylation by the three different Srcs is similar *in vitro*.

However, when the amount of phosphorylation detected at the 2 hour saturation time point was monitored, there was a significant difference in the amount of phosphorylation detected when comparing N1-Src with C- and N2-Src (figure 4.2B). This suggests that the Srcs vary in the amount of Syp they can phosphorylate. The extent of Syp phosphorylation (figure 4.2B) closely resembles that of the GST-pull down using the three different Srcs SH3 domains (figure 4.1A), where C- and N2-Src showed greater levels of interaction with Syp when compared to N1-Src. This could suggest that the different modes of interaction of the three Srcs with Syp regulated the amount of phosphorylation while not affecting the rate.

To confirm the results seen using a PY20 antibody, ATP-γ^{32}P and autoradiography was used to detect any γ^{32}P incorporation to Syp. The reactions were conducted using the same method as the PY20 experiments, with the exception that the non-radio labelled ATP was replaced with ATP- γ^{32}P. Due to the difficulties involved in handling the γ^{32}P, slightly different time points including an endpoint of 30 minutes were used. These time points still allowed capture of the initial rapid phase of the reaction. As data from the PY20 antibody experiments showed that the reaction was at the start of its plateau stage at the 30 minutes time point, the full range of the phosphorylation rate dynamics were captured. The results mirrored those seen using the PY20 antibody. When the autoradiography signal was normalised to its maximum value, there was no difference in the time course of phosphorylation of

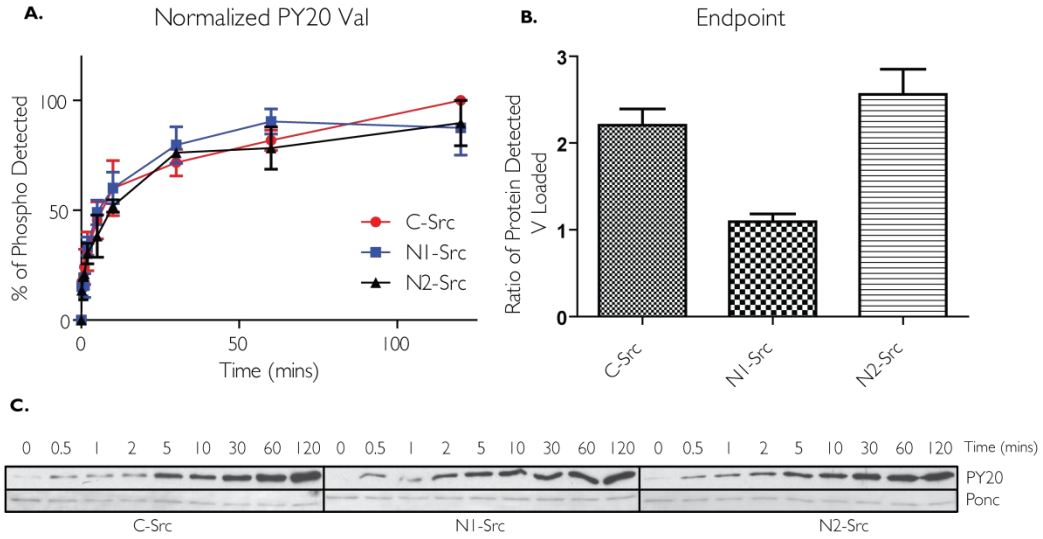

Figure 4-2 Phosphorylation of Synaptophysin by the 3 Different Srcs using a PY20 Antibody

Kinase assays were conducted using the C-terminal of Syp and either C-, N1- or N2-Src. Samples were taken at 0, 0.5, 1, 2, 5, 10, 30, 60 and 120 minutes. The amount of phosphorylation was detected by western blotting using a PY20 antibody. Densitometry analysis revealed the amount of phosphorylation detected, and the results were A) normalised to the maximum PY20 signal. B) To determine the total amount of phosphorylation, the amount of phosphorylation detected was normalised to a ponceau stain of the protein membrane, which provided a loading control, for the 120 minute time point. N=3 independent experiments for C-Src and n = 4 for both N1- and N2-Src. Graph bars and plots are means ± SEM. C) Representative western blots for each set of data are shown.

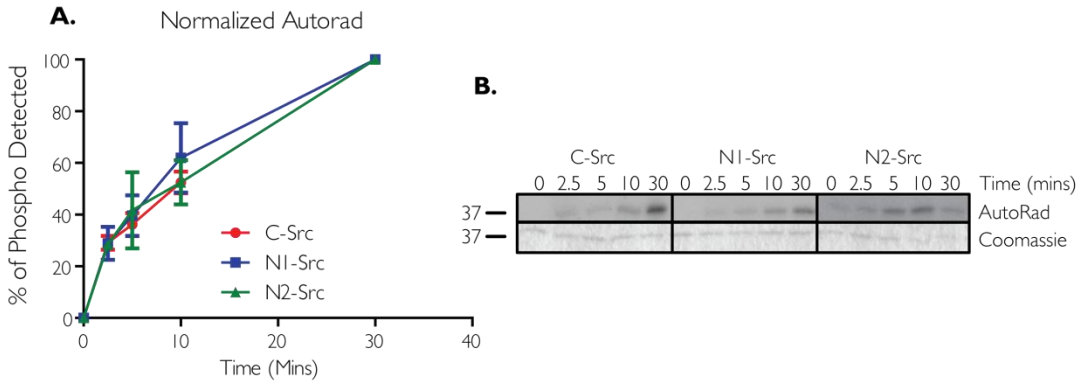

Figure 4-3 Phosphorylation of Synaptophysin by the 3 Different Srcs using Autoradiography

Kinase assays were conducted using the C-terminal of Syp and either C-, N1- or N2-Src. Samples were taken at 0, 2.5, 5, 10 and 30 minutes. The amount of phosphorylation was detected by autoradiography. Densitometry analysis revealed the amount of phosphorylation detected, and the results were A) normalised to the maximum autoradiography signal. n=4 independent experiments for C-Src and n = 3 for both N1- and N2-Src. Graph plots are means ± SEM. B) Representative western blots for each set of data are shown.

Syp by the three different Src kinases (figure 4.3A). The endpoint saturation amounts of phosphorylation were not compared as an earlier different end time point was used in compared to the PY20 experiments.

Taken together, these data suggest that the 3 different Srcs are all able to phosphorylate Syp, at similar rates. They do however appear to achieve different maximum levels of phosphorylation, which might suggest that they have different access and abilities to phosphorylate the 9 different tyrosine residues on the C-terminal of Syp. This pattern corresponded to the amount of interaction that the SH3 domain of the Srcs have with Syp.

4.2.2 - C- and N2-Src are More Efficient in Phosphorylating Synaptophysin than N1-Src

In the previous section there were no obvious differences between the time courses of the three difference Src kinases when phosphorylating the C-terminal of Syp. To gain a more accurate measure of the abilities of the Srcs to phosphorylate Syp, Km values were calculated. The Km value defines the substrate concentration that elicits half of the maximal rate of the reaction, therefore it can be seen as a measure of efficiency of the different Src kinases; a lower Km value would highlight a more efficient kinase for phosphorylating the C-terminal of Syp.

To calculate a Km value, kinase assays were conducted where the different Srcs were aliquoted into eppendorf tubes that contained a range of different C-Syp substrate concentrations (100 nM to 10 µM). ATP was added to start the reaction and a 5 minutes time point was used for the reaction time. The 5 minute time point

was selected because the time course assays showed that this was in the linear region of the initial rate of reaction (figure 4.2A). A 'minus Src' control was conducted; where 1 µM Syp was incubated in the same reaction condition but without Src during the assay. This serves as a control for background signal. The samples were subjected to western blotting with a PY20 antibody, and the amount of phosphorylation detected was normalised to the maximal response, after subtracting the minus Src experiment (figure 4.4A). These values are then used to produce a Hanes-Woofl ([S]/V plotted against [S]) plot. The Km values were then calculated using linear regression, where the y-intercept value equals Km / Vmax. It is clear that C- and N2-Src were very similar in their Km values (2.26 µM and 2.96 µM respectively), which were almost half of the Km value for N1-Src (4.84 µM). Therefore, it can be concluded that C- and N2-Src are more efficient in phosphorylating the C-terminal of Syp when compared to N1-Src.

To confirm, the Km values of the three Src kinses, experiments using ATP-P^{32} and autoradiography were also conducted. Similar results to the PY20 experimentally calculated Km values were seen (figure 4.5); with both C- and N2-Src lower than N1-Src (C-Src Km - 1.33 µM, N1-Src - 8.82 µM, N2-Src - 2.64 µM).

Thus C- and N2-Src are more efficient in phosphorylating the C-terminal of Syp when compared to N1-Src. These data complement pervious experiments where the SH3 domains of C- and N2-Src are able to extract more Syp from synaptosomal

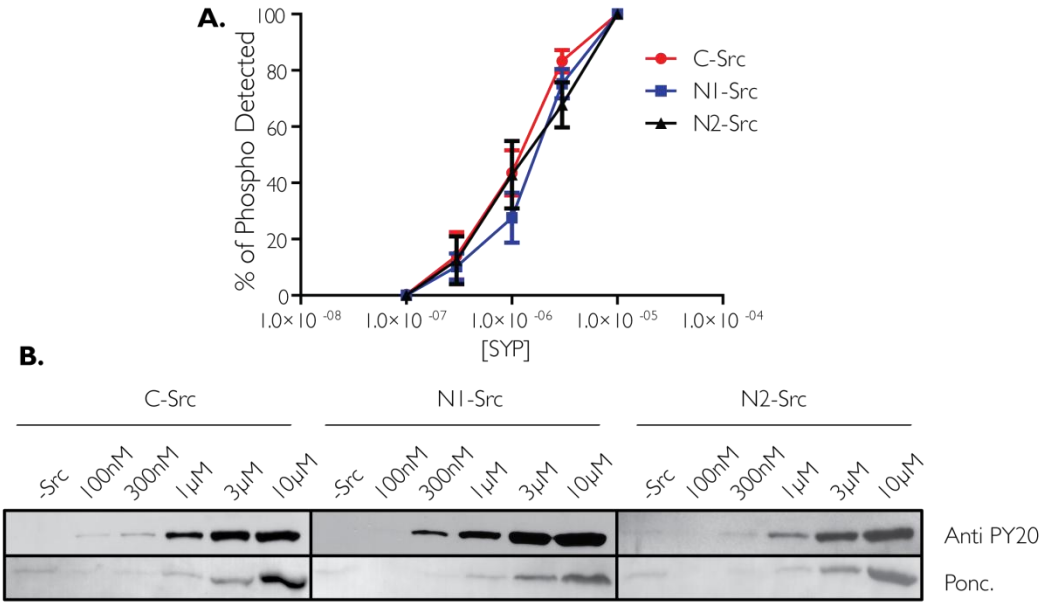

Figure 4-4 Determination of the Kinetic Efficiencies of the Different Srcs using a PY20 antibody

Different concentrations of Syp (100 nM, 300 nM, 1 µM, 3 µM and 10 µM) were used in kinase assays with C-, N1- and N2-Src. A time point of 5 minutes was used. The amount of phosphorylation detected by western blotting with a PY20 antibody, and this was quantified by densitometry analysis. A) The values, minus the control 'minus Src', were normalised to the maximum PY20 signal and plotted against the Syp concentration. n=5 independent experiments for C-Src and n = 4 for N1- and n= 3 for N2-Src. Graph plots are means ± SEM. B) Representative western blots for each set of data are shown.

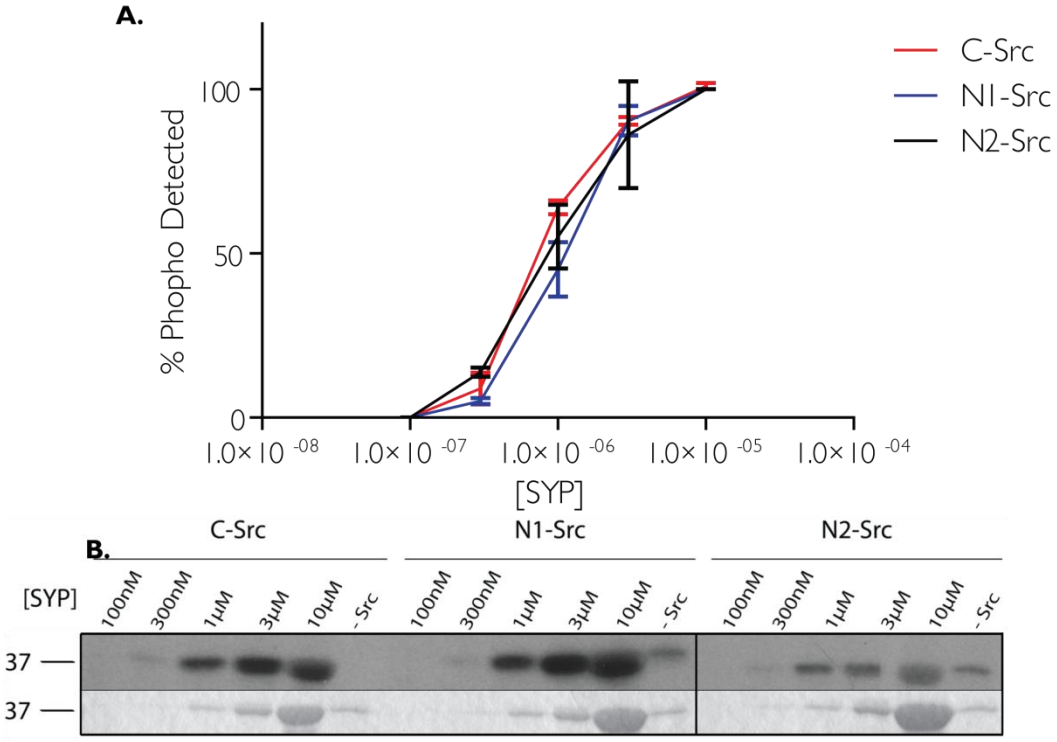

Figure 4-5 Determination of the Kinetic Efficiencies of the Different Srcs using Autoradiography

Different concentrations of Syp (100 nM, 300 nM, 1 µM, 3 µM and 10 µM) were used in kinase assays with C-, N1- and N2-Src. A time point of 5 minutes was used. The amount of phosphorylation detected by autoradiography, and this was quantified by densitometry analysis. A) The values, minus the control 'minus Src', were normalised to the maximum autoradiography signal and plotted against the Syp concentration. Graph plots are means ± SEM. N=3 independent experiments for each of the conditions. B) Representative western blots for each set of data are shown.

lysate (figure 4.1), and to phosphorylate it to a greater extent than N1-Src (figure 4.2B).

4.2.3 - Mutation of Potential Phosphorylation Sites Decreases the Level of Synaptophysin Phosphorylation

The C-terminal of Syp contains 9 potential phosphorylation sites and only one trypsin cleavage site prior to these sites; therefore it has been somewhat difficult to determine which of the tyrosines are phosphorylated in a physiological situation. To try to identify potential phosphorylation sites, single point mutations of key predicted by NetPhos (245, 250, 263, 273, 290) (figure 1.4) were mutated to phenylalanine (F), and were subjected to saturation kinase assays.

Four Y to F mutants were made, Y245F, Y273F, Y290F and a 6F C-Syp. The 6F C-Syp that was used had all the 5 predicated tyrosines mutated to phenylalanines, and additionally Y257. They were subjected to a kinase assay using ATP-γ^{32}P at a single time point at 30 minutes. Autoradiography detailed how the mutations affected the overall level of phosphorylation of the C-terminal of Syp compared to WT (figure 4.6A). Only C- and N2-Src were tested as they showed the highest levels of activity and interactions with Syp when compared to N1-Src.

The C-Src kinase assay revealed that the single mutations of the predicted residues decreased the level of phosphorylation on the C-terminal of Syp slightly, although this was not significantly different from WT levels. The 6F C-terminal mutant of Syp however resulted in a significant reduction in phosphorylation when compared to

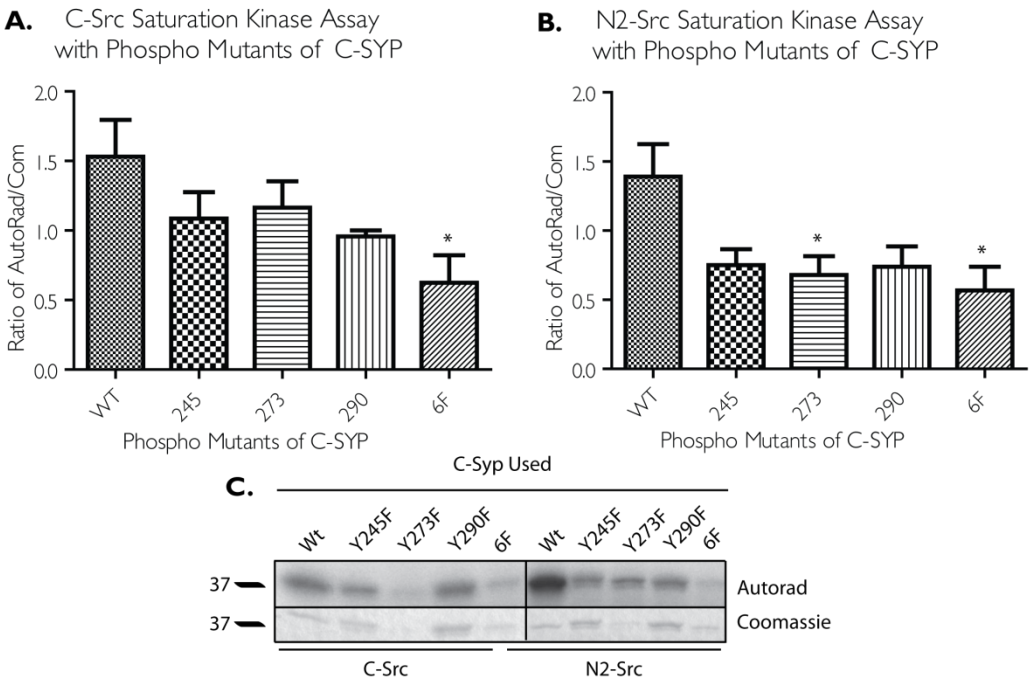

Figure 4-6 Saturation Kinase assays to Identify the Tyrosine Phosphorylation Sites on the C-terminus of Synaptophysin

Phosphorylation mutants (Y245F, Y273F, Y290F and 6F - Y245, 250, 257, 263, 273, 290, 295F) of the C-terminal of Syp were subjected to a saturation kinase assays. A time point of 30 minutes was used. The amount of phosphorylation was detected by autoradiography, and this was quantified by densitometry analysis. Coomassie staining was used as a control for the amount of Syp loaded in each lane, and a ratio of the amount of phosphorylation divided by the amount of protein to produce plots for A) C- and B) N2-Src. Graph plots are means ± SEM. N=3 independent experiments for each of the conditions. One way ANOVA, * = $p<0.05$ C) Representative western blots for each set of data are shown.

WT C-Syp (figure 4.6A, B). This highlights that the predicted phosphorylation sites are phosphorylated *in vitro*.

When N2-Src was tested, there was one single mutant, Y273F, that displayed significantly reduced overall levels of phosphorylation when compared to WT (figure 4.6B, C). The other single point mutations did reduce the overall phosphorylation levels, but not to significant levels. Similar to C-Src, the 6F C-Syp mutant significantly reduced the levels of phosphorylation.

It can therefore be concluded that Y273 may be a key phosphorylation residue for N2-Src. Only when all the NetPhos predicated tyrosine residues are mutated, a significant reduction in the overall levels of phosphorylation detected on the C-terminal of Syp implying that all the NetPhos predicted sites might be important and the other sites are phosphorylated *in vitro* by Src.

4.2.4 - The SH3 Interaction Motif on Synaptophysin is Regulates C-Src Phosphorylation of Synaptophysin

In section 3.2.7, it was demonstrated that single point mutations of the SH3 interaction motif on the C-terminal of Syp disrupted the level of interaction between Syp and C-Src. Further to this, the greater the mutation of the motif, the more disruption of the interaction was seen (figure 3.15). To determine if the SH3 interaction motif was important for C-Src phosphorylation of the C-terminal of Syp, the SH3 interaction motif mutations of C-Syp were used in kinase assays with C-Src.

Time course assays were conducted using western blotting with a PY20 antibody to test how the SH3 interaction motif controlled the ability of C-Src to phosphorylate

the C-terminal of Syp. The same mutants were used as used in section 3.2.7 (R229E (R), PP232 and 235AA (AA) and R229E combined with PP232, 235AA (RA)). When the results were normalised to the maximum PY20 signal, the R and AA C-Syps appear to have an accelerated initial rate of reaction when compared to the WT C-Syp (figure 4.7).

However in direct contrast to this, the RA C-Syp displayed no difference on the time course of phosphorylation when compared to WT C-Syp (figure 4.7), suggesting that the SH3 interaction motif is not important in the mechanism of C-Src phosphorylation of C-Syp.

These experiments suggest that the SH3 interaction motif on the C-terminal of Syp is not a key interaction for C-Src regarding its ability to phosphorylate Syp. This also suggests that the mechanism of phosphorylation might be independent of an ability for C-Src to interact with Syp, as this interaction is mediated via the SH3 domain of C-Src and the SH3 interaction motif on C-Syp, and thus could be a result of another domain on Src.

4.2.5 - Mutation of Predicted Synaptophysin Phosphorylation Sites regulates its Binding to other Proteins

To determine the significance of the phosphorylation of Syp in the SV lifecycle, GST-pull downs were conducted using phospho-null and -mimetic C-Syp mutants as bait. Synaptosomal lysates were used to detect potential phosphorylation dependent synatpic interaction partners. If any interaction partners were lost, or gained,

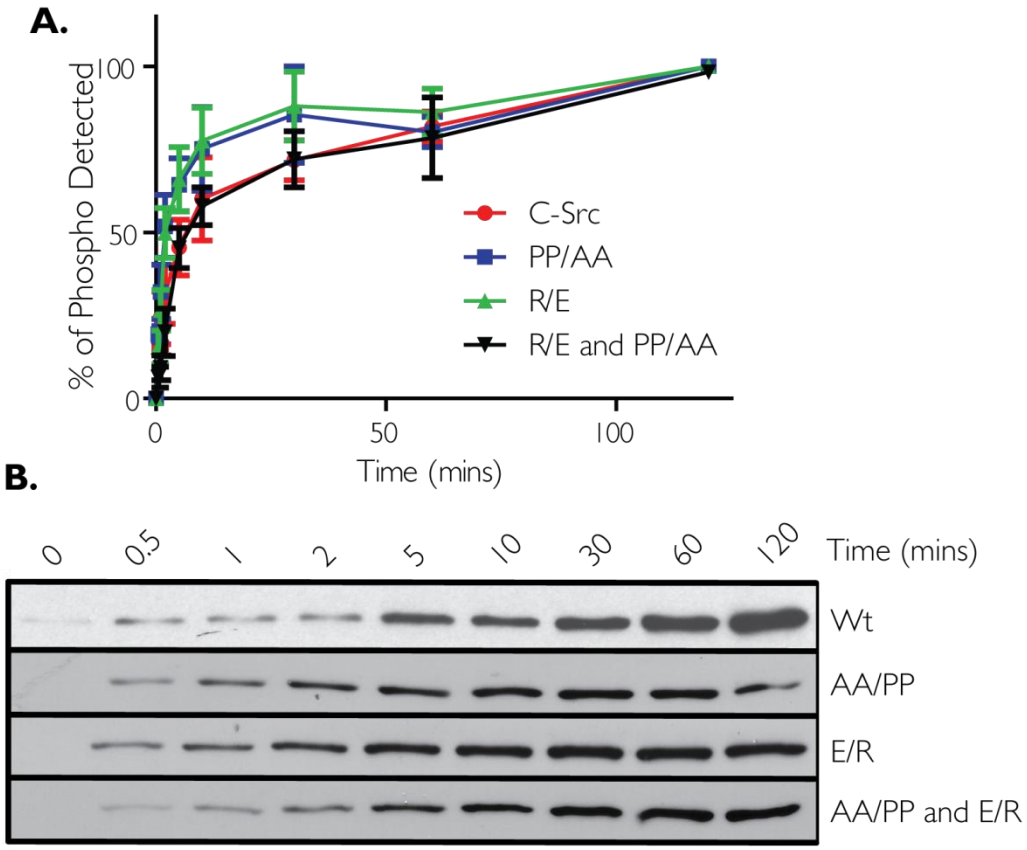

Figure 4-7 Phosphorylation of Synaptophysin SH3 Interaction Mutants by C-Src

Kinase assays were conducted using the C-terminal of Syp, WT and SH3 interaction mutants (R229E (E/R), PP232 and 235AA (AA/PP) and R229E combined with PP232, 235AA (AA/PP and E/R) with C -Src. Samples were taken at 0, 0.5, 1, 2, 5, 10, 30, 60 and 120 minutes. The amount of phosphorylation was detected by western blotting using a PY20 antibody. Densitometry analysis revealed the amount of phosphorylation detected, and the results were A) normalised to the maximum PY20 signal. n=3 independent experiments for each of the conditions. Graph plots are means ± SEM. B) Representative western blots for each set of data are shown.

based on the phosphorylation state of Syp, it would provide clues to which step phosphorylation regulates the physiological role of Syp in the SV lifecycle.

Mutagenesis of all 9 tyrosine residues were completed to turn the whole of the C-terminal of Syp into either a phospho-null, tyrosine (Y) to phenylalanine (F), or a phospho-mimetic, tyrosine (Y) to glutamate (E), bait protein. Residues Y263 and Y273 were also either changed to an F or an E. These specific residues were selected for two reasons; firstly that in section 4.2.5 residues 273 appeared to be a key phosphorylation site for N2-Src. Secondly, previous work stated that there were sites that were phosphorylated following peroxynitrite treatment and via a Src kinase family member Fyn (Mallozzi et al., 2009).

Figure 4.8A shows the results of the GST-pull downs using the phospho C-Syps as bait pulling down from synaptosomal lysate. It is clear that there are many differences in the proteins that the phospho-null and -mineitc C-terminals of Syp can interact with, highlighted by arrows. Further to this, there are differences in the proteins that the 9F and 2F, 9E and 2E Syps can interact with too. This suggests that the Y263 and Y273 are not the only residues that can affect phospho-dependent interactions of the C-terminal of Syp.

4.2.6 - The Synaptophysin Phosphorylation Truncation T1 Disrupts Trafficking of Synaptophysin during Action Potential Stimulation

As a first step in determining the role of Syp phosphorylation in the SV lifecycle, the T1 mutant (as described in chapter 3) was made in full length Syp. The full length T1

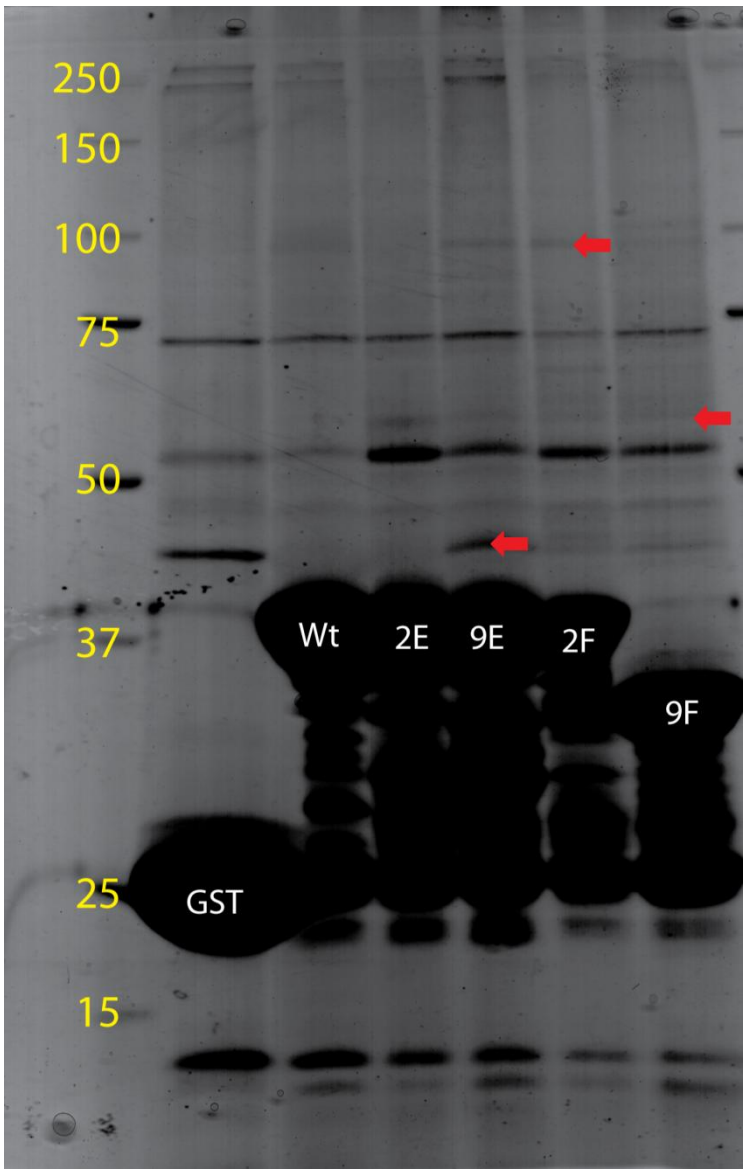

Figure 4-8 Mutation of the Potential Phosphorylation Sites on the C-terminal of Synaptophysin Changes Protein Interactions

GST bait proteins of phosphorylation point mutations of tyrosine on the C-terminal of Syp were generated; all 9 were changed to either Y or (9F and 9E), and Y263 and Y273 were changed to either Y of E (2F and 2E). They were used in pull down experiments using synaptosomal lysates, the samples were separated by use of a large gradient SDS-PAGE gel, and subjected to coomassie staining. A few examples of differences in the protein that interact with the SH3 interaction motif are highlighted by red arrows.

mutant has all nine tyrosine sites removed, so should indicate whether this phospho region of the C-terminal of Syp is important for Syp function.

To determine whether the 9 pentapeptide repeats were important for trafficking of Syp, Syp knockout cortical neurons were transfected with either Cer-Syp Wt of Cer-Syp T1 and were subjected to a trafficking assay, as detailed in section 2.5.4.

The WT trace in figure 4.9 shows a drop in fluorescence upon electrical stimulation (10 Hz for 10 seconds). This is a result of exocytosis, which pushes the Cer Syp in the membrane out of the centre of the synapse away from the nerve terminals (figure 2.5). Following this, the fluorescence signal recovered back to baseline levels as Cer-Syp is returned to the centre of the synapse during endocytosis to complete the SV lifecycle.

The phospho truncation of Cer-Syp, T1, however showed a completely different trend. As shown by the smaller decrease in fluorescence during the electrical stimulation, a smaller amount of the tagged protein moved out of the centre of the synapse, when compared to WT Cer-Syp (figure 4.9A, B). After the simulation, the recovery of fluorescence occurred much sooner than WT. This suggests that the T1 mutant only partially leaves the centre of the synapse, which could be a result of defective exocytosis. Another difference is that once recovery of the T1 mutant began, there was a second phase of fluorescent decrease, suggesting a major trafficking defect. Furthermore, sample images reveal that the phospho mutant begins in a diffuse manner across the neuron while the stimulation causes a slight decrease in fluorescent intensity detected in the ROI. After more time, the Cer-

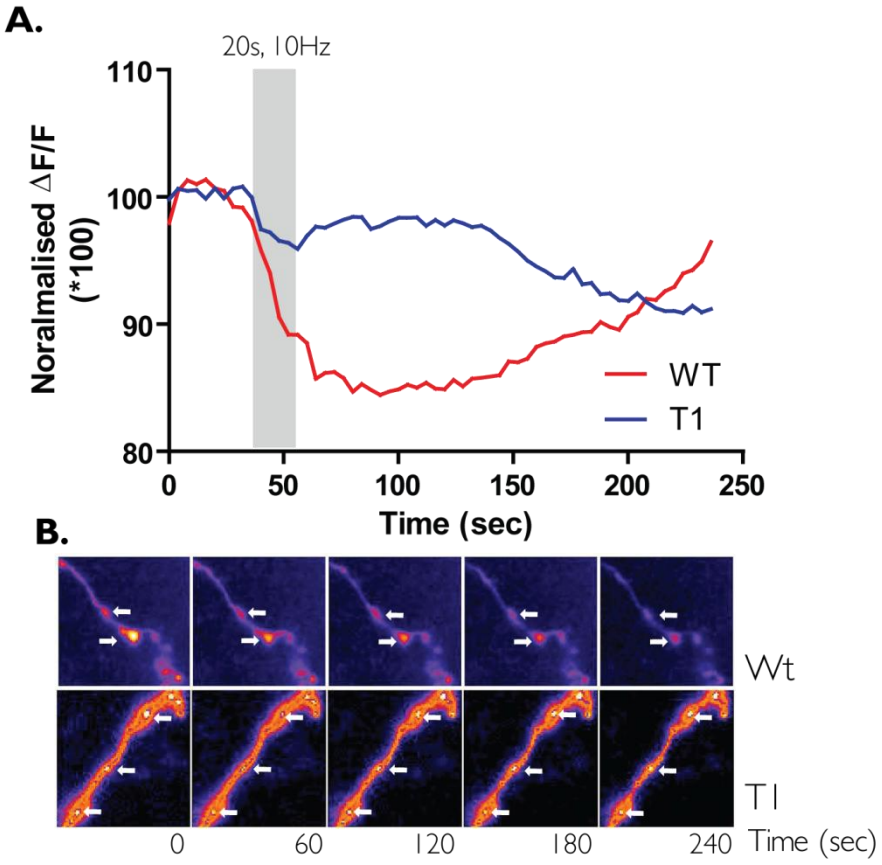

Figure 4-9 Removal of the Phosphorylation Motifs on the C-terminal of Synaptophysin Disrupt its Trafficking

Cortical neurons derived from Syp knockout mice were transfected with either WT or the phosphorylation truncation (T1) of Syp that are tagged with mCerulean. Cells were imaged for 10 frames (4 seconds apart) to establish a baseline level of fluorescence, and then electrical stimulation was applied (10 Hz for 20 seconds - highlighted by the grey shading). Images were captured for a further 50 frames (200 seconds). A) The change in fluorescence was normalised to the baseline level and plotted against time. B) Representative images from various time points during experiments of each condition are shown in false colouring. (n=2 for both conditions). White arrows highlight example ROIs.

phospho mutant appears to start to form puncta and then these slowly revert back to a diffuse localisation. This observation indicates that the potential phospho sequence on the C-terminal of Syp is key in regulating the trafficking of Syp during the SV lifecycle as without it, trafficking of Syp is clearly disrupted.

These results suggest that the phosphorylation of Syp maybe a critical post translational modification that affects the trafficking of Syp during the SV lifecycle. It also appears to be key in the process that allows the formation of punctate expression pattern of WT Syp. Without the phosphorylation sites, the expression profile of Syp was very diffuse and it only returned to a punctate pattern following stimulation.

4.2.7 - Supercliptic Synaptophluorins Show that the Phosphorylation sites of Synaptophysin are not regulators of Synaptophysin trafficking during the Synaptophysin Lifecycle

The Cer trafficking assay (section 4.2.6) using neurons transfected with the T1 mutant of Syp showed that there were potential trafficking defects when compared to neurons transfected with WT Cer-Syp. To test more directly if the phosphorylation of Syp is important in its trafficking, supercliptic Syp phluorin was used. Supercliptic Syp phluorin (SypHy) allowed direct monitoring of Syp movement during the SV lifecycle, as described in the previous chapter. Syp knock out cortical neurons were transfected with either WT SypHy or T1 Syp (SypHy T1), where all the potential tyrosine phosphorylation sites were removed and the SH3 interaction motif was still present on the C-terminal.

To see if the phosphorylation of Syp is important in the regulation of Syp-containing SVs during SV recycling, fluorescent intensity traces from WT SypHy and SypHy T1 were normalised to their maximum fluorescent intensity values during the NH_4Cl perfusion at the end of each experiment. This provided information about the percentage of labelled SVs that are part of the recycling pool of SVs. Figure 4.10A showed that there was no difference in the percentage of labelled SVs that can recycle when comparing the WT and the phospho mutant SypHy, where both conditions show that about 40% of the labelled SVs were in the recycling pool. This value agrees with previously published reports (Kim and Ryan, 2009). Further to this, both fluorescent intensity traces of the WT and phospho mutant SypHy showed that the labelled SVs were able to complete the SV lifecycle in almost identical manner, where no significant differences in the intensities of the traces for either WT Syp of the phospho mutant T1 were found for the duration of the experiments.

To examine the retrieval kinetics of the differing SypHys, the traces of the WT SypHy and T1 SypHy were normalised to the maximum of their peaks during the electrical stimulation and the fluorescent decay was compared (figure 4.10B). Similar τ values revealed that there was no difference when comparing the WT SypHy and the phospho mutant SypHy T1 (42.5 ± 4.56 and 42.4 ± 5.96 respectively).

As the phosphorylation truncation mutant showed no defect in the SypHy traces, it can be concluded that phosphorylation of Syp is not important for regulating Syp trafficking or SV turnover following electrical stimulation.

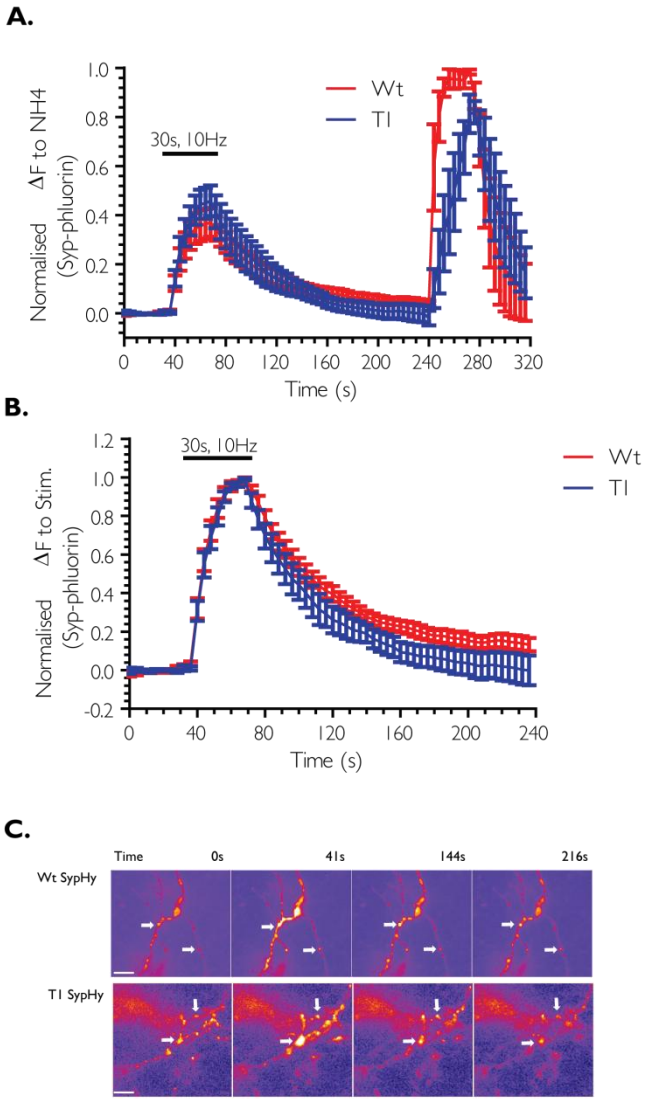

Figure 4-10 Deletion of the Phosphorylation Sites on Synaptophysin Does Not Alter Recycling of Synaptophysin

Cortical neurons derived from Syp knockout mice were transfected with supercliptic Syp phluorin, either WT or the phosphorylation truncation (T1). The neurons were imaged for 40 seconds, to establish a baseline level of fluorescence, and then an electrical stimulation was applied to the neurons (10 Hz for 30 seconds). The cells were imaged for a further 200 seconds where a short perfusion of NH_4Cl was applied for 30 seconds. The changes in fluorescence over time were normalised to A) the peak during the NH_4Cl perfusion or B) the peak of stimulation (where the NH_4Cl induced change in fluorescence was removed for presentation purposes). Graph plots are the mean ± SEM. C) Representative images are shown in false colouring. N=4 for Wt and n=7 for T1. White arrows highlight example ROIs.

4.2.8 - The Synaptophysin Phosphorylation Region is Critical for the Retrieval of VAMP Synaptophluorin

SypHy experiments had shown that phosphorylation of Syp was not important in the trafficking and function of Syp during the SV lifecycle, but chapter three and Gordon et al showed that Syp is responsible for the retrieval of VAMP during SV recycling (Gordon et al., 2011). To test if the mechanism of VAMP retrieval is phosphorylation dependent a VAMP phluorin was used to transfect Syp knock out cortical neurons that had also been transfected with either Cer-Syp or the Cer Syp mutant T1. These cells were then subjected to the synaptophluorin assays as detailed in figure 2.5.2.

A Cer control was compared with WT C-Syp to reveal what occurs to VAMP trafficking in the absence of Syp. These cells were transfected with VAMP phourin and labelled with Cer-tagged Syps. When these traces were normalised to the peak of fluorescent intensity during the NH_4Cl perfusion, there was a significant reduction in the percentage of VAMP labelled SVs that are able to recycle when compared to neurons that were transfected with WT Cer-Syp (figure 4.11A). Further to this, when the fluorescent intensity traces were normalised to the maximal intensity during stimulation the proportion of VAMP phluorin retrieved from the plasma membrane was significantly different from cells that had been transfected with WT Cer-Syp (figure 4.12B). This is revealed by the amount of fluorescent recovery to baseline at the end of the trace. In addition, the rate of this retrieval was different, as reflected by the decay time constant τ (Cer - 57.45 ± 12.06, WT - 30.06 ± 3.18). This demonstrated that WT Syp is key in retrieving VAMP

from the plasma membrane during the SV lifecycle, as observed before (Chapter 3 and (Gordon et al., 2011).

To examine if the phosphorylation of Syp was important for VAMP retrieval from the plasma membrane, Syp knock out cortical neurons were also transfected with the mutant Cer-Syp T1 and the VAMP phluorin. When the fluorescent intensity trace was normalised to the peak intensity during the NH_4Cl perfusion, there was no difference in the percentage of recycling SVs when comparing WT and T1 transfected neurons, which is about 40%. However, there was a significant difference in amount of VAMP phluorin that was retrieved between the WT and the phospho mutant transfected cells (figure 4.11C). The phospho mutant resulted in an incomplete retrieval similar to the Cer control neurons, suggesting that phosphorylation of Syp is critical for the physiological retrieval of VAMP from the plasma membrane during the SV lifecycle.

To examine the different kinetics of VAMP retrieval of the phospho mutant and WT Cer-Syp, fluorescent intensity traces were normalised to the maximum value during the electrical stimulation. Again, there was a significant difference when comparing the amount of VAMP retrieval that occurs in neurons transfected with WT Cer-Syp and the phospho mutant T1 (about 80% retrieval compared to about 40% after 200 seconds) (figure 4.12D). This observation is complemented by the differences found in the τ values of the WT and T1 Syp transfected neurons; where WT has a τ of 30.06 ± 3.18 and T1 has a τ value of 49.45 ± 12.78, indicating a slower retrieval of VAMP with the

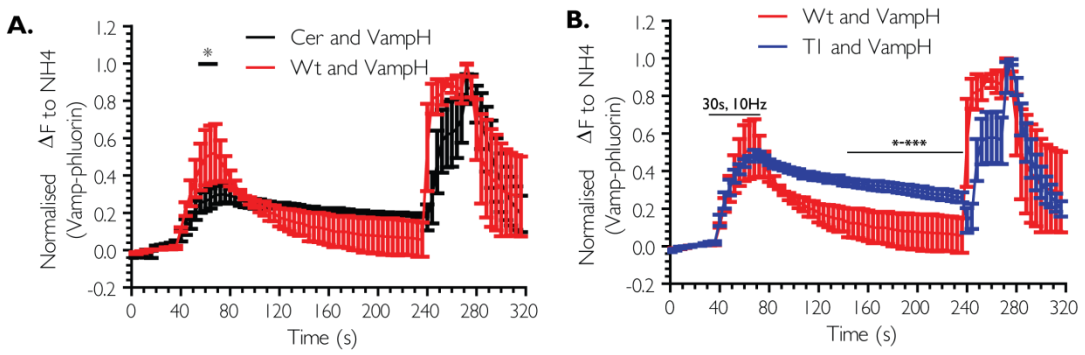

Figure 4-11 The effect of Deleting the Phosphorylation Motif from the C-terminal of Synaptophysin on the Recycling Pool of VAMP

Cortical neurons derived from Syp knockout mice were transfected with supercliptic VAMP phluorin and a mCerulean construct of; the empty mCerulean vector (Cer), wild type Syp (WT) and the phosphorylation truncation (T1). The neurons were imaged for 40 seconds, to establish a baseline level of fluorescence, and then an electrical stimulation was applied to the neurons (10 Hz for 30 seconds). The cells were imaged for a further 200 seconds where a short perfusion of NH_4Cl was applied for 30 seconds. The changes in fluorescence over time were normalised to the peak during the NH_4Cl perfusion to compare the effects of A) Cer with WT and B) Wt and T1 on VAMP recycling. Traces are the mean ± SEM. Statistical testing was conducted by means of a two-way ANOVA, * indicates $p<0.05$, ** indicated $p<0.01$. N = 4 for Cer, n = 3 for WT and n = 5 for T1.

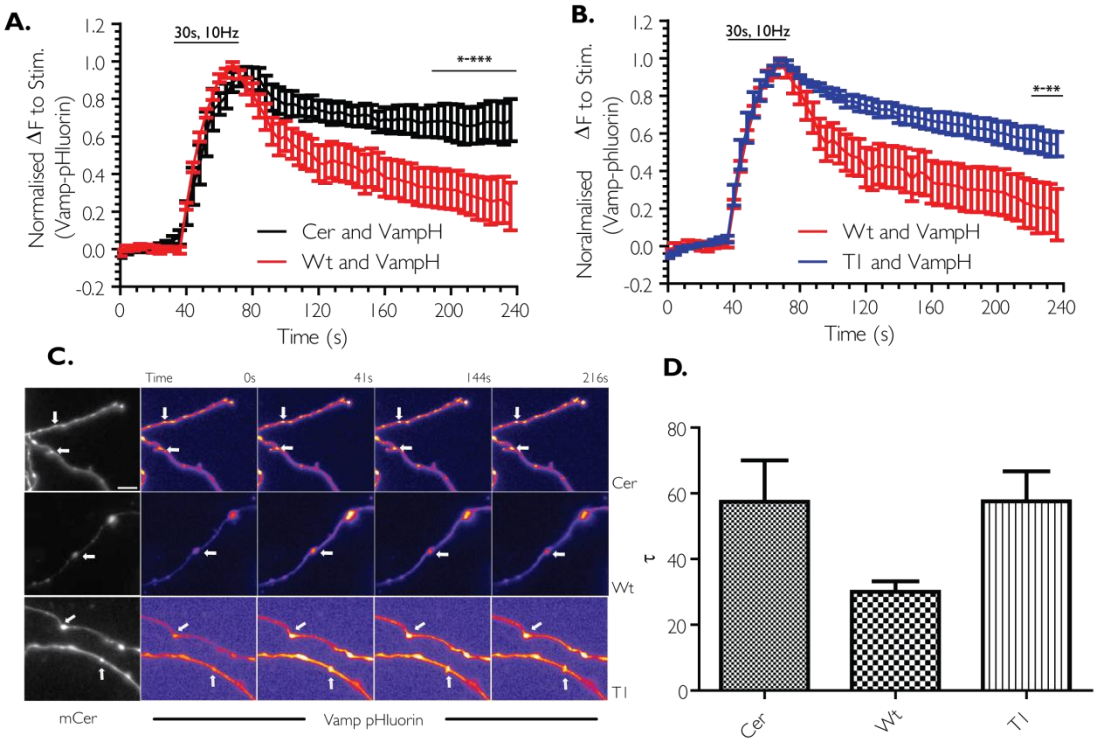

Figure 4-12 The effect of Deleting the Synaptophysin Phosphorylation Region on the Kinetics of VAMP Retrieval

Cortical neurons derived from Syp knockout mice were transfected with superecliptic VAMP phluorin and either a mCerulean construct of; the empty mCerulean vector (Cer), wild type Syp (WT) or the phosphorylation truncation (T1). The neurons were imaged for 40 seconds, to establish a baseline level of fluorescence, and then an electrical stimulation was applied to the neurons (10 Hz for 30 seconds). The cells were imaged for a further 200 seconds. The changes in fluorescence over time were normalised to the peak during stimulation to compare the effects of A) Cer with WT and B) Wt and T1 on VAMP retrieval. Plots are the mean ± SEM. Statistical testing was conducted by means of a two-way ANOVA, * indicates $p<0.05$, *** indicates $p<0.001$. C) Representative images are shown in false colouring. D) τ values for the VAMP retrieval are plotted as their means ± SEM. N = 4 for Cer, n = 3 for WT and n = 5 for T1. White arrows highlight example ROIs.

phospho mutant T1 (figure 4.12F). This difference was very similar to that when comparing the control Cer neurons with WT Syp transfected neurons, implying that the phospho mutant renders VAMP retrieval defective as found in Syp knockout neurons.

These findings clearly suggest that tyrosine phosphorylation region of the C-terminal of Syp is fundamental to the physiological role of Syp in retrieving VAMP from the plasma membrane during the SV lifecycle.

4.3 - Discussion

Results generated in this chapter have provided the starting point for the characterisation of tyrosine phosphorylation of Syp by tyrosine kinases C-, N1 and N2-Src and the effect that this post-translational modification has on regulating the interaction partners of Syp. Further to this, the data has provided further insight of the mechanism by which Syp retrieves VAMP from the plasma membrane during the SV lifecycle, showing that this physiological role of Syp may be phosphorylation dependent.

In vitro kinase assays showed that there were key differences in the efficiency of the 3 different Src splice variants to phosphorylate the C-terminal of Syp. The time courses of phosphorylation for the three Srcs were identical in reaching their maximum levels of phosphorylation. However, differences in the overall amount of phosphorylation were found; C- and N2-Src were able to phosphorylate the C-terminal of Syp to significantly greater levels than N1-Src. This data reflected the ability of the SH3 domains of the 3 difference Srcs to interact with Syp, suggesting

that the SH3 interaction of the different Srcs could be important. C- and N2 Src were found to have lower Km values when compared to N1-Src, highlighting that they are more efficient at phosphorylating the C-terminal of Syp.

NetPhos (an online phosphorylation predictor) was used to make predictions about which of the 9 tyrosine residues might be phosphorylated on the C-terminal of Syp. It was found that when all of the predicted sites were mutated, there were significant reductions in the overall amount of phosphorylation detected on the C-terminal of Syp by either C- or N2-Src. It was also found that a single mutant of Y273 significantly reduced the overall levels of phosphorylation when incubated with N2-Src. In an attempt to further define which sites were phosphorylated *in vitro*, and in which order, mass spectrometry analysis was conducted on time course samples. However, the results are still pending.

Chapter 3 showed that the SH3 interaction motif on the C-terminal of Syp was the site of the C-Src interaction, and SH3 interaction motif mutants were used to examine how the interaction regulates the kinase activity. However a direct link between the interaction of the SH3 domain of C-Src and then SH3 interaction motif on the C-terminal of Syp was hard to interpret. To begin to understand the significance of the role of tyrosine phosphorylation of the C-terminal of Syp, GST-pull downs were conducted from synaptosomal lysate using phospho-null and -mimetic C-Syps. It was found that phosphorylation regulated and facilitated many different protein interactions. Mass spectrometry analysis of these samples to

identify the phosphorylation dependent interactions of Syp is currently being carried out.

To address the physiological role of phosphorylation of Syp, Syp knockout cortical neurons were transfected with a phospho truncation mutant (T1). All the tyrosine repeats had been removed from the C-terminal, while keeping the SH3 interaction motif intact. Trafficking assays determined that this region was important in the global trafficking of Syp following electrical stimulation. However, there were no defects detected when looking at the trafficking of Syp in endocytosis. In addition, a VAMP phluorin showed that the physiological role of Syp, to retrieve VAMP from the plasma membrane, was dependent on this phosphorylation region.

4.3.1 - Appraisal of the Biochemical Experimental Approach

The key technique used to characterise to phosphorylation reaction between the Srcs and the C-terminal of Syp was an *in vitro* kinase assay. This *in vitro* approach has several advantages and disadvantages. The biggest disadvantage is that the proteins in question are not in their natural environment. By placing two proteins in a tube, any chaperones and controlling proteins of the Src kinases are absent. It is thus difficult to assume that the kinase will work in a manner that resembles their physiological function. However, this also has an advantage. As we wanted to compare the different activities of the different Srcs, and relate that to how the Srcs can interact with the C-terminal of Syp, removal of any other proteins that might disrupt this reaction was critical.

One of the problems in using the kinase assay is related to the detection of phosphorylation at the end of the assay via western blotting. The way in which the PY20 antibody produces a signal via chemi-luminsence, or the autoradiography signal, is not linear in the amount that it saturates the X-ray film; therefore the exposure times of the film were critical to the experiments. Indeed, the results obtained showed that there were differences between using PY20 and autoradiography measuring the efficiencies of phosphorylation by the different Srcs. To overcome this, a better measure of phosphate incorporation of Syp would be to cut the coomassie bands of the $\gamma^{32}P$ experiments and subject them to scintillation counting, using a Cerenkov method of detection.

Another concern is having a substrate incubated with a kinase and ATP, phosphorylation of non-physiological sites is likely. For example, while Syp has 9 potential phosphorylation sites on its C-terminal, it is possible that only 5 of these are phosphorylated in an *in vivo* situation. If given enough kinase then other 4 sites might also get compensatory phosphorylated. This situation could be further exacerbated by the fact that a saturating concentration of ATP is used in the assay. However, when comparing the saturation time point assay in section 4.2.1, we saw that C- and N2-Src led to a significantly higher amount of phosphorylation of the C-terminal of Syp when compared to N1-src. These results are reassuring in showing that there is still some specificity for the phosphorylation sites on the C-terminal, as not every kinase produced the same maximum response.

Assessment of the final extent of Syp phosphorylation highlighted a possibility that the three different Srcs phosphorylate Syp to different levels (section 4.2.1, figure 4.2B). This might be because the different Srcs can phosphorylate only some of, or specific, residues of the 9 possible phosphorylation sites on the C-terminal of Syp. If there are different tyrosine residues that are phosphorylated by the different Srcs, then the order in which they phosphorylate the tyrosines might also be important. To investigate this, a collaboration was formed, with Professor Phil Robinson and Doctor Peter Hains (University of Sydney), to conduct mass spectrometry on the time point samples of the kinase assays from the different Srcs. A time course assay for each of the Srcs was repeated, where the volumes of the reaction were scaled up to maximise the amount of protein for analysis by mass spectrometry. A small amount of the samples were subjected to western blotting to confirm that phosphorylation occurred over time. Once confirmed, the remainder of the samples were subjected to SDS-PAGE and coomassie staining which allowed the Syp protein bands to be extracted in a sterile environment. A digestion protocol was designed, based on work by Mallozzi *et al.* (Mallozzi et al., 2009), which would produce enough digested peptide fragments of the C-terminal to allow identification of all the 9 potential tyrosines. The Syp bands were then subjected to a double digest of trypsin and Asp-N to produce multiple phosphopeptides fragments of the C-terminal of Syp. This method of double digestion allowed full coverage of the C-terminal of Syp. The combinations of peptides produced also allowed each tyrosine residues to be detected in a separate peptide fragment.

However, after multiple trails, the results so far have failed to highlight which are the key residues that are phosphorylated.

This was a worrying trend, but we were confident that the kinases were phosphorylating the C-terminal of Syp as we had seen it with a PY20 antibody and when measuring $\gamma^{32}P$ incorporation. Therefore, the reason we failed to detect any phospho-peptides in the mass spectrometry could be that the phosphates were 'falling off' during the digestion of the C-terminal. Vanadate could have been used to ensure that the C-terminal remained heavily phosphorylated *in vitro*.

In section 4.2.2, the Km values of the Srcs were calculated from results generated with a PY20 antibody and autoradiography to detect $\gamma^{32}P$ incorporation. The same trend was found, that C- and N2-Src were more efficient at phosphorylating Syp when compared to N1-Src, but the values were slightly different using the two different methods. A reason for this could be because of the differences in sensitivity of detection of the phosphorylation, using autoradiography compared to ECL illumination of the PY20 antibody. Another reason might be that using the PY20 detection method, we have a lot more control of the exposure time of the X-ray film to the protein containing membrane.

In an attempt to identify which of the NetPhos predicated phosphorylation were actually phosphorylated, point mutations were made of the sites and subjected to a saturation kinase assay (section 4.2.5). A problem with this experiment is that it was conducted in an *in vitro* environment; therefore there could potentially result in off target phosphorylation of the other 8 tyrosine residues. However, this might

not be the case as Y273 was significantly different from WT for the N2-Src kinase. To gain a more physiological sample of phosphorylated Syp, Syp was purified from synaptosomes and subjected to mass spectrometry to identify the *in vivo* phosphorylation sites on the C-terminal of Syp. Immunoprecipitations from synaptosomal lysates were conducted with a Syp antibody; although there was protein purified as detected by western blotting and coomassie staining, very little of the protein was phosphorylated, and therefore not suitable for mass spectrometry. Examination of the Syp antibody used revealed that the epitope was very similar to the pentapeptide repeat sequence, so it is possible that the antibody was not able to purify heavily phosphorylated Syp. After repeating the immunoprecipitations with a different Syp antibody (with an epitope on the 1st inter-vesicular loop of Syp), the Syp that was purified was phosphorylated (detected with a PY20 western blot) and detectable on a coomassie stained gel. After cutting these Syp bands out of an SDS-PAGE gel, they were subjected to mass spectrometry analysis. However, the mass spectrometry analysis has failed to detect any phospho-peptides to date.

In section 4.2.4 where the SH3 interaction motif mutants were subjected to a kinase assay with C-Src we saw that single point mutants accelerated the rate of phosphorylation of Syp, but when the whole motif was mutated we saw no difference in rate from WT. Further to this, there was no difference in the endpoint saturation of the SH3 interaction mutants, highlighting that Syp was still able to be phosphorylated to its WT levels. This suggests that the SH3 interaction motif could be important in the mechanism of how C-Src can phosphorylate Syp. For example,

the interaction between the SH3 domain of C-Src and C-Syp might be a control point for phosphorylation. As the binding mutants reduce the amount of interaction, it is possible that due to this weaker affinity, the Src could bind, phosphorylate and dissociate from Syp faster allowing it to move on to the next substrate more quickly. This therefore suggests that the SH3 domain binds to Syp first via the SH3 interaction motif and phosphorylates Syp, by doing this it creates a binding motif for the SH2 domain of Src; which binds to phosphorylated tyrosines (Songyang et al., 1993). This is supported by the fact that the SH2 domain of Src was found to interact with the C-terminal of Syp in a yeast two-hybrid system (Felkl and Leube, 2008). However, when the full SH3 interaction mutant was used, the rate of phosphorylation was identical to WT. This could be due to a random collision of the substrate and the kinase resulting in phosphorylation of one of the tyrosine phosphorylation sites, creating an motif for the SH2 domain to interaction with Syp, thus restoring the reaction at WT levels. However, further experiments would need to be conducted to further understand the mechanism of phosphorylation. For example, mutants of the C-src SH2 domain could be use to begin to tease apart the differing roles of the SH3 and SH2 domains.

This idea that the SH3 interaction of the Srcs with Syp might be a controlling interaction of the phosphorylation reaction is supported by the Vmax values for the different Srcs. C- and N2-Src have lower Vmax values than N1; C-Src - 132.9, N1-Src -203.6 and N2-Src - 145 determined using a PY20 antibody and C-Src was 2082, N1-Src 2612 and N2-Src 1470 determined using autoradiography. The difference between the values of the PY20 antibody and the autoradiography is likely to be a

result of the difference in sensitivity of detection of phosphorylation by the two different methods. Nevertheless, N1-Src appears to have a higher maximal rate of reaction compared to C- and N2-Src. As C- and N2-Src have lower Km values than N1-Src, it is possible that the apparent higher Vmax rate of N1-Src is a result of a faster reaction in the absence of a strong SH3 interaction with Syp. This may be an artefact of the *in vitro* design, where some kinases will phosphorylate their substrate as a result of random collisions. This fits with the saturation time point, where it was found that C- and N2-Src are able to phosphorylate Syp to a significantly greater extent than N1-Src, suggesting that once C- and N2-Src bind to Syp via the SH3 interaction motif, they are able to phosphorylate more tyrosines than N1-Src which does not bind as well. Therefore N1-src can only phosphorylate a few tyrosines before dissociating from Syp. This is supported by the fact that once the SH3 interaction motif is mutated, the initial rate of reaction is increased. To confirm this, a key experiment would be to determine the Km values of the SH3 interaction mutants for the 3 different Srcs.

To attribute a molecular role to the tyrosine phosphorylation of Syp, GST-pull downs were conducted with a variety of phospho GST-C-Syp mutants from synaptosomal lysates to determine if any of the interaction partners found were phosphorylation dependent (section 4.2.5). The phospho mutants were either total phospho-null or -mimetic, but as this is quite a large mutation and could affect the structure of the C-terminal of Syp, smaller mutations were used; Y263 and Y273 were changed into a phospho-null (Y to F) of phospho-mimetic (Y to E). These key residues were picked due to reports that they are phosphorylated following

peroxynitrie treatment, which initiates oxidative stress conditions and the kinase Fyn (a member of the Src kinase family) (Mallozzi et al., 2009). Further to this, section 4.2.3 also showed that Y273 was important in regulating the overall amount of phosphorylation detected when using the N2-Src in the kinase assay. Therefore, the interactions found with the double mutants might reflect a more physiological situation of phospho regulation of interactions of Syp.

In Section 4.2.5 we found that phosphorylation altered the proteins that were able to be extracted from synaptosomal lysates using different phospho mutants of the C-terminal. To identify proteins pulled down by the different phospho C-Syps, a large gel was run to allow bands to be easily cut out for the purpose of analysis by mass spectrometry. 1 centimetre 'slabs' were cut from each of the lanes and sent for mass spectrometry, where all the proteins present in a slab are to be identified. The slabs were cut so they contain the same molecular weight regions of the different sample lanes, therefore the results will show if a protein is present in a pull down from the different phospho C-Syp bait proteins. Based on these preliminary results, it is expected that phosphorylation is important in regulating the interactions of Syp with an array of proteins. However, at the time of writing, the mass spectrometry results have not yet been finalised.

4.3.2 - Cellular Function Appraisal

In section 4.2.5, mutations of the C-terminal of Syp were produced that singularly mutated either all the nine tyrosines, or two specific tyrosines, to phospho-null and -mimetic versions of Syp where the structure of the C-terminus remained relatively

intact. However, in experiments designed to examine the physiological role of tyrosine phosphorylation of Syp, a gross C-terminal truncation was used (T1, where the C-terminal of Syp was truncated at 238). The reason for using this truncation was that all the pentapeptide potential phosphorylation sites were removed from the C-terminus, while leaving the SH3 interaction motif intact, thus allowing it to conduct its physiological role of retrieving VAMP from the plasma membrane during the SV lifecycle (as detailed in chapter 3). Despite the truncation being a rather large mutation to examine the effect of 9 residues, it consisted of only the pentapeptide repeats and a very short sequence of residues (9 residues - PTSFSNQM) at the end of the C-terminal of Syp. The other main reason for using this truncation mutant as opposed to the tyrosine mutated versions of Syp was that these experiments were conducted prior to the generation of the tyrosine mutants.

In section 4.2.7, supercliptic synaptophluorin showed that pentapeptide repeats on the C-terminal of Syp was not a regulator of the SV lifecycle, since the T1 truncation mutation of SypHy showed normal traces of exocytosis and endocytosis. However this result is in contrast to other results, where the Cer trafficking assay showed that phosphorylation of Syp was important in the localisation and trafficking of Syp. This could be due to the selection method of ROIs during Supercliptic Synaptophluorins assays; ROIs were selected if they responded to both an electrical stimulation and the NH_4Cl perfusion, which discriminates against a potential population of SVs that do not respond at all, and these could be the defective SVs that were highlighted using other methods. Therefore it is important

to conclude that Syp pentapeptide repeats do not appear to affect the lifecycle of SVs that are able to recycle in a physiological manner.

In section 4.2.8 it was shown that the phosphorylation region of Syp was critical in the retrieval of VAMP during the SV lifecycle. However, chapter 3 detailed that this retrieval was mediated by the SH3 interaction motif on the C-terminal of Syp and via a complex of proteins as there was no direct interaction of VAMP with the C-terminal of Syp, therefore these results appear to be somewhat contradictory. To explain this, it is likely that the VAMP retrieval complex, which binds to the SH3 interaction motif on the C-terminal of Syp, may bind in a phosphorylation dependent manner. This idea is further supported by the results in section 4.2.5, were it was shown that phosphorylation can regulate many interactions of the C-terminal of Syp. It is also possible that both phosphorylation and a complex binding to the SH3 interaction motif are required for the retrieval of VAMP.

In experiments which relied on the transfection of neurons with Cer tagged verisons of Syp; the WT and phospho truncation T1. There was a difference in the overall expression of the different proteins; the phospho truncation resulted in a more diffuse staining across the length of the neuron. However, there were still clear puncta visible in the processes, which displayed normal trafficking during the SV recycling processes, and no obvious aggregations in other parts of the neuron (like the cell body or axon). It is possible that the Cer tagged is being removed from the mutant protein and free in the cell cytoplasm, this idea is supported by the fact that the T1 phospho truncation results in defective global trafficking of Cer in the Cer-

trafficking assay. However this expression profile seen in neurons transfected with the T1 phospho truncation differs to those transfected with the control Cer empty vector (observations by the MAC lab). To test to see if the protein is being degraded in the cell, one could immunostain neurons with antibodies targeted against the Cer tag and the protein of interest.

4.3.3 - Further Discussion

The significance of this chapter is that we have shown that the tyrosine phosphorylation region of Syp is fundamental to the role of Syp in retrieving VAMP from the plasma membrane. One of the few reports published about the role of tyrosine phosphorylation of Syp has shown that the tyrosine repeats are the interaction site of dynamin (Daly and Ziff, 2002), therefore it is possible to hypothesise that the roles of phosphorylation of Syp is to regulate the interactions. Mass spectrometry analysis will provide a list of all the potential interactions that are regulated in this manner.

The main drawback with the T1 mutation to examine the effect of tyrosine phosphorylation is that it removes more than just the tyrosine residues. The C-terminal of Syp is known to be the interaction site of some proteins (dynamin (Daly and Ziff, 2002), SIAH (Wheeler et al., 2002)), N2-Src and the amphiphysins (chapter 3), and also host the potential serine phosphorylation sites (Rubenstein et al., 1993). A way to begin to address whether the defect in VAMP retrieval seen using the phospho truncation T1 is caused by phosphorylation or by the removal of other potential binding on the C-terminus would be to create full lengths Cer-Syps which

have different lengths of truncation of the C-terminal, in a similar fashion to figure 3.6.

Other groups have used similar truncations mutants of the C-terminal of Syp to try and address if it is important in Syp function. It has been shown that the truncations of the C-terminal of Syp (very similar to the T1, by removing the pentapeptide repeats but maintaining the SH3 interaction motif) does not affect localisation of Syp with VAMP in FRET experiments (Felkl and Leube, 2008, Pennuto et al., 2002). This suggests that the phosphorylation region of the C-terminal of Syp is not the site of interaction between the two proteins. This agrees with our own data, which shows that there was no direct interaction of the C-terminal of Syp with VAMP in synaptosomal lysates (figure 3.22). However, the fact that VAMP and Syp are reported to interact normally when the phosphorylation region of the C-terminus of Syp is removed suggests that the C-terminal would not be important for retrieval of VAMP, which is in contrast to our data. However, this could be explained by the fact that we looked at the neurons under electrical stimulation, while the FRET experiments were under basal conditions. Although we saw a large defect in VAMP retrieval, there was still some occurring, just very slowly. Therefore, it is possible that in basal conditions VAMP is less likely to be stuck on the plasma membrane, due to a defect of VAMP retrieval during SV recycling. Further to this, it is important to consider that FRET is only indicative of an interaction. As there are 70 copies of VAMP and 30 copies of Syp on the relatively smaller surface area of an SV (Takamori et al., 2006), tagging them with large

fluorescent FRET tags (as an acceptor fluorophore and a donor fluorophore are required for FRET) might not depict the most accurate reading of interactions.

In a recent paper, a very similar truncation of the C-terminus of Syp as our T1 truncation (six amino acids longer) was used in experiments to determine the role of Syp in the kinetics of endocytosis. Using a SV2a superecliptic phluorin and electrophysiological recordings, it was shown that the end of the C-terminus of Syp was important in regulating endocytosis during persistent stimulation, but not after. This suggests that the defects caused by the removal of the phospho region of Syp is important during stimulation, therefore suggesting that efficient retrieval of VAMP is important in maintain efficient endocytosis during persistent stimulation.

A better way would be to employ the mutant of Syp where all the tyrosines are either phosho-null or -mimetic, as used in the biochemical studies. To further test the significance of tyrosine phosphorylation mediated by the Srcs would be to conduct the VAMP phluorin assay in the Syp knockout neurons which have been subjected to knockdowns of the different Srcs, via shRNA. A simpler way would be to inhibit Src activity by application of PP2 in conjunction with the phosphorylation mutants of Syp.

An exciting prospect will be the results of the specific tyrosine residues that are phosphorylated by the three different Srcs. This information will allow one to make Src specific phosphorylation mutants to examine the effect of each of the difference kinase. Further to this, with potential mass spectrometry results identifying the *in vivo* phosphorylation sites of Syp, it will be the first report of their identify and this

facilitate future research in understanding the role of tyrosine phosphorylation of Syp.

In summary, it was found that C- and N2-Src are more efficient at phosphorylating Syp than N1-Src, and truncation of the phosphorylation region of the C-terminal of Syp results in defective VAMP retrieval from the plasma membrane.

Chapter 5 Final Discussion

5.1 - A Potential model for the C-terminal of Syp in VAMP retrieval

This project has provided clear evidence that both the SH3 interaction motif and the potential tyrosine phosphorylation of Syp are important in the in the retrieval of VAMP from the plasma membrane during the SV lifecycle. Interestingly, the τ value for the retrieval of the VAMP phluorin was the same for both the SH3 interaction and phospho mutants (49.44 ± 8.7 and 49.45 ± 12.78 respectively). This suggests that the SH3 mediated interactions and tyrosine phosphorylation regulate the same process responsible for the VAMP retrieval. A model for the retrieval of VAMP during the SV lifecycle can therefore be proposed; C-Src binds to Syp via the SH3 interaction motif and phosphorylates the C-terminal of Syp. Once phosphorylated, the complex of proteins that have a direct interaction with VAMP are then able to bind to the SH3 interaction motif of Syp. This complex then retrieves VAMP from the plasma membrane as the vesicle invaginates (figure 5.1).

This model has important implications, as the retrieval of VAMP is a very important step in the maintenance of the SV lifecycle and a fundamental protein in regulating vesicle fusion (Schoch et al., 2001). Further to this, it has been implicated in a rapid mode of endocytosis in which VAMP is responsible for refilling the readily releasable pool of SVs (Deak et al., 2004). Indeed, it was found in this current study the failure to retrieve VAMP altered the size of the recycling pool (figure 3.20). In particular, both the Syp knockout and the SH3 interaction mutant saw a significant reduction in the proportion of SVs that are available for recycling. Therefore, in

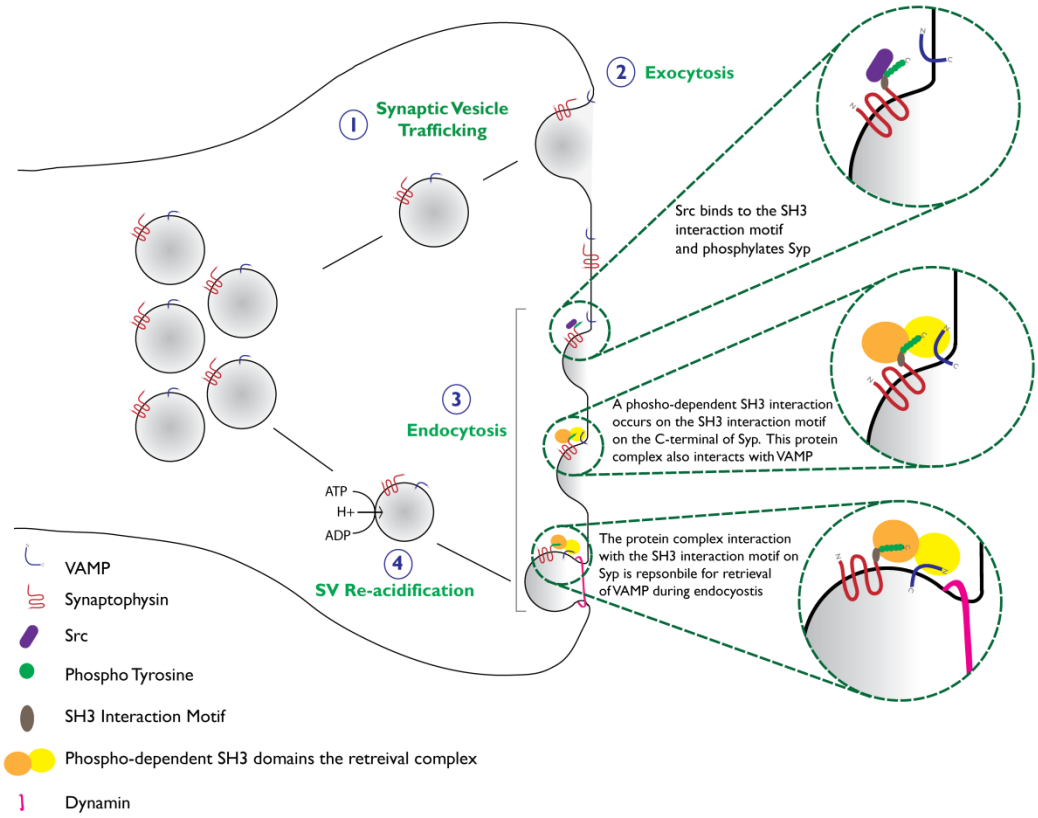

Figure 5-1 Potential role of the Syp C-terminus in VAMP retrieval

Both VAMP and Syp are located on the SV membrane. SVs are trafficked to the cell surface membrane, and following a Ca^{2+} influx the vesicles fuse with the membrane. In order for VAMP to participate in further rounds of SV recycling, and to mediate a rapid form of clathrin independent endocytosis it must be retrieved. It is proposed that Syp plays an important role in this in a phosphorylation dependent manner, mediated by the SH3 interaction motif on its C-terminal. After exocytosis, Src binds to the SH3 interaction motif on the C-terminal of Syp and phosphorylate the tyrosine pentapeptide repeats. This allows a VAMP retrieval complex of proteins to bind to Syp, and this interaction is mediated by the SH3 interaction motif on the C-terminal of Syp. As a result, VAMP is retrieved from the plasma membrane during endocytosis, freeing it to take part in further rounds of SV recycling.

order to maintain the efficient release of NT during this rapid form of endocytosis, VAMP must be efficiently retrieved from the plasma membrane. This idea fits well with the phenotypes in the early Syp studies where reports suggested that defects were found in a clathrin independent form of endocytosis (Daly et al., 2000, Spiwoks-Becker et al., 2001). It is possible to imagine that these endocytosis defects were only found during periods of high stimulation due to its high copy number of VAMP on each SV Takamori et al reported that about 70 copies of VAMP are found on a typical SV, which outnumbers the requirement of only 1-15 VAMPs for the formation of the SNARE complex during SV fusion (Han et al., 2004, Hua and Scheller, 2001, Keller et al., 2004, Montecucco et al., 2005, van den Bogaart et al., 2010). This could suggest that the physiological defect that results from defective VAMP retrieval would only be seen when the system is under stress. This idea is supported by the fact that Syp knockout studies found impaired LTP (Janz et al., 1999, Schmitt et al., 2009). LTP is induced under high and persistent stimulations, where potentially the high copy number of VAMP would be exhausted and mostly stuck in the plasma membrane, due to defective Syp dependent VAMP retrieval. Given that VAMP has been implicated in a rapid form of endocytosis, which mediates rapid reuse of SVs (Deak et al., 2004), it is possible that retrieval of VAMP by Syp might be a critical step in this process. For example, under persistent stimulation, clathrin mediated endocytosis will reach its capacity and the recycling of the SVs becomes insufficient due to its slow speed (Balaji and Ryan, 2007, Dittman and Ryan, 2009). In WT cells, this role is normally completed by VAMP

which is retrieved by Syp, but in Syp knockout neurons VAMP is not retrieved efficiently and thus impairing the replenishment of the recycling pool of SVs, leading to less NT release to induce LTP.

A potential activating step of this VAMP mediated endocytosis is provided by the observation that the retrieval of VAMP was dependent on the potential tyrosine phosphorylation of Syp, as truncation of the phospho region of the C-terminus of Syp resulted in a lack of VAMP retrieval from the plasma membrane. Turnover of tyrosine phosphorylation of Syp has been reported to only occur under LTP-inducing stimulations (Mullany and Lynch, 1998). The current findings revealed that phosphorylation region of the C-terminal of Syp was critical in the retrieval of VAMP, as the complex of protein that binds to the SH3 domain of Syp and interacts directly with VAMP to retrieve may bind in a phosphorylation dependent manner. For this reason, while the phosphorylation state of Syp is unchanged during mild stimulations (Rubenstein et al., 1993), Syp becomes phosphorylated under high or persistent stimulation. This allows the VAMP retrieval complex to bind to Syp and therefore retrieve VAMP, making it available for rapid rounds of SV recycling. It is important to consider that the phospho truncation might also be removing other interaction sites on the C-terminus. In support of this idea, a recent paper published last year showed that truncation of the tyrosine repeats on the C-terminus of Syp (very similar to T1 mutant described in this thesis) impaired the kinetics of endocytosis during, and not after, persistent stimulation (Kwon and Chapman, 2011), where tyrosine phosphorylation of Syp is able to turnover (Mullany and Lynch, 1998).

A possible mechanism to facilitate this tyrosine phosphorylation switch to activate the VAMP rapid clathrin independent endocytosis is provided by the fact that dynamin is known to bind to the tyrosine repeats of the C-terminal of Syp (Daly and Ziff, 2002, Gonzalez-Jamett et al., 2010). Therefore, it is likely that dynamin displays a phosphorylation dependent interaction with Syp. The VAMP mediated endocytosis is more rapid than clathrin dependent endocytosis (Deak et al., 2004), suggesting that it may be performed in a similar fashion to kiss-and-run; where NT release is completed without full fusion of the SV into the plasma membrane. This would mean that the site of this VAMP mediated endocytosis is within the active zone. In the active zone, there is a high level of Ca^{2+}, and the interaction between Syp and dynamin is known to only occur at concentrations of Ca^{2+} akin to the active zones (Daly and Ziff, 2002).

We also demonstrated that syndapin binds to Syp via the SH3 interaction motif. Syndapin is known to have a phosphorylation dependent interaction with dynamin (Anggono et al., 2006), and interestingly this interaction is stimulation dependent. It could be hypothesised that under the levels of LTP inducing stimulation, syndapin might recruit dynamin to the invaginating SV where VAMP is via a direct interaction of the SH3 domain of syndapin and the C-terminal of Syp. If the rapid VAMP mediated endocytosis is undergoing transient fusion, as opposed to full fusion, then the degree of membrane curvature would be different to the clathrin mediated invagination, suggesting that a different BAR domain containing protein to amphiphysin might be involved in recruiting dynamin to the neck of the invaginating SV.

5.2 - Further Experiments

5.2.1 - Is the Retrieval of VAMP Defect seen using the Phosphorylation Truncation T1 a Result of Tyrosine Phosphorylation or Removing Potential Interaction Sites?

It is important that the phospho truncation T1 also removes interaction sites for other synaptic proteins. It is known that the interaction of Syp and dynamin increased with the length of the C-terminus (Daly and Ziff, 2002), and this was also shown in chapter 3 to be true for N1- and N2-Src. It is also known that AP1 binds to the C-terminal (Horikawa et al., 2002) and we also showed in chapter 3 that the amphiphysins also bind to the C-terminal, although the exact site is not known. Further to this, the interaction of Siah1a has been mapped to the end of the C-terminal (Wheeler et al., 2002), which is removed in our T1 truncation. Therefore, it is possible that by removing the phosphorylation sites, which might also act as interaction motifs, we are disrupting VAMP retrieval by simply removing other interaction sites. However, this is unlikely as we have shown that the retrieval of VAMP is defective in a single point mutant of Syp (R) where the phosphorylation repeats are still intact, and any interactions that depend on the pentapetide repeats would still be able to form. However, it is also possible that the retrieval of VAMP depends on interactions mediated by both the SH3 interaction motif and the phosphorylation repeats, or an end fragment of the C-terminal of Syp.

To determine whether the effects seen by the phospho T1 truncation of Syp are as a result of defective tyrosine phosphorylation or loss of interaction sites, one would

need to repeat the VAMP phluorin assays with single point phosphorylation mutations of the pentapeptide repeats, according to results to be obtained from mass spectrometry of *in vitro* and *in vivo* phosphorylated Syp.

Another drawback in using the phosphorylation truncation T1 is that we are also removing serine phosphorylation sites (Rubenstein et al., 1993). To determine if the defect in VAMP retrieval is caused by a lack of serine phosphorylation of Syp, one could repeat the VAMP phluorin assays in the presence of a serine phosphorylation inhibitor, such as KN-93 which is a CamKII inhibitor, the kinase thought to act on the serine residues (Rubenstein et al., 1993). However, this approach would be tricky as serine phosphorylation is important in regulating endocytosis. Therefore a more specific experiment would be to mutate the three serine phosphorylation sites on the C-terminal of Syp to E or A (to produce phospho-null and -mimetic versions), and conduct the VAMP phluorin assays with that construct.

5.2.2 - Definition of the VAMP Retrieval Complex

Although mass spectrometry analysis of GST-pull downs have provided us with a catalogue of proteins that bind to the C-terminal of Syp (appendix table 1), we have only identified two proteins which bind specifically to the SH3 interaction motif of Syp. Thus, further biochemical experiments must be conducted to identify the protein that directly links Syp with VAMP. We are currently awaiting the delivery of the mass spectrometry analysis of GST-pull downs investigating the phosphorylation dependent interactions of the C-terminus of Syp. Together, the mass spectrometry

results of the catalogue of proteins that interact with the C-terminal of Syp and the mass spectrometry results of the phosphorylation dependent interactions should provide a list of potential candidates.

5.2.3 - The Global Effects of SV Turnover

To examine if the SH3 interaction mutant or the phosphorylation truncation T1 mutants, and thus the retrieval of VAMP, affect gobal SV turnover, one could use FM dyes which label recycling SVs (Clayton et al., 2009). This would provide information about the turnover of SVs and the kinetics of exocytosis. This technique has been used to compare WT and Syp knockout neurons, showing no difference between the two systems (Gordon et al., 2011). However, the effect was not studied under LTP inducing stimulations as the defects reported in Syp knockout systems are found at these higher levels of stimulation (Spiwoks-Becker et al., 2001). Further to this, this approach relies on FM dyes being taken up by every SV in every endocytosis pathway. It is possible that the VAMP mediated form of endocytosis differs from that of clathrin mediated and therefore might not be labelled using FM dyes. It has been suggested that FM dyes are not a suitable measure of kiss-and-run as they may not pass through the fusion pore (Chen et al., 2008). With this in mind, one would need to repeat these experiments with quantum dots (Zhang et al., 2007) during high stimulation or to analyse the ultra-structure of the SVs formed during high stimulation, where the defective retrieval of VAMP appears to have its effect.

5.2.4 - The Significance of the SH3 Interaction Motif and Phosphorylation on LTP

The Syp knockout mouse displays defects in LTP (Janz et al., 1999, Schmitt et al., 2009), which suggests that Syp is important in regulating endocytosis during high and persistant levels of stimulation. Therefore to examine if this is due to the defects in the retrieval of VAMP via the phosphorylation dependent SH3 interaction reported in this thesis, one could use electrophysiological methods to determine the postsynaptic responses of Syp knockout neurons that have been transfected with either the SH3 interaction motifs or the phosphorylation mutants of Syp. In particular, paired recordings of neurons would be useful to measure this.

5.3 - Concluding Statement

This is the first study that has provided molecular mapping and definition of the interaction of Syp. Here, I report that both syndapin and C-Src bind to the SH3 interaction motif on the C-terminal of Syp. Functional analysis of these interactions in neurons has suggested that there may be a tyrosine phosphorylation dependent protein complex, which binds to the SH3 interaction motif on the C-terminal of Syp, and is fundamental in the retrieval of VAMP during the SV lifecycle.

Chapter 6 References

AHN, S., KIM, J., LUCAVECHE, C. L., REEDY, M. C., LUTTRELL, L. M., LEFKOWITZ, R. J. & DAAKA, Y. 2002. Src-dependent tyrosine phosphorylation regulates dynamin self-assembly and ligand-induced endocytosis of the epidermal growth factor receptor. *J Biol Chem,* 277**,** 26642-51.

ALBILLOS, A., DERNICK, G., HORSTMANN, H., ALMERS, W., ALVAREZ DE TOLEDO, G. & LINDAU, M. 1997. The exocytotic event in chromaffin cells revealed by patch amperometry. *Nature,* 389**,** 509-12.

ALDER, J., KANKI, H., VALTORTA, F., GREENGARD, P. & POO, M. M. 1995. Overexpression of synaptophysin enhances neurotransmitter secretion at Xenopus neuromuscular synapses. *J Neurosci,* 15**,** 511-9.

ALDER, J., XIE, Z. P., VALTORTA, F., GREENGARD, P. & POO, M. 1992. Antibodies to synaptophysin interfere with transmitter secretion at neuromuscular synapses. *Neuron,* 9**,** 759-68.

ANGGONO, V., SMILLIE, K. J., GRAHAM, M. E., VALOVA, V. A., COUSIN, M. A. & ROBINSON, P. J. 2006. Syndapin I is the phosphorylation-regulated dynamin I partner in synaptic vesicle endocytosis. *Nat Neurosci,* 9**,** 752-60.

ARAC, D., CHEN, X., KHANT, H. A., UBACH, J., LUDTKE, S. J., KIKKAWA, M., JOHNSON, A. E., CHIU, W., SUDHOF, T. C. & RIZO, J. 2006. Close membrane-membrane proximity induced by Ca(2+)-dependent multivalent binding of synaptotagmin-1 to phospholipids. *Nat Struct Mol Biol,* 13**,** 209-17.

ARAVANIS, A. M., PYLE, J. L. & TSIEN, R. W. 2003. Single synaptic vesicles fusing transiently and successively without loss of identity. *Nature,* 423**,** 643-7.

ARTHUR, C. P. & STOWELL, M. H. 2007. Structure of synaptophysin: a hexameric MARVEL-domain channel protein. *Structure,* 15**,** 707-14.

BALAJI, J. & RYAN, T. A. 2007. Single-vesicle imaging reveals that synaptic vesicle exocytosis and endocytosis are coupled by a single stochastic mode. *Proc Natl Acad Sci U S A,* 104**,** 20576-81.

BALDWIN, M. L., CAMMAROTA, M., SIM, A. T. & ROSTAS, J. A. 2006. Src family tyrosine kinases differentially modulate exocytosis from rat brain nerve terminals. *Neurochem Int,* 49**,** 80-6.

BARNEKOW, A., JAHN, R. & SCHARTL, M. 1990. Synaptophysin: a substrate for the protein tyrosine kinase pp60c-src in intact synaptic vesicles. *Oncogene,* 5**,** 1019-24.

BECHER, A., DRENCKHAHN, A., PAHNER, I., MARGITTAI, M., JAHN, R. & AHNERT-HILGER, G. 1999. The synaptophysin-synaptobrevin complex: a hallmark of synaptic vesicle maturation. *J Neurosci,* 19**,** 1922-31.

BENNETT, M. K., CALAKOS, N. & SCHELLER, R. H. 1992. Syntaxin: a synaptic protein implicated in docking of synaptic vesicles at presynaptic active zones. *Science,* 257**,** 255-9.

BEUTNER, D., VOETS, T., NEHER, E. & MOSER, T. 2001. Calcium dependence of exocytosis and endocytosis at the cochlear inner hair cell afferent synapse. *Neuron,* 29**,** 681-90.

BLASI, J., CHAPMAN, E. R., LINK, E., BINZ, T., YAMASAKI, S., DE CAMILLI, P., SUDHOF, T. C., NIEMANN, H. & JAHN, R. 1993a. Botulinum neurotoxin A selectively cleaves the synaptic protein SNAP-25. *Nature,* 365**,** 160-3.

BLASI, J., CHAPMAN, E. R., YAMASAKI, S., BINZ, T., NIEMANN, H. & JAHN, R. 1993b. Botulinum neurotoxin C1 blocks neurotransmitter release by means of cleaving HPC-1/syntaxin. *EMBO J,* 12**,** 4821-8.

BLISS, T. V. & LOMO, T. 1970. Plasticity in a monosynaptic cortical pathway. *J Physiol,* 207**,** 61P.

BOGGON, T. J. & ECK, M. J. 2004. Structure and regulation of Src family kinases. *Oncogene,* 23**,** 7918-27.

BONANOMI, D., RUSCONI, L., COLOMBO, C. A., BENFENATI, F. & VALTORTA, F. 2007. Synaptophysin I selectively specifies the exocytic pathway of synaptobrevin 2/VAMP2. *Biochem J,* 404**,** 525-34.

BRABEK, J., MOJZITA, D., NOVOTNY, M., PUTA, F. & FOLK, P. 2002. The SH3 domain of Src can downregulate its kinase activity in the absence of the SH2 domain-pY527 interaction. *Biochem Biophys Res Commun,* 296**,** 664-70.

BRADSHAW, J. M., MITAXOV, V. & WAKSMAN, G. 1999. Investigation of phosphotyrosine recognition by the SH2 domain of the Src kinase. *J Mol Biol,* 293**,** 971-85.

BRADSHAW, J. M. & WAKSMAN, G. 2002. Molecular recognition by SH2 domains. *Adv Protein Chem,* 61**,** 161-210.

BREMNES, T., LAUVRAK, V., LINDQVIST, B. & BAKKE, O. 1998. A region from the medium chain adaptor subunit (mu) recognizes leucine- and tyrosine-based sorting signals. *J Biol Chem,* 273**,** 8638-45.

BUCKLEY, K. M., FLOOR, E. & KELLY, R. B. 1987. Cloning and sequence analysis of cDNA encoding p38, a major synaptic vesicle protein. *J Cell Biol,* 105**,** 2447-56.

BURGOYNE, R. D. & MORGAN, A. 2003. Secretory granule exocytosis. *Physiol Rev,* 83**,** 581-632.

CALAKOS, N. & SCHELLER, R. H. 1994. Vesicle-associated membrane protein and synaptophysin are associated on the synaptic vesicle. *J Biol Chem,* 269**,** 24534-7.

CAO, H., CHEN, J., AWONIYI, M., HENLEY, J. R. & MCNIVEN, M. A. 2007. Dynamin 2 mediates fluid-phase micropinocytosis in epithelial cells. *J Cell Sci,* 120**,** 4167-77.

CAO, H., GARCIA, F. & MCNIVEN, M. A. 1998. Differential distribution of dynamin isoforms in mammalian cells. *Mol Biol Cell,* 9**,** 2595-609.

CARRION-VAZQUEZ, M., FERNANDEZ, A. M., CHOWEN, J. & NIETO-SAMPEDRO, M. 1998. Brain Ac39/physophilin: cloning, coexpression and colocalization with synaptophysin. *Eur J Neurosci,* 10**,** 1153-66.

CECCARELLI, B., HURLBUT, W. P. & MAURO, A. 1973. Turnover of transmitter and synaptic vesicles at the frog neuromuscular junction. *J Cell Biol,* 57**,** 499-524.

CESARENI, G., PANNI, S., NARDELLI, G. & CASTAGNOLI, L. 2002. Can we infer peptide recognition specificity mediated by SH3 domains? *FEBS Lett,* 513**,** 38-44.

CHAN, R. C. & BLACK, D. L. 1995. Conserved intron elements repress splicing of a neuron-specific c-src exon in vitro. *Mol Cell Biol,* 15**,** 6377-85.

CHEN, X., BARG, S. & ALMERS, W. 2008. Release of the styryl dyes from single synaptic vesicles in hippocampal neurons. *J Neurosci,* 28**,** 1894-903.

CHENG, Y., BOLL, W., KIRCHHAUSEN, T., HARRISON, S. C. & WALZ, T. 2007. Cryo-electron tomography of clathrin-coated vesicles: structural implications for coat assembly. *J Mol Biol,* 365**,** 892-9.

CICERO, D. O., CONTESSA, G. M., PERTINHEZ, T. A., GALLO, M., KATSUYAMA, A. M., PACI, M., FARAH, C. S. & SPISNI, A. 2007. Solution structure of ApaG from Xanthomonas axonopodis pv. citri reveals a fibronectin-3 fold. *Proteins,* 67**,** 490-500.

CLAYTON, E. L., ANGGONO, V., SMILLIE, K. J., CHAU, N., ROBINSON, P. J. & COUSIN, M. A. 2009. The phospho-dependent dynamin-syndapin interaction triggers activity-dependent bulk endocytosis of synaptic vesicles. *J Neurosci,* 29**,** 7706-17.

CLAYTON, E. L., EVANS, G. J. & COUSIN, M. A. 2008. Bulk synaptic vesicle endocytosis is rapidly triggered during strong stimulation. *J Neurosci,* 28**,** 6627-32.

COLLINS, B. M., MCCOY, A. J., KENT, H. M., EVANS, P. R. & OWEN, D. J. 2002. Molecular architecture and functional model of the endocytic AP2 complex. *Cell,* 109**,** 523-35.

COUSIN, M. A. 2000. Synaptic vesicle endocytosis: calcium works overtime in the nerve terminal. *Mol Neurobiol,* 22**,** 115-28.

COUSIN, M. A., MALLADI, C. S., TAN, T. C., RAYMOND, C. R., SMILLIE, K. J. & ROBINSON, P. J. 2003. Synapsin I-associated phosphatidylinositol 3-kinase mediates synaptic vesicle delivery to the readily releasable pool. *J Biol Chem,* 278**,** 29065-71.

CREMONA, O., DI PAOLO, G., WENK, M. R., LUTHI, A., KIM, W. T., TAKEI, K., DANIELL, L., NEMOTO, Y., SHEARS, S. B., FLAVELL, R. A., MCCORMICK, D. A. & DE CAMILLI, P. 1999. Essential role of phosphoinositide metabolism in synaptic vesicle recycling. *Cell,* 99**,** 179-88.

DALY, C., SUGIMORI, M., MOREIRA, J. E., ZIFF, E. B. & LLINAS, R. 2000. Synaptophysin regulates clathrin-independent endocytosis of synaptic vesicles. *Proc Natl Acad Sci U S A,* 97**,** 6120-5.

DALY, C. & ZIFF, E. B. 2002. Ca2+-dependent formation of a dynamin-synaptophysin complex: potential role in synaptic vesicle endocytosis. *J Biol Chem,* 277**,** 9010-5.

DAVID, C., MCPHERSON, P. S., MUNDIGL, O. & DE CAMILLI, P. 1996. A role of amphiphysin in synaptic vesicle endocytosis suggested by its binding to dynamin in nerve terminals. *Proc Natl Acad Sci U S A,* 93**,** 331-5.

DEAK, F., SCHOCH, S., LIU, X., SUDHOF, T. C. & KAVALALI, E. T. 2004. Synaptobrevin is essential for fast synaptic-vesicle endocytosis. *Nat Cell Biol,* 6**,** 1102-8.

DEAN, C., DUNNING, F. M., LIU, H., BOMBA, E., BHARAT, V., AHMED, S. & CHAPMAN, E. R. 2012. Axonal and dendritic synaptotagmin isoforms revealed by a pHluorin-syt functional screen. *Mol Biol Cell*.

DI PAOLO, G., SANKARANARAYANAN, S., WENK, M. R., DANIELL, L., PERUCCO, E., CALDARONE, B. J., FLAVELL, R., PICCIOTTO, M. R., RYAN, T. A., CREMONA, O. & DE CAMILLI, P. 2002. Decreased synaptic vesicle recycling efficiency and cognitive deficits in amphiphysin 1 knockout mice. *Neuron,* 33**,** 789-804.

DITTMAN, J. & RYAN, T. A. 2009. Molecular circuitry of endocytosis at nerve terminals. *Annu Rev Cell Dev Biol,* 25**,** 133-60.

DULUBOVA, I., SUGITA, S., HILL, S., HOSAKA, M., FERNANDEZ, I., SUDHOF, T. C. & RIZO, J. 1999. A conformational switch in syntaxin during exocytosis: role of munc18. *EMBO J,* 18**,** 4372-82.

EDELMANN, L., HANSON, P. I., CHAPMAN, E. R. & JAHN, R. 1995. Synaptobrevin binding to synaptophysin: a potential mechanism for controlling the exocytotic fusion machine. *EMBO J,* 14**,** 224-31.

ESHKIND, L. G. & LEUBE, R. E. 1995. Mice lacking synaptophysin reproduce and form typical synaptic vesicles. *Cell Tissue Res,* 282**,** 423-33.

EVANS, G. J. & COUSIN, M. A. 2005. Tyrosine phosphorylation of synaptophysin in synaptic vesicle recycling. *Biochem Soc Trans,* 33**,** 1350-3.

EVANS, G. J. & POCOCK, J. M. 1999. Modulation of neurotransmitter release by dihydropyridine-sensitive calcium channels involves tyrosine phosphorylation. *Eur J Neurosci,* 11**,** 279-92.

EVERGREN, E., MARCUCCI, M., TOMILIN, N., LOW, P., SLEPNEV, V., ANDERSSON, F., GAD, H., BRODIN, L., DE CAMILLI, P. & SHUPLIAKOV, O. 2004. Amphiphysin is a component of clathrin coats formed during synaptic vesicle recycling at the lamprey giant synapse. *Traffic,* 5**,** 514-28.

FALET, H., RAMOS-MORALES, F., BACHELOT, C., FISCHER, S. & RENDU, F. 1996. Association of the protein tyrosine phosphatase PTP1C with the protein tyrosine kinase c-Src in human platelets. *FEBS Lett,* 383**,** 165-9.

FARSAD, K., RINGSTAD, N., TAKEI, K., FLOYD, S. R., ROSE, K. & DE CAMILLI, P. 2001. Generation of high curvature membranes mediated by direct endophilin bilayer interactions. *J Cell Biol,* 155**,** 193-200.

FELKL, M. & LEUBE, R. E. 2008. Interaction assays in yeast and cultured cells confirm known and identify novel partners of the synaptic vesicle protein synaptophysin. *Neuroscience,* 156**,** 344-52.

FENG, S., CHEN, J. K., YU, H., SIMON, J. A. & SCHREIBER, S. L. 1994. Two binding orientations for peptides to the Src SH3 domain: development of a general model for SH3-ligand interactions. *Science,* 266**,** 1241-7.

FENG, S., KASAHARA, C., RICKLES, R. J. & SCHREIBER, S. L. 1995. Specific interactions outside the proline-rich core of two classes of Src homology 3 ligands. *Proc Natl Acad Sci U S A,* 92**,** 12408-15.

FERGUSON, S. M., BRASNJO, G., HAYASHI, M., WOLFEL, M., COLLESI, C., GIOVEDI, S., RAIMONDI, A., GONG, L. W., ARIEL, P., PARADISE, S., O'TOOLE, E., FLAVELL, R., CREMONA, O., MIESENBOCK, G., RYAN, T. A. & DE CAMILLI, P. 2007. A selective activity-dependent requirement for dynamin 1 in synaptic vesicle endocytosis. *Science,* 316**,** 570-4.

FERNÁNDEZ-ALFONSO, T., KWAN, R. & RYAN, T. A. 2006. Synaptic Vesicles Interchange Their Membrane Proteins with a Large Surface Reservoir during Recycling. *Neuron,* 51**,** 179-186.

FERNANDEZ-CHACON, R., WOLFEL, M., NISHIMUNE, H., TABARES, L., SCHMITZ, F., CASTELLANO-MUNOZ, M., ROSENMUND, C., MONTESINOS, M. L., SANES, J. R., SCHNEGGENBURGER, R. & SUDHOF, T. C. 2004. The synaptic vesicle protein CSP alpha prevents presynaptic degeneration. *Neuron,* 42**,** 237-51.

FESCE, R., GROHOVAZ, F., VALTORTA, F. & MELDOLESI, J. 1994. Neurotransmitter release: fusion or 'kiss-and-run'? *Trends Cell Biol,* 4**,** 1-4.

FESSART, D., SIMAAN, M. & LAPORTE, S. A. 2005. c-Src regulates clathrin adapter protein 2 interaction with beta-arrestin and the angiotensin II type 1 receptor during clathrin-mediated internalization. *Mol Endocrinol,* 19**,** 491-503.

FORD, M. G., MILLS, I. G., PETER, B. J., VALLIS, Y., PRAEFCKE, G. J., EVANS, P. R. & MCMAHON, H. T. 2002. Curvature of clathrin-coated pits driven by epsin. *Nature,* 419**,** 361-6.

GAD, H., RINGSTAD, N., LOW, P., KJAERULFF, O., GUSTAFSSON, J., WENK, M., DI PAOLO, G., NEMOTO, Y., CRUN, J., ELLISMAN, M. H., DE CAMILLI, P., SHUPLIAKOV, O. & BRODIN, L. 2000. Fission and uncoating of synaptic clathrin-coated vesicles are perturbed by disruption of interactions with the SH3 domain of endophilin. *Neuron,* 27**,** 301-12.

GAIDAROV, I. & KEEN, J. H. 1999. Phosphoinositide-AP-2 interactions required for targeting to plasma membrane clathrin-coated pits. *J Cell Biol,* 146**,** 755-64.

GALLI, T., MCPHERSON, P. S. & DE CAMILLI, P. 1996. The V0 sector of the V-ATPase, synaptobrevin, and synaptophysin are associated on synaptic vesicles in a Triton X-100-resistant, freeze-thawing sensitive, complex. *J Biol Chem,* 271**,** 2193-8.

GEPPERT, M., GODA, Y., HAMMER, R. E., LI, C., ROSAHL, T. W., STEVENS, C. F. & SUDHOF, T. C. 1994. Synaptotagmin I: a major Ca2+ sensor for transmitter release at a central synapse. *Cell,* 79**,** 717-27.

GINCEL, D. & SHOSHAN-BARMATZ, V. 2002. The synaptic vesicle protein synaptophysin: purification and characterization of its channel activity. *Biophys J,* 83**,** 3223-9.

GONZALEZ-JAMETT, A. M., BAEZ-MATUS, X., HEVIA, M. A., GUERRA, M. J., OLIVARES, M. J., MARTINEZ, A. D., NEELY, A. & CARDENAS, A. M. 2010. The association of dynamin with synaptophysin regulates quantal size and duration of exocytotic events in chromaffin cells. *J Neurosci,* 30**,** 10683-91.

GORDON, S. L., LEUBE, R. E. & COUSIN, M. A. 2011. Synaptophysin is required for synaptobrevin retrieval during synaptic vesicle endocytosis. *J Neurosci,* 31**,** 14032-6.

GRAHAM, M. E., ANGGONO, V., BACHE, N., LARSEN, M. R., CRAFT, G. E. & ROBINSON, P. J. 2007. The in vivo phosphorylation sites of rat brain dynamin I. *J Biol Chem,* 282**,** 14695-707.

GRANSETH, B., ODERMATT, B., ROYLE, S. J. & LAGNADO, L. 2006. Clathrin-mediated endocytosis is the dominant mechanism of vesicle retrieval at hippocampal synapses. *Neuron,* 51**,** 773-86.

GRAY, N. W., FOURGEAUD, L., HUANG, B., CHEN, J., CAO, H., OSWALD, B. J., HEMAR, A. & MCNIVEN, M. A. 2003. Dynamin 3 is a component of the postsynapse, where it interacts with mGluR5 and Homer. *Curr Biol,* 13**,** 510-5.

GREENGARD, P., VALTORTA, F., CZERNIK, A. J. & BENFENATI, F. 1993. Synaptic vesicle phosphoproteins and regulation of synaptic function. *Science,* 259**,** 780-5.

GURD, J. W. 1997. Protein tyrosine phosphorylation: implications for synaptic function. *Neurochem Int,* 31**,** 635-49.

HAASS, N. K., KARTENBECK, M. A. & LEUBE, R. E. 1996. Pantophysin is a ubiquitously expressed synaptophysin homologue and defines constitutive transport vesicles. *J Cell Biol,* 134**,** 731-46.

HAN, X., WANG, C. T., BAI, J., CHAPMAN, E. R. & JACKSON, M. B. 2004. Transmembrane segments of syntaxin line the fusion pore of Ca2+-triggered exocytosis. *Science,* 304**,** 289-92.

HANNAH, M. J., SCHMIDT, A. A. & HUTTNER, W. B. 1999. Synaptic vesicle biogenesis. *Annu Rev Cell Dev Biol,* 15**,** 733-98.

HANSON, P. I., HEUSER, J. E. & JAHN, R. 1997. Neurotransmitter release - four years of SNARE complexes. *Curr Opin Neurobiol,* 7**,** 310-5.

HAO, W., LUO, Z., ZHENG, L., PRASAD, K. & LAFER, E. M. 1999. AP180 and AP-2 interact directly in a complex that cooperatively assembles clathrin. *J Biol Chem,* 274**,** 22785-94.

HARATA, N. C., CHOI, S., PYLE, J. L., ARAVANIS, A. M. & TSIEN, R. W. 2006. Frequency-dependent kinetics and prevalence of kiss-and-run and reuse at hippocampal synapses studied with novel quenching methods. *Neuron,* 49**,** 243-56.

HAUCKE, V. & DE CAMILLI, P. 1999. AP-2 recruitment to synaptotagmin stimulated by tyrosine-based endocytic motifs. *Science,* 285**,** 1268-71.

HAUCKE, V., WENK, M. R., CHAPMAN, E. R., FARSAD, K. & DE CAMILLI, P. 2000. Dual interaction of synaptotagmin with mu2- and alpha-adaptin facilitates clathrin-coated pit nucleation. *EMBO J,* 19**,** 6011-9.

HE, L., WU, X. S., MOHAN, R. & WU, L. G. 2006. Two modes of fusion pore opening revealed by cell-attached recordings at a synapse. *Nature,* 444**,** 102-5.

HENNE, W. M., KENT, H. M., FORD, M. G., HEGDE, B. G., DAUMKE, O., BUTLER, P. J., MITTAL, R., LANGEN, R., EVANS, P. R. & MCMAHON, H. T. 2007. Structure and analysis of FCHo2 F-BAR domain: a dimerizing and membrane recruitment module that effects membrane curvature. *Structure,* 15**,** 839-52.

HEUSER, J. 1980. Three-dimensional visualization of coated vesicle formation in fibroblasts. *J Cell Biol,* 84**,** 560-83.

HEUSER, J. E. & REESE, T. S. 1973. Evidence for recycling of synaptic vesicle membrane during transmitter release at the frog neuromuscular junction. *J Cell Biol,* 57**,** 315-44.
HILL, E., VAN DER KAAY, J., DOWNES, C. P. & SMYTHE, E. 2001. The role of dynamin and its binding partners in coated pit invagination and scission. *J Cell Biol,* 152**,** 309-23.
HORIKAWA, H. P., KNEUSSEL, M., EL FAR, O. & BETZ, H. 2002. Interaction of synaptophysin with the AP-1 adaptor protein gamma-adaptin. *Mol Cell Neurosci,* 21**,** 454-62.
HUA, J. & CULLEN, B. R. 1997. Human immunodeficiency virus types 1 and 2 and simian immunodeficiency virus Nef use distinct but overlapping target sites for downregulation of cell surface CD4. *J Virol,* 71**,** 6742-8.
HUA, Y. & SCHELLER, R. H. 2001. Three SNARE complexes cooperate to mediate membrane fusion. *Proc Natl Acad Sci U S A,* 98**,** 8065-70.
JAHN, R., SCHIEBLER, W., OUIMET, C. & GREENGARD, P. 1985. A 38,000-dalton membrane protein (p38) present in synaptic vesicles. *Proc Natl Acad Sci U S A,* 82**,** 4137-41.
JANZ, R., SUDHOF, T. C., HAMMER, R. E., UNNI, V., SIEGELBAUM, S. A. & BOLSHAKOV, V. Y. 1999. Essential roles in synaptic plasticity for synaptogyrin I and synaptophysin I. *Neuron,* 24**,** 687-700.
JENA, B. P., WEBSTER, P., GEIBEL, J. P., VAN DEN POL, A. N. & SRITHARAN, K. C. 1997. Localization of SH-PTP1 to synaptic vesicles: a possible role in neurotransmission. *Cell Biol Int,* 21**,** 469-76.
JOHNSTON, P. A., JAHN, R. & SUDHOF, T. C. 1989. Transmembrane topography and evolutionary conservation of synaptophysin. *J Biol Chem,* 264**,** 1268-73.
JOHNSTON, P. A. & SUDHOF, T. C. 1990. The multisubunit structure of synaptophysin. Relationship between disulfide bonding and homo-oligomerization. *J Biol Chem,* 265**,** 8869-73.
JORGENSEN, E. M., HARTWIEG, E., SCHUSKE, K., NONET, M. L., JIN, Y. & HORVITZ, H. R. 1995. Defective recycling of synaptic vesicles in synaptotagmin mutants of Caenorhabditis elegans. *Nature,* 378**,** 196-9.
JOVANOVIC, J. N., CZERNIK, A. J., FIENBERG, A. A., GREENGARD, P. & SIHRA, T. S. 2000. Synapsins as mediators of BDNF-enhanced neurotransmitter release. *Nat Neurosci,* 3**,** 323-9.
KALIA, L. V., GINGRICH, J. R. & SALTER, M. W. 2004. Src in synaptic transmission and plasticity. *Oncogene,* 23**,** 8007-16.
KELLER, J. E., CAI, F. & NEALE, E. A. 2004. Uptake of botulinum neurotoxin into cultured neurons. *Biochemistry,* 43**,** 526-32.
KELLY, B. T., MCCOY, A. J., SPATE, K., MILLER, S. E., EVANS, P. R., HONING, S. & OWEN, D. J. 2008. A structural explanation for the binding of endocytic dileucine motifs by the AP2 complex. *Nature,* 456**,** 976-79.
KHVOTCHEV, M. V. & SUDHOF, T. C. 2004. Stimulus-dependent dynamic homo- and heteromultimerization of synaptobrevin/VAMP and synaptophysin. *Biochemistry,* 43**,** 15037-43.
KIBBEY, R. G., RIZO, J., GIERASCH, L. M. & ANDERSON, R. G. 1998. The LDL receptor clustering motif interacts with the clathrin terminal domain in a reverse turn conformation. *J Cell Biol,* 142**,** 59-67.
KIM, S. H. & RYAN, T. A. 2009. Synaptic vesicle recycling at CNS snapses without AP-2. *J Neurosci,* 29**,** 3865-74.
KIRCHHAUSEN, T., BONIFACINO, J. S. & RIEZMAN, H. 1997. Linking cargo to vesicle formation: receptor tail interactions with coat proteins. *Curr Opin Cell Biol,* 9**,** 488-95.

KIRCHHAUSEN, T. & HARRISON, S. C. 1981. Protein organization in clathrin trimers. *Cell,* 23**,** 755-61.

KLINGAUF, J., KAVALALI, E. T. & TSIEN, R. W. 1998. Kinetics and regulation of fast endocytosis at hippocampal synapses. *Nature,* 394**,** 581-5.

KNAUS, P., MARQUEZE-POUEY, B., SCHERER, H. & BETZ, H. 1990. Synaptoporin, a novel putative channel protein of synaptic vesicles. *Neuron,* 5**,** 453-62.

KOCH, D., SPIWOKS-BECKER, I., SABANOV, V., SINNING, A., DUGLADZE, T., STELLMACHER, A., AHUJA, R., GRIMM, J., SCHULER, S., MULLER, A., ANGENSTEIN, F., AHMED, T., DIESLER, A., MOSER, M., TOM DIECK, S., SPESSERT, R., BOECKERS, T. M., FASSLER, R., HUBNER, C. A., BALSCHUN, D., GLOVELI, T., KESSELS, M. M. & QUALMANN, B. 2011. Proper synaptic vesicle formation and neuronal network activity critically rely on syndapin I. *EMBO J,* 30**,** 4955-69.

KOENIG, J. H. & IKEDA, K. 1989. Disappearance and reformation of synaptic vesicle membrane upon transmitter release observed under reversible blockage of membrane retrieval. *J Neurosci,* 9**,** 3844-60.

KWON, S. E. & CHAPMAN, E. R. 2011. Synaptophysin regulates the kinetics of synaptic vesicle endocytosis in central neurons. *Neuron,* 70**,** 847-54.

LARSON, D. R., ZIPFEL, W. R., WILLIAMS, R. M., CLARK, S. W., BRUCHEZ, M. P., WISE, F. W. & WEBB, W. W. 2003. Water-soluble quantum dots for multiphoton fluorescence imaging in vivo. *Science,* 300**,** 1434-6.

LEMMON, S. K., PELLICENA-PALLE, A., CONLEY, K. & FREUND, C. L. 1991. Sequence of the clathrin heavy chain from Saccharomyces cerevisiae and requirement of the COOH terminus for clathrin function. *J Cell Biol,* 112**,** 65-80.

LEUBE, R. E., KAISER, P., SEITER, A., ZIMBELMANN, R., FRANKE, W. W., REHM, H., KNAUS, P., PRIOR, P., BETZ, H., REINKE, H. & ET AL. 1987. Synaptophysin: molecular organization and mRNA expression as determined from cloned cDNA. *EMBO J,* 6**,** 3261-8.

LEVY, J. B., DORAI, T., WANG, L. H. & BRUGGE, J. S. 1987. The structurally distinct form of pp60c-src detected in neuronal cells is encoded by a unique c-src mRNA. *Mol Cell Biol,* 7**,** 4142-5.

LI, Z. & MURTHY, V. N. 2001. Visualizing postendocytic traffic of synaptic vesicles at hippocampal synapses. *Neuron,* 31**,** 593-605.

LINSTEDT, A. D. & KELLY, R. B. 1991. Endocytosis of the synaptic vesicle protein, synaptophysin, requires the COOH-terminal tail. *J Physiol (Paris),* 85**,** 90-6.

LLINAS, R., SUGIMORI, M. & SILVER, R. B. 1992. Microdomains of high calcium concentration in a presynaptic terminal. *Science,* 256**,** 677-9.

LU, Y. M., RODER, J. C., DAVIDOW, J. & SALTER, M. W. 1998. Src activation in the induction of long-term potentiation in CA1 hippocampal neurons. *Science,* 279**,** 1363-7.

LYLES, V., ZHAO, Y. & MARTIN, K. C. 2006. Synapse formation and mRNA localization in cultured Aplysia neurons. *Neuron,* 49**,** 349-56.

LYNCH, K. L., GERONA, R. R., KIELAR, D. M., MARTENS, S., MCMAHON, H. T. & MARTIN, T. F. 2008. Synaptotagmin-1 utilizes membrane bending and SNARE binding to drive fusion pore expansion. *Mol Biol Cell,* 19**,** 5093-103.

MALLOZZI, C., CECCARINI, M., CAMERINI, S., MACCHIA, G., CRESCENZI, M., PETRUCCI, T. C. & DI STASI, A. M. 2009. Peroxynitrite induces tyrosine residue modifications in synaptophysin C-terminal domain, affecting its interaction with src. *J Neurochem,* 111**,** 859-69.

MARKS, B., STOWELL, M. H., VALLIS, Y., MILLS, I. G., GIBSON, A., HOPKINS, C. R. & MCMAHON, H. T. 2001. GTPase activity of dynamin and resulting conformation change are essential for endocytosis. *Nature,* 410**,** 231-5.

MARTENS, S., KOZLOV, M. M. & MCMAHON, H. T. 2007. How synaptotagmin promotes membrane fusion. *Science,* 316**,** 1205-8.
MASUDA, M., TAKEDA, S., SONE, M., OHKI, T., MORI, H., KAMIOKA, Y. & MOCHIZUKI, N. 2006. Endophilin BAR domain drives membrane curvature by two newly identified structure-based mechanisms. *EMBO J,* 25**,** 2889-97.
MATSUNAGA, T., SHIRASAWA, H., TANABE, M., OHNUMA, N., TAKAHASHI, H. & SIMIZU, B. 1993. Expression of alternatively spliced src messenger RNAs related to neuronal differentiation in human neuroblastomas. *Cancer Res,* 53**,** 3179-85.
MAYER, A., WICKNER, W. & HAAS, A. 1996. Sec18p (NSF)-driven release of Sec17p (alpha-SNAP) can precede docking and fusion of yeast vacuoles. *Cell,* 85**,** 83-94.
MAYER, B. J. & ECK, M. J. 1995. SH3 domains. Minding your p's and q's. *Curr Biol,* 5**,** 364-7.
MCMAHON, H. T., BOLSHAKOV, V. Y., JANZ, R., HAMMER, R. E., SIEGELBAUM, S. A. & SUDHOF, T. C. 1996. Synaptophysin, a major synaptic vesicle protein, is not essential for neurotransmitter release. *Proc Natl Acad Sci U S A,* 93**,** 4760-4.
MEDINE, C. N., RICKMAN, C., CHAMBERLAIN, L. H. & DUNCAN, R. R. 2007. Munc18-1 prevents the formation of ectopic SNARE complexes in living cells. *J Cell Sci,* 120**,** 4407-15.
MICHEVA, K. D., RAMJAUN, A. R., KAY, B. K. & MCPHERSON, P. S. 1997. SH3 domain-dependent interactions of endophilin with amphiphysin. *FEBS Letters,* 414**,** 308-312.
MILLER, T. M. & HEUSER, J. E. 1984. Endocytosis of synaptic vesicle membrane at the frog neuromuscular junction. *J Cell Biol,* 98**,** 685-98.
MILLER, W. T. 2003. Determinants of substrate recognition in nonreceptor tyrosine kinases. *Acc Chem Res,* 36**,** 393-400.
MILOSEVIC, I., GIOVEDI, S., LOU, X., RAIMONDI, A., COLLESI, C., SHEN, H., PARADISE, S., O'TOOLE, E., FERGUSON, S., CREMONA, O. & DE CAMILLI, P. 2011. Recruitment of endophilin to clathrin-coated pit necks is required for efficient vesicle uncoating after fission. *Neuron,* 72**,** 587-601.
MITTER, D., REISINGER, C., HINZ, B., HOLLMANN, S., YELAMANCHILI, S. V., TREIBER-HELD, S., OHM, T. G., HERRMANN, A. & AHNERT-HILGER, G. 2003. The synaptophysin/synaptobrevin interaction critically depends on the cholesterol content. *J Neurochem,* 84**,** 35-42.
MONTECUCCO, C., SCHIAVO, G. & PANTANO, S. 2005. SNARE complexes and neuroexocytosis: how many, how close? *Trends Biochem Sci,* 30**,** 367-72.
MORGAN, J. R., PRASAD, K., JIN, S., AUGUSTINE, G. J. & LAFER, E. M. 2001. Uncoating of clathrin-coated vesicles in presynaptic terminals: roles for Hsc70 and auxilin. *Neuron,* 32**,** 289-300.
MORRIS, R. G., ANDERSON, E., LYNCH, G. S. & BAUDRY, M. 1986. Selective impairment of learning and blockade of long-term potentiation by an N-methyl-D-aspartate receptor antagonist, AP5. *Nature,* 319**,** 774-6.
MULLANY, P. M. & LYNCH, M. A. 1998. Evidence for a role for synaptophysin in expression of long-term potentiation in rat dentate gyrus. *Neuroreport,* 9**,** 2489-94.
NAITO, S. & UEDA, T. 1985. Characterization of Glutamate Uptake into Synaptic Vesicles. *Journal of Neurochemistry,* 44**,** 99-109.
NESTEROV, A., WILEY, H. S. & GILL, G. N. 1995. Ligand-induced endocytosis of epidermal growth factor receptors that are defective in binding adaptor proteins. *Proc Natl Acad Sci U S A,* 92**,** 8719-23.
NEVES, G., GOMIS, A. & LAGNADO, L. 2001. Calcium influx selects the fast mode of endocytosis in the synaptic terminal of retinal bipolar cells. *Proc Natl Acad Sci U S A,* 98**,** 15282-7.

NICHOLSON-TOMISHIMA, K. & RYAN, T. A. 2004. Kinetic efficiency of endocytosis at mammalian CNS synapses requires synaptotagmin I. *Proceedings of the National Academy of Sciences of the United States of America,* 101**,** 16648-16652.

NONET, M. L., SAIFEE, O., ZHAO, H., RAND, J. B. & WEI, L. 1998. Synaptic transmission deficits in Caenorhabditis elegans synaptobrevin mutants. *J Neurosci,* 18**,** 70-80.

OHNISHI, H., YAMAMORI, S., ONO, K., AOYAGI, K., KONDO, S. & TAKAHASHI, M. 2001. A src family tyrosine kinase inhibits neurotransmitter release from neuronal cells. *Proc Natl Acad Sci U S A,* 98**,** 10930-5.

ONOFRI, F., GIOVEDI, S., KAO, H. T., VALTORTA, F., BONGIORNO BORBONE, L., DE CAMILLI, P., GREENGARD, P. & BENFENATI, F. 2000. Specificity of the binding of synapsin I to Src homology 3 domains. *J Biol Chem,* 275**,** 29857-67.

ONOFRI, F., GIOVEDI, S., VACCARO, P., CZERNIK, A. J., VALTORTA, F., DE CAMILLI, P., GREENGARD, P. & BENFENATI, F. 1997. Synapsin I interacts with c-Src and stimulates its tyrosine kinase activity. *Proc Natl Acad Sci U S A,* 94**,** 12168-73.

ONOFRI, F., MESSA, M., MATAFORA, V., BONANNO, G., CORRADI, A., BACHI, A., VALTORTA, F. & BENFENATI, F. 2007. Synapsin phosphorylation by SRC tyrosine kinase enhances SRC activity in synaptic vesicles. *J Biol Chem,* 282**,** 15754-67.

PAILLART, C., LI, J., MATTHEWS, G. & STERLING, P. 2003. Endocytosis and vesicle recycling at a ribbon synapse. *J Neurosci,* 23**,** 4092-9.

PANG, D. T., WANG, J. K., VALTORTA, F., BENFENATI, F. & GREENGARD, P. 1988. Protein tyrosine phosphorylation in synaptic vesicles. *Proc Natl Acad Sci U S A,* 85**,** 762-6.

PENNUTO, M., BONANOMI, D., BENFENATI, F. & VALTORTA, F. 2003. Synaptophysin I controls the targeting of VAMP2/synaptobrevin II to synaptic vesicles. *Mol Biol Cell,* 14**,** 4909-19.

PENNUTO, M., DUNLAP, D., CONTESTABILE, A., BENFENATI, F. & VALTORTA, F. 2002. Fluorescence resonance energy transfer detection of synaptophysin I and vesicle-associated membrane protein 2 interactions during exocytosis from single live synapses. *Mol Biol Cell,* 13**,** 2706-17.

PERIN, M. S., BROSE, N., JAHN, R. & SUDHOF, T. C. 1991. Domain structure of synaptotagmin (p65). *J Biol Chem,* 266**,** 623-9.

PETER, B. J., KENT, H. M., MILLS, I. G., VALLIS, Y., BUTLER, P. J., EVANS, P. R. & MCMAHON, H. T. 2004. BAR domains as sensors of membrane curvature: the amphiphysin BAR structure. *Science,* 303**,** 495-9.

PIGUET, V., CHEN, Y. L., MANGASARIAN, A., FOTI, M., CARPENTIER, J. L. & TRONO, D. 1998. Mechanism of Nef-induced CD4 endocytosis: Nef connects CD4 with the mu chain of adaptor complexes. *EMBO J,* 17**,** 2472-81.

POLITIS, M. J., PELLEGRINO, R. G. & RITCHIE, J. M. 1985. The role of post-traumatic mitosis in elevation of anaerobic metabolism enzyme (lactic acid dehydrogenase) activity in degenerating central and peripheral nerve. *Brain Res,* 359**,** 187-93.

PREKERIS, R. & TERRIAN, D. M. 1997. Brain myosin V is a synaptic vesicle-associated motor protein: evidence for a Ca2+-dependent interaction with the synaptobrevin-synaptophysin complex. *J Cell Biol,* 137**,** 1589-601.

PURCELL, A. L. & CAREW, T. J. 2003. Tyrosine kinases, synaptic plasticity and memory: insights from vertebrates and invertebrates. *Trends Neurosci,* 26**,** 625-30.

PYLE, J. L., KAVALALI, E. T., PIEDRAS-RENTERIA, E. S. & TSIEN, R. W. 2000. Rapid reuse of readily releasable pool vesicles at hippocampal synapses. *Neuron,* 28**,** 221-31.

PYPER, J. M. & BOLEN, J. B. 1989. Neuron-specific splicing of C-SRC RNA in human brain. *J Neurosci Res,* 24**,** 89-96.

QUALMANN, B., KOCH, D. & KESSELS, M. M. 2011. Let's go bananas: revisiting the endocytic BAR code. *EMBO J,* 30**,** 3501-15.

QUALMANN, B., ROOS, J., DIGREGORIO, P. J. & KELLY, R. B. 1999. Syndapin I, a synaptic dynamin-binding protein that associates with the neural Wiskott-Aldrich syndrome protein. *Mol Biol Cell,* 10**,** 501-13.

RAIMONDI, A., FERGUSON, S. M., LOU, X., ARMBRUSTER, M., PARADISE, S., GIOVEDI, S., MESSA, M., KONO, N., TAKASAKI, J., CAPPELLO, V., O'TOOLE, E., RYAN, T. A. & DE CAMILLI, P. 2011. Overlapping role of dynamin isoforms in synaptic vesicle endocytosis. *Neuron,* 70**,** 1100-14.

RAPOPORT, I., CHEN, Y. C., CUPERS, P., SHOELSON, S. E. & KIRCHHAUSEN, T. 1998. Dileucine-based sorting signals bind to the beta chain of AP-1 at a site distinct and regulated differently from the tyrosine-based motif-binding site. *EMBO J,* 17**,** 2148-55.

REGNIER-VIGOUROUX, A., TOOZE, S. A. & HUTTNER, W. B. 1991. Newly synthesized synaptophysin is transported to synaptic-like microvesicles via constitutive secretory vesicles and the plasma membrane. *EMBO J,* 10**,** 3589-601.

REHM, H., WIEDENMANN, B. & BETZ, H. 1986. Molecular characterization of synaptophysin, a major calcium-binding protein of the synaptic vesicle membrane. *EMBO J,* 5**,** 535-41.

REISINGER, C., YELAMANCHILI, S. V., HINZ, B., MITTER, D., BECHER, A., BIGALKE, H. & AHNERT-HILGER, G. 2004. The synaptophysin/synaptobrevin complex dissociates independently of neuroexocytosis. *J Neurochem,* 90**,** 1-8.

RICHARDS, D. A., BAI, J. & CHAPMAN, E. R. 2005. Two modes of exocytosis at hippocampal synapses revealed by rate of FM1-43 efflux from individual vesicles. *J Cell Biol,* 168**,** 929-39.

RICHARDS, D. A., GUATIMOSIM, C., RIZZOLI, S. O. & BETZ, W. J. 2003. Synaptic vesicle pools at the frog neuromuscular junction. *Neuron,* 39**,** 529-41.

RICKMAN, C., MEDINE, C. N., BERGMANN, A. & DUNCAN, R. R. 2007. Functionally and spatially distinct modes of munc18-syntaxin 1 interaction. *J Biol Chem,* 282**,** 12097-103.

RINGSTAD, N., GAD, H., LOW, P., DI PAOLO, G., BRODIN, L., SHUPLIAKOV, O. & DE CAMILLI, P. 1999. Endophilin/SH3p4 is required for the transition from early to late stages in clathrin-mediated synaptic vesicle endocytosis. *Neuron,* 24**,** 143-54.

RIZO, J. & ROSENMUND, C. 2008. Synaptic vesicle fusion. *Nat Struct Mol Biol,* 15**,** 665-74.

RIZO, J. & SUDHOF, T. C. 2002. Snares and Munc18 in synaptic vesicle fusion. *Nat Rev Neurosci,* 3**,** 641-53.

ROBINSON, M. S. 1997. Coats and vesicle budding. *Trends Cell Biol,* 7**,** 99-102.

RODAL, S. K., SKRETTING, G., GARRED, O., VILHARDT, F., VAN DEURS, B. & SANDVIG, K. 1999. Extraction of cholesterol with methyl-beta-cyclodextrin perturbs formation of clathrin-coated endocytic vesicles. *Mol Biol Cell,* 10**,** 961-74.

ROOS, J. & KELLY, R. B. 1999. The endocytic machinery in nerve terminals surrounds sites of exocytosis. *Curr Biol,* 9**,** 1411-4.

ROSKOSKI, R., JR. 2004. Src protein-tyrosine kinase structure and regulation. *Biochem Biophys Res Commun,* 324**,** 1155-64.

ROUX, A., UYHAZI, K., FROST, A. & DE CAMILLI, P. 2006. GTP-dependent twisting of dynamin implicates constriction and tension in membrane fission. *Nature,* 441**,** 528-31.

ROYLE, S. J. & LAGNADO, L. 2003. Endocytosis at the synaptic terminal. *The Journal of Physiology,* 553**,** 345-355.

RUBENSTEIN, J. L., GREENGARD, P. & CZERNIK, A. J. 1993. Calcium-dependent serine phosphorylation of synaptophysin. *Synapse,* 13**,** 161-72.

RYAN, T. A., SMITH, S. J. & REUTER, H. 1996. The timing of synaptic vesicle endocytosis. *Proc Natl Acad Sci U S A,* 93**,** 5567-71.

SALTER, M. W. & KALIA, L. V. 2004. Src kinases: a hub for NMDA receptor regulation. *Nat Rev Neurosci,* 5**,** 317-28.
SANCHEZ-PULIDO, L., MARTIN-BELMONTE, F., VALENCIA, A. & ALONSO, M. A. 2002. MARVEL: a conserved domain involved in membrane apposition events. *Trends Biochem Sci,* 27**,** 599-601.
SANKARANARAYANAN, S., DE ANGELIS, D., ROTHMAN, J. E. & RYAN, T. A. 2000. The use of pHluorins for optical measurements of presynaptic activity. *Biophys J,* 79**,** 2199-208.
SCHIAVO, G., BENFENATI, F., POULAIN, B., ROSSETTO, O., POLVERINO DE LAURETO, P., DASGUPTA, B. R. & MONTECUCCO, C. 1992. Tetanus and botulinum-B neurotoxins block neurotransmitter release by proteolytic cleavage of synaptobrevin. *Nature,* 359**,** 832-5.
SCHMID, S. L., MATSUMOTO, A. K. & ROTHMAN, J. E. 1982. A domain of clathrin that forms coats. *Proc Natl Acad Sci U S A,* 79**,** 91-5.
SCHMITT, U., TANIMOTO, N., SEELIGER, M., SCHAEFFEL, F. & LEUBE, R. E. 2009. Detection of behavioral alterations and learning deficits in mice lacking synaptophysin. *Neuroscience,* 162**,** 234-43.
SCHOCH, S., DEAK, F., KONIGSTORFER, A., MOZHAYEVA, M., SARA, Y., SUDHOF, T. C. & KAVALALI, E. T. 2001. SNARE function analyzed in synaptobrevin/VAMP knockout mice. *Science,* 294**,** 1117-22.
SCHRODER, S. & UNGEWICKELL, E. 1991. Subunit interaction and function of clathrin-coated vesicle adaptors from the Golgi and the plasma membrane. *J Biol Chem,* 266**,** 7910-8.
SCHULZE, K. L., BROADIE, K., PERIN, M. S. & BELLEN, H. J. 1995. Genetic and electrophysiological studies of Drosophila syntaxin-1A demonstrate its role in nonneuronal secretion and neurotransmission. *Cell,* 80**,** 311-20.
SHARMA, M., BURRE, J. & SUDHOF, T. C. 2011. CSPalpha promotes SNARE-complex assembly by chaperoning SNAP-25 during synaptic activity. *Nat Cell Biol,* 13**,** 30-9.
SHIH, W., GALLUSSER, A. & KIRCHHAUSEN, T. 1995. A clathrin-binding site in the hinge of the beta 2 chain of mammalian AP-2 complexes. *J Biol Chem,* 270**,** 31083-90.
SHUPLIAKOV, O., LOW, P., GRABS, D., GAD, H., CHEN, H., DAVID, C., TAKEI, K., DE CAMILLI, P. & BRODIN, L. 1997. Synaptic vesicle endocytosis impaired by disruption of dynamin-SH3 domain interactions. *Science,* 276**,** 259-63.
SIMPSON, F., HUSSAIN, N. K., QUALMANN, B., KELLY, R. B., KAY, B. K., MCPHERSON, P. S. & SCHMID, S. L. 1999. SH3-domain-containing proteins function at distinct steps in clathrin-coated vesicle formation. *Nat Cell Biol,* 1**,** 119-24.
SINGLETON, D. R., WU, T. T. & CASTLE, J. D. 1997. Three mammalian SCAMPs (secretory carrier membrane proteins) are highly related products of distinct genes having similar subcellular distributions. *J Cell Sci,* 110 (Pt 17)**,** 2099-107.
SMITH, C. J., GRIGORIEFF, N. & PEARSE, B. M. 1998. Clathrin coats at 21 A resolution: a cellular assembly designed to recycle multiple membrane receptors. *EMBO J,* 17**,** 4943-53.
SOLLNER, T., BENNETT, M. K., WHITEHEART, S. W., SCHELLER, R. H. & ROTHMAN, J. E. 1993. A protein assembly-disassembly pathway in vitro that may correspond to sequential steps of synaptic vesicle docking, activation, and fusion. *Cell,* 75**,** 409-18.
SOLOMAHA, E., SZETO, F. L., YOUSEF, M. A. & PALFREY, H. C. 2005. Kinetics of Src homology 3 domain association with the proline-rich domain of dynamins: specificity, occlusion, and the effects of phosphorylation. *J Biol Chem,* 280**,** 23147-56.
SONG, K. S., SARGIACOMO, M., GALBIATI, F., PARENTI, M. & LISANTI, M. P. 1997. Targeting of a G alpha subunit (Gi1 alpha) and c-Src tyrosine kinase to caveolae membranes: clarifying the role of N-myristoylation. *Cell Mol Biol (Noisy-le-grand),* 43**,** 293-303.

SONGYANG, Z., SHOELSON, S. E., CHAUDHURI, M., GISH, G., PAWSON, T., HASER, W. G., KING, F., ROBERTS, T., RATNOFSKY, S., LECHLEIDER, R. J. & ET AL. 1993. SH2 domains recognize specific phosphopeptide sequences. *Cell,* 72**,** 767-78.

SORKIN, A., MAZZOTTI, M., SORKINA, T., SCOTTO, L. & BEGUINOT, L. 1996. Epidermal growth factor receptor interaction with clathrin adaptors is mediated by the Tyr974-containing internalization motif. *J Biol Chem,* 271**,** 13377-84.

SPIWOKS-BECKER, I., VOLLRATH, L., SEELIGER, M. W., JAISSLE, G., ESHKIND, L. G. & LEUBE, R. E. 2001. Synaptic vesicle alterations in rod photoreceptors of synaptophysin-deficient mice. *Neuroscience,* 107**,** 127-42.

STENIUS, K., JANZ, R., SUDHOF, T. C. & JAHN, R. 1995. Structure of synaptogyrin (p29) defines novel synaptic vesicle protein. *J Cell Biol,* 131**,** 1801-9.

STOWELL, M. H., MARKS, B., WIGGE, P. & MCMAHON, H. T. 1999. Nucleotide-dependent conformational changes in dynamin: evidence for a mechanochemical molecular spring. *Nat Cell Biol,* 1**,** 27-32.

SUBTIL, A., GAIDAROV, I., KOBYLARZ, K., LAMPSON, M. A., KEEN, J. H. & MCGRAW, T. E. 1999. Acute cholesterol depletion inhibits clathrin-coated pit budding. *Proc Natl Acad Sci U S A,* 96**,** 6775-80.

SUDHOF, T. C. 2002. Synaptotagmins: why so many? *J Biol Chem,* 277**,** 7629-32.

SUDHOF, T. C., LOTTSPEICH, F., GREENGARD, P., MEHL, E. & JAHN, R. 1987. A synaptic vesicle protein with a novel cytoplasmic domain and four transmembrane regions. *Science,* 238**,** 1142-4.

SUGRUE, M. M., BRUGGE, J. S., MARSHAK, D. R., GREENGARD, P. & GUSTAFSON, E. L. 1990. Immunocytochemical localization of the neuron-specific form of the c-src gene product, pp60c-src(+), in rat brain. *J Neurosci,* 10**,** 2513-27.

SUTTON, R. B., FASSHAUER, D., JAHN, R. & BRUNGER, A. T. 1998. Crystal structure of a SNARE complex involved in synaptic exocytosis at 2.4 A resolution. *Nature,* 395**,** 347-53.

SVERDLOV, M., SHAJAHAN, A. N. & MINSHALL, R. D. 2007. Tyrosine phosphorylation-dependence of caveolae-mediated endocytosis. *J Cell Mol Med,* 11**,** 1239-50.

SWEITZER, S. M. & HINSHAW, J. E. 1998. Dynamin undergoes a GTP-dependent conformational change causing vesiculation. *Cell,* 93**,** 1021-9.

TAKAMORI, S., HOLT, M., STENIUS, K., LEMKE, E. A., GRONBORG, M., RIEDEL, D., URLAUB, H., SCHENCK, S., BRUGGER, B., RINGLER, P., MULLER, S. A., RAMMNER, B., GRATER, F., HUB, J. S., DE GROOT, B. L., MIESKES, G., MORIYAMA, Y., KLINGAUF, J., GRUBMULLER, H., HEUSER, J., WIELAND, F. & JAHN, R. 2006. Molecular anatomy of a trafficking organelle. *Cell,* 127**,** 831-46.

TAKEI, K., SLEPNEV, V. I., HAUCKE, V. & DE CAMILLI, P. 1999. Functional partnership between amphiphysin and dynamin in clathrin-mediated endocytosis. *Nat Cell Biol,* 1**,** 33-9.

TAKESHIMA, H., SHIMUTA, M., KOMAZAKI, S., OHMI, K., NISHI, M., IINO, M., MIYATA, A. & KANGAWA, K. 1998. Mitsugumin29, a novel synaptophysin family member from the triad junction in skeletal muscle. *Biochem J,* 331 (Pt 1)**,** 317-22.

TATOSYAN, A. G. & MIZENINA, O. A. 2000. Kinases of the Src family: structure and functions. *Biochemistry (Mosc),* 65**,** 49-58.

TENG, H. & WILKINSON, R. S. 2000. Clathrin-mediated endocytosis near active zones in snake motor boutons. *J Neurosci,* 20**,** 7986-93.

THIELE, C., HANNAH, M. J., FAHRENHOLZ, F. & HUTTNER, W. B. 2000. Cholesterol binds to synaptophysin and is required for biogenesis of synaptic vesicles. *Nat Cell Biol,* 2**,** 42-9.

THOMAS, L. & BETZ, H. 1990. Synaptophysin binds to physophilin, a putative synaptic plasma membrane protein. *J Cell Biol,* 111**,** 2041-52.
THOMAS, L., HARTUNG, K., LANGOSCH, D., REHM, H., BAMBERG, E., FRANKE, W. W. & BETZ, H. 1988. Identification of synaptophysin as a hexameric channel protein of the synaptic vesicle membrane. *Science,* 242**,** 1050-3.
UBACH, J., ZHANG, X., SHAO, X., SUDHOF, T. C. & RIZO, J. 1998. Ca2+ binding to synaptotagmin: how many Ca2+ ions bind to the tip of a C2-domain? *EMBO J,* 17**,** 3921-30.
ULLRICH, B., LI, C., ZHANG, J. Z., MCMAHON, H., ANDERSON, R. G., GEPPERT, M. & SUDHOF, T. C. 1994. Functional properties of multiple synaptotagmins in brain. *Neuron,* 13**,** 1281-91.
UMBACH, J. A., ZINSMAIER, K. E., EBERLE, K. K., BUCHNER, E., BENZER, S. & GUNDERSEN, C. B. 1994. Presynaptic dysfunction in Drosophila csp mutants. *Neuron,* 13**,** 899-907.
VALTORTA, F., PENNUTO, M., BONANOMI, D. & BENFENATI, F. 2004. Synaptophysin: leading actor or walk-on role in synaptic vesicle exocytosis? *Bioessays,* 26**,** 445-53.
VAN DEN BOGAART, G., HOLT, M. G., BUNT, G., RIEDEL, D., WOUTERS, F. S. & JAHN, R. 2010. One SNARE complex is sufficient for membrane fusion. *Nat Struct Mol Biol,* 17**,** 358-364.
VAN DER BLIEK, A. M. & MEYEROWITZ, E. M. 1991. Dynamin-like protein encoded by the Drosophila shibire gene associated with vesicular traffic. *Nature,* 351**,** 411-4.
VARMUS, H. E., PADGETT, T., HEASLEY, S., SIMON, G. & BISHOP, J. M. 1977. Cellular functions are required for the synthesis and integration of avian sarcoma virus-specific DNA. *Cell,* 11**,** 307-19.
WALAAS, S. I., LUSTIG, A., GREENGARD, P. & BRUGGE, J. S. 1988. Widespread distribution of the c-src gene product in nerve cells and axon terminals in the adult rat brain. *Brain Res,* 427**,** 215-22.
WANG, S. J. 2003. A role for Src kinase in the regulation of glutamate release from rat cerebrocortical nerve terminals. *Neuroreport,* 14**,** 1519-22.
WASHBOURNE, P., SCHIAVO, G. & MONTECUCCO, C. 1995. Vesicle-associated membrane protein-2 (synaptobrevin-2) forms a complex with synaptophysin. *Biochem J,* 305 (Pt 3)**,** 721-4.
WASHBOURNE, P., THOMPSON, P. M., CARTA, M., COSTA, E. T., MATHEWS, J. R., LOPEZ-BENDITO, G., MOLNAR, Z., BECHER, M. W., VALENZUELA, C. F., PARTRIDGE, L. D. & WILSON, M. C. 2002. Genetic ablation of the t-SNARE SNAP-25 distinguishes mechanisms of neuroexocytosis. *Nat Neurosci,* 5**,** 19-26.
WENG, Z., RICKLES, R. J., FENG, S., RICHARD, S., SHAW, A. S., SCHREIBER, S. L. & BRUGGE, J. S. 1995. Structure-function analysis of SH3 domains: SH3 binding specificity altered by single amino acid substitutions. *Mol Cell Biol,* 15**,** 5627-34.
WESTHEAD, E. W. 1987. Lipid composition and orientation in secretory vesicles. *Ann N Y Acad Sci,* 493**,** 92-100.
WHEELER, T. C., CHIN, L. S., LI, Y., ROUDABUSH, F. L. & LI, L. 2002. Regulation of synaptophysin degradation by mammalian homologues of seven in absentia. *J Biol Chem,* 277**,** 10273-82.
WIEDENMANN, B. & FRANKE, W. W. 1985. Identification and localization of synaptophysin, an integral membrane glycoprotein of Mr 38,000 characteristic of presynaptic vesicles. *Cell,* 41**,** 1017-28.
WU, W. & WU, L. G. 2007. Rapid bulk endocytosis and its kinetics of fission pore closure at a central synapse. *Proc Natl Acad Sci U S A,* 104**,** 10234-9.
XU, W., HARRISON, S. C. & ECK, M. J. 1997. Three-dimensional structure of the tyrosine kinase c-Src. *Nature,* 385**,** 595-602.

YAGI, T. 1994. Src Family Kinases Control Neural Development and Function. *Development, Growth & Differentiation,* 36**,** 543-550.
YEATMAN, T. J. 2004. A renaissance for SRC. *Nat Rev Cancer,* 4**,** 470-80.
YELAMANCHILI, S. V., REISINGER, C., BECHER, A., SIKORRA, S., BIGALKE, H., BINZ, T. & AHNERT-HILGER, G. 2005. The C-terminal transmembrane region of synaptobrevin binds synaptophysin from adult synaptic vesicles. *Eur J Cell Biol,* 84**,** 467-75.
YU, X. M., ASKALAN, R., KEIL, G. J., 2ND & SALTER, M. W. 1997. NMDA channel regulation by channel-associated protein tyrosine kinase Src. *Science,* 275**,** 674-8.
YU, X. M. & SALTER, M. W. 1999. Src, a molecular switch governing gain control of synaptic transmission mediated by N-methyl-D-aspartate receptors. *Proc Natl Acad Sci U S A,* 96**,** 7697-704.
ZENISEK, D., STEYER, J. A., FELDMAN, M. E. & ALMERS, W. 2002. A membrane marker leaves synaptic vesicles in milliseconds after exocytosis in retinal bipolar cells. *Neuron,* 35**,** 1085-97.
ZHANG, Q., CAO, Y. Q. & TSIEN, R. W. 2007. Quantum dots provide an optical signal specific to full collapse fusion of synaptic vesicles. *Proc Natl Acad Sci U S A,* 104**,** 17843-8.
ZHANG, Q., LI, Y. & TSIEN, R. W. 2009. The dynamic control of kiss-and-run and vesicular reuse probed with single nanoparticles. *Science,* 323**,** 1448-53.
ZHAO, W., CAVALLARO, S., GUSEV, P. & ALKON, D. L. 2000. Nonreceptor tyrosine protein kinase pp60c-src in spatial learning: synapse-specific changes in its gene expression, tyrosine phosphorylation, and protein-protein interactions. *Proc Natl Acad Sci U S A,* 97**,** 8098-103.
ZIMMERMAN, B., SIMAAN, M., LEE, M. H., LUTTRELL, L. M. & LAPORTE, S. A. 2009. c-Src-mediated phosphorylation of AP-2 reveals a general mechanism for receptors internalizing through the clathrin pathway. *Cell Signal,* 21**,** 103-10.

Chapter 7 Appendix

A)

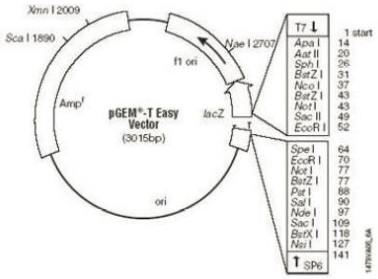

B)

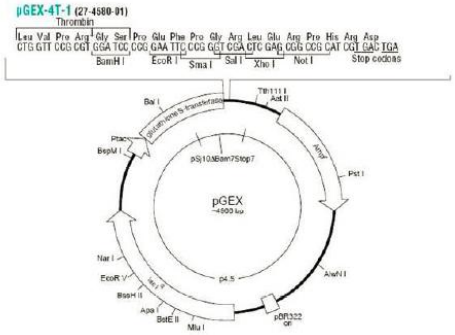

C)

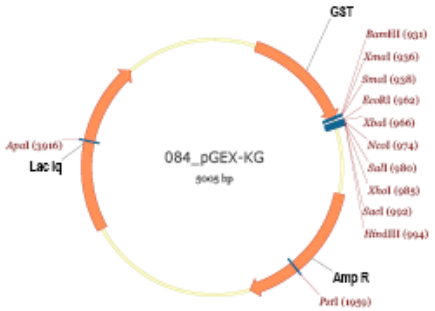

Appendix Figure 1 - Map of the Biochemical Vectors used

Schematics of showing the A) pGEM, B) pGEX 4T-1 and C) pGEX KG vectors used in the biochemical experiments

Appendix Table 1 Mass Spectrometry Results from GST-Pull Downs from Synaptosomal Lysate using the SH3 Interaction Motif Mutants as Bait

#	MS/MS View:Identified Proteins (106)	Accession Number	Molecular Weight
1	Anionic trypsin-1 OS=Rattus norvegicus GN=Prss1 PE=1 SV=1	TRY1_RAT	26 kDa
2	Sodium/potassium-transporting ATPase subunit alpha-3 OS=Mus musculus GN=Atp1a3 PE=1 SV=1	AT1A3_MOUSE (+1)	112 kDa
3	Tubulin beta-2A chain OS=Mus musculus GN=Tubb2a PE=1 SV=1	TBB2A_MOUSE (+1)	50 kDa
4	Keratin, type I cytoskeletal 10 OS=Rattus norvegicus GN=Krt10 PE=2 SV=1	K1C10_RAT	57 kDa
5	Keratin, type II cytoskeletal 1 OS=Rattus norvegicus GN=Krt1 PE=2 SV=1	K2C1_RAT	65 kDa
6	Heat shock cognate 71 kDa protein OS=Mus musculus GN=Hspa8 PE=1 SV=1	HSP7C_MOUSE (+1)	71 kDa
7	Tubulin alpha-1A chain OS=Cricetulus griseus GN=TUBA1A PE=2 SV=1	TBA1A_CRIGR (+2)	50 kDa
8	ATP synthase subunit alpha, mitochondrial OS=Rattus norvegicus GN=Atp5a1 PE=1 SV=2	ATPA_RAT	60 kDa
9	Stress-70 protein, mitochondrial OS=Rattus norvegicus GN=Hspa9 PE=1 SV=3	GRP75_RAT	74 kDa
10	Keratin, type II cytoskeletal 5 OS=Rattus norvegicus GN=Krt5 PE=1 SV=1	K2C5_RAT	62 kDa
11	AP-2 complex subunit beta OS=Mus musculus GN=Ap2b1 PE=1 SV=1	AP2B1_MOUSE (+1)	105 kDa
12	ATP synthase subunit beta, mitochondrial OS=Rattus norvegicus GN=Atp5b PE=1 SV=2	ATPB_RAT	56 kDa
13	Synaptophysin OS=Mus musculus GN=Syp PE=1 SV=2	SYPH_MOUSE	34 kDa
14	Anionic trypsin-2 OS=Mus musculus GN=Prss2 PE=2 SV=1	TRY2_MOUSE (+1)	26 kDa
15	Vesicle-fusing ATPase OS=Cricetulus griseus GN=NSF PE=1 SV=1	NSF_CRIGR (+2)	83 kDa
16	Synapsin-2 OS=Rattus norvegicus GN=Syn2 PE=1 SV=1	SYN2_RAT	63 kDa
17	Synapsin-1 OS=Rattus norvegicus GN=Syn1 PE=1 SV=3	SYN1_RAT	74 kDa

18	Tubulin beta-3 chain OS=Mus musculus GN=Tubb3 PE=1 SV=1	TBB3_MOUSE (+1)	50 kDa
19	AP-2 complex subunit alpha-1 OS=Mus musculus GN=Ap2a1 PE=1 SV=1	AP2A1_MOUSE	108 kDa
20	Dynamin-1 OS=Rattus norvegicus GN=Dnm1 PE=1 SV=2	DYN1_RAT	97 kDa
21	Glutamate dehydrogenase 1, mitochondrial OS=Rattus norvegicus GN=Glud1 PE=1 SV=2	DHE3_RAT	61 kDa
22	Sodium/potassium-transporting ATPase subunit alpha-1 OS=Mus musculus GN=Atp1a1 PE=1 SV=1	AT1A1_MOUSE (+1)	113 kDa
23	Keratin, type I cytoskeletal 14 OS=Mus musculus GN=Krt14 PE=1 SV=2	K1C14_MOUSE	53 kDa
24	Phosphatidylinositol-4-phosphate 5-kinase type-1 gamma OS=Rattus norvegicus GN=Pip5k1c PE=1 SV=1	PI51C_RAT	76 kDa
25	78 kDa glucose-regulated protein OS=Mus musculus GN=Hspa5 PE=1 SV=3	GRP78_MOUSE (+1)	72 kDa
26	60 kDa heat shock protein, mitochondrial OS=Mus musculus GN=Hspd1 PE=1 SV=1	CH60_MOUSE (+1)	61 kDa
27	Dihydropyrimidinase-related protein 2 OS=Mus musculus GN=Dpysl2 PE=1 SV=2	DPYL2_MOUSE (+1)	62 kDa
28	Microtubule-associated protein 1B OS=Rattus norvegicus GN=Map1b PE=1 SV=2	MAP1B_RAT	270 kDa
29	Aconitate hydratase, mitochondrial OS=Rattus norvegicus GN=Aco2 PE=1 SV=2	ACON_RAT	85 kDa
30	Plasma membrane calcium-transporting ATPase 1 OS=Rattus norvegicus GN=Atp2b1 PE=2 SV=2	AT2B1_RAT	139 kDa
31	Excitatory amino acid transporter 1 OS=Mus musculus GN=Slc1a3 PE=1 SV=2	EAA1_MOUSE (+1)	60 kDa
32	ADP/ATP translocase 1 OS=Mus musculus GN=Slc25a4 PE=1 SV=4	ADT1_MOUSE (+1)	33 kDa
33	AP-2 complex subunit alpha-2 OS=Mus musculus GN=Ap2a2 PE=1 SV=1	AP2A2_MOUSE (+1)	104 kDa
34	Synaptotagmin-1 OS=Mus musculus GN=Syt1 PE=1 SV=1	SYT1_MOUSE (+1)	47 kDa
35	Keratin, type II cytoskeletal 73 OS=Mus musculus GN=Krt73 PE=1 SV=1	K2C73_MOUSE (+1)	59 kDa

36	Elongation factor 1-alpha 1 OS=Cricetulus griseus GN=EEF1A1 PE=2 SV=1	EF1A1_CRIGR (+2)	50 kDa
37	2',3'-cyclic-nucleotide 3'-phosphodiesterase OS=Rattus norvegicus GN=Cnp PE=1 SV=2	CN37_RAT	47 kDa
38	Tubulin beta-2C chain OS=Mus musculus GN=Tubb2c PE=1 SV=1	TBB2C_MOUSE (+1)	50 kDa
39	Cytoplasmic FMR1-interacting protein 2 OS=Mus musculus GN=Cyfip2 PE=1 SV=2	CYFP2_MOUSE	146 kDa
40	AP-2 complex subunit mu OS=Mus musculus GN=Ap2m1 PE=1 SV=1	AP2M1_MOUSE (+1)	50 kDa
41	Hexokinase-1 OS=Mus musculus GN=Hk1 PE=1 SV=2	HXK1_MOUSE (+1)	108 kDa
42	Microtubule-associated protein 1A OS=Rattus norvegicus GN=Map1a PE=1 SV=1	MAP1A_RAT	300 kDa
43	Keratin, type I cytoskeletal 42 OS=Mus musculus GN=Krt42 PE=1 SV=1	K1C42_MOUSE	50 kDa
44	Keratin, type II cytoskeletal 2 epidermal OS=Rattus norvegicus GN=Krt2 PE=2 SV=1	K22E_RAT	69 kDa
45	Band 4.1-like protein 1 OS=Mus musculus GN=Epb41l1 PE=1 SV=2	E41L1_MOUSE (+1)	98 kDa
46	Neural cell adhesion molecule 1 OS=Mus musculus GN=Ncam1 PE=1 SV=3	NCAM1_MOUSE (+1)	119 kDa
47	Nck-associated protein 1 OS=Rattus norvegicus GN=Nckap1 PE=2 SV=1	NCKP1_RAT	129 kDa
48	Keratin, type I cytoskeletal 17 OS=Mus musculus GN=Krt17 PE=1 SV=3	K1C17_MOUSE (+1)	48 kDa
49	DNA-dependent protein kinase catalytic subunit OS=Mus musculus GN=Prkdc PE=1 SV=2	PRKDC_MOUSE	471 kDa
50	Synaptic vesicle glycoprotein 2A OS=Mus musculus GN=Sv2a PE=1 SV=1	SV2A_MOUSE (+1)	83 kDa
51	Syntaxin-binding protein 1 OS=Mus musculus GN=Stxbp1 PE=1 SV=2	STXB1_MOUSE (+1)	68 kDa
52	Importin subunit beta-1 OS=Mus musculus GN=Kpnb1 PE=1 SV=1	IMB1_MOUSE (+1)	97 kDa
53	Calcium/calmodulin-dependent protein kinase type II subunit beta	KCC2B_MOUSE	60 kDa

	OS=Mus musculus GN=Camk2b PE=1 SV=2	(+1)	
54	Band 4.1-like protein 3 OS=Mus musculus GN=Epb41l3 PE=1 SV=1	E41L3_MOUSE	103 kDa
55	Reticulocalbin-2 OS=Rattus norvegicus GN=Rcn2 PE=1 SV=2	RCN2_RAT	37 kDa
56	Septin-11 OS=Mus musculus GN=Sept11 PE=1 SV=4	SEP11_MOUSE (+1)	50 kDa
57	2-oxoglutarate dehydrogenase, mitochondrial OS=Mus musculus GN=Ogdh PE=1 SV=3	ODO1_MOUSE (+1)	116 kDa
58	Elongation factor 1-gamma OS=Rattus norvegicus GN=Eef1g PE=1 SV=3	EF1G_RAT	50 kDa
59	Dihydrolipoyllysine-residue succinyltransferase component of 2-oxoglutarate dehydrogenase complex, mitochondrial OS=Rattus norvegicus GN=Dlst PE=1 SV=2	ODO2_RAT	49 kDa
60	Dihydrolipoyllysine-residue acetyltransferase component of pyruvate dehydrogenase complex, mitochondrial OS=Rattus norvegicus GN=Dlat PE=1 SV=3	ODP2_RAT	67 kDa
61	Nucleosome assembly protein 1-like 4 OS=Rattus norvegicus GN=Nap1l4 PE=2 SV=1	NP1L4_RAT	44 kDa
62	Microtubule-associated protein 6 OS=Rattus norvegicus GN=Map6 PE=1 SV=1	MAP6_RAT	100 kDa
63	Heat shock protein HSP 90-alpha OS=Mus musculus GN=Hsp90aa1 PE=1 SV=4	HS90A_MOUSE (+1)	85 kDa
64	Phosphofurin acidic cluster sorting protein 1 OS=Rattus norvegicus GN=Pacs1 PE=2 SV=1	PACS1_RAT	105 kDa
65	Amphiphysin OS=Rattus norvegicus GN=Amph PE=1 SV=1	AMPH_RAT	75 kDa
66	Glycogen phosphorylase, muscle form OS=Mus musculus GN=Pygm PE=1 SV=3	PYGM_MOUSE	97 kDa
67	CaM kinase-like vesicle-associated protein OS=Rattus norvegicus GN=Camkv PE=1 SV=1	CAMKV_RAT	54 kDa
68	Tubulin beta-4 chain OS=Mus musculus GN=Tubb4 PE=1 SV=3	TBB4_MOUSE	50 kDa
69	Solute carrier family 12 member 5 OS=Mus musculus GN=Slc12a5 PE=1 SV=2	S12A5_MOUSE (+1)	126 kDa
70	Sodium/potassium-transporting ATPase subunit alpha-2 OS=Mus musculus GN=Atp1a2 PE=1 SV=1	AT1A2_MOUSE (+1)	112 kDa
71	Myelin proteolipid protein OS=Mus musculus GN=Plp1 PE=1 SV=2	MYPR_MOUSE	30 kDa

		(+1)	
72	Keratin, type II cytoskeletal 6A OS=Mus musculus GN=Krt6a PE=2 SV=3	K2C6A_MOUSE	59 kDa
73	Calcium-binding mitochondrial carrier protein Aralar1 OS=Mus musculus GN=Slc25a12 PE=1 SV=1	CMC1_MOUSE	75 kDa
74	Sodium/potassium-transporting ATPase subunit beta-1 OS=Mus musculus GN=Atp1b1 PE=1 SV=1	AT1B1_MOUSE (+1)	35 kDa
75	MAGUK p55 subfamily member 2 OS=Mus musculus GN=Mpp2 PE=1 SV=1	MPP2_MOUSE	62 kDa
76	Sarcoplasmic/endoplasmic reticulum calcium ATPase 2 OS=Mus musculus GN=Atp2a2 PE=1 SV=2	AT2A2_MOUSE (+1)	115 kDa
77	LETM1 and EF-hand domain-containing protein 1, mitochondrial OS=Rattus norvegicus GN=Letm1 PE=1 SV=1	LETM1_RAT	83 kDa
78	Tubulin beta-5 chain OS=Cricetulus griseus GN=TUBB5 PE=2 SV=1	TBB5_CRIGR (+2)	50 kDa
79	V-type proton ATPase catalytic subunit A OS=Mus musculus GN=Atp6v1a PE=1 SV=2	VATA_MOUSE	68 kDa
80	Tubulin alpha-4A chain OS=Mus musculus GN=Tuba4a PE=1 SV=1	TBA4A_MOUSE (+1)	50 kDa
81	Protein kinase C and casein kinase substrate in neurons protein 1 OS=Rattus norvegicus GN=Pacsin1 PE=1 SV=1	PACN1_RAT	50 kDa
82	Collagen alpha-1(I) chain OS=Mus musculus GN=Col1a1 PE=1 SV=4	CO1A1_MOUSE (+1)	138 kDa
83	Dihydrolipoyl dehydrogenase, mitochondrial OS=Rattus norvegicus GN=Dld PE=1 SV=1	DLDH_RAT	54 kDa
84	Microtubule-associated protein tau OS=Mus musculus GN=Mapt PE=1 SV=3	TAU_MOUSE (+1)	76 kDa
85	Myelin basic protein OS=Mus musculus GN=Mbp PE=1 SV=2	MBP_MOUSE (+1)	27 kDa
86	Septin-8 OS=Mus musculus GN=Sept8 PE=1 SV=4	SEPT8_MOUSE (+1)	50 kDa
87	Serine/threonine-protein phosphatase 2A 65 kDa regulatory subunit A alpha isoform OS=Mus musculus GN=Ppp2r1a PE=1 SV=3	2AAA_MOUSE	65 kDa
88	Lon protease homolog, mitochondrial OS=Mus musculus GN=Lonp1	LONM_MOUSE	106 kDa

	PE=1 SV=2	(+1)	
89	Regulator of G-protein signaling 7 OS=Mus musculus GN=Rgs7 PE=1 SV=1	RGS7_MOUSE (+1)	55 kDa
90	Long-chain fatty acid transport protein 1 OS=Rattus norvegicus GN=Slc27a1 PE=2 SV=1	S27A1_RAT	71 kDa
91	Collagen alpha-2(I) chain OS=Mus musculus GN=Col1a2 PE=2 SV=2	CO1A2_MOUSE	130 kDa
92	AP-1 complex subunit beta-1 OS=Mus musculus GN=Ap1b1 PE=1 SV=1	AP1B1_MOUSE	104 kDa
93	Plasma membrane calcium-transporting ATPase 2 OS=Mus musculus GN=Atp2b2 PE=1 SV=2	AT2B2_MOUSE (+1)	133 kDa
94	Clathrin heavy chain 1 OS=Mus musculus GN=Cltc PE=1 SV=3	CLH_MOUSE (+1)	192 kDa
95	Trifunctional enzyme subunit alpha, mitochondrial OS=Rattus norvegicus GN=Hadha PE=1 SV=2	ECHA_RAT	83 kDa
96	Heterogeneous nuclear ribonucleoprotein Q OS=Mus musculus GN=Syncrip PE=1 SV=2	HNRPQ_MOUSE	70 kDa
97	Mitochondrial inner membrane protein OS=Mus musculus GN=Immt PE=1 SV=1	IMMT_MOUSE	84 kDa
98	cAMP-dependent protein kinase type II-beta regulatory subunit OS=Mus musculus GN=Prkar2b PE=1 SV=3	KAP3_MOUSE (+1)	46 kDa
99	Pyruvate dehydrogenase E1 component subunit alpha, somatic form, mitochondrial OS=Mus musculus GN=Pdha1 PE=1 SV=1	ODPA_MOUSE (+1)	43 kDa
100	Dynamin-like 120 kDa protein, mitochondrial OS=Mus musculus GN=Opa1 PE=1 SV=1	OPA1_MOUSE (+1)	111 kDa
101	Pyruvate carboxylase, mitochondrial OS=Mus musculus GN=Pc PE=1 SV=1	PYC_MOUSE (+1)	130 kDa
102	T-complex protein 1 subunit delta OS=Mus musculus GN=Cct4 PE=1 SV=3	TCPD_MOUSE (+1)	58 kDa
103	V-type proton ATPase subunit B, brain isoform OS=Mus musculus GN=Atp6v1b2 PE=1 SV=1	VATB2_MOUSE (+1)	57 kDa
104	Catenin beta-1 OS=Mus musculus GN=Ctnnb1 PE=1 SV=1	CTNB1_MOUSE (+1)	85 kDa
105	Cationic trypsin-3 OS=Rattus norvegicus GN=Try3 PE=2 SV=1	TRY3_RAT	26 kDa
106	ATP-citrate synthase OS=Rattus norvegicus GN=Acly PE=1 SV=1	ACLY_RAT	121 kDa